Arrhythmia In Fabry Disease

Ashwin Roy

BSc (Hons), MBChB, MRCP, PGCert

Student ID: [redacted]

A thesis submitted to the University of Birmingham for the degree of:

Doctor of Philosophy

Institute of Cardiovascular Sciences

School of Medical and Dental Sciences

University of Birmingham

September 2024

Dedication

To my pillars of support - my incredible wife, Smita, and my parents. Thank you for your unwavering strength and encouragement.

Abstract

Fabry Disease (FD) is an X-linked lysosomal disorder, characterised by multi-organ accumulation of glycosphingolipid due to α-galactosidase A deficiency. Cardiac Gb3 accumulation triggers left ventricular hypertrophy (LVH), interstitial fibrosis and chronic myocardial inflammation manifesting in the advanced stages; all of which are a trigger for therapy initiation. These form a powerful substrate for ventricular and atrial arrhythmia, responsible for the high burden of SCD and stroke. It is clear, however, that FD-cardiomyopathy develops before LVH is present. Yet it not well understood which abnormalities develop first, what the drivers are to these changes, and when these start. The aims of this thesis were to understand the pro-arrhythmic role of the atria in FD as a primary atrial myopathy, characterise early markers of FD cardiomyopathy that might provoke arrhythmia, identify novel risk predictors for arrhythmia and identify clinical strategies to document significant arrhythmia. This thesis has provided new insights into pro-arrhythmic, cellular, atrial alterations which are mimicked *in-vivo*. It has identified evidence of early cardiomyopathy in patients thought to be negative for a cardiac phenotype, diagnosed using routine investigations. This thesis also identifies potential mechanisms relating to ischaemia and inflammation that drive arrhythmia. Finally, it highlights the importance of risk stratification for arrhythmia and initiating continuous cardiac monitoring in those deemed high risk. The content of this thesis enhances our understand of some of the mechanisms driving this complex pro-arrhythmic inflammatory cardiomyopathy.

.Acknowledgments

Firstly, I would like to extend my sincerest gratitude to my PhD supervisors. Specifically, my lead supervisor, Professor Richard Steeds and co-supervisors Professor Tarekegn Geberhiwot and Professor Katja Gehmlich. Without their mentorship, guidance and support, I would not have been able to develop and mature as an academic researcher or achieve my targets for this PhD. Together, they have motivated me and ensured I stayed on track, particularly during challenging times of navigating projects around a pandemic. Despite an incredibly busy schedule, Professor Steeds has always dedicated time to meet with me, discussing various aspects of the PhD and beyond. His honesty in identifying areas for development and his praise where it is due have been invaluable to my growth. I have been extremely fortunate to have had the opportunity to work under him. I find it remarkable how he manages his time so effectively, juggling so many responsibilities and yet excelling in everything he does. It is inspiring how he finds times to work as a Cardiologist, engage in academic research, pursue hobbies and find time for his family. I aspire to follow in his footsteps and achieve a similar balance and dedication in my career.

Secondly, I would like to express my gratitude to colleagues at the Institute of Cardiovascular Sciences who took me under their wing and guided me through the complexities of working in a laboratory. Despite my lack of prior experience, they were incredibly generous with their time and effort, ensuring that I received thorough training. Their support enabled me to achieve a high level of independence early on, which has been invaluable to my development. My specific gratitude goes to Miss Leena Patel, Dr Amar Azad, Dr Max Cumberland, Dr Christopher O'Shea and Dr

Sophie Broadway-Stringer. I would like to express my sincere thanks to Professor Jonathan Townend for providing his senior input on this thesis. I am also grateful to Dr Davor Pavlovic for his senior support with the electrophysiological and calcium handling work.

Thirdly, I wish to extend my gratitude to clinical collaborators who supported various projects presented in this thesis, specifically Ms Heather Small and Dr Sophie Thompson. Additionally, I am grateful to Mr James Hodson for his regular statistical advice and input throughout this journey. His patience and understanding, especially during the early days when my knowledge of statistics was limited, have been invaluable.

Finally, thank you to my family. To my late grandmother, Thama, whom we lost during my first year, and to my sister Ameeta and brother-in-law Nathan, thank you for your continued support and encouragement in both my personal and professional life. You have always guided me in the right direction and offered invaluable advice. To my parents, Meera and Ashok, you have been my biggest supporters from day one, patiently standing by me emotionally and financially, no matter what path I chose. Finally, to my incredible team at home – my wonderful wife Smita, and my beautiful children Sarina and Arjun. Thank you for being my motivation, my drive and my anchor. You make me who I am, and I would not have achieved what I have without you all by my side.

Table of Contents

List of Figures

Chapter 1

Chapter 2

Chapter 3

Chapter 4

Chapter 5

Chapter 6

Chapter 7

List of Tables

Chapter 1

Chapter 2

Chapter 3

Chapter 4

Chapter 5

Chapter 6

List of Abbreviations

18F-FDG	Fludeoxyglucose 18F
2D	2-Dimensional
6MWD	6-Minute Walk Distance
6MWT	6-Minute Walk Test
a-Gal A	Alpha Galactosidase A
A2C	Apical-2-Chamber
A4C	Apical-4-Chamber
ACE	Angiotensin Converting Enzyme
ACR	Albumin Creatinine Ratio
AF	Atrial Fibrillation
AHRE	Atrial High-Rate Episode
ANOVA	Analysis of Variance
AP	Action Potential
APD	Action Potential Duration
ARB	Angiotensin Receptor Blocker
AV	Atrioventricular
AV	Aortic Valve

AV V Max	Aortic Valve Maximum Velocity
BMI	Body Mass Index
BMP-4	Bone Morphogenic Protein-4
BP	Blood Pressure
BSA	Body Surface Index
CABG	Coronary Artery Bypass Grafting
CAD	Coronary Artery Disease
cDNA	Complementary Deoxyribose Nucleic Acid
CKD	Chronic Kidney Disease
CM	Cardiomyocyte
CMR	Cardiac Magnetic Resonance Imaging
COVID-19	Coronavirus 2019
CPEX	Cardiopulmonary Exercise Test
CRISPR/Cas9	Clustered Regularly Interspace Short Palindromic Repeat-Associated Protein 9
CT	Computed Tomography
CTCA	Compute Tomography Coronary Angiography
CTD	Calcium Transient Duration
CVA	Cerebrovascular Accident

DAD	Delayed Afterdepolarisation
DAPI	4',6-Diamidino-2-Phenylindole
DCCV	Direct Current Cardioversion
DM	Diabetes Mellitus
DMEM	Dulbecco's Modified Eagle Medium
ECG	Electrocardiogram
ECM	Extracellular Matrix
ECV	Extracellular Volume
EDF	Eosinophil-Differentiation Factor
EDV	End-Diastolic Volume
eGFR	Estimated Glomerular Filtration Rate
ELISA	Enzyme Linked Immunosorbent Assay
ERT	Enzyme Replacement Therapy
ESV	End-Systolic Volume
FAC	Fractional Area Change
FACS	Fluorescence Activated Cell Sorting
FD	Fabry Disease
FEV_1	Forced Expiratory Volume In 1 Second
FGF2	Fibroblast Growth Factor 2

Flt-3 Ligand	FMS-Related Tyrosine Kinase 3 Ligand
G-CSF	Granulocyte Colony-Stimulating Factor
GAPDH	Glyceraldehyde-3-Phosphate Dehydrogenase
Gb3	Globotriaosylceramide
GCS	Global Circumferential Strain
GEE	Generalised Estimating Equation
GLA	Galactosidase Alpha
GLS	Global Longitudinal Strain
GM-CSF	Granulocyte -Macrophage Colony-Stimulating Factor
GRO-a	Growth Regulated Protein Alpha
Gro-ß	Growth Regulated Protein Beta
HbA1c	Glycated Haemoglobin
HCM	Hypertrophic Cardiomyopathy
HDL-C	High-Density Lipoprotein Cholesterol
HDR	Homology Directed Repair
HEPES	4-2-Hydroxyethyl-1-Piperazineethanesulfonic Acid
HR	Heart Rate
HS	High-Sensitivity
ICA	Invasive Coronary Angiography

ICAM-1	Intracellular Adhesion Molecule 1
ICC	Intraclass Correlation Coefficient
ICD	Implantable Cardioverter Defibrillator
IFN-a2	Interferon Alpha 2
IFN-ß	Interferon Beta
IFN-γ	Interferon Gamma
IHD	Ischaemic Heart Disease
IL-10	Interleukin 10
IL-12 p70	Interleukin 12 P70
IL-13	Interleukin 13
IL-15	Interleukin 15
IL-17a	Interleukin 17 Alpha
IL-1a	Interleukin 1 Alpha
IL-1ra	Interleukin 1 Receptor Alpha
IL-1ß	Interleukin 1 Beta
IL-2	Interleukin 2
IL-33	Interleukin 33
IL-4	Interleukin 4
IL-6	Interleukin 6

IL-7	Interleukin 7
IL-8	Interleukin 9
ILR	Implantable Loop Recorder
IP10	Interferon Gamma-Induced Protein 10
iPSC	Induced Pluripotent Stem Cell
iPSC-CM	Induced Pluripotent Stem Cell-Derived Cardiomyocyte
IQR	Interquartile Range
IRAS	Integrated Research Application System
IVS	Interventricular Septum
LA	Left Atrium
Lat	Lateral
LDL-C	Low-Density Lipoprotein Cholesterol
LGE	Late Gadolinium Enhancement
LSD	Lysosomal Storage Disease
LV	Left Ventricle
LVEDd	Left Ventricular End-Diastolic Dimension
LVEDP	Left Ventricular End-Diastolic Pressure
LVEDVi	Indexed Left Ventricular End-Diastolic Volume
LVEF	Left Ventricular Ejection Fraction

LVESd	Left Ventricular End-Systolic Dimension
LVESVi	Indexed Left Ventricular End-Systolic Volume
LVH	Left Ventricular Hypertrophy
LVID	Left Ventricular Internal Diameter
LVM	Left Ventricular Mass
LVMi	Indexed Left Ventricular Mass
LVOT	Left Ventricular Outflow Tract
LVOTO	Left Ventricular Outflow Tract Obstruction
LVPW	Left Ventricular Posterior Wall
LVPWd	Left Ventricular Posterior Wall Dimension
LVSVi	Indexed Left Ventricular Stroke Volume
LVWT	Left Ventricular Wall Thickness
lyso-Gb3	Globotriaosylsphingosine
MACE	Major Adverse Cardiac Event
MAPSE	Mitral Annular Plane Systolic Excursion
MCP-1	Monocyte Chemoattractant Protein-1
MIP-1ß	Macrophage Inflammatory Protein 1 Beta
MIP-3a	Macrophage Inflammatory Protein 3 Alpha
MIP-3ß	Macrophage Inflammatory Protein 3 Beta

MOLLI	Modified Look-Locker Inversion Recovery
MPO	Myeloperoxidase
MPS	Myocardial Perfusion Scan
mRNA	Messenger Ribonucleic Acid
MSSI	Mainz Severity Score Index
mTOR	Mammalian Target of Rapamycin
MV	Mitral Valve
MV A Max	Mitral Valve Maximum A-Wave Velocity
MV E Max	Mitral Valve Maximum E-Wave Velocity
MWT	Maximum Wall Thickness
MYH6	Myosin Heavy Chain Alpha
MYH7	Myosin Heavy Chain Beta
MYL2	Myosin Regulatory Light Chain 2
MYL7	Myosin Regulatory Light Chain 2 Atrial Isoform
NANOG	Homeobox Protein
NK	Natural Killer
NO	Nitric Oxide
NSVT	Non-Sustained Ventricular Tachycardia
NT-proBNP	N-Terminal Pro B-Type Natriuretic Peptide

OCT	Oral Chaperone Therapy
OCT4	Octamer-Binding Transcription Factor 4
PAC	Premature Atrial Complex
PBS	Phosphate-Buffered Solution
PCI	Percutaneous Coronary Intervention
PCR	Polymerase Chain Reaction
PDF	Portable Document Format
PDGF	Platelet-Derived Growth Factor
PDGF-AA	Platelet-Derived Growth Factor AA
PDL1- B17 H1	Programmed Cell Death 1 Ligand
PET	Positron Emission Tomography
PPM	Permanent Pacemaker
QEHB	Queen Elizabeth Hospital Birmingham
qPCR	Quantitative Polymerase Chain Reaction
RANTES	Regulated On Activation Normal T Cell Expressed and Secreted
RER	Respiratory Exchange Ratio
ROS	Reactive Oxygen Species
RPMI	Roswell Park Memorial Institute
RV	Right Ventricle

RVEDVi	Indexed Right Ventricular End-Diastolic Volume
RVEF	Right Ventricular Ejection Fraction
RVESVi	Indexed Right Ventricular End-Systolic Volume
RVH	Right Ventricular Hypertrophy
RVSVi	Indexed Right Ventricular Stroke Volume
SCD	Sudden Cardiac Death
SD	Standard Deviation
Sep	Septal
sgRNA	Single Guide Ribonucleic Acid
SNO	Single Nucleotide Polymorphism
SOX2	Sex Determining Region Y Box 2
SpO_2	Oxygen Saturation
SSEA4	Stage-Specific Embryonic Antigen 4
ssODN	Single-Stranded Oligodeoxynucleotide
T-Chol	Total Cholesterol
TAPSE	Tricuspid Annual Plane Systolic Excursion
TDI	Tissue Doppler Imaging
TGF-	Transforming Growth Factor
TGF-a	Transforming Growth Factor Alpha

TIA	Transient Ischaemic Attack
TNF-a	Tumour Necrosis Factor Alpha
TNF-a.	Tumour Necrosis Factor Alpha
TNF-ß	Tumour Necrosis Factor Beta
TNNT2	Cardiac Muscle Troponin T
TR	Tricuspid Regurgitation
TR V Max	Tricuspid Regurgitation Maximum Velocity
TRAIL	Tumour Necrosis Factor-Related Apoptosis-Inducing Ligand
TTE	Transthoracic Echocardiography
UK	United Kingdom
VA	Ventricular Arrhythmia
VEGF	Vascular Endothelial Growth Factor
VEGF	Vascular Endothelial Growth Factor
VF	Ventricular Fibrillation
$\dot{V}O_{2peak}$	Maximum Oxygen Uptake
VT	Ventricular Tachycardia
WCC	White Cell Count
WT	Wild Type

1 Chapter 1 – Introduction

Fabry Disease (FD) is an X-linked inherited lysosomal storage disorder (LSD) which manifests due to pathogenic variants in the galactosidase-α (*GLA*) gene, which encodes the enzyme α-galactosidase A (α-Gal A) (1). Variants in *GLA* result in α-Gal A deficiency and subsequent multiorgan lysosomal accumulation of unmetabolised sphingolipid, namely globotriaosylceramide (Gb3) and globotriaosylsphingosine (lyso-Gb3) (2). Accumulation triggers widespread intracellular and extracellular dysfunction. This results in the development of cardiac, renal and cerebrovascular manifestations with significant associated mortality and morbidity (3).

The *GLA* gene is located on the long arm of the X-chromosome (Xq22.1) which encodes the enzyme α-Gal A (1). α-Gal A hydrolyses the terminal α-galactosyl moieties from glycosphingolipids namely Gb3 and lyso-Gb3. Variants in *GLA* result in α-Gal A deficiency due to alterations in synthesis and stability of the enzyme (4). There are over 1,000 identified variants within the *GLA* gene which include nonsense variants, missense variants and premature stop codons (5, 6). Those resulting in complete loss of function of α-Gal A are termed “classical variants “and are characterised by an early-onset phenotype of FD (often in childhood) with severe multi-organ dysfunction. Variants that reduce α-Gal A activity are termed “non-classical variants” and are often associated with a later-onset, single-organ phenotype (usually cardiac).

1.1 History of Fabry Disease

LSDs are grouped conditions with the common defect relating to lysosomal enzyme activity or production, which triggers lysosomal accumulation of glycolipid that would have otherwise been degraded. Various types of glycolipids may accumulate; hence LSD are often classified by the accumulation material, i.e. mucopolysaccharidoses, glycoproteinoses and sphingolipidoses (including FD). FD was described in 1898 by physicians William Anderson and Johannes Fabry (7). They documented pigmented, maculopapular, dermatological manifestations, termed “angiokeratoma”, a hallmark feature of classical FD (**Figure 1.1**). Following this discovery, neurological manifestations were documented in 1909, with cardiovascular, ocular features and patterns of inheritance documented in 1925 (8). By 1950, autopsy assessment of the peripheral vascular system of a patient with FD showed accumulation of peptide-like structures, which were subsequently characterised as phosphoglycolipid (9).

Figure 1.1: Angiokeratoma on the lateral aspect of the thigh, one of the first documented manifestations of FD. Taken from Luna et al (10)

1.2 Fabry Cardiomyopathy

FD cardiomyopathy is the largest contributor to FD morbidity and mortality (11). Cardiac Gb3 accumulation begins in childhood and has been detected in all cardiac cell types including cardiomyocytes, cardiac fibroblasts, conduction cells, smooth muscle and endothelial cells (12, 13). Traditionally, the most widely recognised feature of cardiomyopathy related to FD is left ventricular hypertrophy (LVH). Prevalence of FD in unexplained LVH is reported at around 1.6% (14). Mechanisms by which cardiac Gb3 accumulation triggers myocardial hypertrophy are not well understood. FD cardiomyopathy was previously thought to be a simple storage disease triggering LVH and associated diastolic dysfunction, with systolic dysfunction developing in the advanced stages, and causing symptoms including breathlessness and heart failure. However, there is increasing evidence now to suggest that FD is a primary arrhythmic disease causing sudden cardiac death (SCD).

1.3 Epidemiology

FD is pan-ethnic with estimated global prevalence ranging between 1:40,000 and 1:117,000 live births (15). However, newborn studies undertaken, examining enzyme activity on dried blood spots with subsequent gene-testing in those with α-Gal A deficiency, report a much higher prevalence (1:4,600) particularly in late-onset variants (16). This suggests that FD is underdiagnosed. Reasons for this are multifactorial and may include the non-specific nature of symptoms with heterogeneous presentations as well as a lack of awareness of FD amongst clinicians. Given the X-linked nature of FD, family screening and detailed pedigree mapping can facilitate a timely diagnosis of at-risk relatives (17). This, combined with a greater

awareness of FD amongst the medical community and improved access to more advanced diagnostic tests (enzyme assays, genetic sequencing, multiparametric cardiovascular imaging and biomarker assessment), is likely to yield a much higher detection rate of FD. Sequencing for *GLA* has also been added to most panels for sarcomeric hypertrophic cardiomyopathy (HCM) with prevalence of FD in HCM reported up to 4% (18). It was previously presumed that females were obligate carriers of FD. However, due to the phenomenon of X-linked chromosomal inactivation, it is now understood that females also develop phenotypic FD with a similar severity to males, albeit later in life (19). Skewed X-chromosome inactivation is the phenomenon whereby 75% of the individual cells silence the X chromosome from one parent as the inactive X chromosome (20). The choice of X chromosome to silence is random and takes place in the gastrulation stage (21). In FD, random and skewed X-chromosome inactivation may take place and skewed X-linked inactivation is the likely underpinning mechanisms for phenotype variability in female FD patients (22).

1.4 Incidence and Prevalence of Arrhythmia

1.4.1 Tachyarrhythmia and Sudden Cardiac Death

The prevalence of arrhythmia in FD is high. Patients with FD may experience tachyarrhythmia with varying symptomatology and an underlying supraventricular or ventricular source. Of the supraventricular arrhythmias, atrial fibrillation (AF) is the most prevalent, with regular supraventricular re-entrant tachycardias less frequently documented despite shortening of the PR interval being one of the earliest cardiac manifestations in FD cardiomyopathy (23-25). The prevalence of ventricular

arrhythmia (VA), specifically ventricular tachycardia (VT) and ventricular fibrillation (VF) requiring implantable cardioverter defibrillator (ICD) implantation ranges between 13-18% (26-29). These arrhythmias may be non-sustained or sustained with varying symptom profile. **Figure 1.2** illustrates a typical run of implantable loop recorder (ILR)-detected non-sustained VT (NSVT) in an adult with FD and associated cardiomyopathy. SCD in the context of FD cardiomyopathy is likely secondary to an underlying life-threatening VA event and incidence of SCD in FD is documented between 0.5-3% (follow-up range 1.2-8 years) (26, 30-34). These figures are far higher than the rate of SCD in other forms of HCM and the general population (35, 36). Details of studies describing incidence and prevalence of VA and SCD are summarised in **Table 1.1** (37).

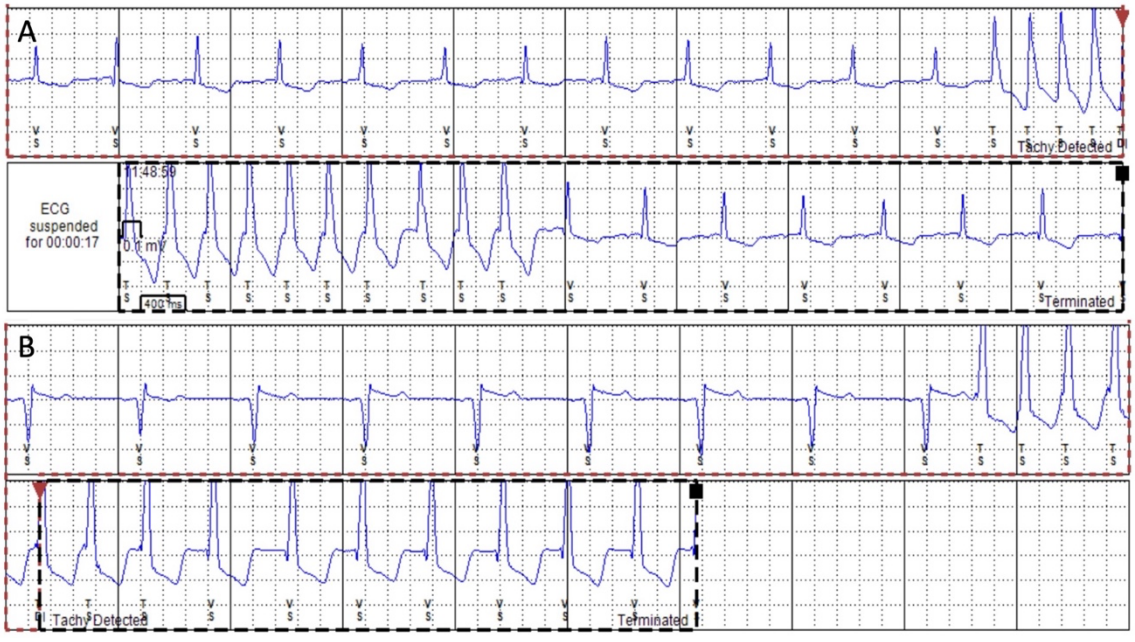

Figure 1.2: ILR recording demonstrating a run of NSVT in an adult with FD. Taken from Roy et al (37).

There are demographic, imaging and electrocardiographic biomarkers reported to increase risk of VA in FD (**Figure 1.3**). These include advancing age, progressive late gadolinium enhancement (LGE) indicative of myocardial fibrosis on cardiac magnetic resonance imaging (CMR), QRS prolongation on 12-lead electrocardiography (ECG) and a general increase in FD-severity, measured using the Mainz Severity Score Index (MSSI) (27, 30). A higher prevalence of VA is also reported in males compared to females, which is expected given the X-linked nature with hemizygous males. Though X-linked inactivation means that females remain at significant risk (26, 38). Interestingly the burden of tachyarrhythmia does not vary according to the genetic variant type in FD (39).

1.4.2 Bradyarrhythmia

Compared with tachyarrhythmia, bradycardia is more prevalent, with weighted estimates for bradycardia-related event rates up to 10% (median follow up time 4.5 years) (40). The type of bradyarrhythmia reported varies and includes bradycardia originating from the sinus node (sinus bradycardia, sinus pauses and chronotropic incompetence) and originating from the atrioventricular (AV) node (namely high degree AV block) (41). The prevalence of bradycardia in one study (N=29, 82% male and mean age 43 ± 11 years) was reported as high as 72% (14% had evidence of PR-interval abnormalities), suggesting early chronotropic incompetence and autonomic dysfunction (42). Bradycardia has been documented early in childhood with one study reporting a prevalence of 23% for bradycardia detected on 12 lead ECG (N=26, 46% male, mean age 10 ± 4 years) (43). Resting bradycardia may have significant implications in adulthood as the prevalence of clinically significant bradyarrhythmia detected related to sinus node disease is documented up to 12% (44) and requiring

cardiac device implantation is 2.5-11% (follow up 1.2-8 years (26, 28, 30, 31, 34, 45-48). A typical sinus pause detected on ILR in an adult with FD is illustrated in **Figure 1.4**. Details of studies describing incidence and prevalence of bradyarrhythmia are summarised in **Table 1.2** (37). As with VA, there are demographic, imaging and

Authors	Number of patients	Study type	Median follow up	Type of monitoring	Incidence	Prevalence
Shah et al (2005) (26)	78 baseline 66 follow up	Single centre longitudinal prospective	1.9 years	Holter	Sudden cardiac death: 1.5% ICD implantation: 1.5%	NSVT: 13%
Acharya et al (2012) (28)	19	Single centre retrospective observational	4.7 years	ECG		ICD implantation: 37% Indications: NSVT and syncope
Kramer et al (2014) (27)	73	Single centre retrospective observational	7.1 years	Holter		Malignant VA: 18% (39% of whom experienced sudden cardiac death)
Patel et al (2015) (30)	207	Single centre longitudinal prospective	7.1 years	ECG	Sudden cardiac death 3%	
Frustaci et al (2015) (29)	13	Single centre retrospective observational	N/A	ECG / Holter		VA: 15.3%
Deva et al (2016) (49)	39	Single centre retrospective observational	N/A	ECG / Holter		VA: 13%
Weidemann et al (2016) (31)	16	Multi-centre longitudinal prospective	1.2 years	ILR	ICD implantation: 25% Indication: Malignant VA	

Vijapurapu et al (2019 (34)	880	Multi-centre retrospective observational	4.3 years	ECG / Cardiac device	ICD implantation: 4.8% Indications: Symptomatic VA, NSVT, multiple risk factors and no arrhythmia, symptomatic long QT syndrome, pacemaker indication with NSVT NSVT: 17% in those with ICD Malignant VA requiring ATP / defibrillation: 28% of those with device	
Orsborne et al (2022)(32)	200	Single centre longitudinal prospective	4.5 years	Holter	Sudden cardiac death: 0.5% NSVT: 12%	
Meucci et al (2023) (33)	314	Multicentre retrospective observational	8 years	ECG	Cardiovascular mortality: 3.3% VA: 3.3%	

Table 1.1: Study characteristics of incidence and prevalence of VA, ICD implantation and SCD in Fabry Disease

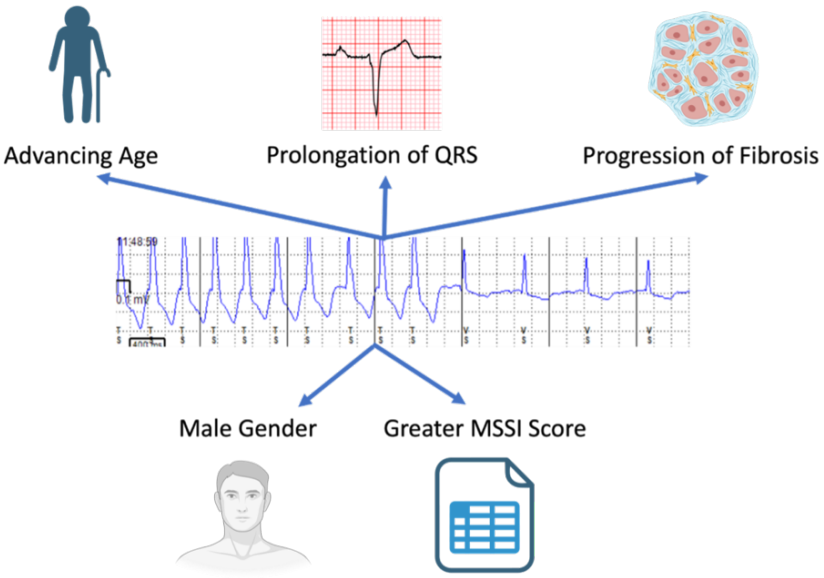

Figure 1.3: Risk factors for ventricular arrhythmias in FD. Abbreviations: QRS: QRS-duration on electrocardiography, MSSI: Mainz Severity Score Index. Taken from Roy et al (37).

electrocardiographic markers reported to increase risk of bradyarrhythmia in FD (**Figure 1.5**). These include advancing age, left atrial (LA) dilatation and dysfunction, resting sinus bradycardia, prolongation of PR-interval and QRS duration, beta-blocker pharmacotherapy and impairment in left ventricular (LV) global longitudinal strain (GLS) on transthoracic echocardiography (TTE) (44, 45, 47). Interestingly, the burden of bradyarrhythmia does not vary according to the genetic variant type in FD (39).

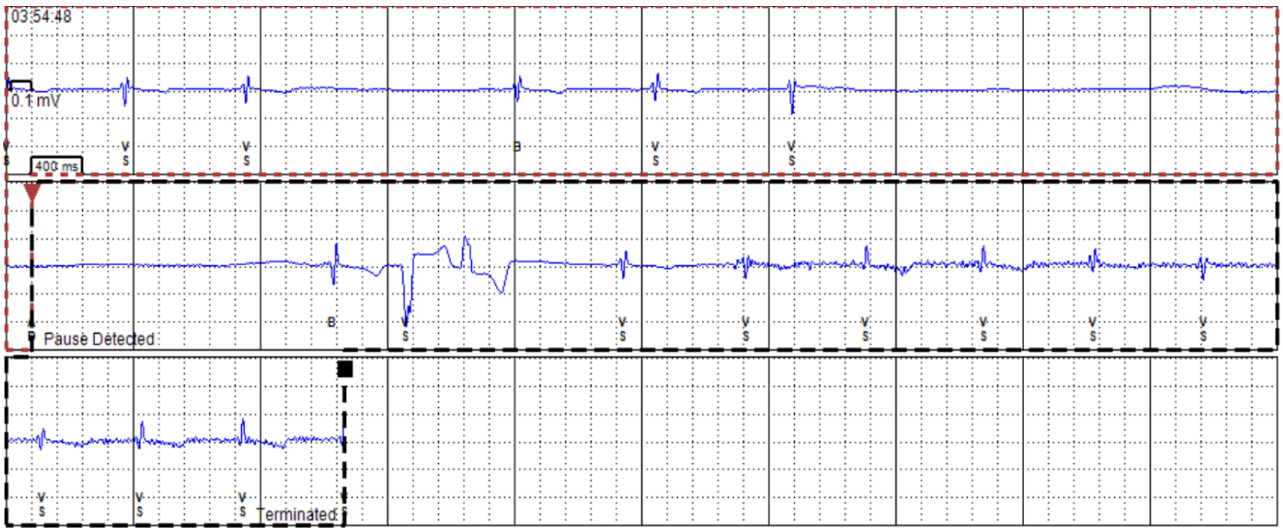

Figure 1.4: ILR recording in a patient with FD demonstrating an asymptomatic 6.5 second nocturnal pause. Taken from Roy et al (37).

1.4.3 Atrial Fibrillation

AF arises from the pulmonary veins (supraventricular) and is characterised by irregular, disorganised atrial conduction due to electrophysiological disruption. The burden of AF is significant, given the high prevalence of stroke in FD (50). Various mechanisms contribute to the AF substrate in FD (structural, functional and electrical) contributing to AF onset and persistence. Reported prevalence ranges between 3-21% (28, 44, 45). and incidence 3-31% (follow up 1.2-8 years) (26, 28, 30, 31, 34, 45-48). The incidence is likely to be higher with various mechanisms specific to FD that contribute to the structural, functional and electrical substrate for AF development. LVH raises LV end-diastolic pressure LVEDP which transmits to the LA, resulting in dilation and impaired LA function (**Figure 1.6**).

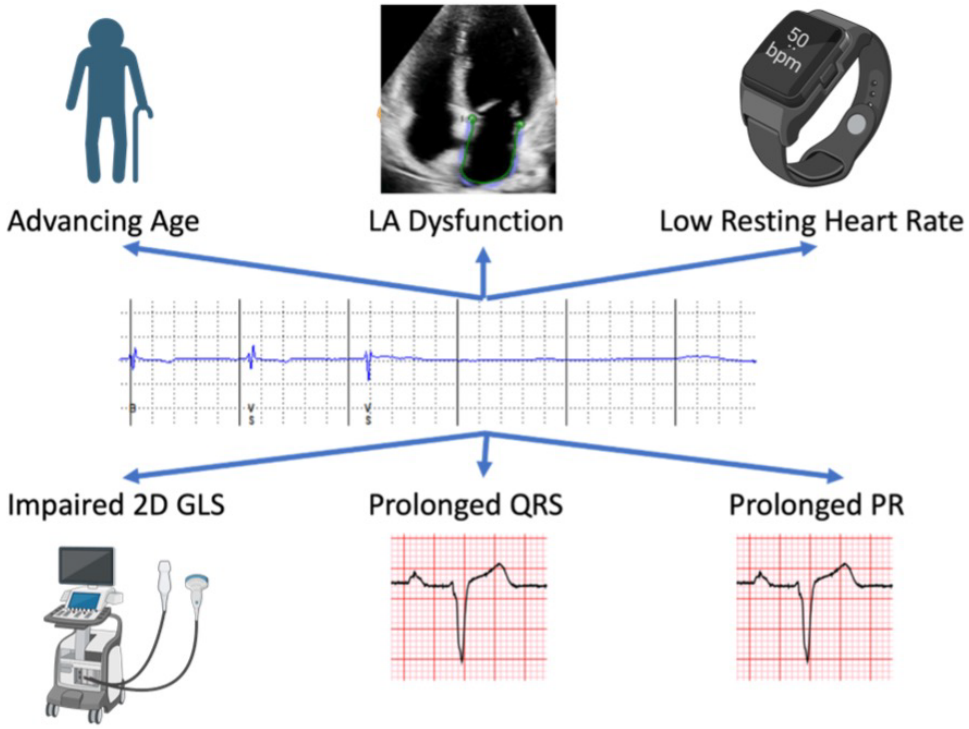

Figure 1.5: Risk factors for bradycardia in FD. Taken from Roy et al (37).

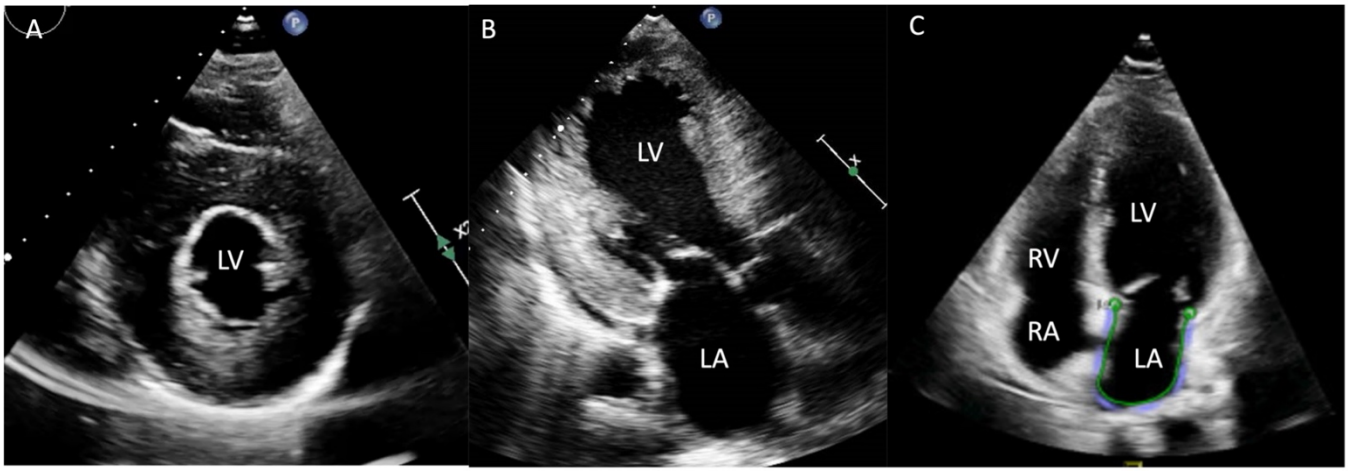

Figure 1.6: Transthoracic echocardiogram images in a patient with Fabry Disease. ***A:*** *Parasternal short axis view of the mid-LV demonstrating concentric LVH.* ***B:*** *Apical 2-chamber view demonstrating LVH and LA dilatation.* ***C*** *Apical 4-chamber view demonstrating LA strain assessment. Taken from Roy et al (51)*

Authors	Number of patients	Study type	Median follow up	Type of monitoring	Incidence	Prevalence
Shah et al (2005) (26)	78 baseline 66 follow up	Single centre longitudinal prospective	1.9 years	Holter	Permanent Pacemaker Implantation: 10.6% Indications: complete heart block, symptomatic bradycardia, left ventricular outflow tract reduction Atrial fibrillation: 3%	Atrial fibrillation: 3.9% on ECG, 13% on Holter
O'Mahoney et al (2011) (45)	204 baseline 188 follow up	Single centre retrospective observational	4.8 years	ECG and Holter	Permanent pacemaker implantation: 6% Indications: Atrioventricular nodal disease, sinus node disease	Permanent pacemaker implantation: 2.5% Indications: Atrioventricular nodal disease, sinus node disease Atrial fibrillation: 3%
Acharya et al (2012) (28)	19	Single centre retrospective observational	4.7 years	ECG	Atrial fibrillation: 10%	Permanent pacemaker implantation: 10.5% Indications: Symptomatic bradycardia, conduction abnormalities

Patel et al (2015) (30)	207	Single centre longitudinal prospective	7.1 years	ECG	Permanent pacemaker implantation: 6% Indications: not specified Atrial fibrillation: 6%	
Talbot et al (2015) (48)	25	Single centre retrospective observational	10 years	ECG	Permanent pacemaker implantation: 4% Indications: Not specified	
Sene et al (2016) (46)	49	Single centre retrospective observational	8 years	ECG	Permanent pacemaker implantation: 12% Indications: Sinus node dysfunction, atrioventricular disease	
Weidemann et al (2016) (31)	16	Multi-centre longitudinal prospective	1.2 years	ILR	Permanent pacemaker implantation: 19% Indications: Asystole, symptomatic bradycardia Atrial fibrillation: 31%	
Pichette et al (2017) (47)	43	Single centre retrospective observational	4.2 years	ECG	Atrial fibrillation: 13%	

Di et al (2018) (44)	53	Cross sectional retrospective	N/A	ECG		Permanent pacemaker implantation: 11% Atrial fibrillation: 21%
Vijapurapu et al (2019) (34)	880	Multi-centre retrospective observational	4.3 years	ECG / Cardiac device	Permanent pacemaker implantation: 4.3% Indications: Tachy-brady syndrome, sinus node dysfunction, bi-fascicular/ tri-fascicular block, second/third degree atrioventricular block AF: 19% (Device-detected AF out of 90 with devices)	
Orsborne et al (2022)(32)	200	Single centre longitudinal prospective	4.5 years	Holter	Bradyarrhythmia requiring PPM: 3% Indications not specified Atrial fibrillation: 4%	
Meucci et al (2023) (33)	314	Multicentre retrospective observational	8 years	ECG	Bradyarrhythmia: 7.2% Atrial fibrillation: 7.6%	

Table 1.2: Study characteristics of incidence and prevalence PPM implantation due to bradycardia and AF in Fabry Disease

1.4.4 Limitations of the Data on Arrhythmia

As there are limited guidelines detailing the frequency and duration of cardiac monitoring in FD, this has contributed to the wide variability in the reporting of tachyarrhythmia, bradyarrhythmia and AF because the detection rate depends, in part, on the duration of monitoring. For example, in studies of patients with advanced FD cardiomyopathy using continuous cardiac monitoring (ILR), arrhythmia detection is higher than those using intermittent short-term monitoring (31, 52). In the UK this is particularly relevant as current guidelines recommend annual 24-hour Holter monitoring which is likely to under-detect clinically significant arrhythmia requiring intervention (53). It is important to reflect on the fact that compared to sarcomeric HCM, it is likely that FD cardiomyopathy is associated with a significant higher arrhythmia burden (54).

1.5 Clinical Presentation

Classical FD typically presents as a multisystemic disease in the first decade of life with non-classical variants often in adulthood and predominantly single organ involvement (55).

1.5.1 Childhood

In the context of classical FD, manifestations in infancy include that of neuropathic pain, termed “acroparaesthesia”, heat/cold intolerance and impairments in sweating (hyper or hypohidrosis). This is due to Gb3 accumulation, ion channel dysfunction and microvascular ischaemia in the peripheral nervous system (56, 57). The development of angiokeratoma (**Figure 1.1**) also may begin in childhood due to endothelial Gb3

accumulation. Microvascular Gb3 accumulation in mesenteric arteries and autonomic ganglia of the small and large intestine also trigger the onset of gastrointestinal symptoms, typically nausea and vomiting, bloating, diarrhoea and constipation which can begin in the first decade of life (58). Renal manifestations may also arise in childhood with Gb3 accumulation in podocytes manifesting as proteinuria. Podocyte loss and tubular atrophy lead to renal impairment in adulthood (59-61). Ocular manifestations may be present from birth with cornea verticillata the most documented. These are bilateral corneal opacities which deposit in the superficial layers of the cornea (**Figure 1.7**) (62).

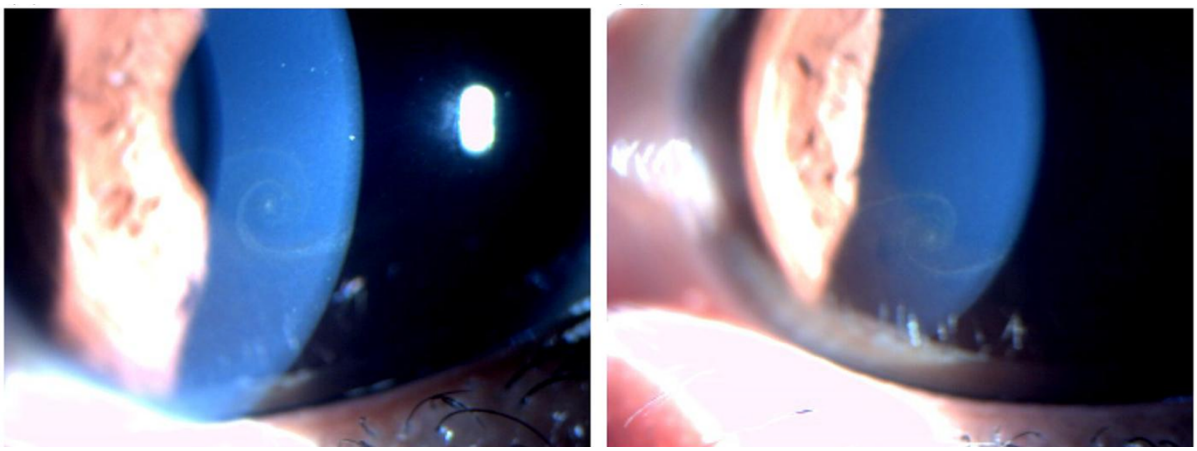

Figure 1.7: Slit lamp examination of the right (left panel) and left (right panel) eye demonstrating whorl-like pattern corneal verticillata in a 21-year-old female with FD. Taken from Idrus et al (63).

1.5.2 Adulthood

In adulthood, FD patients may develop cerebrovascular manifestations including transient ischaemic attacks (TIA) and ischaemic stroke. These manifestations are largely due to small vessel microvascular disease, development of cerebral white

matter lesions and the development of atrial arrythmia, namely AF, causing cardio-embolic stroke (**Figure 1.8**) (50, 64). Peripheral atherosclerosis is prevalent in FD due to accelerated classical atherosclerotic pathways and mechanisms specific to FD (**Figure 1.9**) (65). The burden of living with a multisystemic and chronic disease, combined with the development of cerebrovascular manifestations result in neuropsychological manifestations including depression and anxiety, with onset often in early adulthood (66). Almost all patients with FD develop cardiomyopathy, most frequently in adulthood.

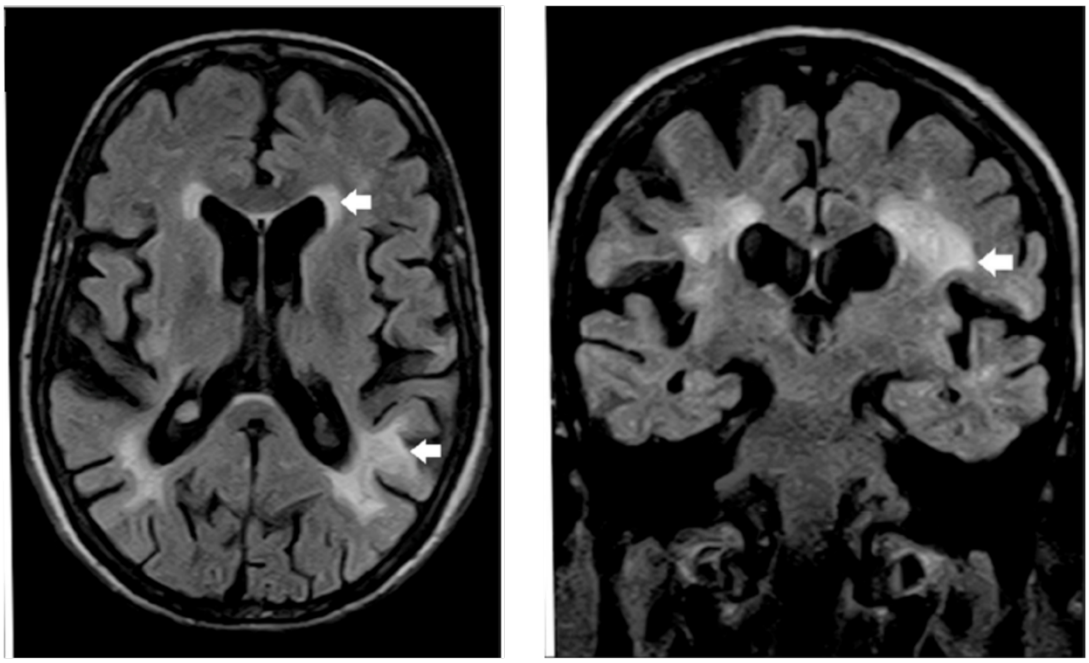

Figure 1.8: Apical (left) and coronal (right) fluid attenuated inversion recovery magnetic resonance imaging demonstrated a high burden of white matter lesions (white arrows) in a 59-year-old male with FD. Adapted from Esposito et al (67).

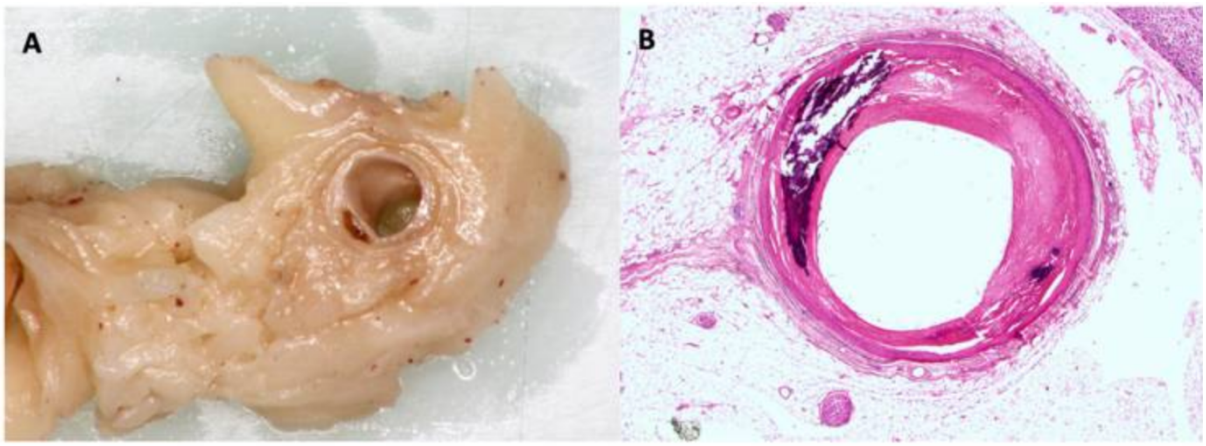

Figure 1.9: Cross sectional slice through the mid-right main coronary artery demonstrating atherosclerotic plaque with localised medial calcification. (B) Corresponding histological section of mid right main coronary artery depicting fibro-intimal atheromatous thickening and multi-centric fractured mineralisation of tunica media Taken from Roy et al (65).

1.5.3 Cardiovascular presentation

FD cardiomyopathy often presents in adulthood, with classical variants usually earlier in onset compared to non-classical, single organ cardiac variants (68). However, the onset of cardiac symptoms and manifestations do not reflect accurately the insidious nature of cardiac Gb3 accumulation. Cardiac symptoms develop due to myocardial Gb3 accumulation, LVH, diastolic dysfunction, atrial or ventricular arrhythmias, development of valvular heart disease, and systolic dysfunction in the more advanced stages (69). Over half of males and a third of females develop LVH, and over 60% present with associated symptoms including chest pain, reduced exercise tolerance, palpitations, shortness of breath, pre-syncope and syncope (70, 71).

1.6 Diagnosis and monitoring

1.6.1 Enzyme and genetic confirmation

In the context of males with a classical variant of FD, reduction or absent α-Gal A levels is all that is required for confirmation of FD. However, in cases where α-Gal A may be only mildly deficient or normal (females and males with a non-classical variant), genotype confirmation is required. In the UK however, all patients ultimately undergo formal genetic testing and formal cascade screening on diagnosis.

1.6.2 Diagnosing and staging Fabry cardiomyopathy

1.6.2.1 Cardiac rhythm monitoring

Given the high prevalence of arrhythmia documented in FD, cardiac monitoring is essential for arrhythmia-detection. As such, 12-lead ECGs are routinely recommended as part of standard clinical work up (53). One of the earliest signs of cardiac involvement in FD is shortening of the PQ interval on 12-lead ECG, specifically shortening of the P-wave duration (**Figure 1.10**) (24).

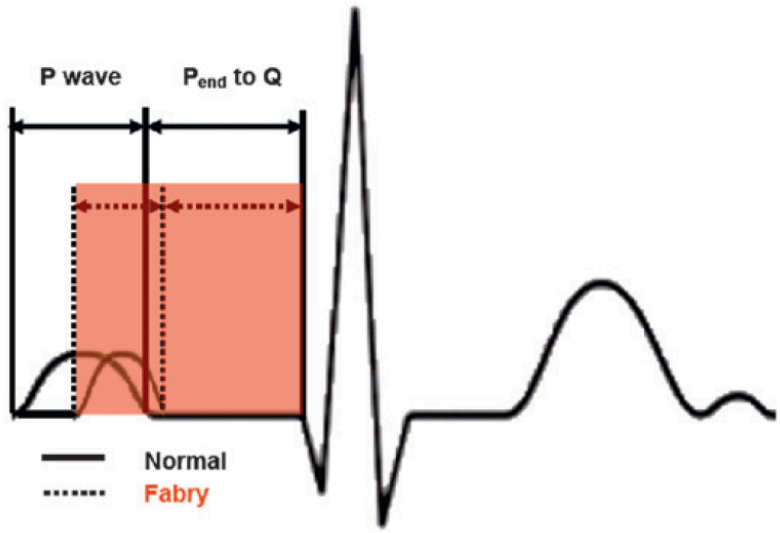

Figure 1.10: Schematic illustration highlighting P-wave duration and subsequent PQ interval shortening in adults with FD compared with non-FD controls. Taken from Namdar et al (24).

With advancing disease, PQ interval and QRS duration may prolong, thus increasing the risk of higher degrees of atrioventricular (AV) block. 12-lead ECG monitoring may detect some of the prevalent arrhythmias documented in FD, including AF, AV block and VA. However, given the sporadic nature of arrhythmia onset in FD, 10 seconds of ECG monitoring are unlikely to be sufficient alone for arrhythmia-detection. For this reason, patients routinely undergo intermittent cardiac monitoring in the form of Holter monitoring, recommended annually in the UK (53). If patients are deemed at high risk for arrythmia, clinicians may consider continuous cardiac monitoring in the form of ILR, with a high burden of arrhythmia detected on ILR in adults with FD and advanced cardiomyopathy (31).

1.6.2.2 Multimodality Imaging

1.6.2.2.1 Transthoracic Echocardiography

TTE is a readily available and accessible imaging modality that is widely used for screening, assessment, and monitoring of cardiac involvement in FD by determining systolic and diastolic function, LV mass, LV wall thickness (LVWT), presence of LV outflow tract obstruction (LVOTO), and the degree of valvular heart disease (**Figure 1.11**) (71). In those with confirmed 'classical' variants FD (in whom leucocyte enzyme activity is less than 5%), Fabry-specific therapy is considered at the point of diagnosis of the phenotype (53). In those with later-onset non-classical variants, TTE imaging triggers the initiation of enzyme replacement therapy (ERT) or oral chaperone therapy (OCT) in patients with a maximum wall thickness (MWT) >12 mm in males and >11 mm in females (72), or an increase in LV mass above the normal range for age and sex.

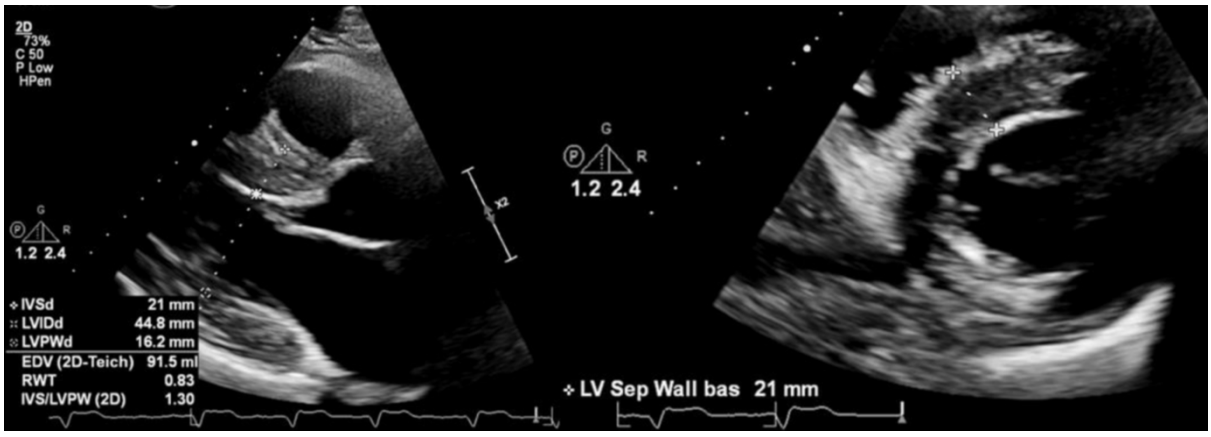

Figure 1.11: Left: Parasternal long axis 2D TTE demonstrating linear measurements of intraventricular septum (IVS), left ventricular internal diameter (LVID) and left ventricular posterior wall (LVPW) demonstrating severe LVH. Right: Parasternal short axis 2D TTE demonstrating severe LVH with MWT of 21mm. Taken from a 56-year-old male with advanced FD cardiomyopathy. Taken from Roy et al (51).

1.6.2.2.1.1 Early disease

With the recognition that Gb3 deposition precedes LVH, TTE remains a useful modality to assess for early FD cardiomyopathy using tissue Doppler imaging (TDI). Reduction in age-adjusted TDI systolic (s') velocity and early myocardial relaxation velocity (e') is a consistent early finding in FD cardiomyopathy (**Figure 1.12**). Case-control studies demonstrate reductions in both in "gene positive, phenotype negative" patients compared to non-FD controls. This reduction was intermediate in size compared to that found in gene positive patients with LVH. Interestingly, in a study of 20 patients with FD (10 with LVH and 10 without), endomyocardial biopsies demonstrated that Gb3 accumulation was proportional to the reduction in TDI velocities in patients with and without LVH, compared to controls (73).

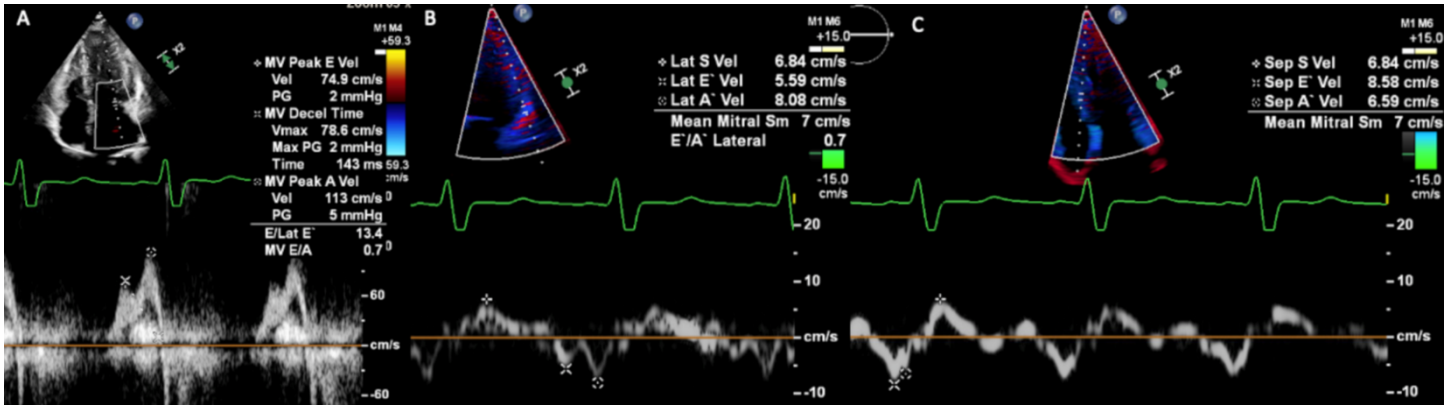

Figure 1.12: Pulsed-wave Doppler and TDI TTE in a patient with FD cardiomyopathy. (A) Pulsed-wave Doppler through the mitral valve leaflet showing E/A 0.7, deceleration time 143 ms and LA dilatation. (B) Lateral TDI showing reduced lateral s' and e' velocities. (C) Septal TDI showing reduced septal s' and e' velocities. Taken from Roy et al (51)

Both Doppler-derived and 2D speckle tracking measurements of strain and stain rate are further useful developments for detection of subclinical dysfunction in FD (**Figure 1.13**). Impaired regional and longitudinal GLS have been used to quantify response to ERT. In a study of 16 patients with FD, impaired GLS improved with ERT initiation. In another study of 32 patients over 2 years, improvements in GLS with early ERT initiation were demonstrated in patients without fibrosis.

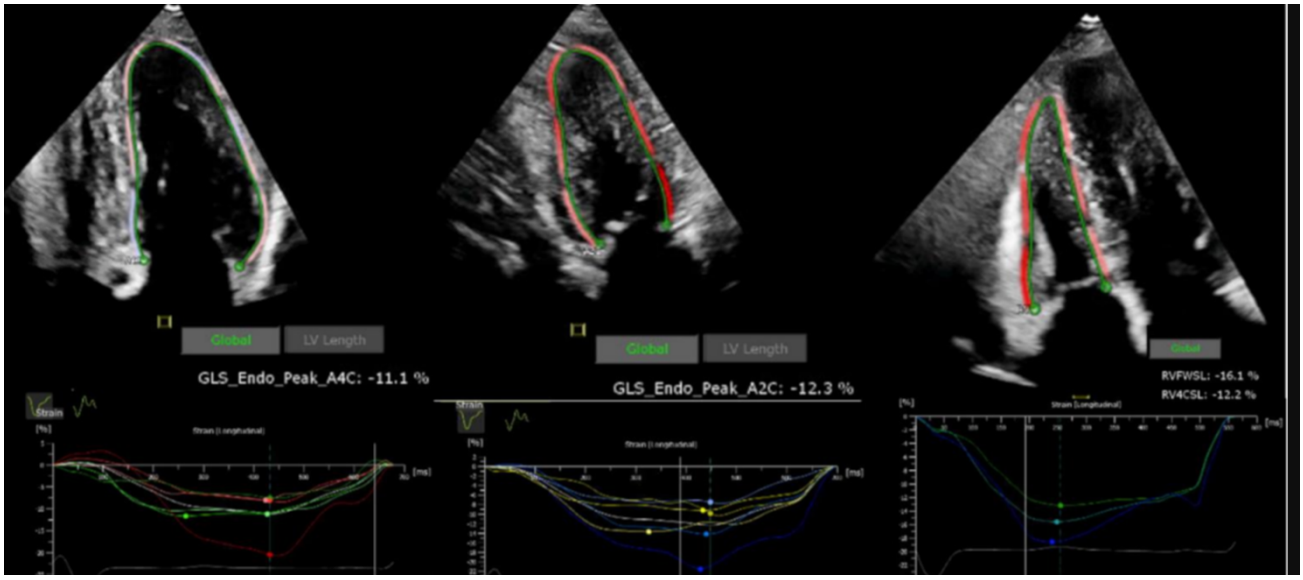

Figure 1.13: Strain TTE in FD cardiomyopathy. Left: GLS assessment of the LV from apical-4-chamber view demonstrating impaired GLS (-11.1%). Middle: GLS assessment of the LV from the apical-2-chamber view demonstrating impaired GLS (-12.3%). Right: GLS assessment of the TV from the apical-4-chamber view demonstrating reduced GLS (free wall strain -16.1%, longitudinal strain -12.2%). Taken from Roy et al (51)

1.6.2.2.1.2 Prognosis

TTE remains useful in combination with other investigations when determining prognosis in FD. In the Fabry Outcome survey, patients with LVH on TTE were more likely to develop cardiovascular and renal events compared to those without. Furthermore, the use of GLS and strain-based myocardial work efficiency have been shown to independently predict poor cardiac outcomes in FD (74).

1.6.2.2.2 Cardiac Magnetic Resonance Imaging

Despite the ease of access and cost of TTE, CMR remains the gold standard non-invasive tool for measurement of wall thickness and LV mass (LVM) (**Figure 1.14**). In FD, the clinical impact of CMR use over TTE has been emphasised in a study of 78 patients, whereby eligibility for FD-therapy changed in 26% of patients with TTE over-estimating wall thickness (75).

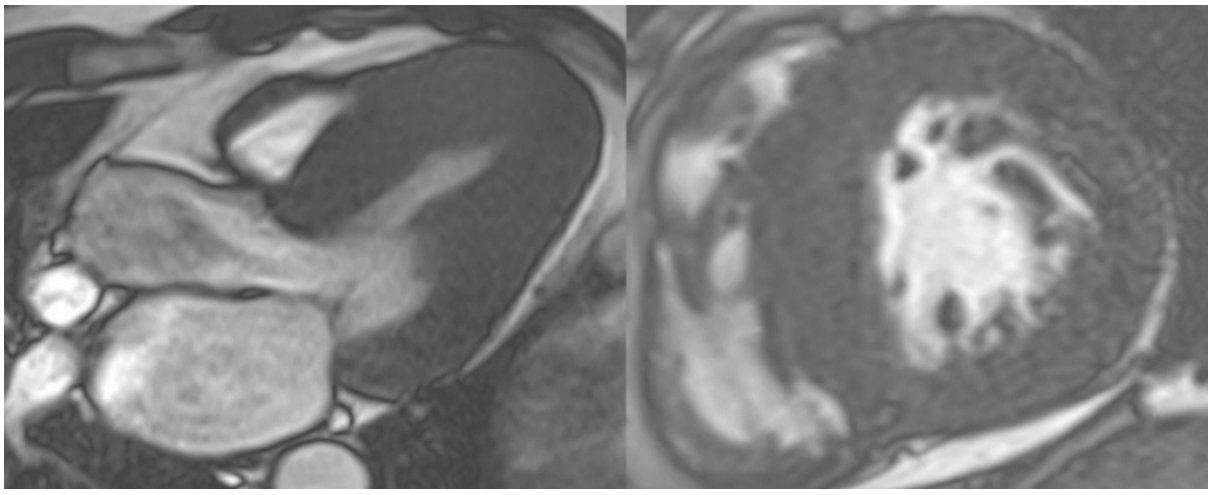

Figure 1.14: CMR in a patient with FD cardiomyopathy. Left: apical-3-chamber view demonstrating concentric LVH with basal inferolateral wall thinning, typical of FD.

Right: Short axis image demonstrating severe concentric LVH. Taken from Roy et al (51)

1.6.2.2.2.1 Early disease

CMR also has the added advantage of being able to accurately assess for early FD cardiomyopathy. The development of T1 mapping as an imaging marker for Gb3 storage has allowed for visualisation and quantification of Gb3, which substantially lowers T1 values below those found in other causes of LVH (**Figure 1.15**) (76).

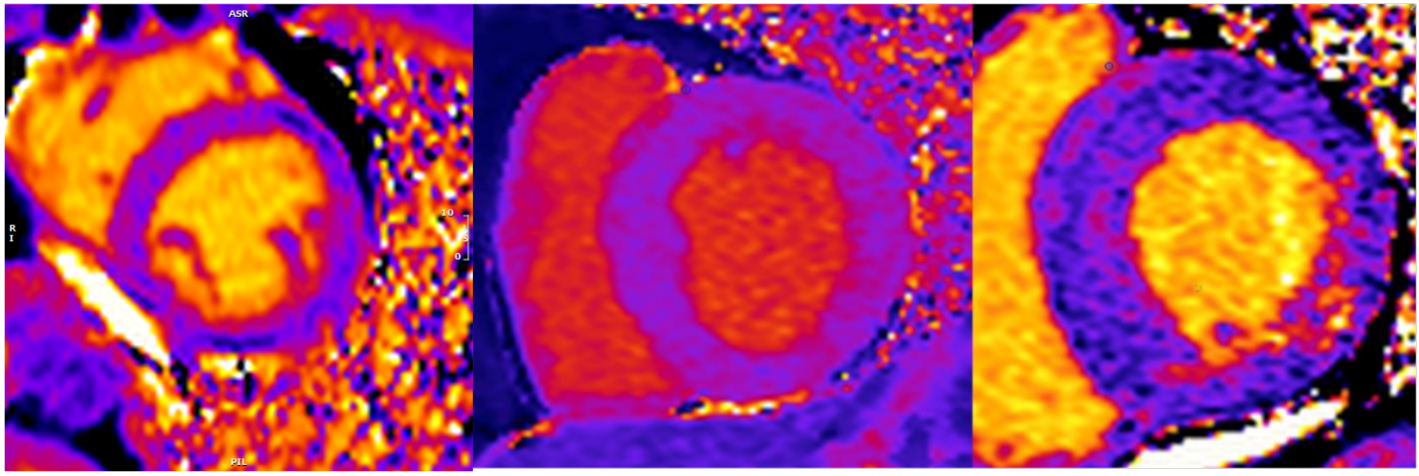

Figure 1.15: CMR T1 mapping sequence. Left: T1 map with normal relaxation times in a patient with FD. Middle: T1 map with a reduction in relaxation times indicating early Gb3 storage in a patient with FD and early FD-cardiomyopathy. Right: T1 map with "pseudonormalisation" of T1 representing fibrosis within the myocardium, evident predominantly in the basal inferolateral wall, typical of advanced FD cardiomyopathy. Taken from Roy et al (51)

T1 lowering may be patchy but is easily measured and does not require extra imaging-based contrast (77). Low T1 has been found in about half of FD patients prior to development of LVH and appears to track reduction in TDI and GLS on TTE (78). In the later stages of FD cardiomyopathy, when fibrosis develops within the myocardium, typically in the basal inferolateral wall, T1 relaxation times subsequently increase or "pseudonormalise" (79). T1 lowering in FD tends to be progressive up until relaxation times "pseudonormalise". Native non-contrast T1 may lengthen with interstitial expansion due to the development of myocardial fibrosis and inflammation, due to increased free fluid associated with this (80). T1 lowering tends to be more pronounced in males and the decline in values continue despite disease-modifying therapy (81). Furthermore, as is expected given the X-linked inheritance of FD, T1 mapping has confirmed that there is sex-dimorphism in FD cardiomyopathy, with men following a pattern of T1 lowering to LVH before development of LGE, whereas in women, T1 lowering associated with LGE before LVH onset.

1.6.2.2.2.2 Advanced disease

CMR allows for the detection of myocardial fibrosis using LGE imaging. In the advanced stages of FD where fibrosis has developed, elevated T2 values have been found in regions of LGE which also correlate with high-sensitivity troponin release (**Figure 1.16**) (82).

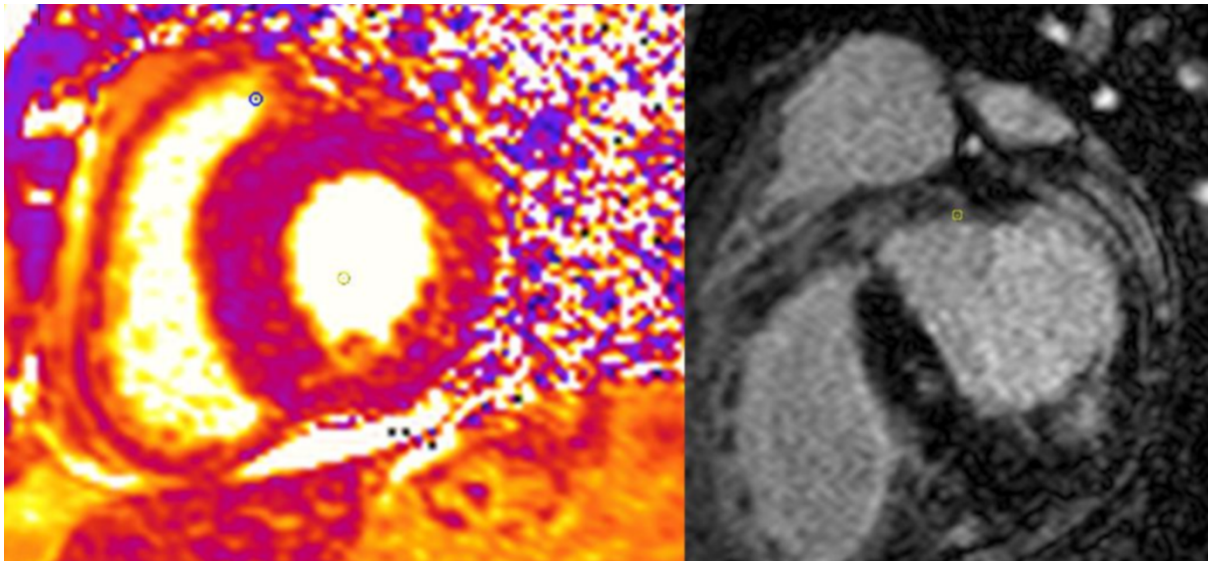

Figure 1.16: Left: Short axis basal CMR T2 map with increased relaxation times representing inflammation and oedema within the myocardium. Right: Corresponding LGE short axis CMR images in the same patient demonstrating inferior and inferolateral enhancement with corresponding T2 elevation. Images from a patient with FD and advanced cardiomyopathy. Taken from Roy et al (51)

T2 mapping provides both visual and quantitative assessment of intracellular and extracellular water and can detect focal as well as diffuse myocardial oedema. T2 signal is high in areas of LGE, consistent with oedema and suggesting the role of inflammation in the final pathway of FD cardiomyopathy. There are limited data on the use of CMR to define long-term risk of cardiovascular disease. In a study of 73 adults with FD, LGE detection independently predicted arrhythmic events in FD, consistent with its ability to predict arrhythmia in ischaemic cardiomyopathy and other cardiac diseases (27).

1.6.2.2.3 Positron emission tomography

Multiparametric CMR builds on data from other modalities of advanced cardiovascular imaging, namely 18-fludeoxyglucose (18-FDG) positron emission tomography (PET) that myocardial inflammation may precede the development of LGE, suggesting the role of inflammation as a more sustained process (83). This was supported by data in females with FD and no LVH, in whom focal myocardial 18F-FDG uptake was found on PET which correlated with impairments in GLS (84). This study linked early inflammation in FD cardiomyopathy with functional decline, before LVH, consistent with elevation of inflammatory biomarkers (85).

1.7 Pathophysiology of arrhythmia

A summary of the pathophysiology of arrhythmia in FD is illustrated in (**Figure 1.17)**.

1.7.1 Direct effects of Gb3 and arrhythmia

The presence of ECG abnormalities in children with FD combined with histological evidence on endomyocardial biopsies of Gb3 deposition in conduction tissue suggest that the arrhythmia substrate in FD begins early in the disease course (29). Shortening of the P-wave duration is one of the earliest manifestations and has been documented in patients without significant LVH, indicating accelerated depolarisation. In the same study, prolonged repolarisation time has also been observed, manifesting as QTc prolongation and dispersion (24). It is well known that QTc prolongation predisposes to life-threatening VA (86). AV-node and crista terminalis Gb3 deposition may account for acceleration of atrial conduction and the consequent P-wave duration shortening

(87, 88). The observed early detectable ECG abnormalities may reflect direct Gb3 accumulation, providing rationale to the risk of arrhythmia prior to the onset of LVH, atrial structural changes and systolic dysfunction. The advancement in digital ECG-acquiring technology holds significant promise in the ability to detect early Gb3 accumulation (89).

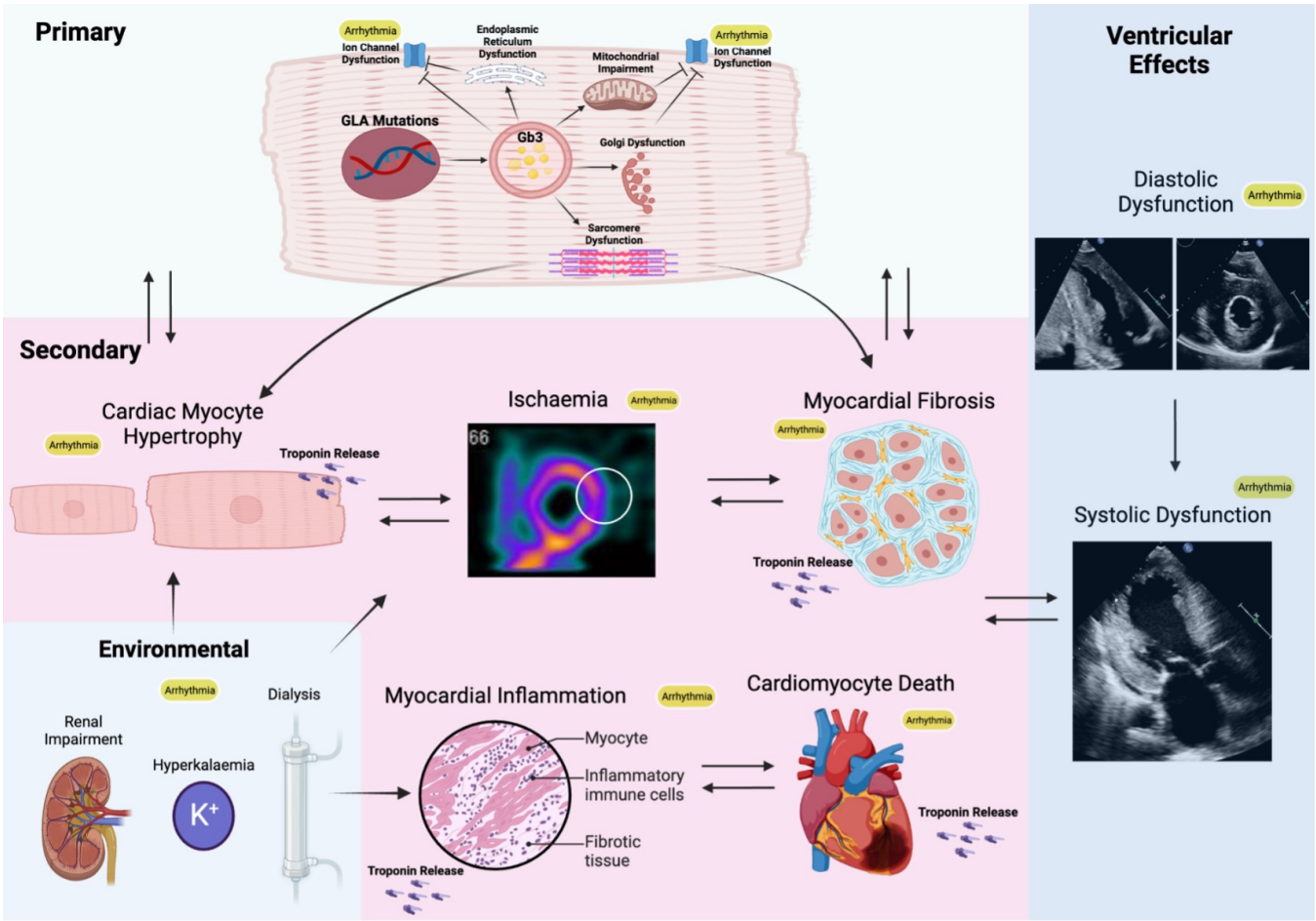

Figure 1.17: Pathophysiology of arrhythmia in Fabry Disease: Primary, secondary, and tertiary mechanisms. Taken from Roy et al (37).

1.7.2 Primary effects

As well as the described direct pro-arrhythmic effect of Gb3 deposition, the effects of Gb3 deposition may trigger other intracellular and extracellular processes in a cascade

effect, contributing to the pro-arrhythmic substrate. Firstly, lysosomes play a key role in cellular autophagy and a key regulator of this is the mechanistic target of rapamycin (mTOR) dependent signalling pathway. mTOR is located on the surfaces of lysosomes and on activation through accumulation of amino acids, triggers autophagy via the regulation of mitochondrial function and autophagy-lysosomal fusion (90, 91). Its role in mitochondrial function is to promote translation of mitochondrial-related proteins. Gb3 accumulation disrupts the activation of mTOR in cardiac fibroblasts which is likely to inhibit autophagy-lysosomal fusion (92). Gb3 accumulation also disrupts the translation of mitochondrial-related proteins, altering mitochondrial metabolism (93). The combination of these effects promote structural and functional changes within cardiac cells, altering their properties and directly provoking arrhythmia (94).

Perinuclear vacuoles of Gb3 have been visualised on electron microscopy of endomyocardial biopsies taken from adults with FD. These single membrane-bound vesicles appeared to displace cardiac myofibrils to the cell periphery, a process termed myofibrillolysis. When calculating the percentage of cardiomyocytes occupied by vacuoles, similar values were ascertained, suggesting that the increase in cardiomyocyte size may in part be due to the presence of the Gb3 filled vacuoles. Stiffening of cardiomyocytes was also demonstrated on these cardiomyocytes. TDI studies conducted on the patients from whom the cells were derived from demonstrated impaired TDI, suggesting the development of diastolic dysfunction, in keeping with the cell findings of stiffening (95). The effect of myofibrillolysis triggered by the development of Gb3-rich vacuoles, as well as mitochondrial dysfunction contribute as trophic stimuli for myocardial hypertrophy which increases arrhythmic risk (96).

In experimental models of FD using patient-derived induced pluripotent stem cell (iPSC) derived ventricular cardiomyocytes (iPSC-CM), pro-arrhythmic cellular properties have also been identified (97). A greater spontaneous action potential (AP) frequency, coupled with a shorter AP duration, and quicker upstroke velocity was observed, suggesting increased excitability (**Figure 1.18)**. In the same study, disruptions in intracellular calcium handling were also observed (greater amplitude and reduced peak width duration), further increasing excitability.

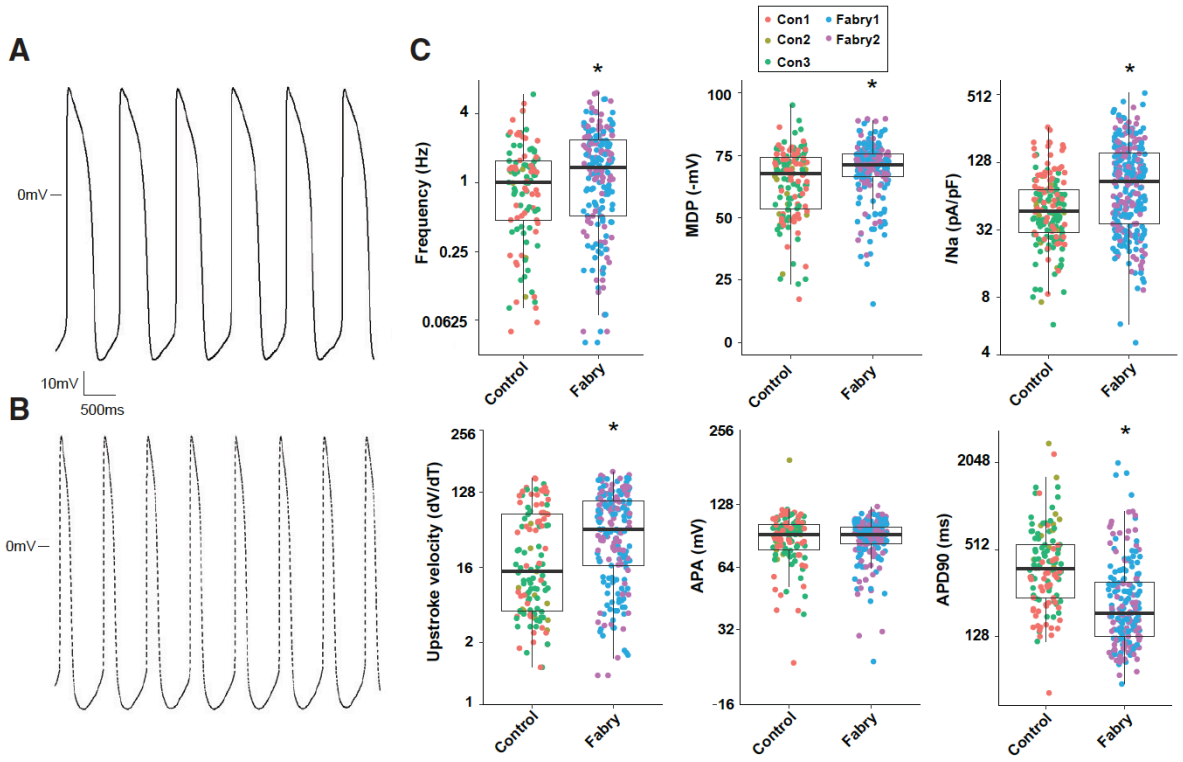

Figure 1.18: (A) Action potential traces in control ventricular cardiomyocytes (B) Action potential traces in FD ventricular cardiomyocytes. (C) Quantification of electrophysiological parameters in spontaneously active cells. Data indicates a greater beating frequency, more positive diastolic membrane potential, greater peak sodium

current density, upstroke velocity, peak amplitude and AP duration at 90% repolarisation. Adapted from Birket et al (97).

Changes in expression of calcium and sodium channels due to the effects of Gb3 accumulation may account for the alterations in the cellular and electrophysiological properties of ventricular iPSC-CMs, as changes in ion channel expression triggered by Gb3 accumulation has been documented in both neuronal and endothelial cells (98, 99). These changes are likely to increase propensity for VA with disease progression (97). The summary of these primary effects highlights the scope for using combined *in-vivo* and *in-vitro* models for evaluation of arrhythmia in FD (100).

1.7.3 Secondary effects

1.7.3.1 Ischaemia, LVH and scar.

Interestingly, myocardial Gb3 accumulation itself only accounts for a small proportion (5%) of the increase in LVM observed in FD. Furthermore, the increase in LVM is not explained by changes in the interstitial space (77). Myocardial Gb3 accumulation is detected by a reduction in T1 mapping times on multiparametric CMR and often precedes the onset of LVH. However, the mechanisms by which accumulation triggers myocyte hypertrophy is poorly understood. Smooth muscle infiltration of Gb3, particularly within the myocardial vasculature may induce structural and functional modifications which causes both macrovascular and microvascular ischaemia. This has been detected using advanced cardiovascular imaging in the form of stress perfusion CMR. Ischaemia has been documented in FD on CMR in the absence of significant coronary stenosis and interestingly the ischaemia was documented prior to

the development of LVH in the ischaemic area of myocardium (79). In the more advanced stages of FD cardiomyopathy, interstitial myocardial fibrosis develops, quantified by the amount of extracellular and extravascular deposition of gadolinium-based contrast agents, LGE on CMR (101, 102). Typically, fibrosis is identified in the mid-wall of the LV in the basal inferolateral segment (**Figure 1.14)**. Interestingly in women, this may develop prior to the onset of LVH, whereas in men this tends to develop in response to a hypertrophic stimulus (69). Ischaemia, LVH and myocardial fibrosis are established high-risk features for arrhythmia in ischaemic and non-ischaemic cardiomyopathy.

1.7.3.2 Inflammation and Arrhythmia.

LSDs, of which FD is the second most prevalent (103), are presumed to have a significant impact on the immune system (104). Within human cells, the lysosome functions as a complex regulatory organelle and degrades substrate received via endocytosis, phagocytosis or autophagy (105). Lysosomal function also involves maintenance of a normal immune system via antigen presentation, phagocytosis, and release of pro-inflammatory mediators (106, 107). In FD, the accumulation of Gb3 may cause damage-associated molecular pattern production in cells, triggering apoptotic pathways and secretion of pro-inflammatory cytokines. This has been confirmed in a study whereby Gb3 was cultured with non-FD monocyte-derived dendritic cells and macrophages. These cells demonstrated a pro-inflammatory cytokine production profile (108). In the same study using peripheral blood mononuclear cells from patients with FD, the same profile was identified of greater pro-inflammatory cytokine expression and production, without the addition of Gb3, indicating Gb3 to be a direct inducer of pro-inflammatory pathways in FD. The study demonstrated a similar pattern

of inflammatory activation in leukocytes and endothelial cells, including reactive oxygen species generation. The wide intra-familial phenotypic variability in organ involvement and severity in FD (109) may be explained by a patient-specific inflammatory and immune response.

In a large study of adults with FD cardiomyopathy who underwent extensive invasive and non-invasive studies including multiparametric CMR and endomyocardial biopsy, 56% had evidence of CD3+ T-lymphocyte infiltrative myocarditis on histological assessment (110). CD3+ T-lymphocyte count correlated with wall thickness on CMR, though interestingly, 38% of those without LVH also demonstrated histological myocarditis on biopsy **(Figure 1.19)**.

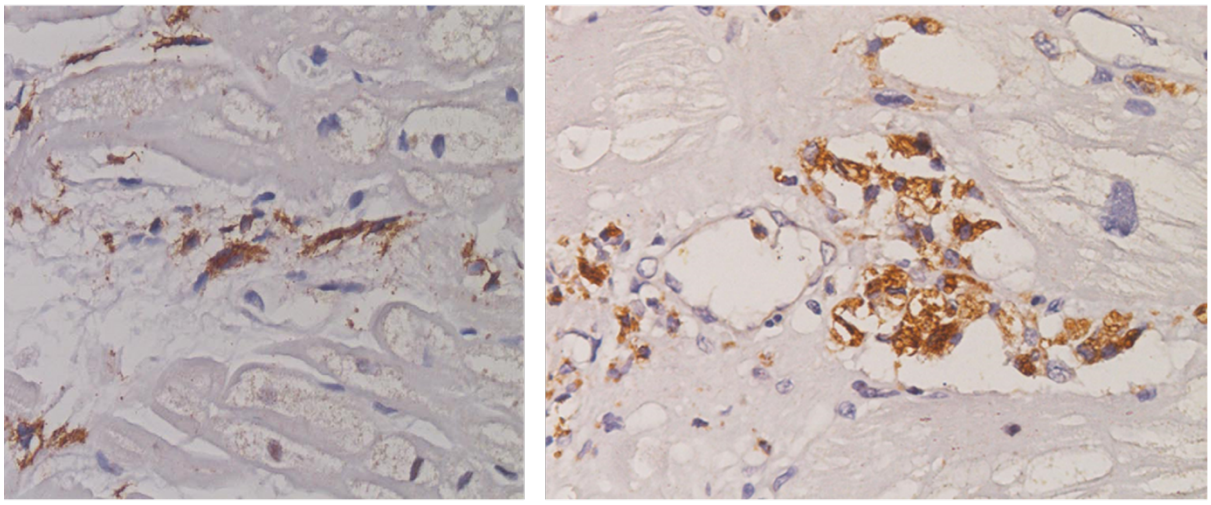

Figure 1.19: Left: Histological assessment of endomyocardial biopsy (200x magnification, immunoperoxidase for T lymphocyte CD3+ antigen) demonstrating intermittently enlarged cardiomyocytes with focal surrounding of CD3+ infiltrates with associated cell necrosis in a 22-year-old female with pre-hypertrophic FD cardiomyopathy. Right: Histological assessment of endomyocardial biopsy (200x magnification, immunoperoxidase for T lymphocyte CD3+ antigen) demonstrating

widespread CD3+ T lymphocyte infiltration of myocardial capillaries in a 63-year-old male with advanced FD cardiomyopathy. Adapted from Frustaci et al (110).

In those who underwent CMR, 31% had evidence of focal T2 elevation indicating tissue oedema likely due to myocardial inflammation. This suggests immune-mediated myocardial inflammation secondary to Gb3 deposition detectable on histological assessment as well as non-invasive multiparametric CMR. The presence of myocarditis was associated with arrhythmia and troponin elevation, suggesting a pro-arrhythmic immune-mediated response to Gb3 deposition.

Multiparametric CMR studies using LGE and T1/T2 mapping have enabled non-invasive detection and quantification of myocardial inflammation, consistent with these biopsy studies. Scar in the inferolateral wall detected on LGE imaging has conventionally been considered either to be replacement or reparative fibrosis. In FD however, elevated T2 scores that reflect oedema have been found not only to co-locate to the inferolateral scar on LGE (**Figure 1.16**) but also correlate closely to increased high sensitivity troponin and pro-inflammatory cytokines such as interleukin 6 (85, 111). T2 elevation in the basal inferolateral wall suggestive of focal myocardial oedema has been associated with the ECG abnormalities that may provoke arrhythmia including abnormal PR-interval, bundle branch block and QTc prolongation (82). That this oedema and troponin release is related to inflammation has been confirmed using 18-FDG PET. In a study of 13 adults with FD, FDG-PET/CMR confirmed that focal LGE with increased T2 values corresponded to focal, increased 18-FDG uptake and associated high-sensitivity troponin elevation. (112). Moreover, in

a study of female adults without LVH who underwent 18-FDG PET/CMR, increased focal 18-FDG myocardial uptake was detected in 54% of patients of whom only 15% had LGE on CMR. Uptake of 18-FDG uptake correlated with impaired LV GLS but in this 'early group', high-sensitivity troponin levels were normal. A further study in females with FD demonstrated an association between focal 18-FDG uptake and pseudonormalisation of T1 values, indicating this to be another marker of inflammation at the intermediate stage before the development of fibrosis associated with cell death (**Figure 1.20**) (83). These findings suggest inflammation may be an insidious process that occurs before LVH and LGE and is not inevitably associated with myocyte cell death, so may be a modifiable target for therapy (84).

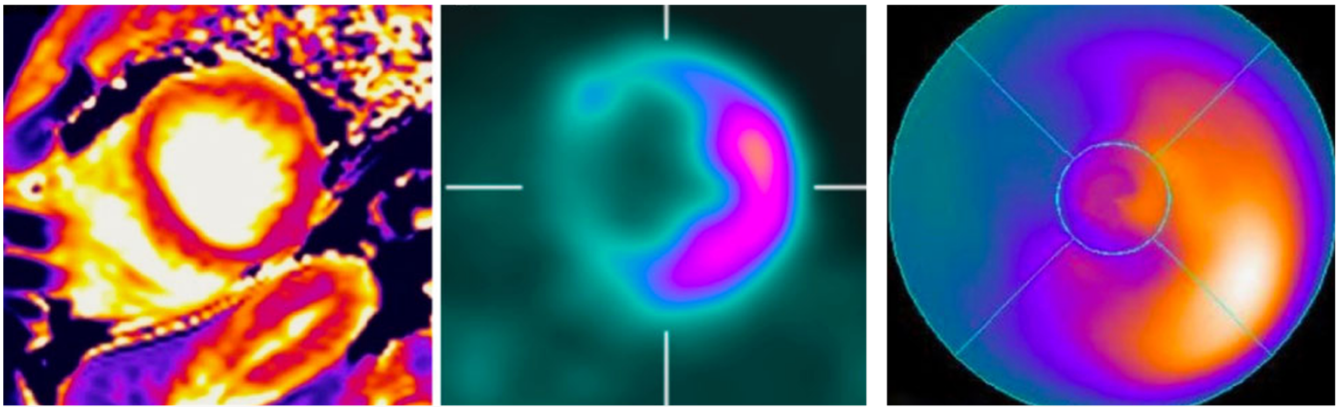

Figure 1.20: Left: Short axis T1 map on CMR demonstrating lateral wall pseudonormalisation of relaxation times. Middle: 18-FDG PET short axis views demonstrating focal uptake in regions of T1 elevation (lateral segments of the mid-wall of the LV). Right: 18-FDG polar map demonstrating focal 18-FDG uptake. Images from a patient with FD and pseudonormalisation of T1 on CMR without LGE. Images adapted from Imbriaco et al (83).

1.7.3.3 Multiorgan involvement.

Renal Gb3 accumulation is prevalent and prominent in podocytes (59). This manifests as progressive renal dysfunction including microalbuminuria, proteinuria, and progressive decline in estimated glomerular filtration rate (113). In advanced stages, FD patients may require long term dialysis and assessment for renal transplantation (114). Renal dysfunction predisposes to various arrhythmias including AF, bradyarrhythmia, VA and SCD in the general population and its high prevalence in FD is likely to be a contributory mechanism to the arrhythmia substrate (**Figure 1.17**). The effects of electrolyte imbalance associated with renal dysfunction (namely potassium) as well as rapid fluctuation in electrolyte levels and haemodynamic shifts during dialysis further contributes to this increase in risk in the later stages of disease (115).

1.8 Risk Stratification

1.8.1 Lack of Fabry-specific risk-prediction models

Given the susceptibility to arrhythmia in patients with FD across all spectrums of the disease, risk stratification is imperative to establish those who would benefit from therapy. In the case of sarcomeric HCM, there is a validated and universally accepted prediction model to evaluate individualised risk of SCD (116). Those in a high-risk category are offered a primary-prevention ICD to reduce the risk of VA and SCD. No such tool is available in FD on which to base decisions on therapy. To-date, there have been single centre studies and systematic reviews confirming risk factors for arrhythmia discussed so far, including advancing age, male gender, prior arrhythmia, LVH and scar on LGE (11, 40). One important note is that, once patients have a risk

of one type of arrhythmia, the change in substrate that takes place in FD seems to place the individual at increased risk of any arrythmia. For example, in a study evaluating device implantation in FD, one patient with a PPM died from sustained VF detected on device interrogation (34). This suggests that, given the progressive nature of FD cardiomyopathy, considerable caution should be taken on implanting cardiac devices without a defibrillator function even in the absence of VA. In the absence of an individual risk calculator, there have been two recent large studies that used deep cardiac phenotyping to develop risk models in FD, with arrhythmia a major component of cardiovascular events recorded (32, 33).

1.8.2 Multimodality cardiovascular imaging for risk prediction

A longitudinal prospective cohort study of 200 adults (average age 46 years; 61% female) with FD undergoing CMR developed a prognostic model to generate risk estimates for major adverse cardiac events (MACE) over a median follow-up of 4.5 years (32). MACE outcomes, based on time to first event, included hospitalisation for heart failure, myocardial infarction, coronary revascularisation, VT, new onset AF, bradycardia requiring implantation of a PPM, aborted SCD, implantation of an ICD or cardiovascular death. A new parameter was developed from the CMRI data, T1-dispersion, calculated as a standard deviation of T1 times extracted from all voxels consisting of the basal and mid-ventricular short axis T1 maps in the mid-wall of the myocardium. In this study, the composite outcome occurred in 43 participants (21% total), at an annualised rate of 4.8% per year, and the most frequent component of the composite outcome was NSVT. The rate of VA was 0.44% per year, AF 1.67% per year and bradycardia requiring pacemaker implantation 1.11% per year. Pooled univariable cox regression for time to the composite outcome was performed, and

variables with the highest statistic were age, MWT, indexed LV mass (LVMi), LV GLS, QRS duration and MSSI. An internally validated model was developed which accurately predicted the 5-year risk of MACE using age, LVMi and native non-contrast T1-dispersion in all adults with FD.

In a recently published retrospective observational multi-centre study of 314 adults with FD, patients were staged on the degree of FD cardiomyopathy using TTE-based parameters (**Figure 1.21**) (33).

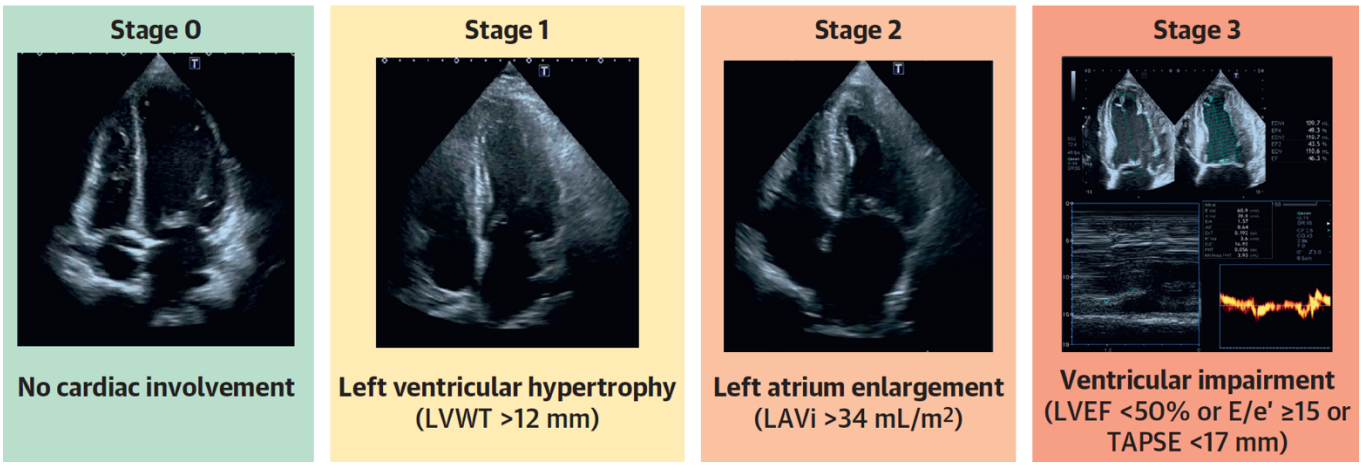

Figure 1.21: Proposed staging system using routinely collected TTE parameters of cardiac involvement in FD. Taken from Meucci et al (33).

Study endpoints were used to test the prognostic value of the staging classification. Endpoints included all-cause mortality, cardiac mortality, major arrhythmia (bradyarrhythmia requiring PPM or tachyarrhythmia cardioversion/ ICD therapy), new onset AF, heart failure hospitalisation and ischaemic stroke. Patients were classified as stage 0 (no cardiac involvement), stage 1 (LVH with MWT >12mm), stage 2 (LA

enlargement with indexed LA indexed volume >34ml/m^2) or stage 3 (ventricular impairment). Older patients had more advanced disease and the majority with AF or cardiac device implantation were in stages 2 and 3. In total, 18% of patients met a study endpoint. Occurrence of cardiac events increased with stage and arrhythmic events accounted for 45% of these over the 8 years follow up, with event rates for bradyarrhythmia 7.2%, VA 3.3% and new-onset AF 7.6% with a higher prevalence in more advanced stages. Interestingly the stage with the highest frequency of PR duration abnormalities was stage 0, consistent with the known early electrical changes. Importantly, the role of LA dilatation and dysfunction as a parameter for prognosticating is highlighted here. LA dilatation may reflect elevated LVEDP from LVH but dilatation may pre-date LVH secondary to direct atrial myopathy (117). A greater proportion of female patients were in stage 2 (atrial enlargement) compared with males. Conversely, a greater proportion of male patients were in stage 1 (LVH), highlighting the varied pathophysiology and arrhythmic risk based on gender observed in FD (33). This study highlights how a greater burden of cardiac involvement correlates with cardiac events but with the large number of endpoints forming the composite (with arrhythmia included), this precludes accurate arrhythmic prediction.

Various risk-prediction data provide conclusive evidence of arrhythmic risk in other cardiomyopathies including sarcomeric HCM, Lamin A/C, dilated cardiomyopathy, cardiac sarcoid and cardiac amyloid (116, 118-121). These enable clinicians to assess an individual's risk of arrhythmia using conventional investigations including 12-lead ECG, Holter, TTE and CMR. The existing risk-prediction studies in FD provide more detailed information confirming that arrythmia is common but that other major adverse cardiovascular events traditionally included in cardiovascular outcome trials, including

hospitalisation for heart failure, myocardial infarction, and cardiovascular death, are less frequent and follow-up time needs to be longer. For arrhythmia, which clearly represent a significant burden to the patient in terms of quality of life, further work is needed to define individual risk in the way that the HCM-SCD risk calculator performs (116). A prospective multi-centre international randomised control trial is currently underway in adults with FD comparing the rate of significant arrhythmia using ILRs, which will be introduced in this thesis (122). This trial will also collect data from a wide variety of investigations with the aim to develop a robust risk stratification tool in FD.

1.9 Therapy for arrhythmia in Fabry Disease

1.9.1 Conventional risk modification

Prevalence of conventional risk factors for atherosclerosis in FD is higher than in the general population suggesting accelerated atherosclerosis (65). Interestingly, novel mechanisms of atherosclerotic disease have also been shown specifically in FD suggesting accelerated atherosclerosis via non-conventional mechanisms (65). Although there is no randomised evidence of benefit specifically in FD, these data highlight the importance of aggressive risk factor modification including lipid-lowering therapy, antihypertensive therapy, and strict glycaemic control. Lifestyle modification including smoking cessation and regular physical exercise is also recommended (123). Elevated systolic blood pressure has an incremental impact on progression of cardiomyopathy and subsequent arrhythmic risk due to relation with myocardial hypertrophy and geometry (124). The benefits of angiotensin converting enzyme

(ACE) inhibitors and angiotensin receptor blocker (ARB) therapy in reducing cardiovascular risk have been demonstrated in sarcomeric HCM (125)

1.9.2 Arrhythmia

Patients with FD tolerate arrhythmia supraventricular tachycardia and AF poorly due to impaired diastolic filling. Therefore, rhythm control is the favoured strategy with either pharmacological intervention, direct current cardioversion (DCCV) or ablation, although long-term success is compromised by progressive atrial dilatation, impaired atrial function and change in atrial structure. Although there is now general support for early ablation in all patients presenting with AF, there remain concerns regarding long-term efficacy in FD (126). In those with refractory AF not amenable to DCCV, careful rate control is important, with the additional concern regarding co-existing risk of bradyarrhythmia and conduction disease. Beta blockers or calcium channel antagonists are generally favoured as first line for rate-limiting strategies, although amiodarone is generally avoided long term in FD. Amiodarone may alter lysosomal pH, subsequent enzyme activity and trigger lysosomal dysfunction. It has also been shown to induce phospholipidosis via inhibition of lysosomal phospholipase activity, triggering phospholipid accumulation and development of lamellar bodies (127). Amiodarone may induce acute heart failure with features of amiodarone toxicity confirmed on endomyocardial biopsy in a case study in FD (128). Frequent Holter or wearable ECG monitoring is recommended.

Although anticoagulation is recommended for life in all FD patients with AF due to the high incidence of stroke, none of the current scoring systems for assessing risk of

stroke, such as the $CHA_2DS_2VAS_c$ scoring system (129), have been validated for use in FD. There is little systematic data on choice of anticoagulation (direct oral anticoagulant versus warfarin). However, direct oral anticoagulation may be advantageous due to lower risks of intracranial bleeding, as FD may be associated with cerebral micro-bleeding (130).

As described, cardiac device implantation with PPM or ICD is high due to increased risk of bradyarrhythmia and VA, particularly in advanced disease (11, 40). However, with no specific guide for device implantation in FD currently available and as FD is specifically excluded from conventional risk calculators for HCM for primary prevention, device implantation is generally for secondary prevention after a significant arrhythmic event or aborted SCD (123).

1.9.3 Enzyme Replacement Therapy

The mainstay of systemic FD-related therapy is ERT (recombinant α-GAL A) to replace deficient α-GAL A. Current recommendations are that in adult males with classical variants and enzyme activity <5%, FD therapy is to be considered at diagnosis. In adult females and males with non-classical variants, FD therapy is recommended in those with an LV MWT >13mm in males and >12mm in females, LVMi on TTE/CMR above normal for age and sex or the presence of LGE on CMR (53). As with all FD therapy, better outcomes are reported with early initiation. There is limited efficacy if commenced >50 years of age in terms of stabilising LVMi compared to if started <30 years of age (113). Those without LGE have seen improvements in LVMi, strain and exercise capacity with ERT, which is not observed

in those with LGE (**Figure 1.22**) (131). Efficacy in FD cardiomyopathy is mixed. Once many of the cardinal features of FD cardiomyopathy have developed, which increase arrhythmic risk, the benefits of ERT initiation are significantly limited. There is currently no definitive evidence that ERT reduces the burden of arrhythmia in FD (70, 113)

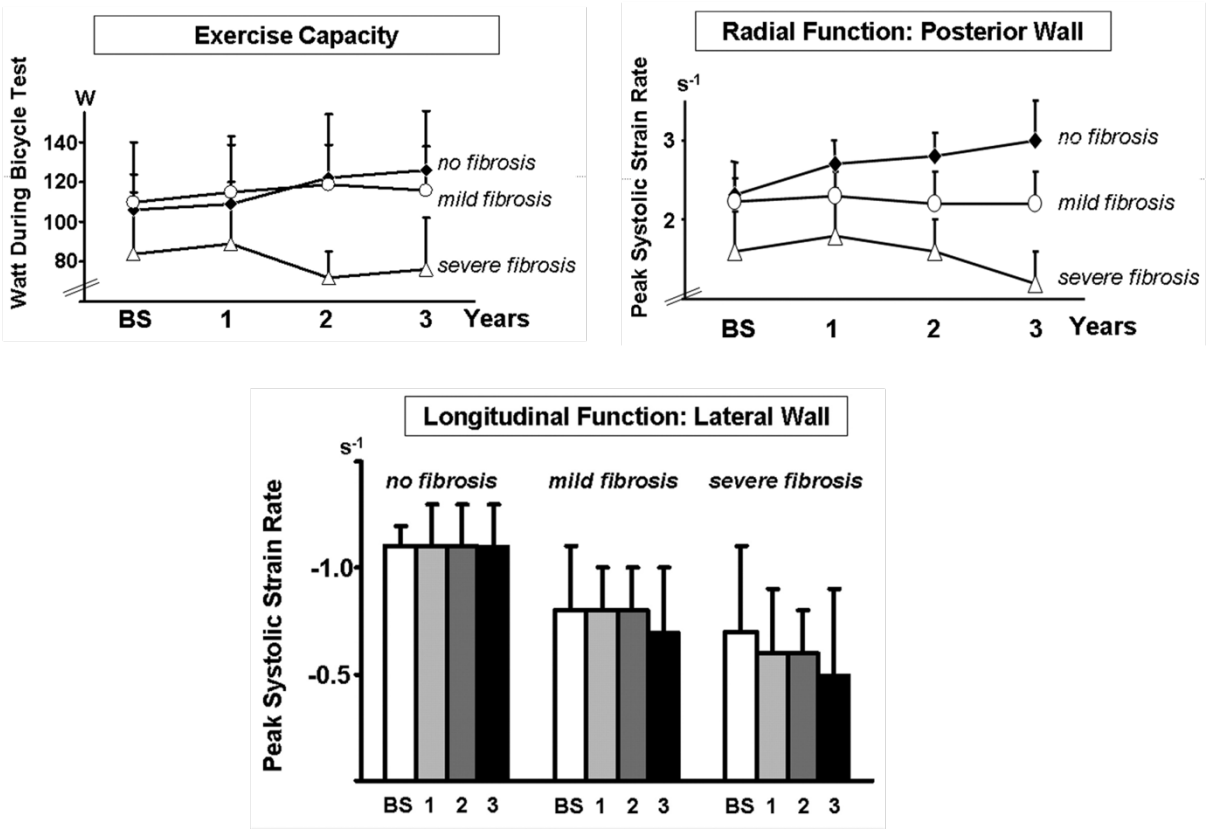

Figure 1.22: Left. Changes in exercise capacity after 3 years ERT demonstrating a mild improvement only in the group without ERT. Right: Changes in LV radial peak systolic strain rate with 3 years ERT demonstrating a linear increase in function in the group without LGE. Bottom: Changes in longitudinal function after 3 years ERT, demonstrating no changes in the group without LGE and worsening function in the groups with LGE with more pronounced worsening in those with a higher burden of LGE. Adapted from Weidemann et al (131).

1.9.4 Oral Chaperone Therapy

OCT is a pharmacological chaperone licensed for use in adults with FD with residual enzyme and an amenable *GLA* mutation. The mechanism is to stabilise the mutant enzyme, increase bioavailability and traffic this to the lysosome whereby metabolism of Gb3 can take place (132). As with ERT, efficacy of OCT in established cardiomyopathy is limited and there is no evidence demonstrating the benefit of OCT on reducing arrhythmia burden. OCT may slow organ damage with studies showing a stabilisation and, in some cases, mild reduction in LVMi (133, 134). However, in those with evidence of LGE, cardiomyopathy still progresses even with OCT (**Figure 1.23**) (135).

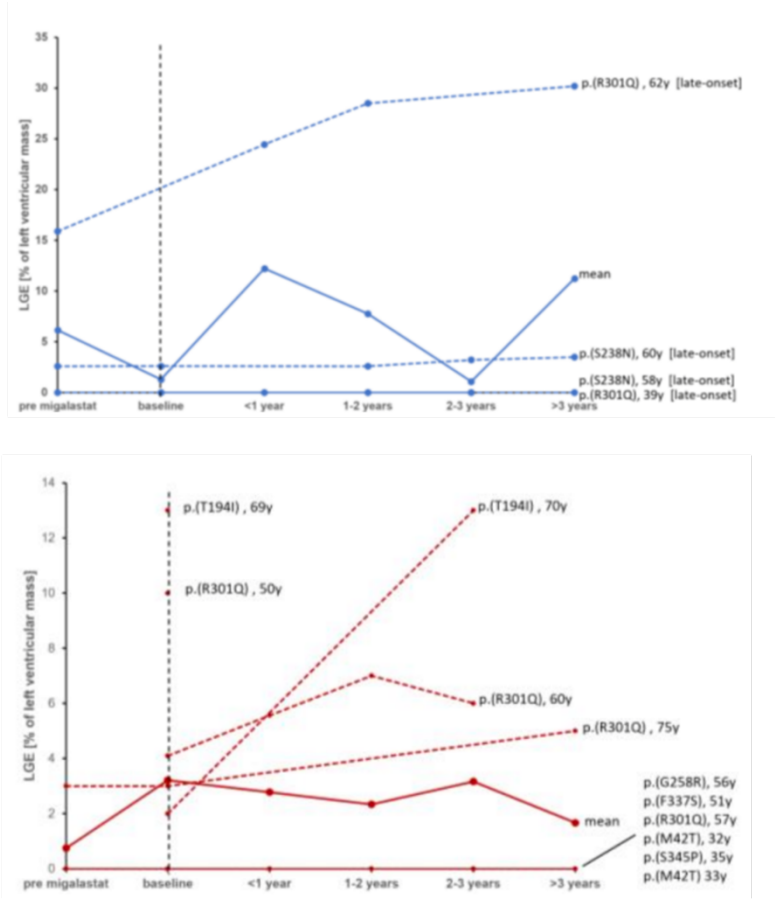

Figure 1.23: Top: Individual courses of LGE burden on CMR in males pre-treatment with OCT and after 3 years follow up. Bottom: Individual courses of LGE burden on

CMR in females pre-treatment with OCT and after 3 years follow up. Taken from Gatterer et al (135).

1.9.5 Transplantation

In patients with significant symptomatic heart failure, intractable arrhythmia despite all optimal therapy (medical and cardiac devices including synchronisation), transplantation may be a viable option. The major barrier to cardiac transplantation in FD is the progressive and multi-organ nature of the disease. Patients often have co-existing end-organ renal disease and so combined cardiac and renal transplantation may need to be considered. The involvement of multiple organs and increased disease burden has a significant impact on exercise capacity and mental health which affects transplant candidacy (136). Finally, in patients with non-classical disease including cardiac variants, these are often late onset in age which presents another barrier to transplantation (62).

1.10 Research Aims

The burden of arrhythmia in FD is high, yet the underpinning mechanisms require further exploration. This is particularly in the context of the underlying pathogenesis of atrial arrhythmia-development and how early detectable changes on cardiac imaging, biochemistry and symptom profile may influence future arrhythmic risk.

1.10.1 Thesis Hypotheses

The main hypotheses from this thesis are:

1. Atrial arrhythmia in FD reflects a primary atrial myopathy due to Gb3 accumulation and intrinsic intracellular changes that increase arrhythmic risk.
2. Cardiac Gb3 accumulation begins early, progresses insidiously and is detectable using current routinely performed investigations during FD follow up.
3. Symptoms begin early in FD and whilst many are non-specific (given the multisystemic nature of the disease), particular symptoms including exercise intolerance may have an underlying cardiac aetiology. The current risk factors for do not explain the increased risk of arrhythmia

1.10.2 Thesis Aims

Therefore, the main aims of this thesis are to:

1. Characterise mechanisms of atrial cardiomyopathy in FD to understand how identified early changes may provoke atrial arrhythmia.

2. Identify markers of early cardiomyopathy, detectable on routine clinical investigations and through assessment of symptom status in patients with FD, to understand which may predispose to arrhythmia.
3. Explore how additional potential risk factors in FD cardiomyopathy contribute to the pro-arrhythmic substrate in FD.

2 Chapter 2 – Molecular and electrophysiological changes in an atrial "disease in a dish" model of Fabry cardiomyopathy

Data from this chapter has been submitted for publication at Circulation: Arrhythmia and Electrophysiology for which I am the first author. The manuscript is under peer review.

2.1 Personal Contribution

iPSCs were gene edited with the *GLA* p. *N215S* variant, checked for pluripotency and karyotyped at the University of Oxford, before being sent to the University of Birmingham. I performed cell culture, atrial differentiation, passaging and harvesting. I performed immunofixation, confocal microscopy, RNA extraction, cDNA conversion, Western Blotting and qPCR under supervision of members of the Gehmlich lab. I performed the steps for MUSCLEMOTION and optical mapping analysis. I prepared the cells for patch clamping, which was performed by lab member Max Cumberland who has experience in this technique. I completed all the statistical analyses for each lab component. For the ECG component, I acquired, anonymised and performed signal average ECG analysis as well as completing the statistical analyses.

2.2 Background

2.2.1 Arrhythmia in Fabry Disease

In FD, cardiac symptoms, typically in the form of palpitations, are common and occur in up to 50% of women and 75% of men. Weighted mean estimates suggest that the incidence of atrial AF is especially high (12.2%, 95% confidence interval 7.2-19.7%) (40). There are numerous identified atrial structural alterations that contribute to the substrate for AF. These include passive LA dilatation, impaired atrial strain due to elevated LVEDP, as well as direct atrial Gb3 accumulation resulting in an atrial myopathy (47). In the general population, developing AF is associated with greater morbidity, including stroke, heart failure, and cardiovascular mortality (137). The risks from AF are considered even greater in those with FD, with stroke prevalence reported up to 6.9% in males and 4.3% in females with FD (50). Furthermore, heart failure symptoms are reported in up to 25% FD patients in large cohort studies (71).

2.2.2 ECG changes in Fabry Disease

There are early detectable electrical changes identified in FD on 12-lead ECG that suggest early cardiac involvement (**Figure 1.10**) (24). In a small cohort of FD patients without LVH, P-wave duration and QRS-width shortening was identified which suggest accelerated depolarisation. The same study also demonstrated an increase in repolarisation time, as evidenced by QTc prolongation. Preliminary evidence from small cohorts of FD patients without LVH, suggest shortening of the P-wave duration and QRS-width, indicative of accelerated depolarisation. Increased repolarisation times have also been demonstrated in the same cohort manifesting as QTc

prolongation (24, 25, 138). However, detailed ECG analysis measured at various cardiac disease stages in larger cohorts of FD patients is currently lacking, as is the link to AF risk.

2.2.3 Atrial involvement in Fabry Disease

It is likely that atrial cardiomyopathy in FD is an early manifestation of the disease. Atrial cardiomyopathy is likely to be a significant contributor to AF substrate and subsequent burden of stroke in FD. However, the cellular mechanisms underpinning pro-arrhythmic atrial electrical remodelling in FD are currently unknown. Given the adverse effects of atrial dilatation and dysfunction on morbidity and mortality in hypertrophic cardiomyopathies, it is important to understand the direct impact of FD on a cellular level. Enhancing our mechanistic understanding of atrial involvement in FD could identify early therapeutic targets, allow for robust risk-stratification for stroke, and may trigger initiation of disease-specific therapy to reduce the burden of cardiac complications.

2.3 Hypotheses

There are intrinsic changes in the properties of gene-edited *GLA* p. *N215S* atrial iPSC-CMs which are pro-arrhythmic in nature which may in part, explain some of the early P-wave changes demonstrated in adults with early-stage FD cardiomyopathy.

2.4 Aims and Objectives

Our aim was to conduct signal-averaged P-wave analysis from 12-lead ECGs collected from a large patient cohort with FD and correlate identified findings with a "disease in dish" model of FD, aiming to explore intrinsic electrophysiological cellular alterations, using genome-engineered atrial iPSC-CMs with the *GLA* p. *N215S* variant.

2.5 Materials and Methods

2.5.1 12-lead ECG

12-lead ECGs were acquired from 115 adults with FD attending the centre for rare disease at the Queen Elizabeth Hospital Birmingham between July 2014 and November 2023. As part of their clinical workup, annual ECGs, and TTEs were routinely acquired. The most recent ECGs were obtained from patients in sinus rhythm, to include those who subsequently developed AF. ECGs were obtained from patients with FD and varying degrees of cardiomyopathy. Patients were scored using a proposed staging criterion in, using a combination of biochemical, imaging, and electrocardiographic parameters (69). Two Fabry experts (myself and Richard Steeds) reviewed the staging of patients, with discrepancies resolved by consensus. ECGs were also acquired from 40 age/sex-matched healthy non-FD controls for comparison.

2.5.1.1 ECG analysis

Firstly, the presence of premature atrial complexes (PACs) was quantified. Secondly, 10 seconds of the lead II signal from the ECG portable document formats (PDFs) were digitised using an in-house developed algorithm and analysed as previously described (139). Briefly, all R-waves were identified, and averaged to produce the signal averaged ECG complex. Once this was produced, P-wave start and end, QRS start and end, and T-wave start and end were identified. The isoelectric line was defined from start to end of the P-wave, and duration and amplitude parameters automatically measured (**Figure 2.1**).

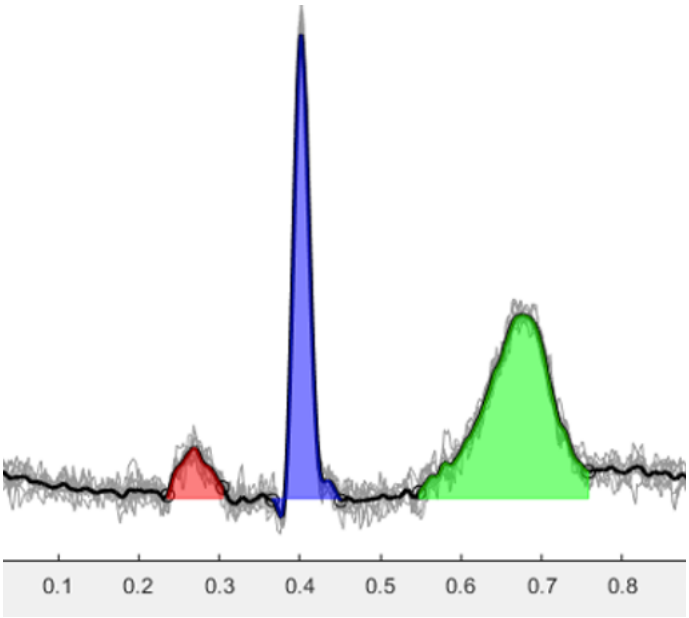

Figure 2.1: Digitalised ECG signal, developed by identifying the R-waves on ECG complexes in lead 2 and averaging to produce the signal-averaged complex.

2.5.2 Transthoracic Echocardiography

TTE data were collected by an accredited sonographer using ie33 and EPIC ultrasound systems (Phillips) according to the British Society for Echocardiography minimum dataset (140). Biplane LA volume was collected from the TTE report where available.

2.5.3 Haematology and Biochemistry

Data for haematology and biochemistry tests performed at the nearest date to ECG acquirement were additionally extracted and included high-sensitivity (HS) troponin I, and N-terminal pro- brain natriuretic peptide (NTpro-BNP). NTpro-BNP was measured

by sandwich immunoassay with magnetic particle separation and chemiluminescent detection on an E170 analyser (Roche Diagnostics, Burgess Hill, United Kingdom)

2.5.4 Generation of genome-edited iPSCs

The aim was to introduce the *N215S* mutation into the endogenous *GLA* gene, which involves the introduction of an A>G single nucleotide polymorphisms (SNP). *GLA* p. *N215S* gives rise to a predominantly cardiac phenotype in FD, without overt effects in other organs (39). It is the most prevalent mutation in the United Kingdom (141).

iPSCs were engineered via CRISPR-Cas9 mediated genome-engineering to introduce the *GLA* p. *N215S* variant into male KOLF2 iPSC line. As WT controls, cells which are not carrying the *GLA* variant, but have undergone the same genome editing procedure, were used. The KOLF2-C1 (WTSIi018-B-1) human iPSC line was used for all experiments in this study and was provided by the Wellcome Sanger Institute. A single guide RNA (sgRNA) was designed to target the following spacer sequence: 5'-CTGTCGGATTTCTGTATAAT-3', which lies close to the nucleotides encoding the Asparagine 215 residue. A single-stranded oligodeoxynucleotide (ssODN) harboring the desired A>G SNP for homology directed repair (HDR) was designed:

5'CTCAAGAGAAGGCTACAAGTGCCTCCTTTAAACTGTTTTCATCTCACAAGGAT
GTTAGTAGAAAGTAAACAGAAGAGTCATATCTGTTTTCACAGCCCAGTTACACA
GAAATTCGACAGTACTGCAATCACTGGCGAAATTTTGCTGACATTGATGATTCCT
GGAAAAGTATAAAGAGTATCTTGGACTGGACATCTTTT-3'.

Two additional silent mutations (T>C; Y216Y and C>T; I219I) were additionally introduced to inhibit re-cleavage and mutagenesis of the locus after successful HDR. The A>G SNP mutation, following successful HDR creates a *de novo BmrI* restriction site in proximity of the target region, facilitating the detection of the targeted allele. PCR primers (GLA-F1: 5'- GTGCCCAGCCTCTACAAACTT-3' and GLA-R1: 5'-AAAGCCTCCTCCCAGGAACT-3') were designed to amplify 610 bases surrounding the SNP site and *BmrI* restriction digestion of the PCR products was used for genotyping. *GLA* is located on the X-chromosome and the KOLF2-C1 iPSC line is male, so all resulting clones were hemizygous for the introduced mutations.

The site-specific CRISPR/Cas9 nuclease as a ribonucleoprotein complex (Cas9 protein (890nM) / sgRNA (1.48µM)) and the ssODN (3.7µM) were electroporated into early passage KOLF2-C1 cells using the Neon Electroporation System (Thermo Fisher Scientific; 1200V, 30ms, 2 pulses). Monoclonal expansion and *BmrI*-based genotyping of individual clones led to the identification of putative mutant hemizygous

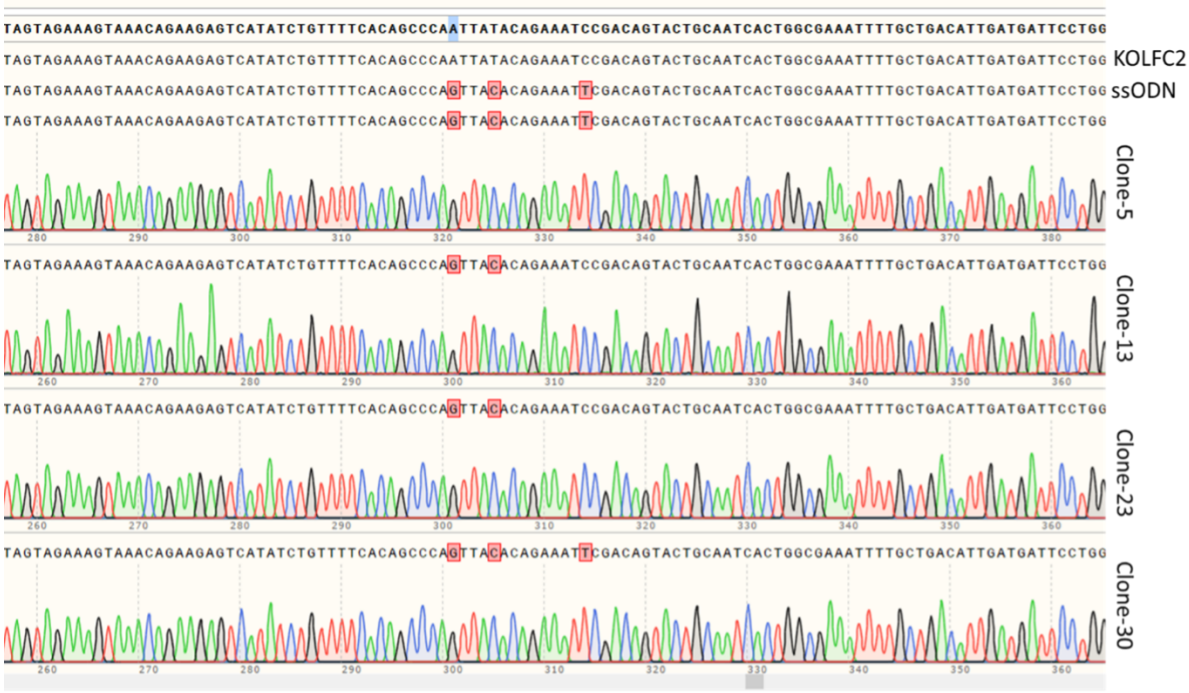

Figure 2.2: Sanger sequencing of GLA F1/R2 PCR products from Clone 5, 13, 23 and 30 confirming GLA p. N215S A>G SNP at the CRISPR target site

iPSC clones. Sanger sequencing of the clones confirmed the correct HDR of the locus and the introduction of the *N215S* mutation in 4 independent clones (Clone-5, 13, 23 and 30) (**Figure 2.2).** Interestingly, although all the clones harboured the desired *N215S* mutation, the clones differed in the number of silent mutations introduced during the engineering. Clones 13 and 23 only had the additional T>C (Y216Y) mutation, whereas clones 5 and 30 had both the C>T (Y216Y) and T>C (I219I) silent mutations.

The resulting hemizygous *N215S* iPSC clones were validated as pluripotent by fluorescence activated cell sorting (FACS) analysis for expression of stem cell markers including *OCT4, SOX2, NANOG a*nd *SSEA4* using Human Pluripotent Stem Cell transcription factor Analysis Kit (BD Biosciences 560589) (**Figure 2.3**). A normal karyotype was confirmed for all 4 clones by chromosomal counting at metaphase (**Figure 2.4**) performed by the Chromosome Dynamics Core Facility at the Wellcome Centre for Human Genetics, UK.

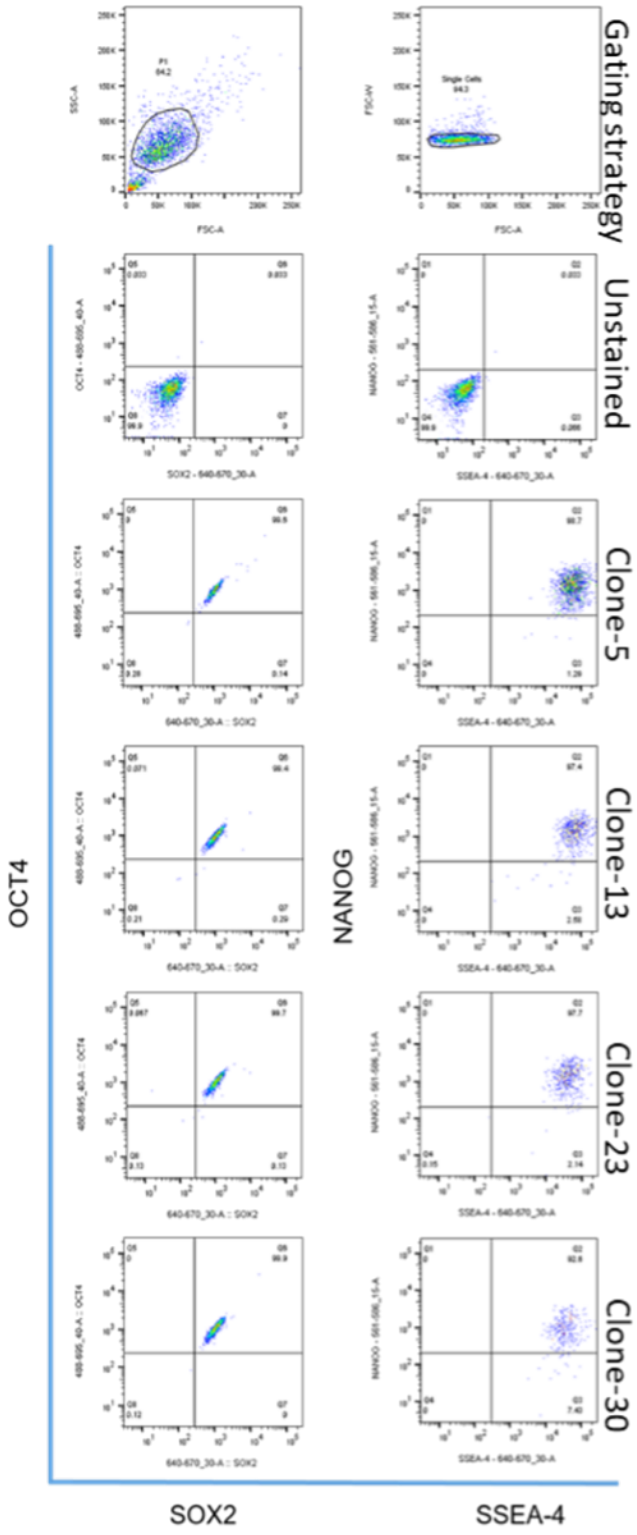

Figure 2.3: FACS analysis for pluripotent stem cell markers. All four clones (Clone 5, 13, 23 and 30) showed high expression of pluripotent stem cell markers.

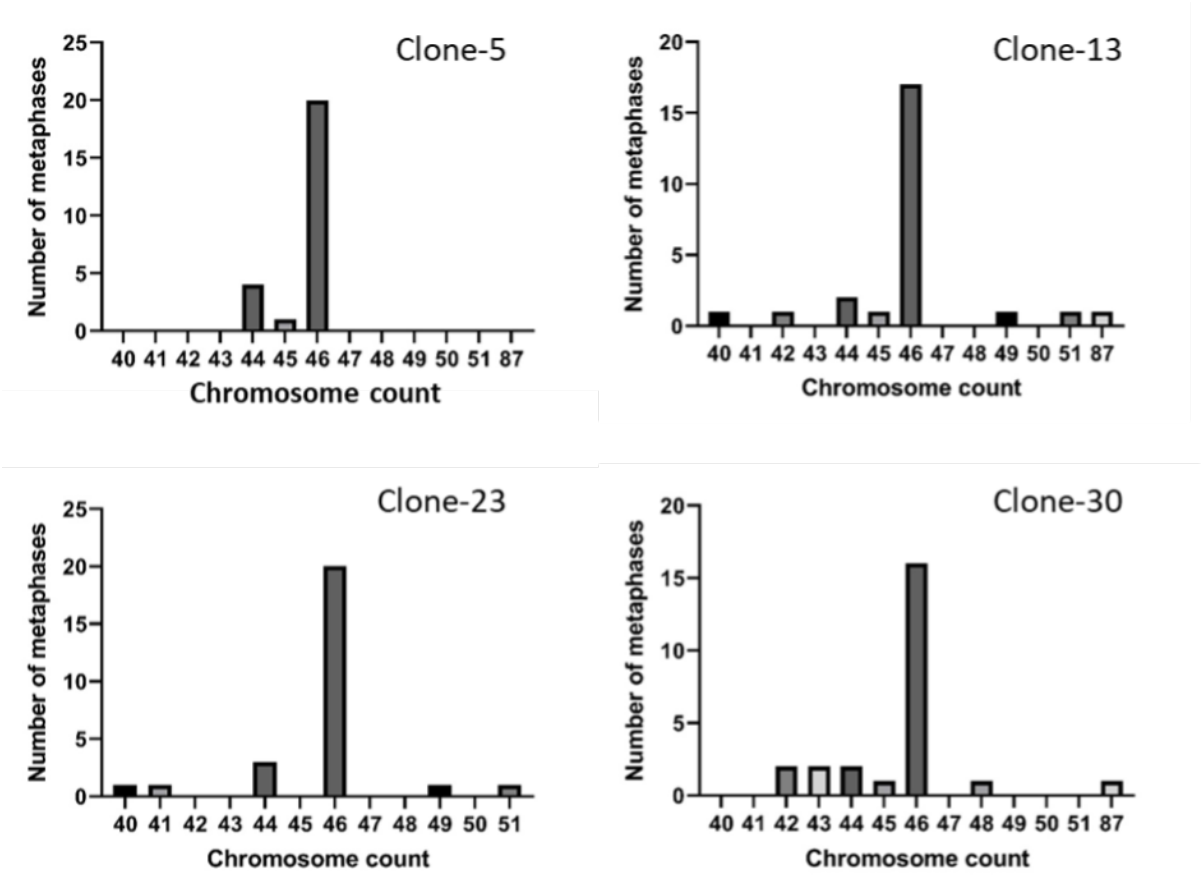

Figure 2.4: Karyotype Analysis. Chromosome counts of individual clones. All four analysed clones demonstrated a diploid chromosome count. More than 20 spreads (out of 25) from each clone were counted as normal with 46 chromosomes.

2.5.5 iPSC culture

iPSCs were cultured in mTeSR Plus medium (StemCell Technologies, 100-0276) on 6-well plates coated with 1:100 GelTrex™ LDEV-Free Reduced Growth Factor Basement Membrane Matrix (Thermo Fisher Scientific A1413201). GelTrex™ was diluted in ice-cold Dulbecco's Modified Eagle Medium F12 (DMEM/F12) and stored at 4°C. Cells were incubated in 6-well plates at 37°C with 5% CO_2. Cells underwent media change every 48 hours until 80% confluency at which point they were passaged. At this stage, mTeSR Plus medium was aspirated and 2mL 1mM EDTA in

phosphate-buffered (PBS) solution was added to dissociate cells. The cells were left for 5 minutes at room temperature and checked for detachment under microscopy. An aliquot of mTeSR Plus with Rock-inhibitor (1:100) Y-27632 (Selleck S1049) was then prepared and 1mL pipetted around each well to dissociate the cells. This was then transferred to a falcon with mTeSR Plus and Rock-inhibitor. The wells were further washed with mTeSR Plus and Rock-inhibitor and added to the falcon. The solution was then triturated. Cells were then spun and counted using a Neubauer and plated between 10,000 and 20,000 cells/cm^2. Cells were then incubated overnight at 37°C with a media change the next day with mTeSR Plus without Rock-inhibitor.

2.5.6 Atrial iPSC-CM differentiation

iPSCs were differentiated into atrial iPSC-CMs following a published protocol (142), illustrated in (**Figure 2.5**). Cells were passaged at-least twice prior to commencing differentiation. At 60% confluency, pre-conditioning medium was added (Day-1). All supplements and media were pre-warmed and filtered (0.2 um) prior to use.

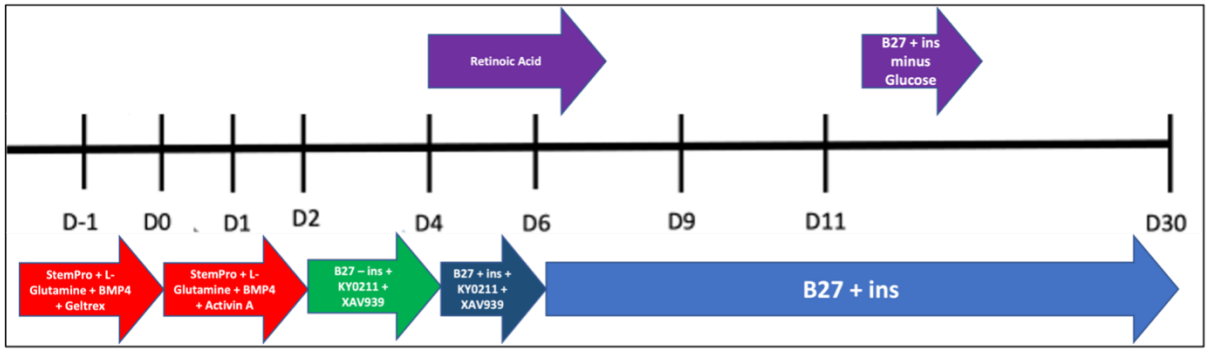

Figure 2.5: Schematic representation of the differentiation protocol of iPSCs into beating iPSC-CM monolayers. The addition of retinoic acid from Days 4-8 drives differentiation into an atrial line.

mTeSR Plus medium was removed and a solution of StemPro™-34 (Thermo Fisher Scientific, 10639011) supplemented with Recombinant Human BMP-4 Protein (1ng/mL) (R&D Systems, 314-BP-010/CF), L-Glutamine 2mM (Thermo Fisher Scientific, 25030024) and GelTrex™ (1:100) was added. The next day (Day 0), the media was removed and a solution of StemPro™-34 supplemented with L-Glutamine 2mM, Recombinant Human BMP-4 (10ng/mL) and Human Activin-A Recombinant Protein (Thermo Scientific PHC9564) (8ng/mL) was added for 48 hours. After this time (Day 2) the medium was removed and Roswell Park Memorial Institute (RPMI) 1640 Medium (Thermo Fisher, Scientific, 21875034) supplemented with B-17™, minus insulin (Thermo Fisher Scientific, A1895601), XAV 939 (10μM) (TOCRIS, 3748) and KY02111 (10μM) (TOCRIS, 4731) was added for 48 hours. At this point the cells were fragile, and so media change was done carefully and in the dark due to the light-sensitive nature of XAV 939 and KY02111. After this time (Day 4) the medium was removed and a solution of RPMI 1640 supplemented with B-27™ (50X with insulin) (Gibco 17504-044), XAV 939, (10μM), KY02111 (10 μM) and Retinoic Acid 1:50,000 (Sigma-Aldrich, R2625) was added in the dark for 48 hours. After this time (Day 6), the media was removed and a solution of RPMI 1640 supplemented with B-27™ (50X with insulin) (Gibco 17504-044) and Retinoic Acid 1:50,000 was added for 48 hours. After this time (Day 8) the media was removed and RPMI 1640 with B-27™ supplement (50X with insulin) (Gibco 17504-044) was added. Media was subsequently changed every 48 hours. At Day 12, the media was removed and RPMI 1640, no glucose (Thermo Fisher Scientific, 11879020) supplemented with B-27™ (50X with insulin) was added for 48 hours to ensure sufficient glucose starvation. At Day 14 this was removed and RPMI 1640 supplemented with B-27™ Supplement

(50X with insulin) was added with subsequent media changes completed every 48 hours until Day 30 to ensure sufficient maturation of iPSC-CMs.

2.5.7 Confirmation of model

The model was confirmed and validated by Western blotting for α-GAL A deficiency in *GLA* p. *N215S* IPSC-CMs, immunofluorescence for Gb3 over-accumulation in *GLA* p. *N215S* IPSC-CMs and qPCR for expression of atrial and ventricular markers.

2.5.7.1 Harvesting iPSC-CMs for Western Blotting and qPCR

To perform molecular experiments on atrial iPSC-CMs, iPSC-CMs were harvested on reaching maturity (Day 30). Media was removed and 1ml TrypLE™ Select enzyme (10X) (Thermo Fisher, Scientific A1217701) was added and placed in the incubator at 30°C for 15 minutes. TrypLE was then removed and 1mL PBS was added for washing and cell dissociation. This was then transferred into pre-labelled Eppendorf tubes and spun at 13,000g for 5 minutes in a pre-chilled centrifuge at 4°C. The PBS was then aspirated, and dry pellet stored at -80°C in the Eppendorf tubes.

2.5.7.2 Expression of α-GAL A: Western Blotting

GLA p. *N215S* iPSC-CM and WT iPSC-CM pellets that had been cultured to day 30, ensuring sufficient maturation, were washed twice with PBS and lysed directly in 2xSDS sample buffer (100mM Tris-HCL pH 6.8, 4% sodium dodecyl sulphate, 0.2% bromophenol blue, 200mM dithiothreitol and 20% glycerol). After heating at 95 degrees for 3 minutes, samples were sonicated and stored at -80°C.

Western blotting was performed as described (143) with an antibody (Proteintech ® 66121-1-lg) (1:2000) to assess for α-GAL A expression and Rabbit ACTN2 (Abcam Ab68167) (1:500). Secondary antibodies were Rabbit HRP (Cytiva NA934V) (1:5000) and Mouse HRP (Cytiva NXA931V) (1:5000). Imaging was using a Chemidoc system and quantitative expression was conducted using a script on ImageJ. Expression was normalised to GAPDH (Cell Signalling Technology 14C10) (1:1000) to ensure that changes were not due to variations in loading volumes. The values were then normalised to the mean expression of the WT control set to 1.

2.5.7.3 Expression of atrial and ventricular markers: qPCR

RNA was isolated from day 30 iPSC-CMs (atrial and ventricular) using an RNEasy Mini Kit (Qiagen 74104) as per protocol. 200ng of RNA from iPSC-CMs were converted to complementary deoxyribose nucleic acid (cDNA) using reverse transcriptase PCR with High-Capacity cDNA Reverse Transcription Kit protocol (Applied Biosystems 4368814). qPCR was conducted using TaqMan™ probes in combination with TaqMan™ Gene expression Fast Advanced Master Mix 2X (Applied Biosystems 4444557) with the following probes: Atrial: *MYH7* (Hs001110632 m1), *MYH6* (Hs01101425 m1), Ventricular: *MYL2* (Hs00166405 m1), *MYL7* (Hs01085598 g1), Cardiac: *TNNT2* (Hs00943911) and *GAPDH* (4626317E) (Thermo Fisher Scientific). The probes were FAM-labelled and duplexed with VIC-labelled GAPDH probe, allowing simultaneous measurement of two transcripts from the same samples. Changes in expression were calculated using the ΔΔCt method using GAPDH as the control, and data made relative to ventricular cells.

2.5.7.4 Accumulation of Gb3: Immunofluorescence and confocal microscopy

Day 30 atrial iPSC-CMs were fixed at room temperature for 15 minutes using 4% paraformaldehyde in phosphate buffer solution (PBS) (Thermo Fisher Scientific, J19943.K2). Cells were permeabilised using 0.2% Nonidet™ P40 Substitute (Sigma-Aldrich 74385) solution in PBS for 1 hour at room temperature. Primary antibodies, mouse Gb3 (TCI Chemicals A2506) (1:200) and rabbit α-actinin (Abcam AB68167) (1:500) were diluted in PBS and added to cells overnight at 4°C (3 washes in PBS for 5 minutes). Secondary antibodies, Alexa-fluor 488 anti-mouse IgG (Invitrogen) (1:200), Alexa-fluor 568 anti-rabbit IgG (Invitrogen) (1:200) and DAPI (Thermo Fisher Scientific) (1:400) were diluted in PBS and incubated with cells at room temperature for 1 hour (3 washes in PBS for 5 minutes). Coverslips were mounted onto glass microscopy slides using Hydromount mounting medium (National Diagnostics). Coverslips were imaged using a Zeiss LSM880 confocal microscope, using a C-Apochromat 63x/1.20 W Korr M27 objective oil immersion lens. Gb3 accumulation quantification in *GLA* p. *N215S* IPSC-CMs at day 30 was compared with WT controls. Gb3 accumulation in cells was quantified using a custom-written macro in Fiji (ImageJ). Firstly, the α-actinin channel was thresholded to give a mask of the cell area. The Gb3 channel was also thresholded, with the threshold set to the minimum intensity for the edges of Gb3 puncta. The thresholded images were then turn into a binary mask, and single pixel masks were filtered out of the data using the erode and dilate functions within Fiji, to remove noise pixels and retain Gb3 puncta. The number of retained puncta within the Gb3 channel was then divided by the previously calculated area of the α-actinin mask to yield the number of Gb3 puncta per square micron.

2.5.8 Functional Experiments

2.5.8.1 Passaging of iPSC-CMs for patch clamping and optical mapping

iPSC-CMs were washed with PBS solution and TrypLE Select (10X) was added and stored in the incubator at 37°C to ensure sufficient dissociation. 2mL plating medium, consisting of RPMI 1640, B-27™ supplement (1:50), KnockOut™ Serum Replacement (10%) (Thermo Fisher Scientific, 10828028) and Thiazovivin (8μM) (StemCell Technologies, 100-0247) was then added to each well. This was then washed and transferred to a falcon via a cell strainer. The wells were further washed with plating medium and then spun at 220g for 3 minutes at room temperature. The media was aspirated, and cell pellet resuspended in plating medium. Seeding of iPSC-CMs were different for patch clamping and optical mapping, as outlined below.

2.5.8.1.1 Patch Clamping

The cells were counted and 50,000 iPSC-CMs were seeded onto Corning™ BioCoat™ 12mm German Glass Coverslips (Fisher Scientific, 10468681) which had been sterilised, pre-coated with GelTrex™ (1:100) and inserted into wells of a Corning™ 24-well plate. This was to ensure single cells for patch clamping. The medium was changed after 24 hours to RPMI 1640 with B-27™ supplement (50X with insulin). Cells were passaged at day 27 after initiation of differentiation to ensure recovered, beating single cells by day 30, ready for use in experiments

2.5.8.1.2 Optical mapping

The cells were counted and 2,000,000 iPSC-CMs were seeded onto 35mm dishes which had been pre-coated with GelTrex™ (1:100) to form a dense monolayer of cells.

The media was changed after 24 hours to RPMI 1640 with B-27™ supplement (1:50). Cells were passaged at day 17 of the differentiation protocol to ensure a beating dense monolayer of cells by day 24, ready for use in experiments

2.5.8.2 Assessment of electrophysiological properties: Patch clamping

Stimulated and spontaneous APs were recorded from iPSC-CMs using a manual current clamp configuration. APs were recorded at 37°C using an internal solution containing (in mM): KCl 135, NaCl 10, MgATP 5, HEPES 10, EGTA 0.1, pH 7.2 (adjusted using KOH). Micropipette resistances were between 3-4 MΩ. The extracellular solution contained (in mM): NaCl 145, KCl 5.4, $MgSO_4.7H_2O$ 0.83, NaH_2PO_4 0.33, HEPES 5, Glucose 11, $CaCl_2$ 1.8, pH 7.4 (NaOH). A 60 second period after breakthrough allowed cell stabilisation. Spontaneous APs were recorded for 60 seconds prior to stimulation. A continuous hyperpolarising current was then applied to the cells to hold the diastolic membrane potential at –75mV prior to recording of stimulated APs (144, 145). Only those cells that required a hyperpolarising current of less than 150 pA were used (144). APs were stimulated using a 1nA, 2ms current injection at a frequency of 1 Hz (145).10 successive spontaneous and stimulated APs were analysed from each cell using custom algorithms developed in MatLab.

Delayed afterdepolarisations (DADs) may develop after the repolarisation phase of an AP, are triggered by dysregulated calcium homeostasis and are thought to be pro-arhythmic in nature. These were visualised and quantified during analysis. DADs were defined as a sustained spontaneous depolarisation of greater than or equal to 10mV taking place following terminal repolarisation, during the diastolic interval.

2.5.8.3 Assessment of contractile properties

Contractile properties were assessed using a GoPro Inc. H6 camera at 20x magnification. Video recordings were obtained from atrial iPSC-CMs at day 30 of the differentiation protocol in multiple areas of the same well and for multiple wells of beating atrial cardiomyocyte monolayers. These were 20 second videos recorded at room temperature in a quiet setting with no other activity in the room of recording to ensure minimal interference. Videos were converted to TIFF format using DaVinci Resolve (Blackmagic Design). A TIFF-stack and single sub-stack file was then created using a script run in ImageJ. The sub-stack file was then run using a MUSCLEMOTION (146) script on ImageJ (add-on Macro); a validated tool for quantitative analysis of cardiac contraction by determining changes in pixel intensity between image frames. Outputs expressed were measures of movement during contraction and relaxation. Three 20-second videos were taken in each well with 6 wells for each batch. The MUSCLEMOTION script generates a graphical representation of contraction and relaxation; expressed outputs are outlined below with values expressed relative to the mean value of WT controls:

- Contraction amplitude – Peak contraction force from beginning of wave.
- Peak amplitude – Peak contraction force from 0.
- Relaxation time – Interval between peak contraction and beginning of following contraction.
- Time-to-peak time - Interval between beginning of contraction and peak contraction.
- Peak-to-peak time - Interval between each contraction.

2.5.8.4 Assessment of calcium transients: Optical mapping

Between days 23 and 27, calcium optical mapping was performed using intracellular calcium dye Fura-2-AM (Invitrogen). Cells were incubated with 5 μM Fura-2-AM in 1 mL RPMI B27 + Insulin (Thermo Fisher Scientific 17504044) at 37°C for 20 minutes, followed by a further 20 minutes in Tyrode's solution (Concentrations in mM: NaCl 129, KCl 5.4, Hepes 10, $MgCl_2$ 48, $CaCl_2$ 1.8, and D-Glucose 9.99, pH 7.44-7.48).

Dye loaded cells were excited at 380nm, and emission imaged at 10x magnification through 510/40nm bandpass filter. Images were collected at 1.7ms exposure time (588 Hz) using an Evolve delta 512x512 EMCCD camera. Binning was set to 10, giving a final resolution of 51x51 pixels, pixel size = 8μm. Images were collected for 10-30 seconds using WinFluor (University of Strathclyde, UK), and converted to .MAT files for analysis with ElectroMap (147). Images were pre-conditioned with a 3x3 gaussian spatial filter. Time to peak was measure from 10-90% calcium intrusion before peak. Calcium transient duration (CTD) was measured to 30%, 50% and 80% extrusion from both maximum upstroke time (the maximum positive differential) and peak amplitude.

2.6 Statistical Analysis

Where two variables were being compared, normality was assessed using the Shapiro-Wilk test. If the data was normally distributed and groups had similar standard deviation (SD), unpaired t-tests were performed. If the data was normally distributed but standard deviations were not equal, unpaired t-tests with Welch's correction were performed. Where data was not normally distributed, the Mann-Whitney test was used. Where more than two variables were being compared, an Ordinary one-way ANOVA

was performed with Turkey's multiple comparisons test for normally distributed data. For non-normally distributed data where more than two variables were compared, the Kruskal-Wallis test was performed (with Dunn's test for multiple comparisons). For categorical and contingency data, Fishers exact test was performed. Data is presented as mean ± SD for normally distributed data and median (interquartile range) for non-normally distributed data with $p<0.05$ deemed to be indicative of statistical significance. Data was analysed and presented in GraphPad Prism version 10.0.01.

2.7 Statement of ethics

The use of 12-lead ECGs in the FD cohort was approved by West Midlands – South Birmingham Research Ethics Committee (23/WM/0180 IRAS 325613). The studies were conducted in accordance with the local legislation and institutional requirements. The Ethics Committee / institutional review board waived the requirement of written informed consent for participation from the participants or participant's legal guardians / next of kin because data were acquired from a research database using routinely collected clinical data for the purpose of research. The use of 12-lead ECGs in healthy controls was approved by the West Midlands Solihull Research Ethics Committee (17/WM/0048) and approved by the Health Research Council. All healthy controls gave informed consent to take part in accordance with the principles set out in the Declaration of Helsinki.

iPSCs were engineered with the pathogenic *N215S* variant with the support of the Genome Engineering Core Facility at the Wellcome Centre for Human Genetics, University of Oxford. The variant was introduced into male iPSCs (KOLF2 line). KOLF2

are Human Induced Pluripotent Stem Cell Initiative lines from a consortium at the Sanger Institute. They do not fall under the Human Tissue Act (2004) as an established cell line for which the volunteer has given prior consent under an open access agreement.

2.8 Results

2.8.1 Early atrial changes on ECGs of Fabry Disease patients

In the cohort of 115 adults with FD, mean age was 45 ± 17.3 years, 52 (45%) were male and 93 (81%) were of Caucasian descent. 43 (37%) had a classical FD mutation and 72 (63%) had the *GLA* p. *N215S* non-classical cardiac variant. At the time of ECG acquirement, 35 (30%) patients were on ERT and 26 (23%) on OCT. 16 (14%) had a diagnosis of AF and therefore ECG was acquired when they were last in sinus rhythm. Baseline characteristics for the FD and control cohort are summarised in **Table 2.1**. The cohort split between cardiac disease stages was as follows: Stage 1 (n=39), stage 2 (n=30), stage 3 (n=24), and stage 4 (n=22). Age, male predominance, body-mass index, systolic BP and LA volume increased with cardiac disease stage. There was also an observed trend to worsening of cardiac, renal and AF-associated biomarkers with elevations in NTpro-BNP, HS troponin I and serum creatinine with cardiac disease stage.

P-wave morphology changes in non-FD controls, stage 1 FD and stage 4 FD are illustrated in **Figure 2.6A**. In the cohort of adults with FD, there was a significant shortening of P-wave duration on 12-lead ECGs in adults with FD but no overt

evidence of a cardiac phenotype (stage 1), when compared to non-FD controls (p=0.0002) (**Figure 2.6B**). PQ interval shortening in FD stage 1 was also documented when compared to non-FD controls (**Figure 2.6C**) (p=0.0043). Interestingly, prolongation of P-wave duration and PQ interval were seen to be associated with worsening severity of FD cardiac phenotype (stages 1-4) (p=<0.0001 and p=0.0043 respectively). Prolongation of P-wave duration and PQ interval in the later stages of cardiac disease also correlated with greater LA volume on TTE (**Figure 2.6D**). The trend of P-wave duration and PQ interval shortening between healthy controls and stage 1 FD was also observed when comparing healthy controls with the *N215S* cohort only (p=0.0136 and p=0.0131 respectively).

	Control (N=40)	All (N=115)	Stage 1 (N=39)	Stage 2 (N=30)	Stage 3 (N=24)	Stage 4 (N=22)	P-Value
Demographics							
Age (Years)	51.0 ± 11.7	45.4 ± 17.4	30.4 ± 11.9	42.6 ± 13.3	57.6 ± 10.0	62.4 ± 12.3	**<0.0001**
Female Sex N (%)	27 (68)	63 (55)	31 (80)	13 (43)	11 (46)	8 (36)	
Ethnicity N (%)							
White Caucasian	34 (85)	93 (81)	28 (72)	23 (77)	21 (88)	21 (96)	
Black and Minority Ethnic	6 (15)	22 (19)	11 (28)	7 (23)	3 (12)	1 (4)	
Height (m)	1.7 ± 0.1	1.7 ± 0.1	1.7 ± 0.1	1.7 ± 0.1	1.7 ± 0.1	1.7 ± 0.1	0.2190
Weight (kg)	76 ± 12	76 ± 21	77 ± 18	72 ± 18	82 ± 27	76 ± 23	0.4457
BMI (kg/m2)	27 ± 4	27 ± 7	28 ± 5	25 ± 6	29 ± 8	27 ± 7	**0.0258**
Systolic BP (mmHg)	122 ± 16	133 ± 17	127 ± 14	132 ± 20	141 ± 15	136 ± 19	**0.0125**
Diastolic BP (mmHg)	79 ± 9	79 ± 11	79 ± 8	75 ± 12	82 ± 11	80 ± 12	0.1541
Bloods							
Creatinine (umol/L)		74 [60-96]	61 [65-70]	74 [67-90]	89 [61-110]	94 [81-117]	**<0.0001**
NT-proBNP (ng/L)		128 [51-490]	51 [32-115]	68 [41-104]	243 [147-641]	880 [356-2343]	**<0.0001**
Troponin I (ng/L)		8 [4-37]	5 [4-5]	7 [4-12]	29 [14-78]	122 [60-230]	**<0.0001**

Haemoglobin (g/L)		135 ± 14	131 ± 10	138 ± 14	138 ± 17	133 ± 16	0.7930
Comorbidities							
Stroke N (%)	0 (0)	9 (8)	1 (3)	3 (10)	1 (4)	4 (18)	
Hypercholesterolaemia N (%)	7 (18)	35 (30)	3 (8)	6 (20)	16 (67)	10 (46)	
Ischaemic Heart Disease N (%)	0 (0)	7 (6)	0 (0)	2 (7)	1 (4)	4 (18)	
Statin Therapy N (%)	5 (13)	34 (30)	1 (3)	7 (23)	14 (58)	12 (55)	
Current Smoker N (%)	1 (2.5)	8 (7.0)	1 (2.6)	3 (10.0)	2 (8.3)	2 (9.1)	
Fabry Therapy							
Enzyme Replacement Therapy N (%)		35 (30)	7 (18)	10 (33)	8 (33)	10 (45)	
Oral Chaperone Therapy N (%)		26 (22.6)	2 (5.1)	8 (26.7)	11 (45.8)	5 (22.7)	
ECG and TTE							
Rate (bpm)	63 ± 15	64 ± 13	68 ± 12	61 ± 11	64 ± 15	60 ± 12	0.0888
P wave duration (ms)	110 ± 17	106 ± 18	96 ± 16	108 ± 14	110 ± 15	116 ± 20	**<0.0001**
P wave area (mV/ms)	6.2 ± 3.3	7.9 ± 3.9	5.9 ± 3.7	8.8 ± 3.8	8.2 ± 3.7	8.5 ± 3.9	**0.0015**
P wave amplitude (mV)	0.085 ± 0.038	0.12 ± 0.041	0.10 ± 0.048	0.13 ± 0.043	0.12 ± 0.041	0.12 ± 0.035	**<0.0001**
PQ interval (ms)	171 ± 30	159 ± 34	145 ± 26	162 ± 33	159 ± 26	177 ± 46	**0.0013**
QRS duration (ms)	89 ± 18	104 ± 22	94 ± 17	98 ± 16	107 ± 18	124 ± 27	**<0.0001**

QTc interval (ms)	406 ± 53	402 ± 48	403 ± 25	390 ± 52	428 ± 48	428 ± 49	**0.0086**
LA volume (ml)	63 ± 17	68 ± 34	56 ± 15	54 ± 25	86 ± 38	84 ± 43	**<0.0001**

Table 2.1: Cohort Characteristics of FD and Healthy control cohorts, total and according to cardiac disease stage. BMI: body mass index, BP: Blood pressure, LA: left atrium, ECG: electrocardiography, TTE: transthoracic echocardiography, NT-proBNP: N-terminal pro brain natriuretic peptide. Data presented as N (%) or mean ± SD. Ordinary one-way ANOVA performed for normally distributed data. Kruskal-Wallis test performed for non-normally distributed

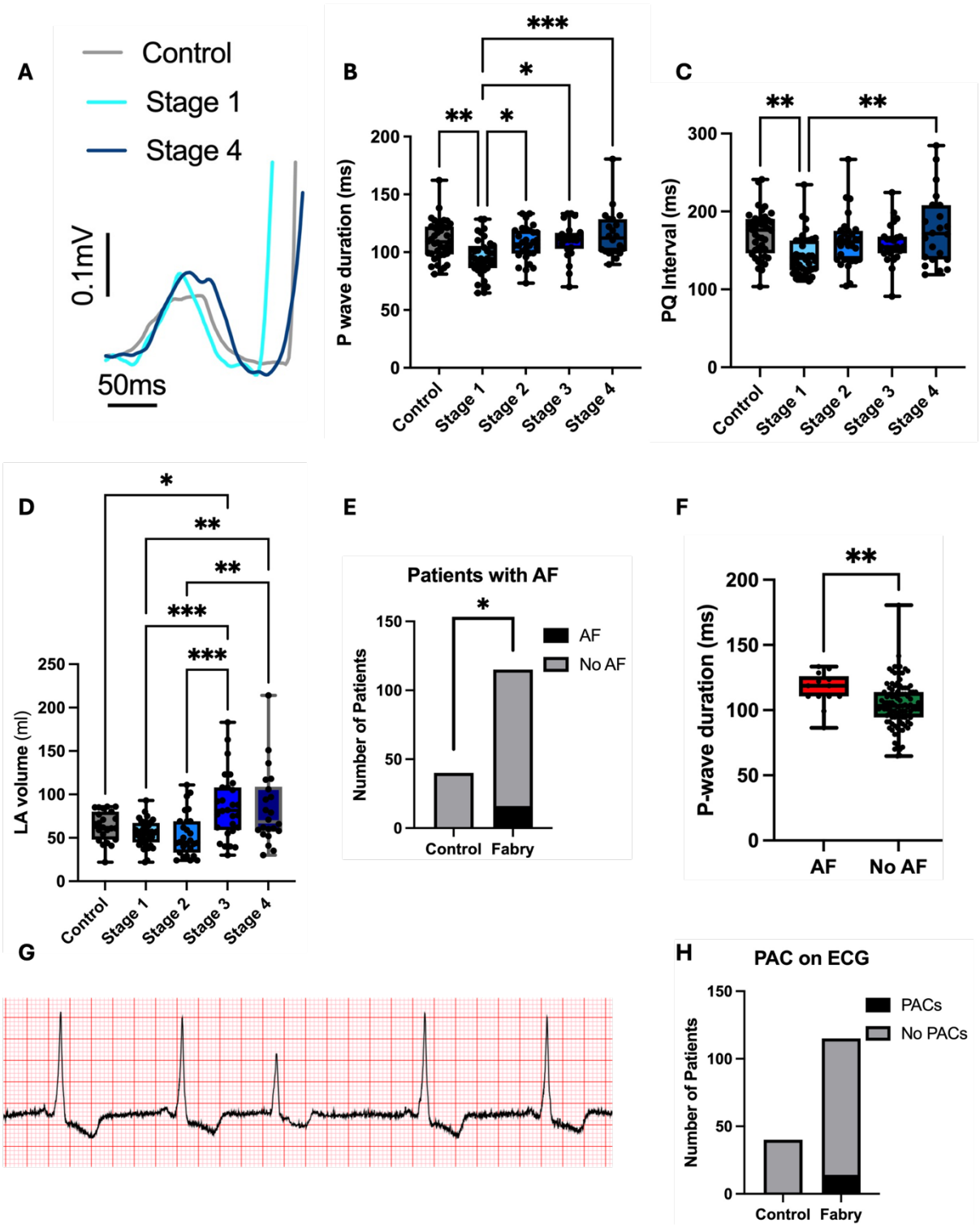

Figure 2.6: 12-lead ECG analysis: (A) P-wave morphology changes on ECG (control vs stage 1 vs stage 4) (B-C) P-wave duration and PQ interval changes in controls and FD cardiomyopathy stages (D) LA volume changes in controls and FD cardiomyopathy stages on TTE. (E) Proportion of patients with AF Fabry vs control

*(F) P-wave duration in AF vs no AF (G) PAC on ECG of adult with FD (H) Proportion of PACs Fabry Vs control. Ordinary one-way ANOVA with Turkey's multiple comparisons statistical test used comparing stages. Mann Whitney Test used to compare P-wave duration in AF vs no AF. Fisher's exact test used for proportion of patients with PACs and AF. Data presented as mean ± SD. * p ≤ 0.05, ** p ≤ 0.01, *** p ≤ 0.001*

In the sub-analysis of patients with AF (N=16) using their most recent ECG in sinus rhythm, more FD patients had AF compared to non-FD controls (**Figure 2.6E**), and this group had a more prolonged P-wave duration compared to those remaining in sinus rhythm throughout (**Figure 2.6F**) (p=0.0094). There was an equal spread of patients with FD developing AF across the cardiac disease stages. The presence of PACs on ECG (**Figure 2.6G)** were observed in 14/115 adults with FD vs 0/40 for controls (**Figure 2.6H)**. Prevalence of PACs in cardiac disease stages were as follows: Stage 1 (N=4/39, stage 2 (N=1/30), stage 3 (N=5/24) and stage 4 (N=4/22).

2.8.2 Successful generation of atrial Fabry Disease model

Sanger sequencing confirmed the presence of *GLA* p. *N215S* at the CRISPR target site, FACS analysis confirmed high expression of pluripotent stem cell markers and normal chromosomal count was confirmed by karyotype analysis.

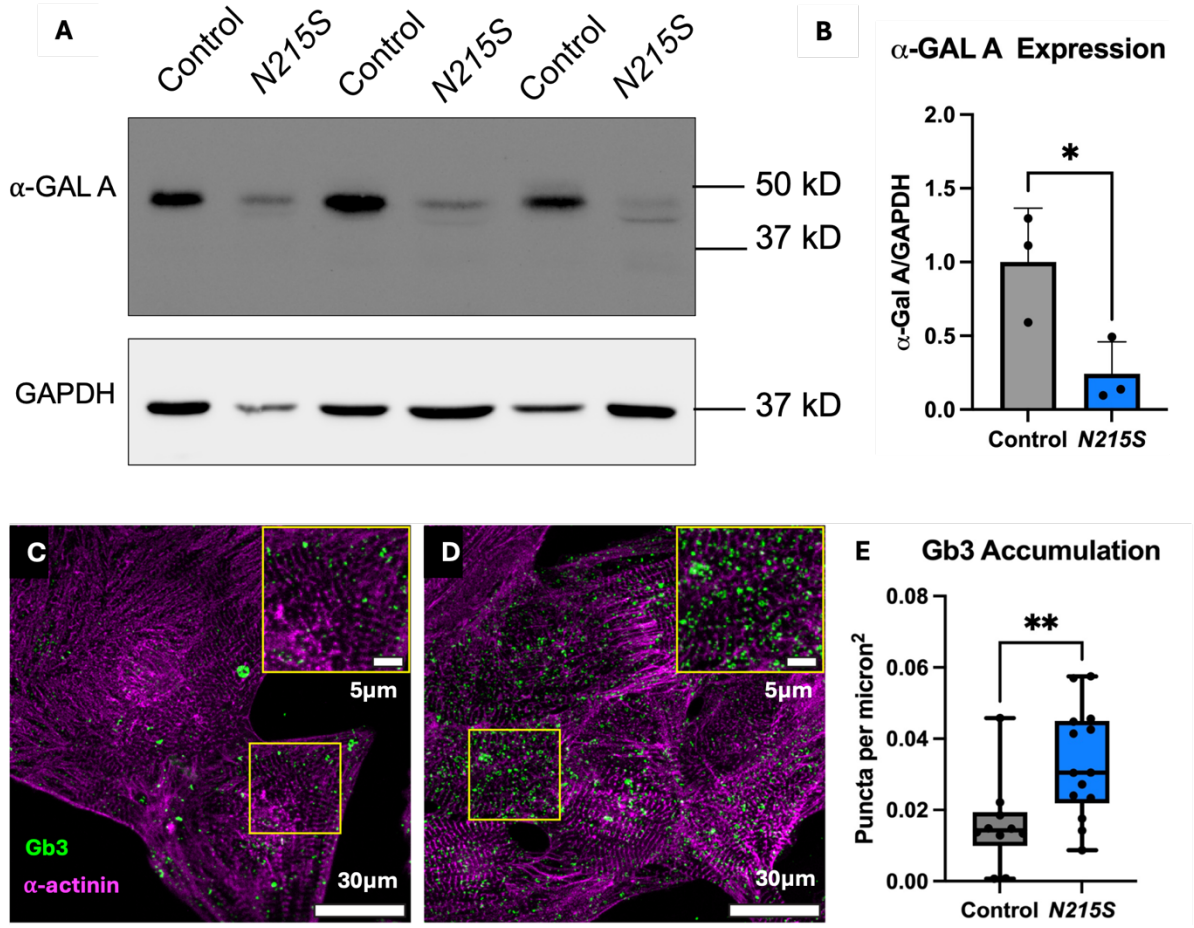

Figure 2.7: Confirmation of FD model. (A) Western blot for α-GAL A protein levels (control vs N215S) in iPSC-CMs. (B) Quantification of α-GAL A expression (control vs N215S) in iPSC-CMs. Data presented as mean ± SD (C-D) Immunofluorescence Gb3 (green) stain using confocal microscopy (C: control D: N215S) in atrial iPSC-CMs (α-actinin, purple) (E) Quantification of Gb3 accumulation (control vs N215S) in atrial iPSC-CMs. Data presented as mean ± SD. Mann Whitney U statistical test used, p=<0.05, ** p=<0.01.*

α-GAL A is a homodimer, consisting of two 49 kDA subunits. Western blotting confirmed under-expression of α-GAL A as visualised by less prominent bands at 49

kDA in *GLA* p.*N215S* iPSC-CMs compared to WT (**Figure 2.7A**). Significant quantitative under-expression of α-GAL A in *GLA* p.*N215S* iPSC-CMs was also confirmed when compared to WT (p=0.0368) (**Figure 2.7B).** When stained with a Gb3 antibody and visualised on confocal microscopy, mature atrial *GLA* p.*N215S* iPSC-CMs displayed greater accumulation of Gb3 compared to WT (**Figure 2.7C-D).** On Gb3 quantification, *GLA* p.*N215S* iPSC-CMs exhibited a greater number of puncta per micron^2 compared to WT (p=0.0073) (**Figure 2.7E).** Markers of atrial and ventricular expression on qPCR are illustrated in **Figure 2.8A-D**. Atrial iPSC-CMs had greater expression of atrial markers *MYL7* (p=0.0184) and a trend towards increased *MYH6* with under-expression of ventricular markers (*MYL2* and *MYH7*) (p=0.0021 and p=0.0142 respectively) compared with ventricular iPSC-CM expression. All iPSC-CMs expressed the cardiac marker troponin (*TNNT2*) on qPCR (**Figure 2.8E**).

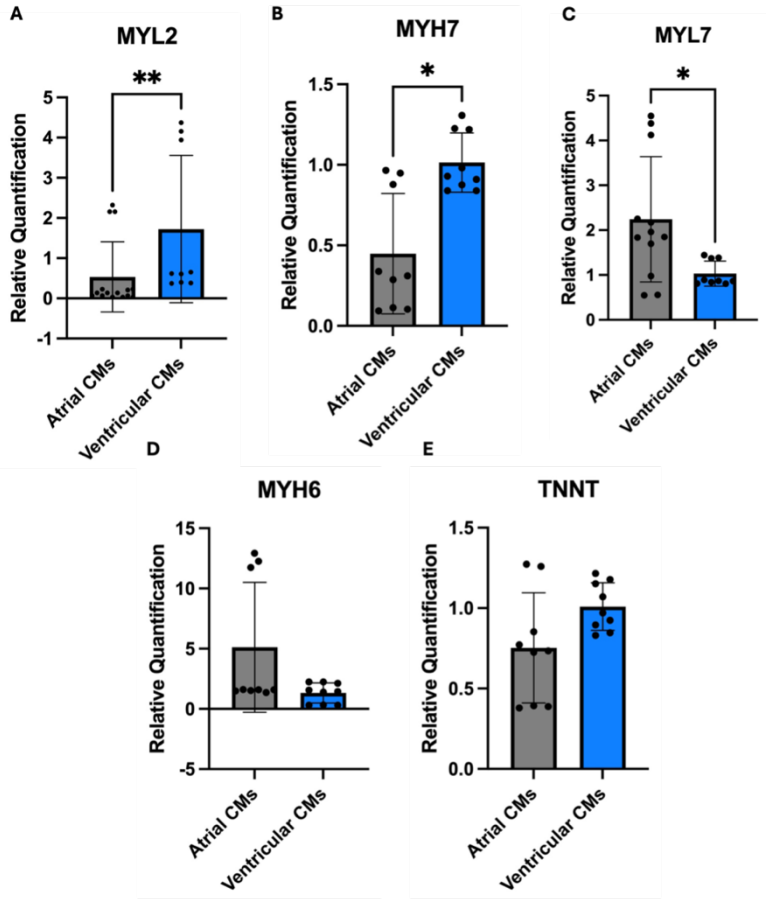

Figure 2.8: Expression of cardiac markers on qPCR. Data presented as individual

*values + SD. Mann-Whitney statistical test used. *p ≤ 0.05, **p ≤0.01*

Taken together, these results confirm the cellular atrial FD model of α-GAL A deficiency and Gb3 accumulation.

2.8.3 Quicker upstroke in atrial APs of GLA p. N215S IPSC-CMs identified.

Findings from single cell patch clamping assessment of atrial APs are summarised in **Figure 2.9**. In the first step, we assessed spontaneous action potentials. *GLA* p. *N215S* atrial iPSC-CMs demonstrated a more positive resting diastolic membrane potential (**Figure 2.9A**) (p=0.0153). There were no significant changes in firing frequency or APD30, APD50, APD70 or APD90 (data not shown).

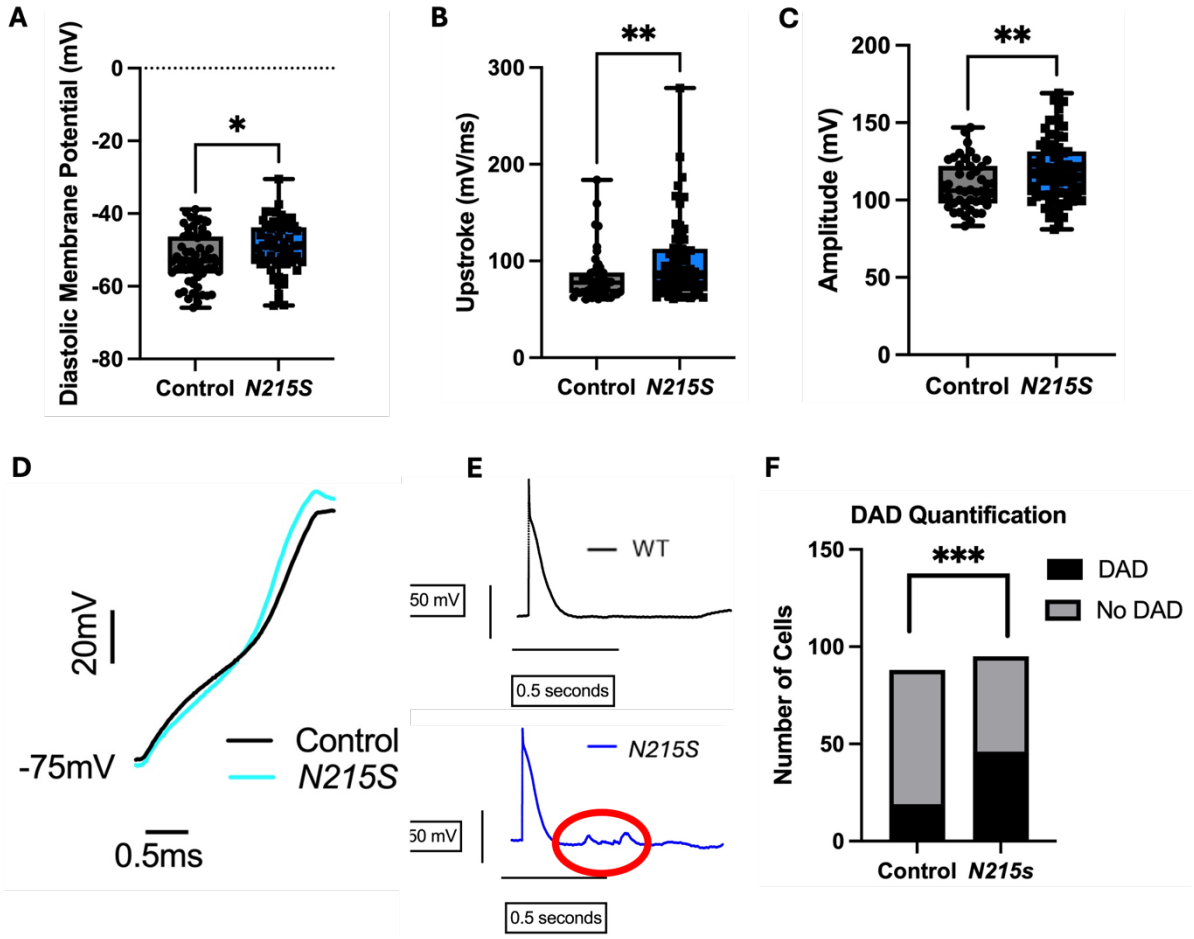

Figure 2.9: (A-C) Diastolic membrane potential, upstroke and amplitude from APs from iPSC-CMs at 1Hz (WT vs N215S). (D) Single cell atrial APs (WT vs N215S) illustrating quicker upstroke in N215S. (E) Stimulated atrial APs (WT vs N215S) illustrating DAD activity in N215S (circled in red) compared to no DAD activity in WT. (F) DAD quantification documenting a greater number of N215S iPSC-CMs with DAD activity compared to WT. Welch's unpaired t-test statistical test used for Diastolic membrane potential. Mann Whitney U test used for Stimulated Upstroke and Amplitude. Fisher's exact test used for comparison of number of DADs. Data presented as mean ± SD. $p \leq 0.05$, *** $p \leq 0.001$, **** $p \leq 0.0001$,*

In the second step, we assessed stimulated APs. When stimulating cells at a held resting potential of -75mV with 1nA, 2ms current injection, we demonstrated a significantly faster action potential upstroke and a greater action potential amplitude (**Figure 2.9B-D**) in *GLA* p. *N215S* atrial iPSC-CMs ($p<0.0001$ and $p<0.0001$ respectively). There were no significant changes in APD30, APD50, APD70 or APD90 (data not shown).

The development of DADs in a *GLA* p. *N215S* atrial iPSC-CM stimulated AP is illustrated in (**Figure 2.9E**), compared to a WT control AP without DADs. Quantitative assessment of stimulated APs showed that there were more cells with APs displaying DADs in *GLA* p. *N215S* atrial iPSC-CMs (N=46) compared with WT (N=19) (**Figure 2.9F**) and these cells demonstrated a greater number of DADs per cell ($p=0.0002$).

2.8.4 Greater contraction in atrial GLA p. N215S iPSC-CMs identified.

Findings from MUSCLEMOTION analysis of contraction in the 2D monolayers are summarised in **Figure 2.10**. Graphical representations of contraction and relaxation are illustrated for *GLA* p. *N215S* iPSC-CMs (**Figure 2.10A**) and WT iPSC-CMs (**Figure 2.10B)**. *GLA* p. *N215S* iPSC-CMs generated a significantly longer contraction duration (**Figure 2.10C)** and time to peak (**Figure 2.10D)** (p=0.0055 and p=0.0296 respectively) with a longer peak-to-peak distance (**Figure 2.10H)** (p=0.0032) indicating a slower beat rate compared to WT. Coupled with this, *GLA* p. *N215S* iPSC-CMs also generated a significantly higher contraction and peak amplitude (**Figure 2.10E and F)** compared to WT (p=0.0074 and p=0.0047 respectively). There were no differences in relaxation time observed between *GLA* p. *N215S* iPSC-CMs and WT (**Figure 2.10G**)

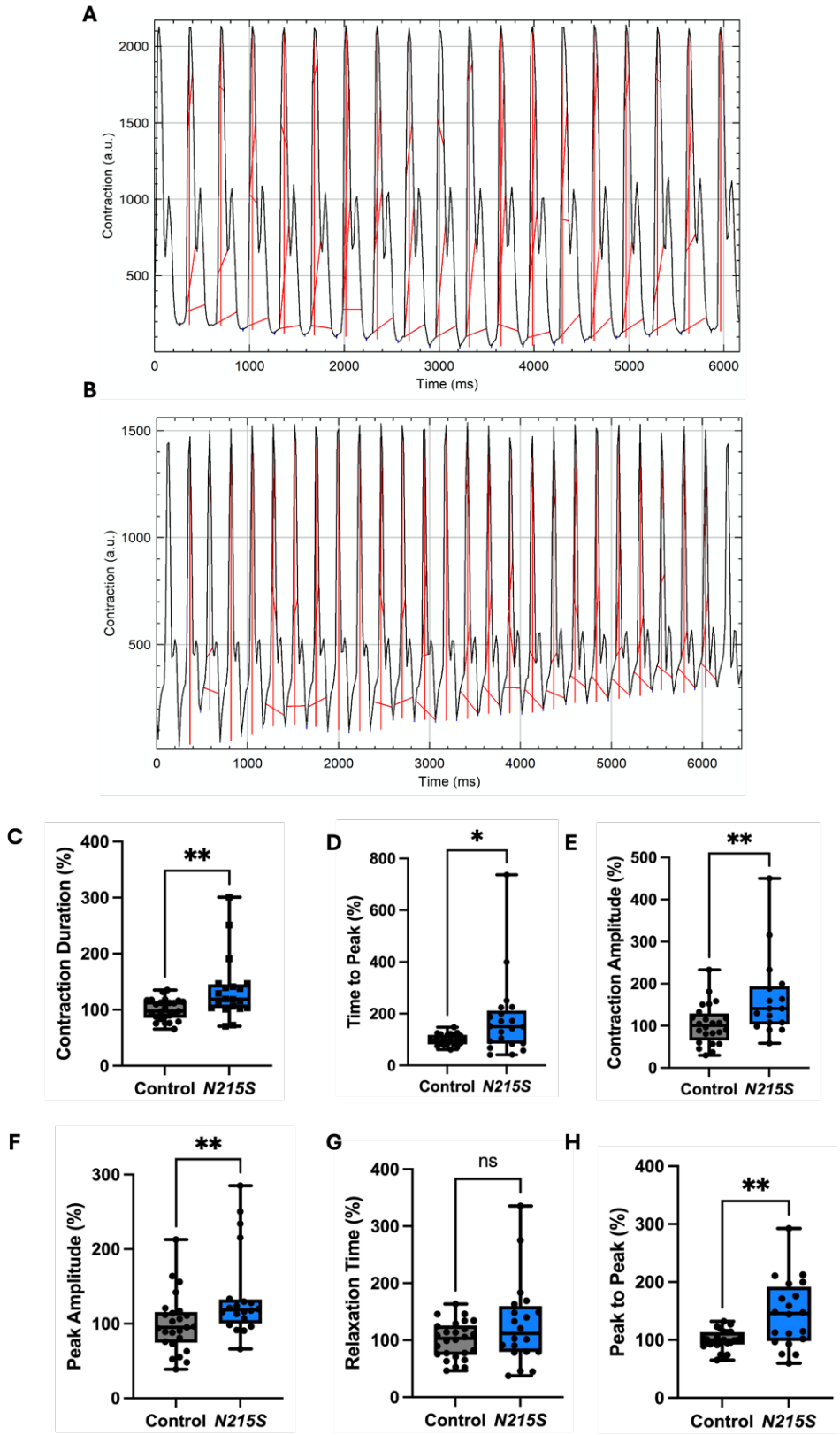

Figure 2.10: (A) Illustration of the outputs from MUSCLEMOTION in an N215S atrial iPSC-CM and (B) WT-iPSC-CM. (C-H) Intervals and contractility parameters from

*atrial iPSC-CMs (N215S vs WT). Values expressed as a percentage difference of the mean value for the WT of each batch. Mann Whitney U statistical test used for Contraction Duration, Time to Peak, Contraction Amplitude, Peak Amplitude and Relaxation time. Welch's unpaired t-test used for Peak-to-Peak time. Data presented as mean ± standard deviation. ns not significant, * p ≤ 0.05, ** p ≤ 0.01.*

Prolonged CTDs in atrial GLA p. N215S iPSC-CMs identified.

To assess calcium handling, optical mapping was performed in the cellular monolayers. CTD was prolonged to all extrusion levels in *GLA* p. *N215S* atrial iPSC-CMs compared to WT controls across the monolayers as demonstrated in the polar maps of each (**Figure 2.11A and 2.11B)**: CTD30 (p=<0.0001), CTD50 (p=<0.0001) and CTD80 (p=<0.0001) (**Figures 2.11D-F)**. Transient morphology was also vastly different in *GLA* p. *N215S* atrial iPSC-CMs compared to WT (**Figure 2.11C**). *GLA* p. *N215S* atrial iPSC-CMs also demonstrated a significantly slower time-to-peak (**Figure 2.11G)** (p=0.0034), and larger peak amplitude (**Figure 2.11H)** (p=0.0004) suggesting a greater total cycling of calcium, and a slower beating frequency (**Figure 2.11I)** (p=<0.0001) consistent with contraction analysis data.

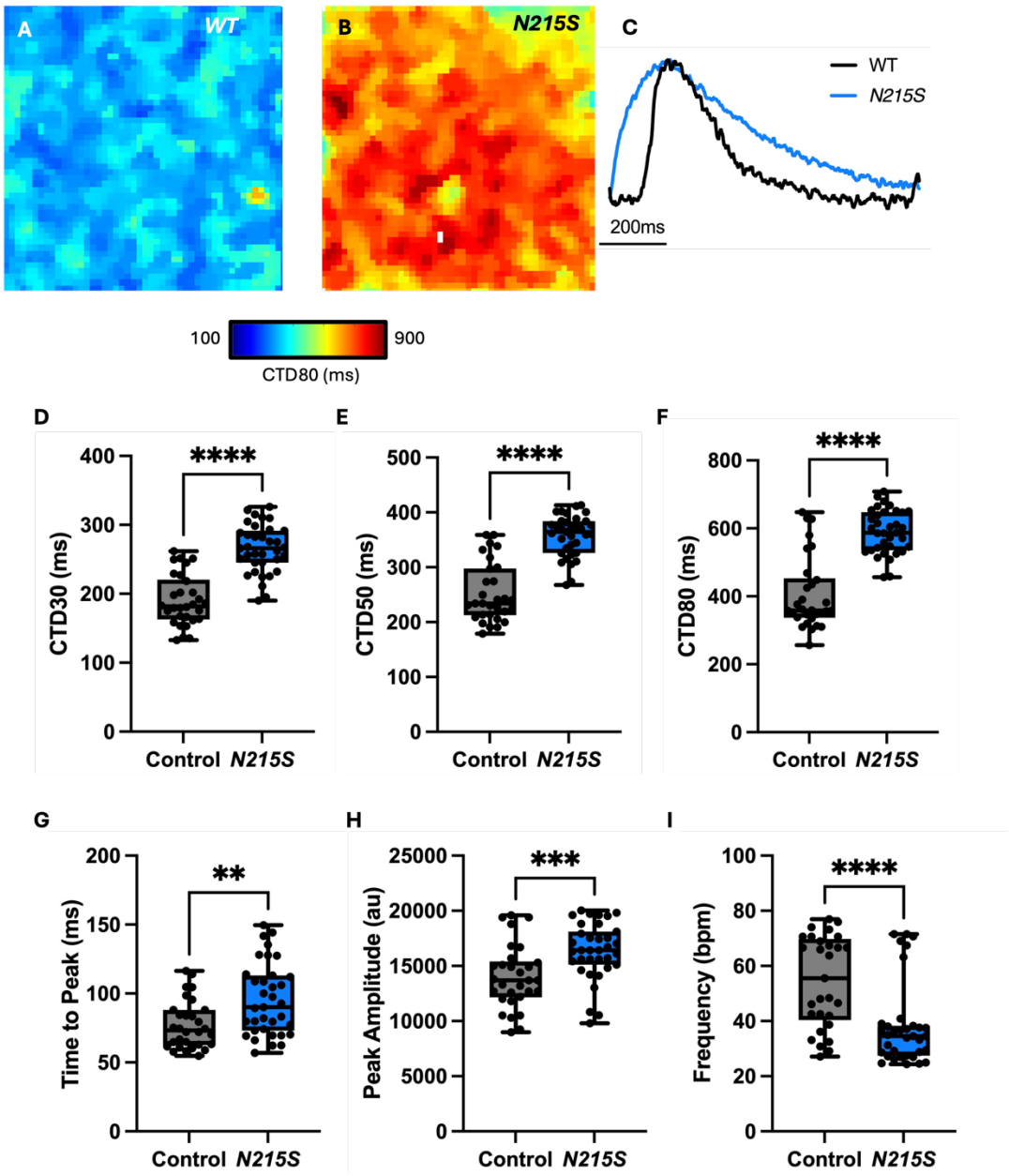

*Figure 2.11: (A) WT atrial iPSC-CM CTD polar map indicating shorter CTDs (blue) (B) N215S atrial iPSC-CM CTD polar map indicating longer CTDs (red) (C) Atrial calcium transients (N215S vs WT) illustrating changes in morphology and CTDs. (D-F) Atrial iPSC-CM CTD30, 50, 80 (N215S vs WT) (G-I) Interval and amplitude parameters (N215S vs WT). Mann Whitney U statistical test used for CTD80, CTD50, Time to peak, Peak Amplitude and Frequency. Welch's Unpaired t-test used for CTD30. Data presented as mean ± standard deviation * $p \leq 0.05$, ** $p \leq 0.01$, *** $p \leq 0.001$, **** $p \leq 0.0001$.*

2.9 Discussion

2.9.1 Early P-Wave changes in Fabry cardiomyopathy

In a deeply phenotyped cohort of FD patients, staged according to degree of cardiomyopathy, we demonstrate P-wave duration and PQ interval shortening in adults with FD and no overt cardiac phenotype that was more pronounced compared age and sex-matched non-FD controls. This has not previously been demonstrated in "phenotype-negative" patients and for the first time suggests early atrial electrical remodelling secondary to Gb3 accumulation in patients with classical disease and in the *GLA* p. *N215S* variant previously thought to be "late-onset". P-wave duration and PQ shortening have been demonstrated previously in a small study of N=30 FD patients without LVH, however these patients did not undergo multiparametric CMR and biomarker assessment to exclude early onset cardiomyopathy due to myocardial Gb3 accumulation (24). Our study demonstrates changes in P-wave characteristics in FD patients with no detectable cardiomyopathy that progress with cardiac disease stage. Crista terminalis and AV nodal Gb3 accumulation may account for P-wave duration shortening via accelerated conduction (29, 87, 88). As cardiac disease stage progresses, P-wave duration and PQ interval prolong, and a positive correlation is observed with LA volume on TTE. These findings suggest multiple mechanisms underlying the pathophysiology of atrial myopathy in FD. Firstly, in early disease, intrinsic electrophysiological cellular changes affecting sodium and calcium, as well as early Gb3 accumulation likely account for the early PQ and P-wave duration shortening on 12-lead ECG which are pro-arrhythmic in nature (25). As Gb3 accumulation progresses and LA volume increases due to the passive effects of elevated LVEDP due to LVH with progressive FD cardiomyopathy, this structural

alteration to the atria results in P-wave duration and PQ prolongation, further adding to the pro-arrhythmic substrate, increasing susceptibility for AF development (148). These mechanisms according to disease stage are summarised in **Figure 2.12**. These are important findings as they provide insight into underpinning mechanisms and may serve as potential biomarkers in the assessment of treatment response.

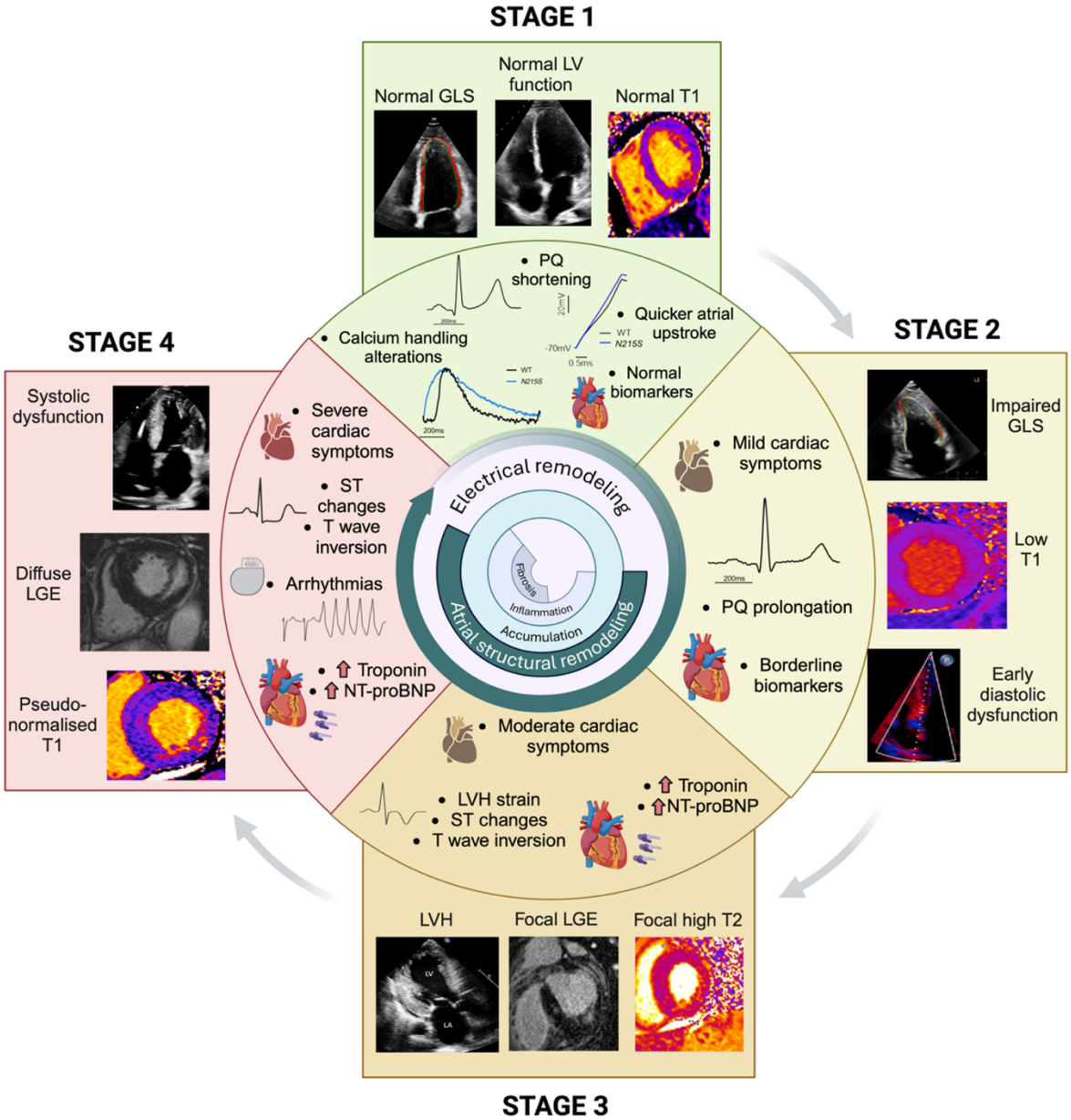

Figure 2.12: Stages of cardiomyopathy in FD. Abbreviations: GLS: global longitudinal strain, LV: left ventricular, LGE: late gadolinium enhancement, LVH: left ventricular

hypertrophy, NT-proBNP: N-terminal-pro brain natriuretic peptide.

2.9.2 Validation of iPSC-CM model

The use of iPSC lines has enabled *in-vitro* work in rare diseases with genetic variants. Gene-edited iPSCs can be differentiated into iPSC-CM via various signalling pathways allowing for the generation of multiple cardiac cell types. We provide mechanistic insight into identified early ECG changes in "phenotype negative" FD patients in this atrial iPSC-CM model of FD. This model suggests that enzyme deficiency and accumulation of unmetabolised Gb3 in atrial cells associated with key alterations in cellular contractility, intracellular calcium handling, AP morphology and DAD occurrence. Pro-arrhythmic properties have been demonstrated in ventricular iPSC-CMs from patient-derived iPSCs with FD including higher spontaneous AP frequency, shorter AP duration, increased sodium current density and increased upstroke velocity; all suggesting increased excitability (97). The same study demonstrated disruption to intracellular calcium handling with transients exhibiting a greater amplitude and reduction in peak-width duration. However, this earlier study did not investigate atrial iPSCs and was not guided by *in-vivo* clinical data.

2.9.3 Changes in atrial electrophysiology

We demonstrate, for the first time, alterations in the atrial APs in *GLA* p. *N215S* iPSC-CMs, which provides mechanistic information underpinning our own, as well as published, clinical data (24). We demonstrate a more positive diastolic membrane potential in *GLA* p. *N215S* iPSC-CMs. Shifting of diastolic membrane potential to a more positive value which is closer to the threshold potential for depolarisation is pro-

arrhythmic as it causes an increase in myocyte excitability and may contribute to an increased risk of ectopic activity (149). We also demonstrate an increased AP upstroke velocity in atrial *N215S* iPSC-CMs compared to WT. The AP upstroke is largely controlled by voltage-gated sodium channels driving the inward sodium current (150). An increase in conduction velocity whilst generally considered anti-arrhythmic, has been proposed as a substrate for arrhythmia in atrial and ventricular CMs (25). It is suggested that rapid intra-atrial conduction velocity counteracts a normally more rapid inter-atrial conduction via Bachmann's bundle, allowing for co-ordinated atrial depolarisation. A shorter AP with a quick upstroke has also been demonstrated in patient-derived stem cell derived ventricular CMs in FD (97). Our findings reflect this in atrial CMs, mimicking the observation of P-wave duration and PQ shortening as the earliest electrical manifestation of FD cardiomyopathy on 12-lead ECG (24). Interpreting the ECG data from adults with FD together with the atrial iPSC-CM stimulated APs, this suggests intrinsic early electrical changes which may be secondary to early Gb3 accumulation, both of which progress insidiously and contribute to the arrhythmia substrate.

2.9.4 Atrial contraction changes

Contraction analysis results demonstrate significantly higher contraction and peak amplitude with prolonged peak-to-peak times in *GLA* p. *N215S* iPSC-CMs compared with WT using a validated tool to assess contraction and relaxation in beating cardiomyocyte monolayers. It is widely understood that in FD, the effects of LVH and elevated LVEDP are reflected in atrial dilatation and dysfunction which may predispose patients to atrial arrhythmia and cardioembolic disease. The reflection of pressure may cause a subsequent increase in atrial contraction force to maintain an

adequate atrial emptying fraction. Impairments in LA strain have been observed in patients with elevated LVEDP and normal LVEF (151). Our study, for the first time, demonstrates intrinsic changes to the properties of atrial myocytes at a cellular level manifesting as changes in contraction force that are not due to passive effects of the elevated LVEDP and LVH. This is in keeping with published clinical data demonstrating that impairments in LA contractile function were weakly associated with parameters of LV diastolic and systolic function, implying primary atrial structural changes accounting for LA strain impairment in FD. (47).

It is also understood that due to a combination of conduction system (29) and neuronal (152) sphingolipid accumulation with subsequent autonomic dysfunction, patients with FD often have a resting sinus bradycardia (42) which may progress to higher degree AV block requiring cardiac device implantation (44). Sinus bradycardia and changes in PR interval on 12-lead ECG can be the earliest features of cardiac involvement in FD (24). The changes observed in this study of a slower beat rate in *GLA* p. *N215S* iPSC-CMs compared to WT are in keeping with published literature and may suggest primary atrial myopathy, with conduction system sphingolipid accumulation as a potential mechanism.

2.9.5 Changes in atrial calcium handling

Another novel finding of this study is the identification of alterations in intracellular calcium handling in atrial *GLA* p. *N215S* iPSC-CMs. Coordinated atrial contraction is dependent on electrical activation and converting this into a mechanical force, i.e. excitation-contraction coupling. This is largely dependent on intracellular intrusion and

extrusion of calcium (153). Our results demonstrate significant effects on the calcium transient, induced directly by the effects of the *GLA* p. *N215S* variant. These include a greater transient amplitude and prolonged duration. Although it should be noted that amplitude measurements from optical mapping of non-ratiometric indicators are influenced by several non-physiological factors including inhomogeneous loading and excitation, together these results suggest an overall increase in calcium that is cycled into and out of the cytosol with each excitation (154). This may therefore explain the increase in contraction force observed in these cells, and also aligns with published data in patient derived ventricular CMs in FD which demonstrate a similar finding of greater amplitude and a greater rising slope with reduced peak width duration (97). Furthermore, the finding of a greater number of atrial *GLA* p. *N215S* iPSC-CMs exhibiting DAD activity compared to WT potentially reflects a greater quantity of intracellular calcium which predispose to DADs (155, 156). DADs can trigger focal activity that can lead to arrhythmogenesis, a potential mechanism explaining the increased arrhythmia burden in these patients, including for AF (157). Furthermore, the higher observed level of DADs in *GLA* p. *N215S* iPSC-CMs may relate to a shift of the diastolic membrane potential in atrial APs to a more positive value, closer to the depolarisation threshold, increasing myocyte excitability and focal ectopic activity risk. Further investigations are required to directly assess sub cellular calcium dynamics in these cells.

2.10 Limitations

This study has several strengths, the primary being the identification of novel atrial mechanisms in FD in an *in-vitro* model that complement *in-vivo* findings in one of the largest ECG studies in a deeply phenotyped cohort of adults with FD. However, there are limitations which need to be considered when interpreting this data. This study involves one of the largest datasets of patients with FD. However, when comparing to studies on related cardiac conditions, the cohort size is comparatively small since FD is a rare disease. The main limitation of the cellular data is that there can be several limitations in the differentiation process when culturing atrial cardiomyocytes which affect the quality and subsequent molecular and functional properties of the cells. To mitigate this, experiments were conducted on multiple batches (minimum of 3) of high-quality cells in a coordinated beating monolayer, suitable for analysis.

2.11 Conclusions

In summary, in this study of adults with FD and atrial iPSC-CMs with the *GLA* p. *N215S* variant for FD, we confirm early P-wave changes in “phenotype negative” patients, supported by our FD atrial model of enzyme deficiency and Gb3 accumulation. In this model, novel cellular changes including alterations in contraction force, intracellular calcium handling, and atrial electrophysiology mimic the early electrical changes observed on 12-lead ECG of FD patients. The identified cellular changes may provoke atrial arrhythmia. This study provides new insights into the underlying mechanisms contributing to the arrhythmic substrate in FD. These identified changes may act as targets for cardioprotective therapy to reduce the burden of arrhythmia, stroke, and sudden cardiac death in FD.

3 Chapter 3 – Longitudinal changes in transthoracic echocardiography and biochemical markers in Fabry Disease

Data from this chapter is based on the first author published article where these data were first presented. The manuscript is currently in press in the Canadian Journal of Cardiology: Open.

3.1 Personal Contribution

I was responsible for data collection for all the patients in the study. I wrote the ethics application for the use of data collected in this chapter for the purposes of research which was approved. I conducted retrospective echocardiography analysis in the assessment of LA strain. I conducted the statistical analysis with support from University Hospitals Birmingham statistician, James Hodson. I wrote the manuscript and led on subsequent revisions

3.2 Background

Advancements in multi-modality cardiovascular imaging have enabled the detection of early FD cardiomyopathy and enhanced monitoring strategies for cardiac disease progression. However, the underpinning mechanisms by which myocardial Gb3 deposition triggers the key features of FD cardiomyopathy such as LVH and fibrosis are not well understood. It is evident however, that hypertrophy is not solely due to the direct effects of Gb3 storage. Based on cross-sectional data (69), a three-phased development process of FD cardiomyopathy has been proposed as follows:

1. Cardiac Gb3 accumulation
2. Myocyte hypertrophy and inflammation
3. Myocardial fibrosis and systolic impairment.

Added to this, cross sectional data also suggest gender dimorphism in cardiomyopathy development in FD. Typically, males develop an earlier onset and more severe form of LVH followed by fibrosis. Females (previously thought to be obligate carriers) develop a milder and later onset cardiac phenotype in which myocardial fibrosis often develops prior to the onset of LVH (19). These cross-sectional data require confirmation by longitudinal assessment.

TTE is the first line modality for assessment of cardiomyopathy in FD and is used routinely for regular clinical view due to ease of access (71). TDI and ventricular and atrial speckle tracking strain have proven useful in the detection of early phase, subclinical cardiomyopathy due to Gb3 accumulation, manifesting prior to the onset of LVH (158-160). Regional LV GLS impairment on TTE, namely in the basal inferolateral LV segment has proven ability to detect myocardial fibrosis comparable to LGE

assessment using CMR (158). Impaired LA strain and early LV diastolic dysfunction may predispose FD patients to adverse cardiac events including atrial arrhythmia, namely AF (47).

Troponin is a reliable biomarker in the assessment of myocardial ischaemia, necrosis and remodelling in various cardiac disease. Its use as a biomarker in the assessment of cardiomyopathy in FD has also been demonstrated (102, 161). Elevated troponin correlated with presence and burden of LGE on CMR in FD, however troponin elevation has been observed in the absence of LGE, highlighting its role as a biomarker in the detection early FD cardiomyopathy. NT-proBNP may increase in the context of pressure overload and increased myocardial wall stress. When used in conjunction with other imaging and biochemical markers, it may have a role in monitoring FD cardiomyopathy in the context of diastolic dysfunction and heart failure (102, 162).

Longitudinal studies documenting the natural history of FD cardiomyopathy using biochemical and TTE parameters in the medium and long term are required to confirm promising cross-sectional data. It is also important to understand if the three-stage model described can be confirmed on TTE and whether early impairments in GLS or TDI may identify changes prior to LVH development that may trigger therapy initiation.

3.3 Hypotheses

Alterations in biochemical and imaging markers on TTE may be sensitive at detecting early onset and progression of FD cardiomyopathy particularly in the early phases of disease. Understanding the rate of progression in biochemical and imaging markers on TTE is important when planning future studies of current and future disease-modifying therapy in FD.

3.4 Aims and Objectives

The primary aim of this chapter was to quantify trends in atrial and ventricular TTE parameters linked to relevant physiological, haematological and biochemical markers from a cohort of patients with FD.

3.5 Methods

3.5.1 Study population

This was a single centre, retrospective, longitudinal study in adults with genetically confirmed FD who have undergone TTE, attending the FD one-stop clinic based at the Centre for Rare Diseases at the Queen Elizabeth Hospital, Birmingham. A genetic diagnosis of FD was confirmed via enzyme assessment of plasma α-Gal A as well as subsequent *GLA* sequencing for confirmation of a disease-causing mutation.

The clinical records for all clinic visits were reviewed between November 2011 and March 2023 to identify patients being followed up during the study period (N=157). Study entry was defined as the date of first TTE performed. Patients were therefore excluded from the study if they did not undergo TTE imaging. Patients attended the one stop clinic for follow up assessment. This began with a detailed clinical history and physical examination. Following this, planned investigations performed on an annual basis included clinical observations, 12-lead ECG, TTE and assessment of biochemical markers. These included relevant cardiac markers, namely high sensitivity troponin and N-terminal pro brain natriuretic peptide (NT-proBNP). The clinic was established with the aim of providing annual face-to-face multi-specialty consultations. However, the impact of the 2019 coronavirus (COVID-19) pandemic reduced outpatient attendances and alternative on-line or telephone consultations were conducted in place. Furthermore, attendance at clinic has taken time to revert to the planned annual review despite the end of the pandemic.

3.5.2 Transthoracic Echocardiography

During the study period, TTE was performed by an accredited sonographer (AMA) using IE33 and EPIC ultrasound systems (Phillips Electronics, Farnborough, United Kingdom), according to the British Society of Echocardiography minimum dataset (140, 163). Diastolic function was assessed, according to existing guidelines (140, 164). Linear internal measurements were obtained from 2D images in the parasternal long axis, measured immediately below mitral valve leaflet tips with LV mass calculated using the Devereux formula (165); 2D volumetric measurements were performed using the biplane summation of discs method, with separate acquisitions optimised for LA volumetric measurement. 2D acquisitions were made at the time of examination for quantification of speckle-tracking strain in each case, following visual assessment of appropriate segmental tracking quality (inadequate quality defined by more than two non-analysable segments), confirmation of two complete consecutive cardiac cycles, absence of ectopy, and a minimum frame rate >40 frames/s. This was using QLAB Cardiac Analysis (Phillips Electronics, Farnborough, United Kingdom) Measures of LA strain were not recorded as part of routine patient follow up in the FD clinic. As such, the apical two-chamber 2D views (with a minimum of two cycle lengths) were retrospectively assessed, where available, by two imaging experts using TomTec off-cart software (Phillips Electronics, Farnborough, United Kingdom). LA strain parameters included LA GLS, LA global circumferential strain (GCS), LA ejection fraction, LA fractional area change, LA end-diastolic volume and LA end-systolic volume. Experts were not blinded to the demographic data and time of the study. Reproducibility was assessed for 10% of the LA strain parameters measured on TTE. Reproducibility of these measurements were assessed using intraclass

classification correlation (ICC) based on a 2-way mixed effects model with absolute agreement.

3.5.3 Data Extraction

The electronic clinical records were reviewed for each patient included in the study, relevant to the patient visit during the study period. Clinical, physiological and biochemical data were extracted for each visit. In some cases, blood tests were not collected on the same day as the TTE. Where this was the case, the blood sample collected closest to the day of the visit was used within a maximum of ± 90 days, where available. With certain biochemical parameters, levels were reported as being lower than a specific value. Where this was the case, a value one significant figure lower than the threshold was assumed for analysis (e.g. a value of 4ng/l for troponin of "<5ng/l"); this impacted albumin: creatinine ratio (ACR) (<2.3mg/mmol; 40% of measurements), troponin (<5ng/l; 21%) and urine protein (<0.005mg/dl; 21%). During the study period, the assay used for quantification of troponin changed. Troponin levels were quantified using a Troponin-T assay when the study commenced. In 2019, the assay used at the QEHB laboratories changes to Troponin-I. As a result, these data were extracted and analysed separately.

Data were also collected for comorbidities at each clinical attendance. Ischaemic heart disease was defined as previous myocardial infarction or prior coronary revascularisation. Diabetes mellitus (DM) included a history of type 1 or type 2 DM, regardless of whether treatment was currently being received. Chronic kidney disease (CKD) was defined as an estimated glomerular filtration rate (eGFR)

<90mL/min/1.73m^2, and divided into stages 1-5 (166). Hypertension was defined based on evidence of a formal diagnosis and the initiation of treatment.

3.6 Ethics

The study was approved by West Midlands South Birmingham Research Ethics Committee (23/WM/0180 IRAS 325613). The study was conducted in accordance with local legislation and institutional requirements. The ethics committee waived the requirement of written informed consent for participation from the participants / legal guardians / next of kin because the data were acquired from a research database using routinely collected clinical data for the purpose of research.

3.7 Statistical analysis

Longitudinal trends in TTE parameters and physiological / biochemical markers were assessed for the cohort of patients who attended at least two visits during the study period. Analyses were performed using a generalised estimating equation (GEE) approach, to account for the non-independence of repeated visits by the same patient. For each visit, the number of years (rounded to the nearest day) from the patient's first visit during the study period was calculated, with the resulting variable set as a continuous covariate in the GEE model. Separate models were produced with each TTE parameter and physiological / biochemical marker as the dependent variable. An autoregressive (AR) (1) correlation structure was assumed, with the within-subjects factor being the timing of the visit relative to the first visit, rounded to the nearest year. Variables that were found to follow positively skewed distributions were $\log_2$-

transformed, prior to the analysis, to normalise the distribution. Negatively skewed distributions were observed for two parameters, LA GCS and LA GLS; since all values of these were negative, the absolute values were taken to reverse the direction of the skew, before applying a $\log_2$-transformation. The direction of the resulting gradient was then reversed, to undo the transformation.

The goodness-of-fit of each GEE model was assessed by examination of the distribution of the residuals and of the predicted vs. residual plots. Where these indicated non-linearity, variables were $\log_2$-transformed, and the GEE analyses were repeated. Coefficients from the GEE models are reported as gradients per year throughout. For parameters where the units were percentages (e.g. LV ejection fraction), gradients represent percentage point (pp) changes per year; for example, a gradient of 10pp per year would represent an increase from 40% to 50% in one year. For parameters that had been $\log_2$-transformed for analysis (e.g. LA GCS), the resulting gradients were anti-logged and converted to percentage increases per year; for example, a gradient of 10% per year would represent an increase from 40% to 44% in a year. The GEE models were also extended to additionally include two additional factors, namely gender, and the interaction between gender and the timing of the visit. As such, these models allowed gradients to be estimated separately for male and female patients, with the p-values for the interaction term representing a comparison between these.

The changes over time in selected TTE parameters/blood markers were then compared, to identify correlations between the observed trends. Initially, linear

regression models were produced for each patient separately, with a TTE parameter/blood marker as the dependent variable, and the timing of the visit as a covariate. Those variables that were found to have non-linear trends over time in the primary analysis of longitudinal trends were log_2-tranformed, as previously described. The gradients from the resulting models were then used to summarise the rate of change in the variable for each patient. Correlations between these gradients were then quantified using Spearman's rank correlation coefficients (rho); only those patients with data for more than two assessments for the pair of TTE parameters/blood markers being compared were included in this analysis, as gradients estimated from only two points would be unreliable. Where significant correlations were detected, regression models were produced to further visualise the associations between the trends.

All analyses were performed using IBM SPSS 24 (IBM Corp. Armonk, NY), with $p<0.05$ deemed to be indicative of statistical significance throughout. Continuous variables are reported as *mean ± standard deviation (SD)* where approximately normally distributed, with non-normal variables reported as *median (interquartile range; IQR)*, unless stated otherwise. Missing data was addressed using pairwise deletion; specifically, visits where data were unavailable for some TTE parameters or physiological / biochemical markers were only excluded from the analyses of the affected parameters/markers.

3.8 Results

3.8.1 Cohort characteristics

157 patients attended the FD clinic between November 2011 (when the one-stop clinic model was introduced) and March 2023 (the date of data collection). Of these, 119 patients had data available for at least one TTE and so were included in the study. 38 patients did not have TTE data available with reasons including poor quality images, remote follow up, non-attendance or deemed not clinically indicated. In those with TTE data available, median age at first clinic visit was 50 years (IQR 34;60) and 67 (56%) were female. 38 (32%) were taking ERT as of March 2023 (22 had previously taken ERT but since discontinued) and 35 (29%) were taking OCT as of March 2023 (3 had previously taken OCT but since discontinued). 39 (33%) were taking an angiotensin converting enzyme inhibitor (ACE-i) and 52 (44%) were taking a statin as of March 2023.

Of the 119 patients with TTE data available, 44 had a single visit during the study visit with reasons highlights in the study flowchart (**Figure 3.1**). Longitudinal data was therefore available for the remaining 75 patients attending more than one clinic visit, who attended a total of 305 visits (median: 4 per patient, range 2-10) over a median off 55 months (IQR 28-82). The characteristics of the full cohort (N=119), and the subgroup of patient with longitudinal data follow-up (N=75) are reported in **Table 3.1**, with TTE parameters at the first visit summarised in **Table 3.2**.

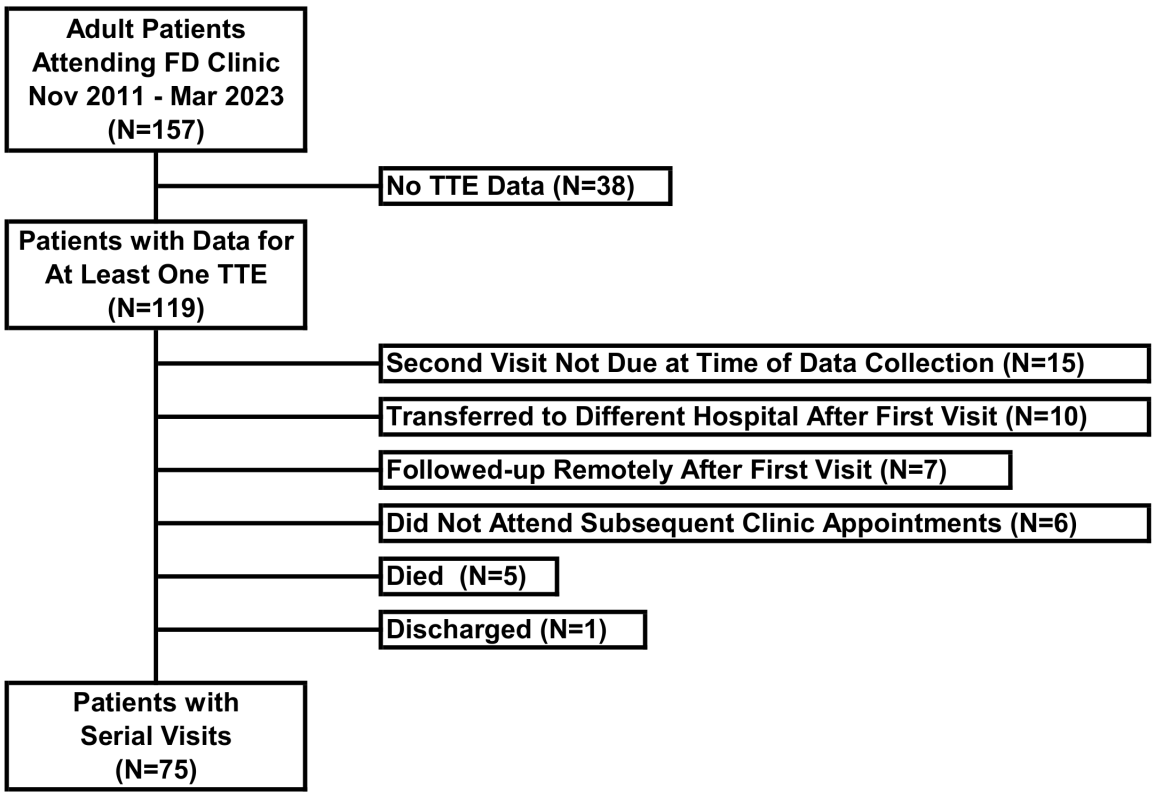

Figure 3.1: Study Flowchart

	Whole FD Cohort (N=119)		Cohort with Serial Visits (N=75)	
	N	***Statistic***	***N***	***Statistic***
Total Number of Visits	119	2 (1, 4)	75	4 (2, 5)
First to Last Visit (Months)	119	25 (0, 69)	75	55 (28, 82)
Age (Years)	119	50 (34, 60)	75	50 (37, 59)
Gender (% Female)	119	67 (56%)	75	40 (53%)
Mutation (% Classical)	119	59 (50%)	75	35 (47%)
Body Surface Area (m^2)	118	1.85 ± 0.25	74	1.85 ± 0.24
Heart Rate (bpm)	119	66 ± 14	75	64 ± 13
Comorbidities				
Diabetes Mellitus	118	7 (6%)	75	5 (7%)
Hypertension	118	27 (23%)	75	17 (23%)
Hypercholesterolemia	118	28 (24%)	75	20 (27%)
Ischaemic Heart Disease	118	9 (8%)	75	5 (7%)
Stroke	118	7 (6%)	75	3 (4%)
Angiokeratoma	118	11 (9%)	75	7 (9%)
Chronic Kidney Disease	118		75	
No		61 (52%)		33 (44%)
Stage 1		14 (12%)		10 (13%)
Stage 2		24 (20%)		18 (24%)
Stage 3a		7 (6%)		5 (7%)
Stage 3b		3 (3%)		3 (4%)
Stage 4		4 (3%)		3 (4%)
Stage 5		4 (3%)		3 (4%)
Unknown Stage [a]		1 (1%)		-
Physiological and Biochemical Markers				

Creatinine (µmol/l)	111 76 (61, 91)	71 79 (66, 100)
Haemoglobin (g/l)	96 137 ± 14	60 137 ± 15
Cholesterol (mmol/l)	104 4.8 ± 1.2	67 4.7 ± 1.0
Troponin-I (ng/l)	38 7 (4, 51)	15 21 (4, 81)
Troponin-T (ng/l)	44 13 (5, 30)	31 10 (4, 37)
NT-proBNP (ng/l)	94 144 (59, 863)	59 144 (58, 1066)
ACR (mg/mmol)	104 2.2 (2.2, 11.6)	66 2.5 (2.2, 15.2)
Urine Protein (mg/dl)	104 0.015 (0.005, 0.079)	66 0.017 (0.004, 0.093)
Systolic BP (mmHg)	119 133 ± 17	75 133 ± 17
Diastolic BP (mmHg)	119 78 ± 10	75 77 ± 10

Table 3.1 – Cohort characteristics at first visit. Data are reported as "N (%)", "median (interquartile range)", or as "mean ± standard deviation", as appropriate. [a] One patient was known to have chronic kidney disease, but had no stage recorded. ACR=Albumin:creatinine ratio, BP=Blood pressure, FD=Fabry disease.

	Whole FD Cohort (N=119)		**Cohort with Serial Visits (N=75)**	
	N	***Statistic***	***N***	***Statistic***
Ventricular Dimensions, Volume and Function				
LVIVSd (cm)	118	1.2 (1.0, 1.6)	74	1.3 (1.0, 1.6)
LVEDd (cm)	118	4.5 ± 0.6	74	4.4 ± 0.4
LVPWd (cm)	118	1.2 ± 0.3	74	1.2 ± 0.3
LVESd (cm)	109	2.9 ± 0.5	67	2.9 ± 0.4
LVEDvol 2D (ml)	90	89 ± 28	54	87 ± 27

LVESvol 2D (ml)	90	33 (26, 41)	54	32 (25, 40)
LVEF-BP (%)	90	62 ± 6	53	63 ± 5
MAPSE (cm)	101	14 ± 4	65	14 ± 4
TAPSE (cm)	106	22 ± 4	66	22 ± 4
LVM (g)	118	187 (142-281)	74	196 (143-292)
LVMi (g/m^2)	117	102 (78-148)	73	104 (80-153)
LV MWT (cm)	118	1.3 ± 0.4	74	1.4 ± 0.4
GLS A4C (%)	60	-17.5 ± 3.7	31	-17.6 ± 3.3
Valves				
MV E max (m/s)	116	81 ± 20	73	80 ± 20
MV A max (m/s)	111	65 ± 19	70	65 ± 19
E/A	111	1.36 ± 0.61	70	1.34 ± 0.56
AV Vmax (m/s)	113	130 (117, 148)	71	131 (118, 150)
LVOT Vmax (m/s)	113	103 (92, 120)	69	106 (93, 120)
TV E (m/s)	99	56 ± 15	61	55 ± 15
TV A (m/s)	92	43 ± 12	56	43 ± 12
TR Vmax (cm/s)	51	219 ± 35	35	214 ± 34
Tissue Doppler Imaging				
TDI Lat s (cm/s)	117	9 ± 3	74	9 ± 3
TDI Lat e (cm/s)	117	11 ± 5	74	11 ± 5
TDI Lat a (cm/s)	110	8 ± 2	69	8 ± 2
TDI Sep s (cm/s)	115	8 ± 2	73	8 ± 2
TDI Sep e (cm/s)	115	9 ± 4	72	8 ± 4
TDI Sep a (cm/s)	109	8 ± 2	68	8 ± 2
TDI RV s (cm/s)	93	13 ± 2	57	13 ± 3
TDI RV e (cm/s)	90	12 ± 4	56	11 ± 4
TDI RV a (cm/s)	86	12 ± 3	53	12 ± 3

Atrial Dimensions and Function		
LAV (ml)	112 43 (35, 57)	69 43 (33, 60)
LA Vi index (ml/m^2)	105 22 (18, 29)	63 23 (18, 31)
LA GCS (%)	94 -26 (-45, -11)	57 -33 (-50, -14)
LA GLS (%)	94 -27 (-35, -15)	57 -28 (-38, -15)
LA EF (%)	94 48 ± 19	57 51 ± 20
LA EDV (ml)	94 28 (17, 40)	57 27 (15, 38)
LA ESV (ml)	94 56 (38, 73)	57 56 (38, 72)
LA FAC (%)	94 36 ± 15	57 39 ± 17

Table 3.2 – TTE parameters at first visit Data are reported "median (interquartile range)", or as "mean ± standard deviation", as appropriate. Abbreviations for TTE parameters are defined in Supplementary Table 1.

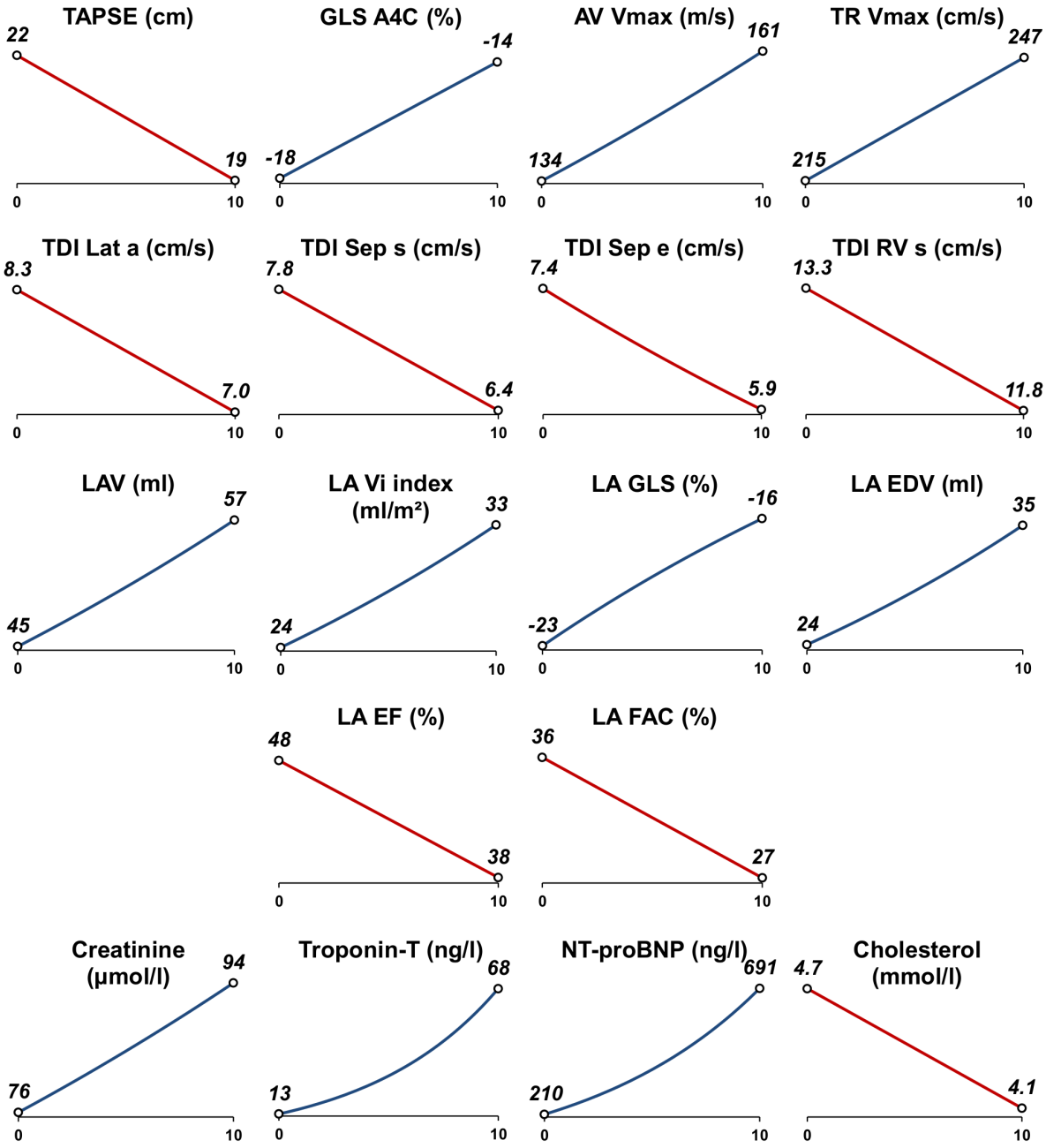

Figure 3.2 – Significant longitudinal changes in TTE and biochemical parameters. Diagrams visualise the generalised estimating equation models in Table 3/Table 4 for parameters found to have significant trends over time. The x-axis represents the number of years from the first scan, with points representing the modelled levels at

the time of the first scan, and after ten years of follow-up. Positive and negative trends are represented by blue and red lines, respectively

3.8.2 Trends in TTE parameters

In the 75 patients with more than one visit, longitudinal trends were performed, the results of which are reported in **Table 3.3**. Significant trends are visualised in **Figure 3.2**. Key findings are summarised below:

3.8.2.1 Ventricles

Ventricular dimensions did not significantly change on longitudinal follow up. There was also no significant change over time in LVM or LVMi, with LVEF remaining stable. However, there were significant impairments over time observed for TAPSE and GLS apical 4-chamber (A4C). Significant changes were also observed in TDI, with septal s', septal e', lateral a' and RV s' all decreasing over time.

3.8.2.2 Atria

Longitudinal assessment of atrial changes was then conducted. On volumetric assessment, LA volume, indexed LA volume and LA end-diastolic volume (EDV) all increased significantly over time. On atrial functional assessment, LA GLS became significantly more impaired, with LA ejection fraction (EF) and LA fractional area change (FAC) both decreasing over time. For the atrial parameters measured retrospectively, following study visit, interobserver variability between assessors was calculated using the intraclass correlation coefficient. When interpreting the intraclass correlation coefficient, values less than 0.5 are indicative of poor reliability, values

between 0.5 and 0.75 indicate moderate reliability, values between 0.75 and 0.9 indicate good reliability, and values greater than 0.90 indicate excellent reliability (167). The intraclass correlation coefficient for each LA parameter ranged between 0.98 and 1 indicating excellent reliability between observers. Values for each parameter are highlighted in **Table 3.4**.

3.8.2.3 Valve Disease

Longitudinal valvular assessment was then conducted. In patients with tricuspid regurgitation (TR) where a trace could be measured, TR maximum velocity (Vmax) increased significantly over time. There were no clinically significant changes noted in the mitral valve (MV) and aortic valve (AV) forward velocities or regurgitation or in MV inflow.

	N Pt.	***N Vis.***	***Gradient per Year (95% CI)***	***p-Value***
Ventricular Dimensions, Volume and Function				
LVIVSd (% per Year) [a]	75	299	0.1% (-0.8%, 1.0%)	0.852
LVEDd (cm per Year)	75	299	0.01 (-0.02, 0.04)	0.436
LVPWd (cm per Year)	75	299	0.01 (0.00, 0.02)	0.162
LVESd (cm per Year)	75	283	0.00 (-0.02, 0.02)	0.825
LVEDvol 2D (% per Year) [a]	73	236	1.1% (-0.3%, 2.6%)	0.126
LVESvol 2D (% per Year) [a]	73	235	1.3% (-0.5%, 3.1%)	0.157
LVEF-BP (pp per Year) [b]	73	234	-0.21 (-0.47, 0.05)	0.111
MAPSE (% per Year) [a]	75	232	-1.2% (-2.5%, 0.0%)	0.052

TAPSE (cm per Year)	75	278	-0.31 (-0.52, -0.10)	**0.004**
LVM (% per Year) [a]	75	299	0.6% (-0.5%, 1.7%)	0.287
LVMi (% per Year) [a]	75	296	0.8% (-0.4%, 1.9%)	0.197
LV MWT (cm per Year)	75	299	0.00 (-0.01, 0.01)	0.785
GLS A4C (pp per Year) [b c]	69	174	0.37 (0.12, 0.63)	**0.004**
Valves				
MV E max (m/s per Year)	75	296	-0.03 (-0.66, 0.61)	0.937
MV A max (m/s per Year)	71	268	0.81 (-0.27, 1.88)	0.140
E/A (% per Year) [a]	71	268	-0.9% (-2.7%, 1.0%)	0.358
AV Vmax (% per Year) [a]	75	293	1.9% (0.6%, 3.1%)	**0.003**
LVOT Vmax (% per Year) [a]	75	288	0.0% (-1.2%, 1.1%)	0.939
TV E (m/s per Year)	74	238	-0.23 (-0.87, 0.42)	0.487
TV A (m/s per Year)	71	213	0.46 (-0.31, 1.23)	0.246
TR Vmax (cm/s per Year)	56	147	3.2 (0.9, 5.5)	**0.007**
Tissue Doppler Imaging				
TDI Lat s (cm/s per Year)	75	290	-0.11 (-0.22, 0.01)	0.064
TDI Lat e (% per Year) [a]	75	289	-1.3% (-3.0%, 0.3%)	0.115
TDI Lat a (cm/s per Year)	73	264	-0.13 (-0.23, -0.02)	**0.017**
TDI Sep s (cm/s per Year)	75	282	-0.13 (-0.20, -0.06)	**<0.001**
TDI Sep e (% per Year) [a]	74	278	-2.2% (-3.7%, -0.7%)	**0.003**
TDI Sep a (cm/s per Year)	71	252	-0.07 (-0.16, 0.02)	0.153
TDI RV s (cm/s per Year)	75	236	-0.15 (-0.29, 0.00)	**0.046**
TDI RV e (cm/s per Year)	74	229	-0.08 (-0.27, 0.11)	0.394
TDI RV a (cm/s per Year)	70	212	-0.11 (-0.34, 0.12)	0.339
Atrial Dimensions and Function				
LAV (% per Year) [a]	75	287	2.4% (0.3%, 4.5%)	**0.022**

LA Vi index (% per Year) [a]	75	268	3.4% (1.5%, 5.4%)	**<0.001**
LA GCS (% per Year) [a c d]	74	238	3.2% (-0.9%, 7.1%)	0.127
LA GLS (% per Year) [a c d]	74	238	3.4% (0.7%, 6.0%)	**0.014**
LA EF (pp per Year) [b]	74	238	-0.99 (-1.80, -0.17)	**0.018**
LA EDV (% per Year) [a]	74	238	4.1% (0.9%, 7.3%)	**0.012**
LA ESV (% per Year) [a]	74	238	1.5% (-0.8%, 3.8%)	0.211
LA FAC (pp per Year) [b]	74	236	-0.83 (-1.41, -0.26)	**0.005**

Table 3.3 – Longitudinal trends in TTE parameters. Results are from generalised estimating equation models on patients with at least two visits (N=75), with the stated TTE parameter as the dependent variable, and the timing of the visit as a covariate. Gradients represent the yearly increases in the stated parameter and are reported alongside 95% confidence intervals (95% CIs). Bold p-values are significant at p<0.05. N Pt./N Vis. represent the number of patients/visits included in each analysis. [a] Values were log_2-transformed prior to analysis, to improve model fit; the resulting gradients were then anti-logged and converted to percentage increases per year. [b] For TTE parameters that are measured as percentages, the gradients represent percentage point (pp) increases per year; for example, a gradient of 1 would represent an increase from 4% to 5% in one year. [c] GCS and GLS values were recorded as negative percentages; hence, the positive gradient indicates a longitudinal trend towards zero. [d] To normalise the negatively skewed distribution, absolute values were taken, to convert values from negative to positive, which were subsequently log_2-transformed; the direction of the resulting gradient was then reversed to reflect the original scale.

Parameter	***Intraclass correlation coefficient***
LA GCS	0.99 (0.99-1)
LA GLS	0.98 (0.93-0.99)
LA EF	0.99 (0.99-1)
LA EDV	1 (0.99-1)
LA ESV	0.99 (0.99-1)
LA FAC	1 (0.99-1)

Table 3.4 – Intraclass correlation coefficient for LA parameters. Intraclass correlation coefficient calculation assessing for interobserver variability in the measurement of LA parameters on TTE. Values expressed as coefficient and 95% confidence intervals.

	N Pt.	***N Vis.***	***Gradient per Year (95% CI)***	***p-Value***
Haemoglobin (g/l per Year)	74	226	-0.58 (-1.38, 0.23)	0.160
Creatinine (% per Year) [a b]	68 [b]	249 [b]	2.2% (0.7%, 3.6%)	**0.004**
Troponin-I (% per Year) [a]	64	115	3.6% (-5.9%, 14.1%)	0.471
Troponin-T (% per Year) [a]	56	101	18.0% (8.2%, 28.7%)	**<0.001**
NT-proBNP (% per Year) [a]	73	237	12.6% (5.5%, 20.2%)	**<0.001**
ACR (% per Year) [a]	73	239	3.9% (-1.3%, 9.5%)	0.145
Urine Protein (% per Year) [a]	71	234	2.5% (-4.3%, 9.8%)	0.484
Cholesterol (mmol/l per Year)	74	258	-0.06 (-0.10, -0.02)	**0.007**
Systolic BP (mmHg per Year)	75	305	-0.46 (-1.00, 0.08)	0.096

Diastolic BP (mmHg per Year)	75 305	0.15 (-0.27, 0.57)	0.480

Table 3.5 – Longitudinal trends in physiological and biochemical markers Results are from generalised estimating equation models on patients with at least two visits (N=75), with the stated physiological / biochemical marker as the dependent variable, and the timing of the visit as a covariate. Gradients represent the yearly increases in the stated parameter and are reported alongside 95% confidence intervals (95% CIs). Bold p-values are significant at p<0.05. N Pt./N Vis. represent the number of patients/visits included in each analysis. [a] Values were log_2-transformed prior to analysis, in order to improve model fit; the resulting gradients were then anti-logged and converted to percentage increases per year. [b] Analysis of creatinine excluded patients with chronic kidney disease stage 4 or 5 at baseline (N=6), to improve model fit. ACR=Albumin:creatinine ratio, BP=Blood pressure.

3.8.3 *Trends in physiological and biochemical markers*

Analysis of physiological and biochemical markers are reported in **Table 3.5**, with significant trends visualised in **Figure 3.2**. This found a tendency for progressive heart disease, with significant increases over time in NT-proBNP and troponin-T; no significant trend in troponin-I was observed. Neither systolic nor diastolic blood pressure were found to change significantly over time. Initial analysis of creatinine produced a poor fitting model, due to the high values in those with advanced CKD being extreme outliers. As such, the six patients with stage 4-5 CKD at the first visit were excluded from the analysis, to produce a reliable model for the remainder of the cohort; this found creatinine levels to increase significantly over time. A significant

reduction over time in cholesterol levels were also observed. Since NT-proBNP increased significantly over time, a post-hoc decision was made to identify other TTE parameters that changed in parallel with NT-proBNP. This found increases over time in NT-proBNP to significantly correlate with increases in LV mass, indexed LV mass, LV GLS A4C and LA GCS, and a reduction in Biplane LVEF (**Table 3.6 and Figure 3.3**).

	N	Rho	p-Value
Ventricular Dimensions, Volume and Function			
LVIVSd [a]	45	0.246	0.104
LVEDd	45	0.254	0.093
LVPWd	45	0.041	0.790
LVESd	45	0.133	0.382
LVEDvol 2D [a]	38	0.031	0.852
LVESvol 2D [a]	38	0.217	0.190
LVEF-BP	37	-0.425	**0.009**
MAPSE [a]	40	-0.284	0.075
TAPSE	45	-0.118	0.438
LVM [a]	45	0.366	**0.013**
LVMi [a]	45	0.347	**0.020**
LV MWT	45	0.250	0.098
GLS A4C [b]	26	0.416	**0.035**
Valves			
MV E max	45	0.052	0.733

MV A max	43	-0.293	0.056
E/A [a]	43	0.262	0.089
AV Vmax [a]	45	0.076	0.618
LVOT Vmax [a]	45	-0.059	0.701
TV E	41	0.187	0.243
TV A	36	0.042	0.808
TR Vmax	21	0.208	0.366
Tissue Doppler Imaging			
TDI Lat s	44	0.171	0.268
TDI Lat e [a]	44	0.066	0.669
TDI Lat a	41	-0.145	0.366
TDI Sep s	43	-0.111	0.480
TDI Sep e [a]	43	0.095	0.546
TDI Sep a	40	-0.192	0.235
TDI RV s	42	-0.164	0.300
TDI RV e	40	0.133	0.413
TDI RV a	38	0.195	0.240
Atrial Dimensions and Function			
LAV [a]	43	-0.038	0.810
LA Vi index [a]	42	0.005	0.977
LA GCS [a b c]	40	0.313	**0.049**
LA GLS [a b c]	40	0.298	0.062
LA EF	40	-0.220	0.172
LA EDV [a]	40	0.106	0.515
LA ESV [a]	40	0.072	0.659
LA FAC	40	-0.165	0.310

Table 3.6 – Correlations between trends in NT-proBNP and trends in TTE parameters. Initially, linear regression models were produced for each patient separately, with the stated TTE parameter as the dependent variable, and the timing of the visit as a covariate. TTE parameters that were found to have non-linear trends over time were log_2-transformed prior to analysis, to improve model fit. The gradients from the resulting models were then used to summarise the rate of change in the TTE parameter for each patient. The rate of change in NT-proBNP for each patient was then estimated using the same approach. Spearman's rho correlation coefficients were then used to compare the rate of change in NT-proBNP to that of each TTE parameter. These analyses included only those patients with data for more than two assessments of NT-proBNP and the TTE parameter being analysed, as gradients estimated from only two points would be unreliable. Bold p-values are significant at $p<0.05$. [a] Values were log_2-transformed prior to analysis, in order to improve model fit. [b] GCS and GLS values were recorded as negative percentages; hence, the positive gradient indicated a longitudinal trend towards zero. [c] To normalise the negatively skewed distribution, absolute values were taken, to convert values from negative to positive, which were subsequently log_2-transformed; the direction of the resulting gradient was then reversed to reflect the original scale.

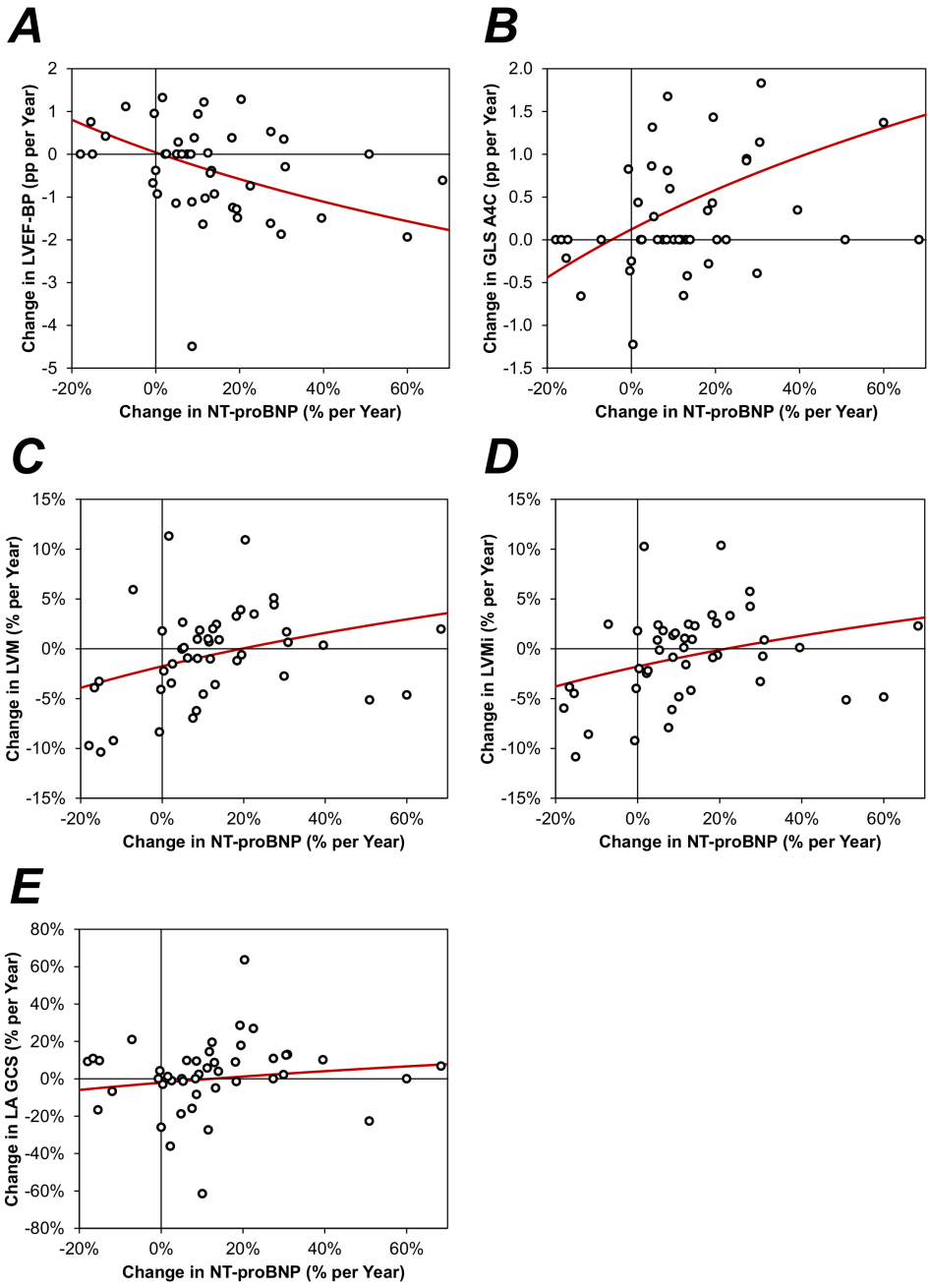

Figure 3.3 – Correlations between trends in NT-proBNP and trends in TTE parameters. Points represent the gradients for individual patients. Trend lines are from regression models, with the gradient in the stated TTE parameter as the dependent variable, and the NT-proBNP gradient as a covariate. For parameters that were log_2-transformed prior to analysis, the gradients for individual patients and

trend line from the resulting regression model were converted to percentage increases per year for the plots, to simplify interpretation. pp=percentage point.

3.8.4 Subgroup analysis by gender

Longitudinal trends in TTE parameters and physiological / biochemical markers were then quantified separately for male and female patients (**Table 3.7**). This found significant interaction effects for LV end-diastolic dimension (LVEDd), 2D LV end-diastolic volume (LVEDvol 2D) and MV E-max, all of which had greater increases over time in males, compared to females. Indexed LV mass was also found to be significantly increasing over time in males but not females, whilst TDI Lateral e' showed a significant decrease over time in females. Of the biochemical markers considered, a significant interaction effect was observed for haemoglobin, which was found to be decreasing over time in males but not in females, whilst ACR and urine protein were found to be significantly increasing in males but not females. Of note, within the 39 patients taking an ACE-i, 17 were male.

	Female		**Male**		**Interaction p-Value**
	Gradient (95% CI)	***p-Value***	***Gradient (95% CI)***	***p-Value***	
Ventricular Dimensions, Volume and Function					
LVIVSd (% per Year) [a]	0.1% (-1.1%, 1.4%)	0.823	-0.3% (-1.3%, 0.7%)	0.602	0.620
LVEDd (cm per Year)	-0.02 (-0.05, 0.01)	0.125	0.05 (0.00, 0.09)	**0.048**	**0.014**
LVPWd (cm per Year)	0.01 (0.00, 0.03)	**0.013**	0.00 (-0.01, 0.01)	0.985	0.127
LVESd (cm per Year)	-0.01 (-0.03, 0.02)	0.659	0.00 (-0.03, 0.04)	0.886	0.715
LVEDvol 2D (% per Year) [a]	-0.6% (-2.1%, 1.0%)	0.470	2.8% (0.6%, 5.0%)	**0.011**	**0.013**

LVESvol 2D (% per Year) [a]	0.1% (-1.4%, 1.7%)	0.850	2.5% (-0.3%, 5.4%)	0.086	0.156
LVEF-BP (pp per Year) [b]	-0.22 (-0.50, 0.05)	0.112	-0.19 (-0.60, 0.22)	0.358	0.896
MAPSE (% per Year) [a]	-1.7% (-3.5%, 0.0%)	0.053	-0.5% (-2.2%, 1.3%)	0.582	0.326
TAPSE (cm per Year)	-0.46 (-0.74, -0.17)	**0.002**	-0.16 (-0.46, 0.14)	0.302	0.162
LVM (% per Year) [a]	0.3% (-1.2%, 1.8%)	0.716	1.3% (-0.3%, 2.9%)	0.106	0.357
LVMi (% per Year) [a]	0.0% (-1.6%, 1.5%)	0.958	1.8% (0.3%, 3.3%)	**0.019**	0.101
LV MWT (cm per Year)	0.01 (-0.01, 0.02)	0.431	-0.01 (-0.02, 0.01)	0.499	0.300
GLS A4C (pp per Year) [b c]	0.20 (-0.08, 0.48)	0.169	0.55 (0.25, 0.84)	**<0.001**	0.092
Valves					
MV E max (m/s per Year)	-0.61 (-1.43, 0.22)	0.148	0.68 (-0.22, 1.57)	0.140	**0.039**
MV A max (m/s per Year)	0.56 (-0.42, 1.55)	0.259	1.12 (-0.88, 3.13)	0.272	0.624
E/A (% per Year) [a]	-1.6% (-3.3%, 0.2%)	0.082	0.0% (-3.4%, 3.5%)	0.998	0.424
AV Vmax (% per Year) [a]	2.1% (0.6%, 3.6%)	**0.005**	1.7% (-0.4%, 3.8%)	0.119	0.743
LVOT Vmax (% per Year) [a]	-0.1% (-1.0%, 0.9%)	0.869	0.1% (-2.2%, 2.4%)	0.952	0.904
TV E (m/s per Year)	0.03 (-0.94, 1.01)	0.946	-0.48 (-1.34, 0.38)	0.270	0.436
TV A (m/s per Year)	0.74 (-0.31, 1.79)	0.169	0.18 (-0.96, 1.32)	0.752	0.484
TR Vmax (cm/s per Year)	1.4 (-1.9, 4.8)	0.397	4.5 (1.2, 7.8)	**0.007**	0.197
Tissue Doppler Imaging					
TDI Lat s (cm/s per Year)	-0.13 (-0.25, -0.02)	**0.025**	-0.08 (-0.27, 0.12)	0.435	0.628
TDI Lat e (% per Year) [a]	-3.2% (-5.2%, -1.1%)	**0.003**	0.9% (-1.5%, 3.3%)	0.467	**0.010**
TDI Lat a (cm/s per Year)	-0.16 (-0.31, -0.01)	**0.032**	-0.10 (-0.25, 0.06)	0.220	0.555
TDI Sep s (cm/s per Year)	-0.16 (-0.24, -0.08)	**<0.001**	-0.09 (-0.20, 0.01)	0.087	0.313
TDI Sep e (% per Year) [a]	-3.3% (-5.1%, -1.5%)	**<0.001**	-1.1% (-3.4%, 1.3%)	0.355	0.142
TDI Sep a (cm/s per Year)	-0.07 (-0.19, 0.05)	0.274	-0.06 (-0.20, 0.07)	0.361	0.948
TDI RV s (cm/s per Year)	-0.24 (-0.41, -0.07)	**0.007**	-0.05 (-0.27, 0.17)	0.649	0.188

TDI RV e (cm/s per Year)	-0.16 (-0.40, 0.08)	0.188	0.00 (-0.29, 0.29)	0.992	0.405
TDI RV a (cm/s per Year)	-0.20 (-0.53, 0.12)	0.218	-0.01 (-0.34, 0.31)	0.930	0.419

Table 3.7 - Longitudinal trends in TTE parameters and physiological / biochemical markers by gender. Results are from generalised estimating equation models on patients with at least two visits (N=75), with the stated parameter as the dependent variable, and the timing of the visit, gender and an interaction term as covariates. The models were then evaluated to estimate the yearly gradients for each parameter for the male and female subgroups separately, which are reported alongside 95% confidence intervals (95% CIs). The p-value for the interaction term represents a comparison between these two gradients. Bold p-values are significant at p<0.05. Definitions of the TTE parameter abbreviations are reported in Supplementary Table 1. [a] *Values were* log_2*-transformed prior to analysis, in order to improve model fit; the resulting gradients were then anti-logged and converted to percentage increases per year.* [b] *For TTE parameters that are measured as percentages, the gradients represent percentage point (pp) increases per year; for example, a gradient of 1 would represent an increase from 4% to 5% in one year.* [c] *GCS and GLS values were recorded as negative percentages; hence, the positive gradient indicates a longitudinal trend towards zero.*

3.9 Discussion

This study is the first of its kind to demonstrate the natural history of atrial and ventricular TTE changes in the long term in FD, incorporating haematological, physiological, and biochemical markers. Trends are highlighted in **Figure 3.4**.

3.9.1 Trends on TTE

Over a median of 55 months, there was a significant, progressive decline in longitudinal ventricular contraction, measured by impairment of LV GLS, decline in septal tissue velocity, decrease in RV TAPSE and reduced RV systolic tissue velocity. In conjunction, there was significant, progressive LA dilatation and impaired atrial function. These complementary changes in ventricular and atrial function were associated with increased pulmonary artery pressure as measured by maximal tricuspid regurgitant velocity. These trends occurred in the absence of significant changes in systolic and diastolic blood pressure over time. Significant increases over time in biomarkers were observed, specifically NT-proBNP and troponin-T. Although LVH has been considered the defining feature of FD cardiomyopathy, and the main cardiac marker for decision-making regarding disease-modifying therapy and evaluation of therapeutic efficacy, this study suggests that other structural and functional markers of cardiac involvement may be better targets.

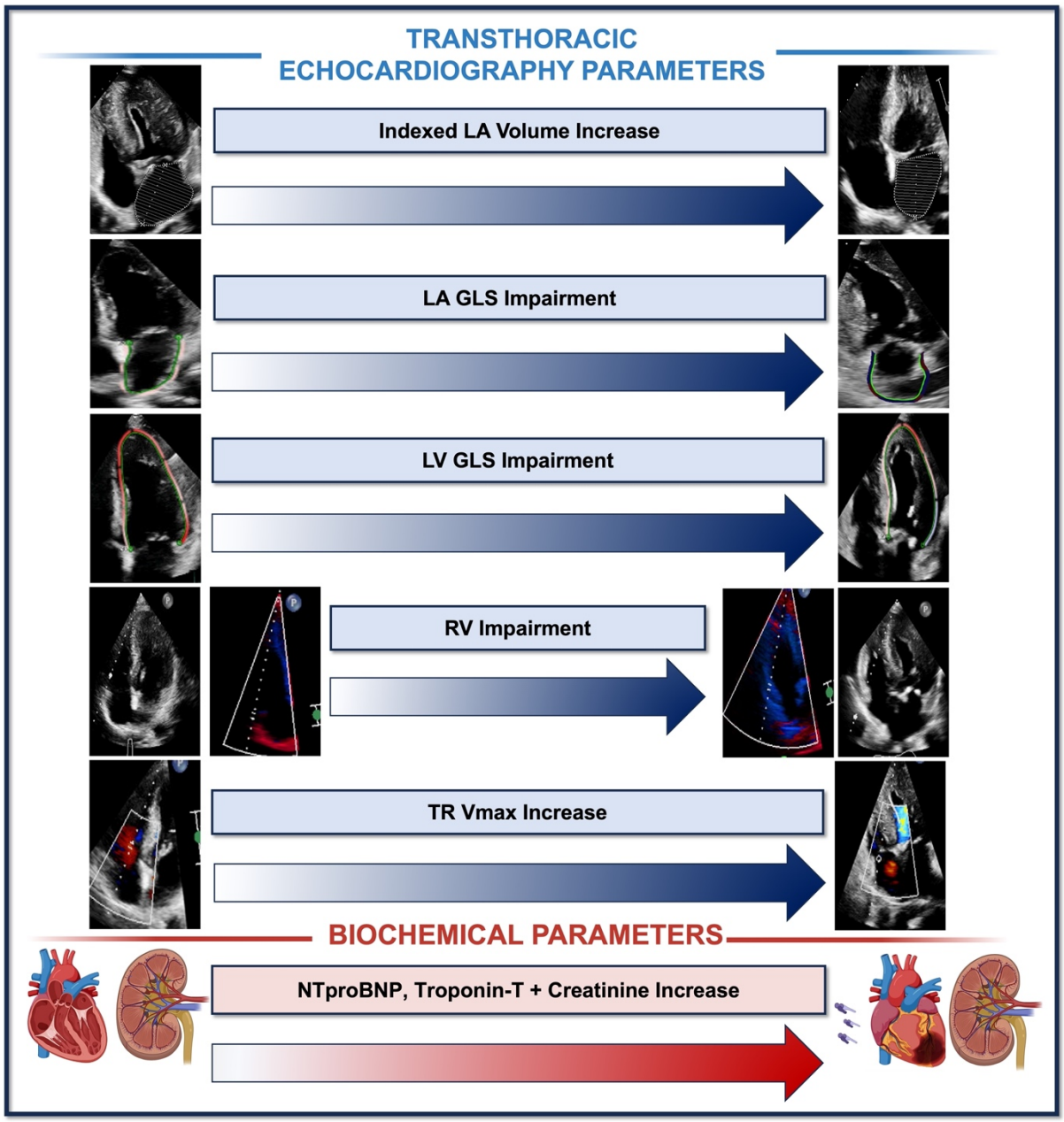

Figure 3.4: Progression of cardiovascular changes over time in Fabry Disease including changes in LA volume and function, longitudinal LV and RV function and increasing TR Vmax, suggestive of the development of a restrictive cardiomyopathy. This is associated with cardiac (troponin and NT-proBNP) and renal biomarker (creatinine) release. These imaging and biomarkers should be routinely assessed in Fabry Disease and may be early markers to guide clinicians regarding initiation of disease modifying therapy.

3.9.2 Therapy

Interestingly, 61% of patients in this study were taking disease-modifying therapy for FD which may, in part, account for the lack of LV mass progression with time. It is well established that in those with more advanced features of FD cardiomyopathy, particularly with LV wall thickness >15mm, efficacy of ERT is limited (62, 168). Reasons for this include the downregulation of mannose-6-phosphate receptor in FD cardiomyocytes, an intracellular carrier of α-galactosidase A, involved in the removal of myocardial Gb3 (169), as well as the long lifespan of cardiomyocytes and associated reduced cell turnover (170). However, there is emerging evidence for the role of ERT in the pre-hypertrophy phase of FD cardiomyopathy, in stabilising hypertrophy and myocardial Gb3 storage (171).

Systematic review of studies assessing disease-specific therapy has emphasised that, although ERT reduces microvascular endothelial Gb3, the long-term impact on morbidity and mortality remains to be established (172). Furthermore, systematic review of the effect of disease-specific therapy on cardiovascular outcomes, including morbidity, mortality and LV mass and wall thickness, has not only emphasised the lack of evidence of benefit, but has also highlighted that all studies were heterogeneous in design, outcome measurements and findings (173). This is important because new therapies are in development and requiring validation in FD cardiomyopathy (174). Furthermore, it is now widely accepted that early treatment is critical to prevent progression to irreversible tissue damage and organ failure, certainly before onset of fibrosis and most likely before LVH (131). Recent groups have also emphasised staging classifications in FD that offer prognostic value based on structural and functional changes on TTE (33) and CMR (175). In this study, we have shown that

structural and functional changes in the ventricles and atria are continual and cannot be divided into specific stages. Using echocardiographic changes as a continuum, a multiparameter approach that combines altered longitudinal deformation, elevated LV filling pressure, atrial enlargement and dysfunction may be a better endpoint for future studies into the effect of early initiation of disease modifying therapy.

3.9.3 Trends in the right ventricle

The RV is frequently involved in FD cardiomyopathy, with RV hypertrophy (RVH) often seen in conjunction with LVH, but rarely resulting in impairments in RV function (176). We demonstrate a significant reduction in TAPSE which was consistent with a reduction in RV s'. TAPSE impairment has been suggested as an important prognostic imaging marker in FD (33). In keeping with this, we also demonstrated a longitudinal increase in TR Vmax, suggesting an increase in pulmonary pressure. Degree of RV involvement correlates with disease stage and is unlikely to improve with ERT initiation (177). In cardiomyopathies of other aetiologies, including sarcomeric HCM and cardiac amyloidosis, RV involvement is secondary to an increase in afterload from pulmonary venous hypertension and often confers an adverse outcome in these diseases (178, 179). In FD, the RV could also be adversely affected by RV Gb3 accumulation which can take place early (180). Contrary to our data, existing cross-sectional prognostic categories include reduced TAPSE as only a late marker of outcome (33). Further data on the timing and importance of RV function In FD is warranted.

3.9.4 Trends in atrial structure and function

13% of FD patients suffer with ischaemic stroke or transient ischaemic attack (181, 182). This may be due to the direct effects of cerebral sphingolipid accumulation (183). However, cardioembolic stroke secondary to undiagnosed AF is likely to contribute given the high prevalence of AF in FD (23). Atrial dysfunction can predict new onset and recurrence of AF in the general population, with similar findings in FD (47, 184). A cross-sectional study found impaired LA reservoir strain in those without other evidence of cardiomyopathy, that was worse in those with LVH and worse still in those with late enhancement (185). An earlier cross-sectional study found that LA dilatation and reduced atrial compliance occurred irrespective of the presence of LVH (117). Interestingly, many of these patients did not have LVH, suggesting direct atrial glycosphingolipid accumulation to be a contributory factor (47), a possibility that has been confirmed on histopathological studies in patients with FD (186). Our findings, from a larger patient cohort, confirmed gradual impairment of LA GLS, LA EF and FAC over time, corresponding with increases in LA volume. Whilst atrial dilatation and altered compliance are an early sign of FD, our study shows this is progressive (185). Targeting early changes in atrial size and compliance may be a worthwhile method of reducing the burden of stroke in FD, which occurs at a much younger age and at more than double the rate of the general population (50).

3.9.5 Trends in biomarkers

We demonstrated a specific increase in troponin-T, consistent with published data (102). Our finding that NT-proBNP increases in parallel with indexed LV mass, GLS A4C and LA GCS but not LA volume is consistent with the concept that this is a biomarker of changes in end-diastolic atrial and ventricular wall stress (187). NT-

proBNP may serve as a partial marker of myocardial fibrosis in sarcomeric HCM (188). Troponin and NT-proBNP are important cardiac biomarkers in FD with their beneficial role in disease staging and prognosis demonstrated in published literature (102, 161, 189). Changes in both may influence therapeutic decision-making.

The longitudinal increase in urine protein and ACR in males reflects a greater progression of nephropathy which doesn't appear to be confounded by ACE-i therapy where just under 50% of those taking an ACE-i were male. ACE-i therapy is widely recognised to reduce the degree of urine protein in the general population (190). In Indexed LV mass also increased significantly over time in males compared to females. The trend of male-specific LV mass increase is in keeping with published literature and reflects gender dimorphism in FD natural progression (19, 191). Typically, hypertrophy develops earlier in males, prior to the onset of fibrosis and indeed fibrosis has been detected in up to 23% of females with no hypertrophy (19). Phenotypic variation in females may be attributed to X-linked inactivation, accounting for a clinical phenotype, albeit less severe (22).

3.10 Limitations

The primary strength of the study was the relatively large sample size, and long period of follow-up, allowing for assessments of long-term trends. However, there were also several limitations, which need to be considered. Primarily, the retrospective and observational design of the study meant that patients had differing follow-up periods, and variability in the time between visits, particularly during COVID-19, resulting in patients contributing different numbers of visits to the analysis. To account for this, the

data were analysed using a GEE approach, to adjust for within-patient correlations, and prevent over-weighting patients with more visits. However, the analysis will still have assigned a greater weight to these patients, which may introduce selection bias, if there were underlying differences between these patients and those that attended less frequently. Selection bias may also have been introduced by excluding those with a single scan, and those who did not have a scan at all. Secondly, for troponin, ACR and urine protein, a considerable proportion of cases had levels that were below the limit of detection of the test. These were assigned a value equal to the test threshold, to allow for the measurements to be included in the analysis. However, this will have resulted in patients with levels that were consistently below the limit of detection being assumed to have a gradient of zero, potentially resulting in an underestimate of the gradient for the cohort. Thirdly, analyses of troponin were limited by the fact that two different tests were used across the study period which needed to be analysed separately, resulting in smaller sample sizes and shorter follow-up periods being included in each analysis. Fourthly, for the comparisons of the trends in NT-proBNP with changes in TTE parameters, the analysis required the gradients to be estimated individually for each patient. Consequently, these gradients were estimated based on a small number of data points, leading to low precision, and inflated variability. This, coupled with the relatively small sample size when analysing patient-level data will have resulted in low statistical power, meaning that only moderate-to-large effect sizes would have been detectable. Finally, the sensitivity to detect changes in LV strain over time is impacted by the fact that apical 4-chamber views alone were used to acquire LV GLS. Data collection started in 2011, when routine GLS assessment was limited to apical 4-chamber views only.

3.11 Conclusions

In conclusion, we demonstrate progressive decline in LV and RV longitudinal contraction, an increase in atrial volume and impairment in atrial function, and an associated increase in maximal velocity of tricuspid regurgitant jet. These changes occurred against a backdrop of increased NT-proBNP over time, likely reflecting greater wall stress in the ventricle from elevated LVEDP resulting in higher pulmonary venous pressure. These processes were continuous, likely reflecting the insidious organ damage that takes place in FD due to sphingolipid deposition, and do not fit easily into a staged approach to prognosis. Understanding these changes and the time course over which these take place should be useful for planning future studies of novel agents to improve cardiovascular outcomes in FD. The study suggests that LVH is not the optimal marker for deciding on initiation of disease-specific therapy in FD

4 Chapter 4 – Changes in peak oxygen consumption on exercise and cardiomyopathy stage in Fabry Disease

Data from this chapter is based on the first author published article where these data were first presented:

Roy A, Thompson SE, Hodson J, van Vliet J, Condon N, Alvior AM, et al. Changes in peak oxygen consumption in Fabry disease and associations with cardiomyopathy severity. *Heart*. 2024.

4.1 Personal Contribution

This was a single centre retrospective study in adults with FD undergoing exercise testing. Exercise testing was performed by an experienced physiologist and physiotherapist. I wrote the ethics application for the use of data collected in this chapter for the purposes of research which was approved. I completed data collection, LA strain analysis and performed the statistical analyses with the support of a statistician. I wrote the manuscript and completed edits of the subsequent revisions.

4.2 Background

Exercise intolerance is common and debilitating in FD. There are various underlying mechanisms that may be responsible for exercise limitation including FD-related cardiomyopathy (192), pulmonary sphingolipid deposition mimicking chronic obstructive pulmonary disease (193), and altered skeletal muscle energetics (194). Cardiopulmonary exercise testing (CPEX) objectively quantifies aerobic fitness, functional capacity, chronotropic and haemodynamic response to exercise, and attributes effort intolerance to various aetiologies, including respiratory and cardiac dysfunction. Exercise intolerance not only impacts quality of life for FD patients but has been used in conjunction with other relevant parameters in staging disease, measuring response to therapy and determining prognosis in various other forms of HCM (195, 196).

Therapies available for FD patients include ERT and OCT, with new developments including substrate reduction therapy and gene editing. It is widely accepted that these therapies are most effective when delivered in early disease, particularly when considering cardiovascular complications (131). This is important because cardiovascular complications are the most common cause of morbidity and premature mortality in FD. Although early therapy is likely to optimise outcomes, current practice guidelines continue to recommend initiation of therapy only when LVH, increased wall thickness or the presence of LGE on CMR have been identified (53). CMR data have given rise to the concept of different phases in FD cardiomyopathy. This begins with an accumulation phase with progressive deposition of sphingolipid before the appearance of LVH. This is followed by a hypertrophy phase, characterised by

progressive LVH, impaired GLS, and biomarker release. In the latter stages of the disease when therapy is considered ineffective, there is accumulation of interstitial myocardial fibrosis and persistent troponin leak, that reflects myocardial oedema, inflammation, risk of heart failure and sudden cardiac death (69).

4.3 Hypotheses

Our hypothesis is that there is progressive effort intolerance that reflects continual sphingolipid accumulation, even in the accumulation phase, becoming common during the hypertrophy phase and disabling at onset of fibrosis and inflammation. If common and quantifiable, exercise tolerance could then be used as a therapeutic target that might be combined with imaging biomarkers, such as T1 mapping and GLS, or ECG biomarkers such as PQ interval and P-wave duration, for future trials.

4.4 Aims and Objectives

The aims of this study were to ascertain frequency and severity of exercise intolerance by investigating the relationship between peak maximal oxygen uptake ($\dot{V}O_{2peak}$) and the phase of cardiac disease. Primarily, the cardiac disease phase was quantified based on a four-point ordinal scale, adapted from published literature (69). Secondary analyses additionally considered selected CMR, TTE, ECG and biochemical parameters.

4.5 Methods

4.5.1 Study population

This was an observational retrospective review of adults (aged over 16 years) with genetically or enzymatically proven FD attending the FD 'one-stop clinic' (incorporating review by metabolic, cardiology and respiratory physicians with input from physiotherapy and dietetics) in the Centre for Rare Disease at the QEHB. Patients attend this clinic for regular follow-up visits. Assessments at these visits include blood sampling, ECG, TTE and CMR, if indicated. Patients reporting cardiopulmonary symptoms are routinely referred for exercise testing using CPEX, as described subsequently. However, in some cases, the six-minute walk test (6MWT) was used, either as an alternative test in patients not physically able to undergo CPEX testing, or as an initial screening assessment, since it can easily be performed in clinic without requiring additional equipment or incurring additional expense.

Patients were included in the review if they underwent either CPEX testing or 6MWT between September 2011 (when the one-stop clinic model was introduced at QEHB) and September 2023. Where patients completed multiple CPEXs or 6MWTs during the study period, only the most recent tests were considered for inclusion. Exercise testing was additionally excluded where it occurred more than two years before or after a CMR or TTE that could be used for cardiac disease staging, such that both variables were measured contemporaneously.

Demographic data, comorbidities, FD-specific therapy history and biochemical data were extracted from the patients' electronic care record at the time of cardiomyopathy phase assessment and included the following:

(a) CPEX: peak values for $\dot{V}O_{2peak}$, forced expiratory volume in 1-second (FEV_1), predicted values and percentage (%) of predicted values.

(b) 6MWT: weight, height, date of birth, sex, to establish predicted 6MWT distance, 6MWT distance, time completed and pre/post heart rate, oxygen saturation (SpO_2), blood pressure (BP) and Borg scale. Reasons for stopping 6MWT were recorded.

(c) CMR data, including indexed values to body surface area (BSA), on LV and RV volumes, mass and function (including ejection fraction, stroke volume, cardiac index, 2D GLS% as well as atrial volumes. Lowest T1 value, highest T2 value and presence/absence of LGE were also collected.

(d) TTE data on LV and RV volumes, function, atrial volumes and function, and markers of diastolic function on TDI.

4.5.2 Haematology and Biochemistry

Data for the standard haematology and biochemistry tests (performed closest to the cardiomyopathy phase classification) including kidney and liver function, glycosylated haemoglobin (HbA1c), lipid panel and cardiac biomarkers were extracted. Specific cardiac biomarkers included high sensitivity troponin I/T (ELISA, Roche Diagnostics) and NTpro-BNP. NTpro-BNP was measured by sandwich immunoassay with

magnetic particle separation and chemiluminescent detection on an E170 analysed (Roche Diagnostics, Burgess Hill, United Kingdom). Normal ranges were high sensitivity troponin T <14ng/L (below the 9th percentile upper reference limit for the test) and NTpro-BNP <47ng/L. NTpro-BNP levels were truncated at a lower limit of 5ng/L by the laboratory; subsequently these values were assigned a value of 4ng/L for the purpose of data analysis and are reported as <5ng/L.

4.5.3 Transthoracic Echocardiography

During the study period, resting TTE was performed by an accredited sonographer using ie33 and EPIC ultrasound systems (Phillips), according to the British Society of Echocardiography minimum dataset (140). Diastolic function was graded by an experienced cardiovascular imaging cardiologist specialising in echocardiography, according to current guidelines (140). Linear internal measurements were obtained from 2D images in the parasternal long axis, measured immediately below mitral valve leaflet tips; 2D volumetric measurements were performed using the biplane summation of discs method, with separate acquisitions optimised for left atrial volumetric measurement. 3D volumetric measurements were not routinely acquired. 2D acquisitions were made for quantification of speckle-tracking strain in each case, following visual assessment of appropriate segmental tracking quality and a minimum frame rate >40 frames/s. Measures of LA strain were not recorded as part of routine patient follow up in the FD clinic. As such, the apical two chamber 2D views (with a minimum of two cycle lengths) were retrospectively assessed, where available, to add data for these parameters to the contemporaneous records for each visit. Study authors were not blinded to the demographic data and time of the study.

4.5.4 Cardiac Magnetic Resonance Imaging

Contrast-enhanced CMR (1.5T Avanto, Siemens Healthcare, Erlangen, Germany) was performed in line with standard protocols to obtain LV dimensions, volumes, and mass (197). A steady-state free precision single breath hold modified Look Locker inversion recovery (MOLLI) sequence was used for T1 mapping in the basal and mid LV short axis levels and horizontal long-axis, before and 15-20 minutes after administration of gadolinium-based contrast agent (198). Imaging for assessment of LGE, calculation of regional and global T1 and myocardial extracellular volume (ECV) were performed as previously described (199).

4.5.5 Cardiopulmonary exercise testing

Before the CPEX test, height, weight and FEV_1 were measured. ECG leads, BP cuff and CPEX mask were fitted. Verbal consent was obtained. CPEX was performed using a treadmill (h/p cosmos quasar®) according to individualised ramp protocols. Patients were questioned on their exercise ability to select a ramped protocol on a treadmill which aimed to bring them to their peak capacity between 8 and 10 minutes. During the CPEX test, talking was discouraged. BP was measured at 3-minute intervals and the patient received encouragement to exercise. After the patient indicated they need to stop, the patient's recovery was monitored for 5 minutes.

Throughout the CPEX, patients received encouragement to exercise as best they could to peak capacity, with a "best effort" CPEX being defined as achieving a respiratory exchange ratio (RER) >1.0 This cut-off has been published in CPEX

research for other HCM studies, including FD (200-202). Performance during the CPEX was then quantified by identifying $\dot{V}O_{2peak}$ using a breath-by-breath analyser (Ultima™ CardiO2®), which was calibrated in accordance with the manufacturers specific instructions prior to being used for the test. The breath-by-breath data acquired was averaged using a moving average algorithm. These involved taking an average of five breaths and excluding the highest and lowest values. Since $\dot{V}O_{2peak}$ is known to vary by age and sex, normalised values of this outcome were additionally calculated. This used the proposed equations in published literature (203), which were, in turn, derived from the normal percentiles published by the Cooper Institute and reported in published guidelines (204). These equations were evaluated for each patient to estimate the 50th percentile of $\dot{V}O_{2peak}$ that would be expected for healthy controls of the same age and sex. The resulting value was then deemed to be the "expected" $\dot{V}O_{2peak}$ for the patient. This was then subtracted from a patient's observed $\dot{V}O_{2peak}$ to produce an age/sex-normalised $\dot{V}O_{2peak}$. As such, negative values of the age/sex-normalised $\dot{V}O_{2peak}$ indicated that a patient had underperformed, relative to what would be expected of an age- and sex-matched healthy control. Prior to CPEX, patients underwent formal pulmonary function testing in the form of spirometry assessment to investigate lung function, from which the FEV_1 was recorded. Normalisation of FEV_1 was performed similarly and as previously described with a "race-neutral" reference equation used to produce age/sex/height-normalised FEV_1 values (205).

4.5.6 Six-minute Walk test

The 6MWTs were performed by an experienced physiotherapist following the American Thoracic Society guidelines (206), using a walking course 20 metres in

length, and were quantified using the total distance walked. Parameters measured pre- and post-6MWT were, BP, heart rate, oxygen saturations, and dyspnoea (using BORG scale). Reasons for underperforming in the 6MWT were also documented (e.g. fatigue or musculoskeletal issues).

4.5.7 Staging Disease

Degree of cardiomyopathy was staged according to published literature (69) by myself and Richard Steeds using a strict criterion (80% of the criteria for a specific stage to be classified). Blood biochemistry, ECG, CMR and TTE imaging of all the patients included in the study were reviewed to clarify the phase of cardiomyopathy on a four-category ordinal scale. Both experts were blinded at the time of classification to patient identifiers and to the results of exercise testing. The criteria used as a guideline for these classifications are visualised in **Figure 4.1**.

	Cardiomyopathy Phase			
	Phase 1	***Phase 2***	***Phase 3***	***Phase 4***
CMR/TTE Parameters				
T1 Mapping	Normal 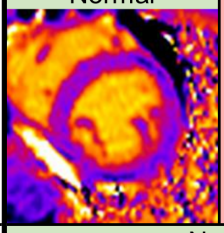	Low 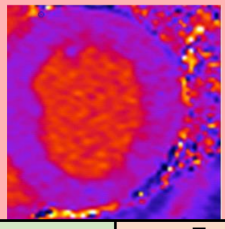		Pseudo-Normal 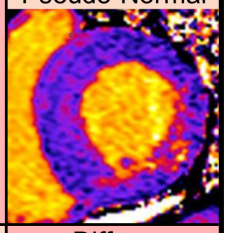
LGE	None 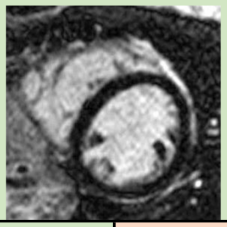		Focal 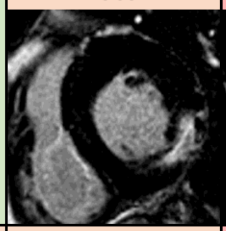	Diffuse 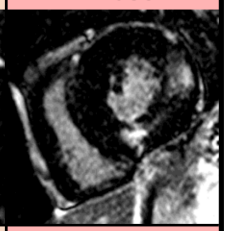
LVH	Absent 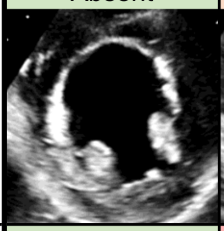	Borderline 	Moderate 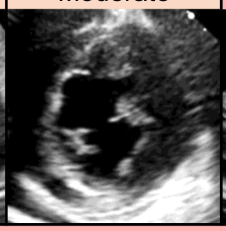	Severe 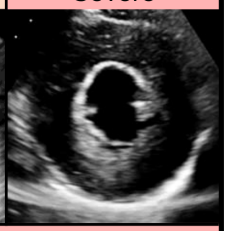
LV GLS	<-17%	≥-17%		
LV EF	≥55%			<55%
Diastolic/Systolic Dysfunction	Normal	≥Grade I Diastolic Dysfunction		Systolic Dysfunction
ECG Parameters				
PR Interval	Normal	<120 / >200ms	>200ms	
ST Segment	Normal		Abnormal	
T-Wave	Normal		Inversion	
Arrythmias	No			Yes
Biochemistry				
HS Troponin	Normal	Borderline [a]	>14 / 16ng/L [b]	
NT-proBNP	Normal	Borderline [a]	>400 ng/L	

Figure 4.1 – Stages of FD Cardiomyopathy. [a] Abnormalities in biochemistry markers are not always observed at cardiomyopathy stage 2, with borderline increases often being observed. [b] Thresholds for abnormality were 14ng/L for troponin-T and 16ng/L for troponin-I. Abbreviations: CMR: cardiac magnetic resonance imaging, ECG: electrocardiogram, EF: ejection fraction, GLS: global longitudinal strain, HS: high sensitivity, LGE: late gadolinium enhancement, LVH: left ventricular hypertrophy,

NTpro-BNP: N-terminal pro B-type natriuretic peptide, TTE: transthoracic echocardiography.

However, the experts were permitted to deviate from these for borderline cases or in the case of those patients with missing data for some of the criteria. Discrepancies between the experts on specific cases were resolved on consensus (N=7). This was particularly the case for patients with incomplete data, including those who did not undergo CMR due to having an existing cardiac device or claustrophobia.

4.6 Ethics

This study was approved by West Midlands South Birmingham Research Ethics Committee (23/WM/0180 IRAS 325613). The studies were conducted in accordance with the local legislation and institutional requirements. The ethics committee waived the requirement of written informed consent for participation from the participants / legal guardians / next of kin because the data were acquired from a research database using routinely collected clinical data with the secondary purpose of research. This study was registered locally at QEHB (CARMS-18469). Patients were consulted and involved in the research question and design for the study

4.7 Statistical methods

Initially, the subgroup of patients who completed both a CPEX and 6MWT were used to produce a linear regression model, with $\dot{V}O_{2peak}$ as the dependent variable, and the 6MWT distance as a covariate. This was then used to impute $\dot{V}O_{2peak}$ values for those

patients who had only undergone a 6MWT. Comparisons between the observed and expected $\dot{V}O_{2peak}$ values were performed using paired t-tests. Patient characteristics were then compared across the four subgroups of cardiac disease stage. Jonckheere-Terpstra tests were used for continuous variables, to account for the fact that the cardiac disease stage categories were ordinal. For binary variables, associations with cardiac disease stage were assessed using Mann-Whitney U tests (i.e. comparing the "average" cardiac disease stage between categories). The association between cardiac disease staging and $\dot{V}O_{2peak}$ was additionally assessed using a linear regression model, which treated the cardiac disease stage as a continuous covariate, to estimate the change in $\dot{V}O_{2peak}$ associated with an increase of one cardiac disease stage. To further interrogate the association between cardiac disease and exercise tolerance, associations between $\dot{V}O_{2peak}$ and both blood markers and CMR/TTE parameters were then assessed using Spearman's rank correlation coefficients (rho).

Continuous variables are reported as "mean ± standard deviation" where approximately normally distributed, or as "median (interquartile range; IQR)" otherwise. Cases with missing data were excluded from the analysis of the affected variable, except for $\dot{V}O_{2peak}$, for which values were imputed from the 6MWT in patients who did not complete a CPEX, as previously described. However, sensitivity analyses were additionally performed after excluding these imputed values, to ensure that the imputation had not unduly influenced the results. All analyses were performed using IBM SPSS v29 (IBM Corp. Armonk, NY), with $p<0.05$ deemed to be indicative of statistical significance throughout.

4.8 Results

4.8.1 Study cohort

The flow of patients through the study is illustrated in **Figure 4.2**. A total of 157 patients were followed up at the FD clinic during the study period. Of these, 6 only attended a single appointment for an initial assessment before being transferred to another hospital for ongoing follow-up, and so did not have the opportunity to undergo exercise testing.

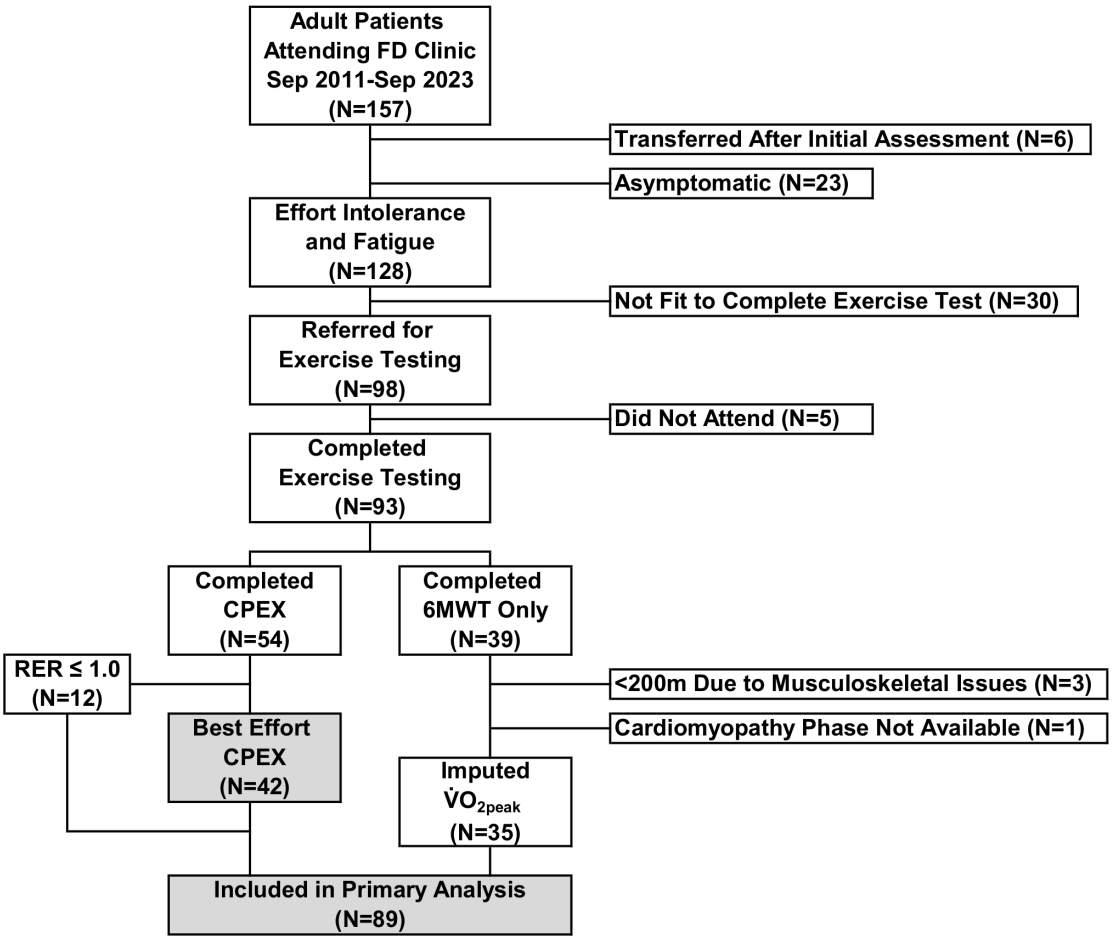

Figure 4.2 – Study Flowchart: The cohorts included in the primary and sensitivity analyses are highlighted in grey. Abbreviations: 6MWT: six-minute walk test, CPEX:

cardiopulmonary exercise testing, FD: Fabry disease, RER: respiratory exchange ratio, $\dot{V}O_{2peak}$: peak oxygen uptake.

A further 23 patients did not report cardiopulmonary symptoms during the follow-up period, and so did not require exercise testing. Of the 128 patients with cardiopulmonary symptoms, 30 were not deemed to be fit to complete an exercise test, whilst 5 were referred for testing but did not attend. Of the remainder, 54 completed a CPEX test, of whom 42 performed with best effort (i.e. RER > 1). A further 39 patients only completed a 6MWT, due to being deemed unsuitable for CPEX testing. The primary analysis included the 54 patients who completed a CPEX (including those with RER <1), in addition to the further 35 patients for whom an estimated $\dot{V}O_{2peak}$ could be imputed from the 6MWT distance as described above. Four patients performed a sub-optimal 6MWT due to fatigue and musculoskeletal pain and so were not included in the analysis, highlighted below.

4.8.2 Imputing $\dot{V}O_{2peak}$

Of the 42 patients with a best effort CPEX test, 18 additionally completed a 6MWT. For these patients, the $\dot{V}O_{2peak}$ was found to be strongly correlated with the 6MWT distance (rho: 0.70, p=0.002). Initial analysis identified two outliers with 6MWT distances <200m, which did not fit the trend of the remaining cases. Further assessment of these patients found that both reported musculoskeletal pain as the cause of their poor performance in the 6MWT; hence, they were excluded from the analysis, since the 6MWT was not a fair assessment of cardiopulmonary exercise

capacity in these cases. A regression model was then produced for the remaining 16 cases, which is visualised in **Figure 4.3**.

The model was then applied to the patients who only completed a 6MWT, to produce estimated $\dot{V}O_{2peak}$ values (N=39). Patients with 6MWT distances <200m were excluded from this cohort, for consistency with the imputation model derivation cohort; review of these found that all had reported musculoskeletal pain as the reason for their poor performance. In addition, one patient was excluded since they had no disease staging assessment. $\dot{V}O_{2peak}$ values were imputed for the remaining 35.

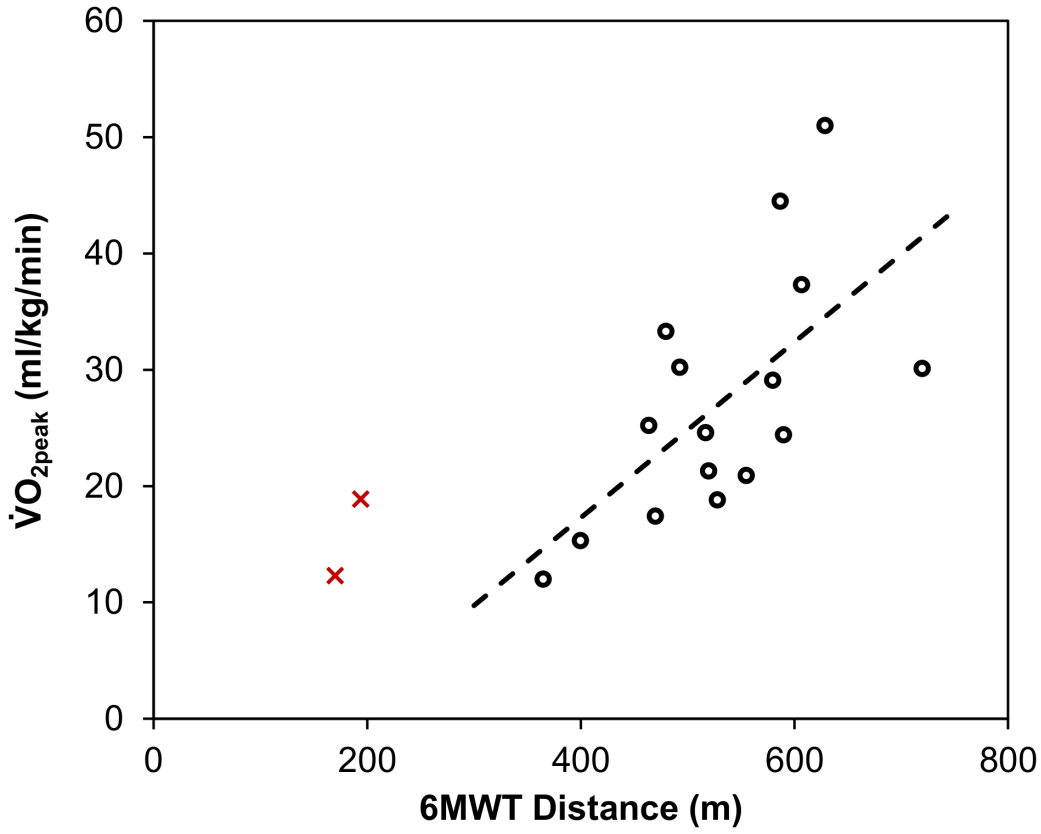

Figure 4.3: Imputation of $\dot{V}O_{2peak}$ from 6MWT. The plot includes data for all N=18 patients who underwent both exercise assessments. Outliers with 6MWT distances <200m (N=2, represented by red crosses) were subsequently excluded, with a linear

regression model produced for the remaining N=16. The equation of the resulting model was: $\dot{V}O_{2peak}$ = 0.076[6MWT Distance] – 12.9. Abbreviations: 6MWT: six-minute walk test, $\dot{V}O_{2peak}$: peak oxygen uptake.*

4.8.3 Cohort characteristics

Initial comparisons between the primary (N=89) and best effort CPEX (N=42) cohorts found the characteristics of these to be similar (**Table 4.1 and 4.2**). As such, subsequent analyses were performed on the larger primary cohort. However, the major analyses were also repeated for the best effort CPEX, to ensure that this gave similar results. The primary cohort had a median age of 54 (IQR: 40-62) years, with 53% of patients being male (**Table 4.3**). Patients were approximately equally distributed across cardiac disease stage 1 (19%; N=17), stage 2 (25%; N=22), stage 3 (29%; N=26) and stage 4 (27%; N=24).

	Primary Cohort (N=89)		**Best Effort CPEX Cohort (N=42)**	
	N	***Statistic***	***N***	***Statistic***
Age (Years)	89	54 (40-62)	42	54 (39-62)
Body Mass Index (kg/m^2)	89	27.1 ± 6.5	42	26.1 ± 5.9
Male Sex	89	47 (53%)	42	26 (62%)
Current Smoker	89	6 (7%)	42	5 (12%)
Non-Classical Mutation	89	44 (49%)	42	24 (57%)
On ERT	89	38 (43%)	42	18 (43%)
On Statin	89	36 (40%)	42	15 (36%)
IHD	89	8 (9%)	42	4 (10%)

Diabetes Mellitus	89	4 (4%)	42	2 (5%)
Chronic Kidney Disease	89	14 (16%)	42	6 (14%)
Stroke/TIA	89	7 (8%)	42	4 (10%)
Proteinuria	87	31 (36%)	42	15 (36%)
Creatinine (umol/L)	88	80 (66-100)	42	77 (67-91)
HS Troponin-I (ng/L) [a]	64	26 (<5-101)	32	20 (<5-97)
HS Troponin-T (ng/L) [a]	23	23 (5-53)	9	49 (12-55)
NTpro-BNP (ng/L)	88	241 (78-936)	42	211 (83-1150)
ACR (mg/mmol)	85	2.5 (0.8-18.5)	41	3.6 (0.8-17.9)
Cholesterol (mmol/L)	87	4.3 (3.8-5.3)	42	4.2 (3.8-5.1)
Haemoglobin (g/L)	86	140 ± 13	42	140 ± 12
Cardiomyopathy Phase				
1		17 (19%)		8 (19%)
2		22 (25%)		11 (26%)
3		26 (29%)		9 (21%)
4		24 (27%)		14 (33%)
$\dot{V}O_{2peak}$ (ml/kg/min)	89		42	
Observed		23.2 ± 8.8		24.8 ± 9.0
Expected [b]		35.5 ± 3.9		36.1 ± 3.7
Age/Sex-Normalised [c]		-12.3 ± 8.0		-11.2 ± 7.7

Table 4.1 – Cohort characteristics in the two study cohorts. Data are reported as "N (%)", "mean ± standard deviation", or as "median (interquartile range)", as applicable. Each factor was assessed both for the primary cohort, and for the subgroup of patients with a best effort CPEX assessment. [a] The laboratory truncated troponin measurements at a lower limit of 5ng/L; measurements below this were assigned a value of 4ng/L for analysis, and are reported as "<5". [b] The expected $\dot{V}O_{2peak}$, based on the normative 50th percentile for a patient's age and sex, using the reported

equations (11). [c] The average difference between the observed vs. expected $\dot{V}O_{2peak}$. Abbreviations: ACR: urine albumin to creatinine ratio, CPEX: cardiopulmonary exercise testing, ERT: enzyme replacement therapy, HS: high sensitivity, IHD: ischaemic heart disease, NTpro-BNP: N-terminal pro B-type natriuretic peptide, TIA: transient ischaemic attack, $\dot{V}O_{2peak}$: peak oxygen uptake.

	Primary Cohort (N=89)		**Best Effort CPEX Cohort (N=42)**	
	N	***Statistic***	***N***	***Statistic***
CMR Parameters				
LV EDVi (ml/m^2)	76	61 ± 14	37	61 ± 14
LV ESVi (ml/m^2)	76	16 (12-21)	37	16 (12-22)
LV Mi (g/m^2)	76	80 (63-134)	37	77 (62-132)
LV SVi (ml/m^2)	75	44 ± 10	36	44 ± 9
LV EF (%)	76	73 (68-77)	37	74 (69-78)
RV EDVi (ml/m^2)	74	63 ± 16	36	64 ± 16
RV ESVi (ml/m^2)	74	21 (15-29)	36	21 (17-27)
RV SVi (ml/m^2)	73	41 ± 10	35	41 ± 10
RV EF (%)	74	66 ± 10	36	66 ± 9
LA Volume (ml)	73	56 (40-69)	36	54 (35-64)
Lowest T1 (ms)	69	875 ± 65	33	871 ± 75
TTE Parameters				
TR Velocity (cm/s)	39	220 (203-245)	19	219 (194-247)
LA EDV (ml)	78	32 (17-49)	37	27 (17-49)
LA ESV (ml)	78	56 (34-81)	37	56 (34-81)
LA GCS (%)	78	25 (9-40)	37	26 (9-40)

LA GLS (%)	78	24 ± 13	37	23 ± 13
LA EF (%)	78	43 ± 20	37	43 ± 20
LA FAC (%)	78	32 ± 16	37	32 ± 16

Table 4.2 – CMR and TTE parameters in the two study cohorts. Data are reported as "N (%)", "mean ± standard deviation", or as "median (interquartile range)", as applicable. Each factor was assessed both for the primary cohort, and for the subgroup of patients with a best effort CPEX assessment. Abbreviations: CMR: cardiac magnetic resonance imaging, CPEX: cardiopulmonary exercise testing, EDV(i): end-diastolic volume (indexed), EF: ejection fraction, ESV(i): end-systolic volume (indexed), FAC: fractional area change, GCS: global circumferential strain, GLS: global longitudinal strain, LA: left atrial, LV: left ventricular, Mi: mass indexed, RV: right ventricular, SVi: stroke volume indexed, TR: tricuspid regurgitation, TTE: transthoracic echocardiography.

As expected, comparisons between the cardiac disease stages found significant trends in age and sex distributions, with the median age increasing from 36 to 60 years ($p<0.001$) and the proportion of males from 12% to 79% ($p<0.001$) between cardiac disease stage 1 and 4. Increasing cardiac disease stage was also associated with higher rates of treatment with ERT ($p=0.005$) and statins ($p<0.001$), as well as a higher prevalence of IHD ($p=0.002$) and CKD ($p=0.001$). Of the blood markers considered, serum creatinine ($p<0.001$), troponin ($p<0.001$), NT-pro-BNP ($p<0.001$), ACR ($p=0.027$) and Hb ($p<0.001$) were all found to increase significantly with cardiac disease stage. Significant changes in CMR and TTE parameters were also observed (**Table 4.4**).

1

	N	Whole Cohort	Cardiomyopathy Phase				p-Value
			Phase 1	***Phase 2***	***Phase 3***	***Phase 4***	
Age (Years)	89	54 (40-62)	36 (23-43)	49 (36-56)	56 (53-64)	60 (52-65)	**<0.001**
Body Mass Index (kg/m^2)	89	27.1 ± 6.5	29.4 ± 6.7	24.2 ± 6.1	28.6 ± 6.3	26.6 ± 6.0	0.889
Male Sex	89	47 (53%)	2 (12%)	10 (45%)	16 (62%)	19 (79%)	**<0.001**
Current Smoker	89	6 (7%)	2 (12%)	2 (9%)	0 (0%)	2 (8%)	0.498
Non-Classical Mutation	89	44 (49%)	6 (35%)	11 (50%)	12 (46%)	15 (63%)	0.126
On ERT	89	38 (43%)	1 (6%)	9 (41%)	16 (62%)	12 (50%)	**0.005**
On Statin	89	36 (40%)	2 (12%)	5 (23%)	14 (54%)	15 (63%)	**<0.001**
IHD	89	8 (9%)	0 (0%)	0 (0%)	2 (8%)	6 (25%)	**0.002**
Diabetes Mellitus	89	4 (4%)	0 (0%)	2 (9%)	1 (4%)	1 (4%)	0.886
Chronic Kidney Disease	89	14 (16%)	0 (0%)	1 (5%)	5 (19%)	8 (33%)	**0.001**
Stroke/TIA	89	7 (8%)	1 (6%)	2 (9%)	3 (12%)	1 (4%)	0.825
Proteinuria	87	31 (36%)	5 (29%)	9 (43%)	7 (27%)	10 (43%)	0.624
Creatinine (umol/L)	88	80 (66-100)	63 (57-68)	73 (67-82)	84 (66-107)	96 (81-129)	**<0.001**
HS Troponin-I (ng/L) [a]	64	26 (<5-101)	<5 (<5-<5)	8 (<5-17)	34 (18-98)	127 (82-407)	**<0.001**

HS Troponin-T (ng/L) [a]	23	23 (5-53)	*<5* (*<5*-*<5*)	11 (*<5*-31)	36 (16-55)	55 (36-123)	**<0.001**
NTpro-BNP (ng/L)	88	241 (78-936)	76 (42-118)	68 (34-162)	363 (179-792)	1294 (356-3041)	**<0.001**
ACR (mg/mmol)	85	2.5 (0.8-18.5)	1.0 (0.6-3.6)	1.8 (0.8-14.2)	2.6 (0.8-19.3)	10.2 (1.6-47.6)	**0.027**
Cholesterol (mmol/L)	87	4.3 (3.8-5.3)	4.6 (3.8-5.1)	4.1 (3.5-4.8)	4.9 (4.0-5.9)	4.1 (3.8-5.2)	0.640
Haemoglobin (g/L)	86	140 ± 13	133 ± 9	138 ± 12	144 ± 11	144 ± 16	**<0.001**

Table 4.3 – Cohort characteristics by cardiomyopathy phase. Continuous variables are reported as "mean ± standard deviation or "median (interquartile range)", as applicable, with p-values from Jonckheere-Terpstra tests. Binary variables are reported as "N (column %)", with p-values from Mann-Whitney U tests (i.e. comparing the "average" cardiomyopathy phase between the two categories). Bold p-values are significant at p<0.05. [a] The laboratory truncated troponin measurements at a lower limit of 5ng/L; measurements below this were assigned a value of 4ng/L for analysis, and are reported as "<5". Abbreviations: ACR: urine albumin to creatinine ratio, ERT: enzyme replacement therapy, HS: high sensitivity, IHD: ischaemic heart disease, NTpro-BNP: N-terminal pro B-type natriuretic peptide, TIA: transient ischaemic attack.

	N	Whole Cohort	Cardiomyopathy Phase				p-Value
			Phase 1	*Phase 2*	*Phase 3*	*Phase 4*	
CMR Parameters							
LV EDVi (ml/m^2)	76	61 ± 14	63 ± 10	61 ± 12	62 ± 18	59 ± 14	0.370
LV ESVi (ml/m^2)	76	16 (12-21)	19 (18-23)	16 (13-19)	17 (10-25)	14 (12-18)	0.055
LV SVi (ml/m^2)	75	44 ± 10	44 ± 7	45 ± 8	44 ± 14	43 ± 10	0.498
LV Mi (g/m^2)	76	80 (63-134)	56 (50-61)	71 (64-87)	115 (80-150)	137 (103-156)	**<0.001**
LV EF (%)	76	73 (68-77)	70 (66-73)	73 (72-76)	72 (65-81)	75 (72-78)	0.055
RV EDVi (ml/m^2)	74	63 ± 16	70 ± 11	65 ± 10	58 ± 18	62 ± 21	**0.014**
RV ESVi (ml/m^2)	74	21 (15-29)	28 (21-31)	23 (20-27)	17 (11-18)	19 (12-29)	**0.012**
RV SVi (ml/m^2)	73	41 ± 10	43 ± 6	41 ± 8	39 ± 13	40 ± 13	0.128
RV EF (%)	74	66 ± 10	63 ± 11	65 ± 6	69 ± 11	66 ± 9	0.066
LA Volume (ml)	73	56 (40-69)	54 (39-62)	45 (32-60)	60 (35-92)	63 (54-79)	**0.017**
Lowest T1 (ms)	69	875 ± 65	939 ± 32	851 ± 65	836 ± 56	880 ± 50	**0.004**
TTE Parameters							
TR Velocity (cm/s)	39	220 (203-245)	220 (215-230)	203 (194-233)	220 (205-245)	248 (219-281)	**0.033**
LA EDV (ml)	78	32 (17-49)	27 (20-32)	18 (13-32)	44 (30-52)	47 (19-69)	**0.003**

LA ESV (ml)	78	56 (34-81)	46 (40-72)	41 (25-57)	72 (56-93)	74 (40-123)	**0.013**
LA GCS (%)	78	25 (9-40)	28 (11-42)	28 (9-39)	19 (10-37)	15 (7-37)	0.204
LA GLS (%)	78	24 ± 13	28 ± 11	27 ± 14	20 ± 11	21 ± 15	**0.016**
LA EF (%)	78	43 ± 20	48 ± 16	46 ± 21	40 ± 19	40 ± 23	0.072
LA FAC (%)	78	32 ± 16	36 ± 12	35 ± 15	29 ± 14	30 ± 19	0.053

Table 4.4 – CMR and TTE parameters by cardiomyopathy phase. Data are reported as "N (%)", "mean ± standard deviation", or as "median (interquartile range)", as applicable, with p-values from Jonckheere-Terpstra tests. Bold p-values are significant at p<0.05. Abbreviations: CMR: cardiac magnetic resonance imaging, EDV(i): end-diastolic volume (indexed), EF: ejection fraction, ESV(i): end-systolic volume (indexed), FAC: fractional area change, GCS: global circumferential strain, GLS: global longitudinal strain, LA: left atrial, LV: left ventricular, Mi: mass indexed, RV: right ventricular, SVi: stroke volume indexed, TR: tricuspid regurgitation, TTE: transthoracic echocardiography.

	Whole Cohort	Cardiomyopathy Phase				p-Value
		Phase 1	***Phase 2***	***Phase 3***	***Phase 4***	
$\dot{V}O_{2peak}$ (ml/kg/min)	*N=89*	*N=17*	*N=22*	*N=26*	*N=24*	
Observed	23.2 ± 8.8	27.7 ± 6.8	26.7 ± 10.8	20.5 ± 7.8	19.8 ± 6.6	**<0.001**
Expected [a]	35.5 ± 3.9	36.8 ± 2.7	36.6 ± 4.3	34.5 ± 4.1	34.8 ± 3.7	0.063
Age/Sex-Normalised [b]	-12.3 ± 8.0	-9.1 ± 6.3	-9.9 ± 10.3	-14.1 ± 6.6	-15.0 ± 7.1	**0.009**
FEV_1 (L)	*N=52*	*N=9*	*N=14*	*N=12*	*N=17*	
Observed	2.50 ± 1.00	2.84 ± 0.93	2.58 ± 1.26	2.44 ± 1.01	2.30 ± 0.79	0.309
Expected [c]	3.11 ± 0.68	3.16 ± 0.65	3.33 ± 0.74	2.92 ± 0.76	3.04 ± 0.58	0.908
Age/Sex/Height-Normalised [b]	-0.61 ± 0.81	-0.32 ± 0.52	-0.74 ± 1.00	-0.49 ± 0.83	-0.74 ± 0.75	0.329

Table 4.5 – $\dot{V}O_{2peak}$ and FEV_1 by cardiomyopathy phase Data are reported as "mean ± standard deviation, with p-values from Jonckheere-Terpstra tests; bold p-values are significant at p<0.05. [a] The expected $\dot{V}O_{2peak}$, based on the normative 50th percentile for a patient's age and sex, using the reported equations (11). [b] The average difference between the observed vs. expected measurements. [c] The expected FEV_1, based on the normative 50th percentile for a patient's age, sex and height, using the reported equations (13). Abbreviations: FEV_1: forced expiratory volume in one second, $\dot{V}O_{2peak}$: peak oxygen uptake.

4.8.4 $\dot{V}O_{2peak}$

For the cohort as a whole, the mean $\dot{V}O_{2peak}$ was 23.2 ± 8.8 ml/kg/min. Comparisons across the cardiac disease stage categories found a significant reduction in $\dot{V}O_{2peak}$, from a mean of 27.7 ml/kg/min in stage 1 to 19.8 ml/kg/min in stage 4 (p<0.001, **Table 4.5**), with regression modelling estimating a reduction of 3.0 ml/kg/min (95% CI: 1.4-4.7) per stage (**Figure 4.4A**).

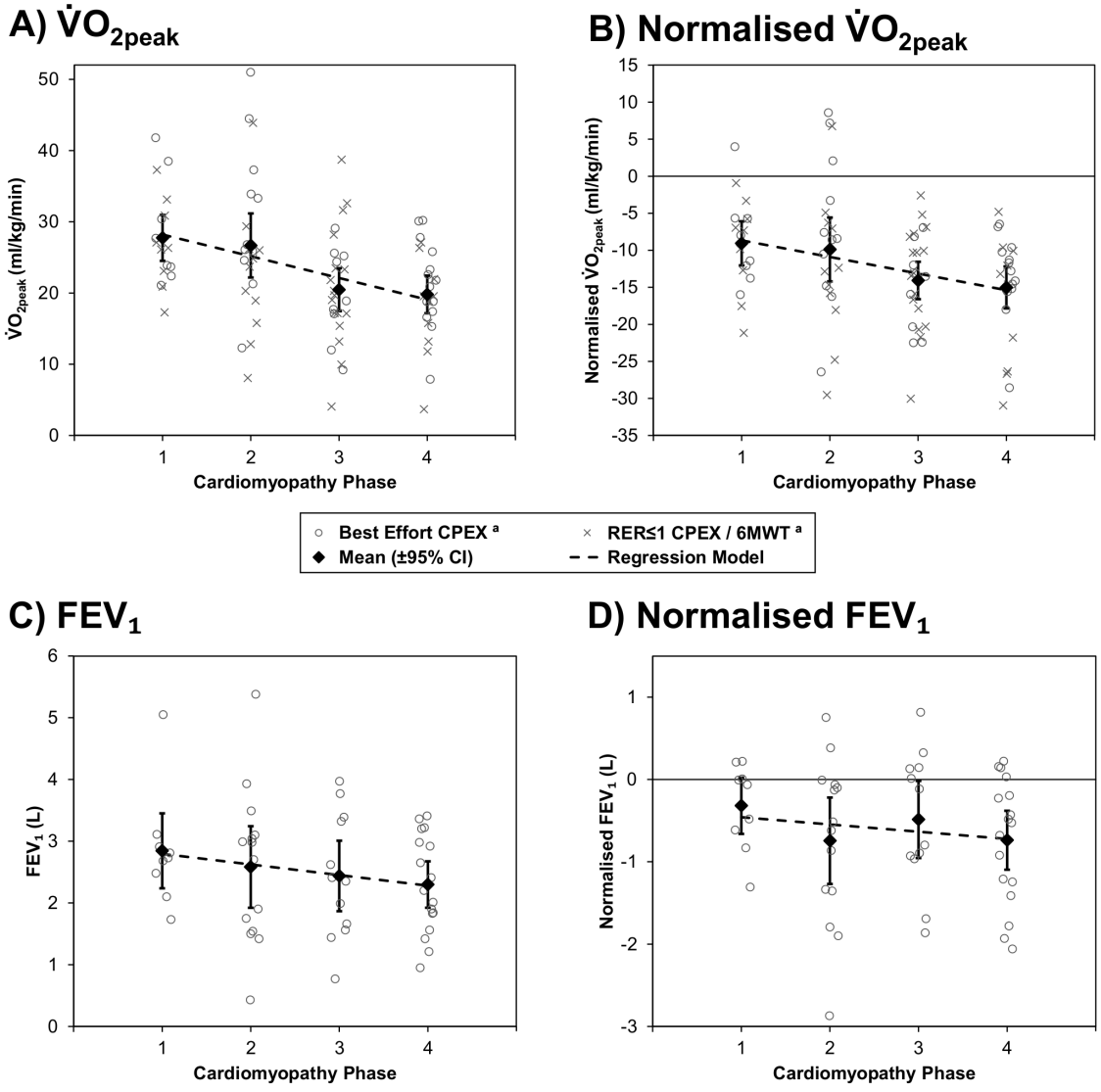

Figure 4.4 – Association between cardiomyopathy phase and $\dot{V}O_{2peak}$ / FEV_1 Grey points represent the values for individual patients and are plotted with jitter. Diamonds represent the mean values within each cardiomyopathy phase subgroup, with

whiskers representing 95% confidence intervals. Broken lines are from linear regression models, with the cardiomyopathy phase treated as a continuous covariate. Analyses are based on N=89 for $\dot{V}O_{2peak}$ and N=52 for FEV_1. For both outcomes, analyses were performed for the observed values, and well as normalised values, as described in Table 2. [a] For $\dot{V}O_{2peak}$, different symbols were used to differentiate values derived from a best effort CPEX, and those that were either from a CPEX with RER≤1.0 or imputed from a 6MWT. Abbreviations: 6MWT: six-minute walk test, CPEX: cardiopulmonary exercise testing, FEV_1: forced expiratory volume in one second, RER: respiratory exchange ratio, $\dot{V}O_{2peak}$: peak oxygen uptake.

However, the significant trends in both age and male sex prevalence with cardiac disease staging likely acted as considerable confounders in this analysis. As such, the normative values of $\dot{V}O_{2peak}$ were calculated for each patient, as per published literature (203), to account for the potential effects of these factors. This returned a mean expected $\dot{V}O_{2peak}$ for the cohort of 35.5 ml/kg/min, which was significantly higher than the observed values ($p<0.001$), with patients underperforming by a mean of 12.3 ± 8.0 ml/kg/min. Patients in all four stages of cardiomyopathy were found to significantly underperform, relative to these expected values (all $p<0.001$). Comparisons of these age/sex-normalised values across the cardiac disease stage groups found the magnitude of this underperformance to increase significantly, from 9.1 ml/kg/min in stage 1 to 15.0 ml/kg/min in stage 4 ($p=0.009$), with regression modelling estimating a change of 2.2 ml/kg/min (95% CI: 0.7-3.7) per stage (**Figure 4.4B**). Sensitivity analysis of the best effort CPEX cohort returned similar results (**Table 4.6**).

		$\dot{V}O_{2peak}$ (ml/kg/min)		Normalised $\dot{V}O_{2peak}$ (ml/kg/min)	
	N	***Statistic***	***p-Value***	***Statistic***	***p-Value***
Cardiomyopathy Phase			**0.010**		0.063
1	8	28.7 ± 7.7		-8.6 ± 6.3	
2	11	30.6 ± 10.9		-7.1 ± 10.4	
3	9	19.9 ± 6.7		-15.0 ± 5.8	
4	14	21.2 ± 6.1		-13.6 ± 5.5	
Gradient (per Phase)	42	-3.3 (-5.6, -1.0)	**0.006**	-2.3 (-4.3, -0.2)	**0.030**

Table 4.6 – Association between cardiomyopathy phase and $\dot{V}O_{2peak}$ for the Best Effort CPEX Cohort. Analyses are based on the Best Effort CPEX Cohort (N=42). Associations between the cardiomyopathy phase and $\dot{V}O_{2peak}$ were assessed using two different approaches. The first reports the mean ± standard deviation of the $\dot{V}O_{2peak}$ for each cardiomyopathy phase subgroup, which were compared using a Jonckheere-Terpstra test. The second reports the gradient from a linear regression model with the cardiomyopathy phase treated as a continuous covariate; hence, represents the change in $\dot{V}O_{2peak}$ per increase of one cardiomyopathy phase. Both analyses were performed for both the observed $\dot{V}O_{2peak}$, and the age/sex-normalised values, based on the reported equations (11). Bold p-values are significant at p<0.05. Abbreviations: CPEX: cardiopulmonary exercise testing, $\dot{V}O_{2peak}$: peak oxygen uptake.

4.8.5 Association between disease markers and $\dot{V}O_{2peak}$

Of the blood markers assessed, increases in creatinine, HS troponin, NT-pro-BNP and ACR were all associated with significant reductions in the age/sex-normalised $\dot{V}O_{2peak}$

(**Table 4.7**). Of the CMR/TTE parameters, increasing indexed LV mass, TR Velocity and LA end-diastolic volume (EDV) were associated with significant reductions in the age/sex-normalised $\dot{V}O_{2peak}$, whilst increasing impairments in LA global circumferential strain (GCS), LA GLS, LA ejection fraction and fractional area change were associated with significant reductions in age/sex-normalised $\dot{V}O_{2peak}$. Analysis of the observed $\dot{V}O_{2peak}$ (i.e. without age/sex-normalisation) and sensitivity analysis of the best effort CPEX cohort returned similar results.

	N	$\dot{V}O_{2peak}$		Age/Sex-Normalised $\dot{V}O_{2peak}$	
		Rho	*p-Value*	*Rho*	*p-Value*
Biochemistry					
Creatinine (umol/L)	88	-0.284	**0.007**	-0.318	**0.003**
HS Troponin-I (ng/L)	64	-0.467	**<0.001**	-0.274	**0.028**
HS Troponin-T (ng/L)	23	-0.699	**<0.001**	-0.624	**0.001**
NTpro-BNP (ng/L)	88	-0.638	**<0.001**	-0.488	**<0.001**
ACR (mg/mmol)	85	-0.375	**<0.001**	-0.314	**0.003**
Cholesterol (mmol/L)	87	-0.114	0.292	-0.071	0.511
Haemoglobin (g/L)	86	0.002	0.988	0.028	0.796
CMR Parameters					
LV EDVi (ml/m^2)	76	0.219	0.057	0.093	0.424
LV ESVi (ml/m^2)	76	0.144	0.214	0.015	0.898
LV SVi (ml/m^2)	75	0.230	**0.047**	0.164	0.159
LV Mi (g/m^2)	76	-0.338	**0.003**	-0.300	**0.009**
LV EF (%)	76	-0.077	0.510	-0.002	0.984

RV EDVi (ml/m^2)	74	0.183	0.119	0.099	0.399
RV ESVi (ml/m^2)	74	0.038	0.747	-0.033	0.779
RV SVi (ml/m^2)	73	0.260	**0.026**	0.229	0.051
RV EF (%)	74	0.023	0.848	0.081	0.491
LA Volume (ml)	73	-0.177	0.134	-0.158	0.183
Lowest T1 (ms)	69	-0.001	0.992	0.043	0.724
TTE Parameters					
TR Velocity (cm/s)	39	-0.534	**<0.001**	-0.477	**0.002**
LA GCS (%)	78	0.275	**0.015**	0.317	**0.005**
LA GLS (%)	78	0.257	**0.023**	0.271	**0.016**
LA EF (%)	78	0.305	**0.007**	0.359	**0.001**
LA EDV (ml)	78	-0.344	**0.002**	-0.304	**0.007**
LA ESV (ml)	78	-0.222	0.051	-0.160	0.162
LA FAC (%)	78	0.285	**0.012**	0.330	**0.003**

Table 4.7 – Correlations between $\dot{V}O_{2peak}$ and biochemistry/imaging parameters for the Primary Cohort. Correlations between each parameter and both the observed and age/sex-normalised $\dot{V}O_{2peak}$ are quantified using Spearman's rank correlation coefficients (rho). Bold p-values are significant at p<0.05. Abbreviations: ACR: urine albumin to creatinine ratio, CMR: cardiac magnetic resonance imaging, EDV(i): end-diastolic volume (indexed), EF: ejection fraction, ESV(i): end-systolic volume (indexed), FAC: fractional area change, GCS: global circumferential strain, GLS: global longitudinal strain, HS: high sensitivity, LA: left atrial, LV: left ventricular, Mi: mass indexed, NTpro-BNP: N-terminal pro B-type natriuretic peptide, RV: right ventricular, SVi: stroke volume indexed, TR: tricuspid regurgitation, TTE: transthoracic echocardiography, $\dot{V}O_{2peak}$: peak oxygen uptake.

4.8.6 FEV_1 by cardiomyopathy stage

Of the 54 patients who underwent a CPEX, 52 additionally had an FEV_1 measurement recorded during lung function testing prior to exercise commencement. The mean FEV_1 was 2.50 ± 1.00 L. Interestingly, as with $\dot{V}O_{2peak}$, this was significantly lower than the mean expected value based on the "race-neutral" reference equation (205) (3.11 ± 0.68, p<0.001), yielding a mean age/sex/height-normalised FEV_1 of -0.61 ± 0.81 L. FEV_1 was found to be strongly correlated with $\dot{V}O_{2peak}$ (rho: 0.603, p<0.001, **Figure 4.4C**). However, unlike $\dot{V}O_{2peak}$, FEV_1 values were not found to differ significantly with cardiac disease stage (p=0.309), with means ranging from 2.84L in stage 1 to 2.30L in stage 4 (**Table 4.5**). Analysis of age/sex/height-normalised FEV_1 returned consistent results, with regression analysis finding no significant trend across cardiac disease stages (gradient: -0.09 L per stage, 95% CI: -0.29, -0.12; p=0.394; **Figure 4.4D**).

4.9 Discussion

4.9.1 Impairments in $\dot{V}O_{2peak}$ in early Fabry cardiomyopathy

This study is the first of its kind to demonstrate significant impairments in peak aerobic capacity in FD with our data suggesting this begins early and is driven largely by progressively worsening of cardiomyopathy, assessed using advanced imaging and biochemical parameters. A previous study assessed exercise capacity using CPEX and demonstrated a general decline in $\dot{V}O_{2peak}$ which improved with ERT (207). However, this was a small study of 15 patients and underlying mechanisms of $\dot{V}O_{2peak}$ impairment were not explored. Another study of 38 patients demonstrated

chronotropic incompetence in FD patients undergoing cycle ergometry suggesting Gb3 deposition within the conduction system and autonomic dysfunction (42). A gender-specific trend was noted with male patients having a lower exercise capacity compared with females. However, the sample size was also small, and most patients were male with LVH. A more recent study of 29 patients demonstrated impairments in $\dot{V}O_{2peak,}$ and oxygen pulse in FD compared to healthy controls. They also identified a positive correlation between aerobic capacity impairment and right ventricular end-diastolic and systolic volumes on CMR in patients with mild myocardial fibrosis and no significant LVH (202). Despite this, there was no correlation observed between $\dot{V}O_{2peak}$ and overall LVM. In a small study of 10 patients with FD, cardiac variants of FD demonstrated a lower $\dot{V}O_{2peak}$ on CPEX testing with cycle ergometry compared to classical disease with both cardiac and classical variants demonstrating a lower $\dot{V}O_{2peak}$ compared with healthy controls (208). A major limitation of this study was the small sample size and all the patients with cardiac variants (n=5) were male, with all those with classical variants (n=5) female.

4.9.2 Cardiac aetiology of $\dot{V}O_{2peak}$ impairment

Compared with previous studies, our cohort has a relatively equal male-to-female ratio with the added benefit of equal distribution across cardiac disease stage. Unlike previously published data, ours is the largest cohort of FD patients who have undergone exercise testing to date and the cohort was deeply phenotyped with TTE, CMR, lung function and biochemical data available. This allows for a better understanding of mechanisms underpinning $\dot{V}O_{2peak}$ limitation in FD. This study, for the first time, highlights objective evidence of impaired aerobic capacity in patients with gene-positive FD but no detectable cardiomyopathy using advanced imaging

techniques for detection, including deformation TTE and CMR. This becomes further impaired with progression of disease stage in the absence of a fall in FEV_1, supporting the notion of an underlying cardiac aetiology. Symptoms relating to exercise impairment in FD are common and include breathlessness (209) and fatigue (42). Due to the multi-systemic nature of FD with a range of non-specific symptoms experienced, it can be a challenge to link symptoms to a specific underlying mechanism related to FD. Early impairments in $\dot{V}O_{2peak}$ exhibited in this study suggest that these symptoms may be, in part, explained by early myocardial disease, not detectable using conventional investigations conducted as part of the patient's standard care. It is becoming increasingly evident that cardiac Gb3 accumulation begins early, and this has been demonstrated on a cellular level in patient-derived ventricular iPSC-CMs, which demonstrate changes in electrophysiology as well as early Gb3 accumulation (97). Early electrocardiographic changes are also detectable in FD patients with PQ shortening being one of the earliest cardiac manifestations before the development of LVH or detectable Gb3 accumulation as seen by T1 relaxation time reduction on CMR (25). These suggest that Gb3 accumulation takes place much earlier than previously thought. The structural consequences of Gb3 accumulation may explain early electrocardiographic changes in vivo and on a cellular level. Early Gb3 accumulation within cardiac cells, both atrial and ventricular, which is not detectable using conventional imaging may also be responsible for impairments in aerobic capacity as evidenced by $\dot{V}O_{2peak}$ impairment. The results of this study are consistent with the cellular data and raise the prospect of potential clinical benefit of commencing disease-modifying FD therapy in early stages of cardiomyopathy.

4.9.3 Impairment of biomarkers with cardiac disease stage

As would be expected with progression of cardiac disease stage, various CMR, TTE and biochemical markers of cardiomyopathy worsened. CMR parameters included greater LVMi and LA volume. TTE parameters included greater LA volume, impaired LA strain and greater TR velocity. These are in keeping with development of a restrictive cardiomyopathy phenotype with advancing disease (69, 210). The phenomenon of T1 relaxation time pseudonormalisation (211) was also observed with a gradual reduction in global T1 relaxation times up to stage 3 with "pseudonormalisation" demonstrated by increased T1 relaxation times in stage 4. Blood biomarker changes with disease stage included elevation of troponin and NT-pro-BNP, in keeping with published literature (175). Serum creatinine and ACR also increased with cardiac disease stage reflecting progressive nephropathy and emphasising the natural progression of multi-organ dysfunction in FD occurring in parallel (62, 212). Interestingly, haemoglobin levels also increased with disease stage which contrasts with the positive correlation demonstrated between $\dot{V}O_{2peak}$ and haemoglobin in the literature due the known role of haemoglobin in oxygen transport in the peripheral circulation (213). As expected with advancing disease, a greater proportion of patients were taking ERT and statins with more advanced cardiac disease stage and patients had more comorbidities, namely ischaemic heart disease and CKD. These findings alongside a greater proportion of males in more advanced cardiac disease stage again highlights the natural progression of FD cardiomyopathy with males generally exhibiting a more severe and earlier-onset phenotype given the X-linked nature of the condition (81). However, with over 20% of those in stage 4 being female, this highlights the importance of skewed X-linked inactivation observed and

the importance of equally close monitoring for organ involvement and organ-related complications in females (214).

4.9.4 Cardiac biomarkers correlate with $\dot{V}O_{2peak}$

Several significant correlations were demonstrated between age/sex-normalised $\dot{V}O_{2peak}$ and various biochemical and imaging parameters providing novel insights into mechanisms underpinning impaired aerobic and exercise capacity in FD. We demonstrate that increasing LVMi was associated with impaired $\dot{V}O_{2peak}$. Myocardial blood flow and reserve can be quantified using stress perfusion CMR and provides information regarding microvascular dysfunction and ischaemia (215). In FD, this has been assessed in patients with and without evidence of LVH. Interestingly they demonstrated impaired myocardial blood flow in the absence of LVH that was more pronounced in those with LVH (79). This suggests that microvascular perfusion abnormalities begin early and may contribute to $\dot{V}O_{2peak}$ impairment. This worsens as LVMi increases, presumably due to progressive microvascular dysfunction and subsequent ischaemia. The observation of troponin increase correlating with $\dot{V}O_{2peak}$ impairment is in keeping with this and may reflect ongoing chronic microvascular ischaemia as well as that of chronic myocardial inflammation in more advanced FD cardiomyopathy (111). The combination of increasing LVMi and increasing TR maximum velocity, both of which correlated with impairments in $\dot{V}O_{2peak}$, suggest the development of a restrictive cardiomyopathy phenotype in FD. The association of elevation in TR maximum regurgitant velocity with progressive LVH suggested increasing pulmonary artery pressure which is likely to contribute to $\dot{V}O_{2peak}$ impairment in our cohort. This observation has also been demonstrated in cohorts of non-FD patients with restrictive cardiomyopathy (216). The finding of worsening

exercise capacity in FD based on degree of cardiomyopathy has been demonstrated in a prior study of 32 patients where cardiomyopathy was graded simply on degree of fibrosis on CMR (131). The study demonstrated improvements in exercise capacity on cycle ergometry with ERT in those without fibrosis with a worsening in exercise capacity in those with “severe” fibrosis. Our findings to an extent are in keeping with this; however, our staging classification takes into consideration the more complex cardiac phenotype.

To put the trend in $\dot{V}O_{2peak}$ into context, the normative ranges reported (203) show the expected $\dot{V}O_{2peak}$ to decline be approximately 2.5 ml/kg/min per decade. As such, the observed reduction of 2.2 ml/kg/min per cardiac disease stage implies that the reduction in exercise tolerance resulting from a progression of one disease stage is similar to that associated with around a decade of aging. On the other hand, published equations for normalisation of FEV_1 estimate a reduction in expected FEV_1 of approximately 0.30L per decade (for a 180cm male) (205); hence, the observed non-significant reduction of 0.09 L per cardiac disease stage represents a change equivalent to that of only three years of aging.

4.10 Limitations

The primary strength of this study is the relatively large sample size of deeply phenotyped patients with a rare disease, incorporating exercise data with imaging and biochemical markers. However, there are limitations which need to be considered when interpreting the results. Firstly, whilst the sample size is the largest to date assessing exercise capacity in FD patients, it remains small compared to non-FD

studies using CPEX. Also, within the cohort, not all were able to undergo CPEX testing. For this reason, 6MWD was used to produce an "estimated" $\dot{V}O_{2peak}$ value. Whilst 6MWD and $\dot{V}O_{2peak}$ were strongly correlated in patients who underwent both 6MWT and CPEX, enabling the use of the 6MWD to impute an estimated $\dot{V}O_{2peak}$, this was still an estimate and not a direct measurement of $\dot{V}O_{2peak}$. However, this is an accurate and published correlation in those not able to undergo CPEX testing due to physical limitations.

Another limitation of this study was the lack of healthy non-FD controls for comparison. Because the study was using routinely collected clinical data as part of the patients' standard care, extra tests were not carried out. For this reason, healthy controls were not recruited to undergo exercise testing. To account for this, as well as variations in $\dot{V}O_{2peak}$ and FEV_1 with age and gender, normalised values were used. For $\dot{V}O_{2peak}$, an equation was used for each patient against normalised percentiles in published literature to provide a value against what would be an expected $\dot{V}O_{2peak}$ for that patients age and gender (204). For FEV_1, a similar equation was used to ascertain what would be expected to be the normal value for a non-FD adult of that specific age, gender and race (205).

The final limitation of this study is that we do not have reproducibility data available when assessing VO_{2peak} on CPEX. This is an important consideration when planning future studies as test-retest reproducibility data would be required to assess the statistical power of $\dot{V}O_{2peak}$ as a reliable outcome measure of aerobic capacity impairment on CPEX.

4.11 Conclusions

In the largest study of its kind, we demonstrate significant impairments in aerobic capacity in FD across all stages of cardiomyopathy which appear be due to cardiac limitation. $\dot{V}O_{2peak}$ was significantly impaired in patients without phenotypic evidence of cardiomyopathy, respiratory limitation or biochemical imbalance suggesting that cardiac Gb3 accumulation takes place early, progresses insidiously and may account for early reduction in exercise capacity. In the future, $\dot{V}O_{2peak}$ could serve as a useful marker of exercise capacity including for baseline assessment and importantly a marker to assess response to therapy.

5 Chapter 5 – The role of atherosclerosis and inflammation on arrhythmia risk stratification in Fabry Disease

Data from this chapter is based on the first author published article where these data were first presented:

Roy A, Umar H, Ochoa-Ferraro A, Warfield A, Lewis N, Geberhiwot T, et al. Atherosclerosis in Fabry Disease-A Contemporary Review. *J Clin Med*. 2021;10(19).

5.1 Personal Contribution

I was responsible for screening the cohorts and collection of data across all sites. Following data collection, I conducted the statistical analyses, wrote the subsequent manuscripts and edited all revisions. Plasma samples were collected from patients enrolled to the randomised controlled trial evaluating arrhythmia burden, risk of sudden cardiac death and stroke in patients with Fabry Disease: the role of implantable loop recorders (RaILRoAD). I collected plasma samples from patients recruited, aliquoted these and conducted the Luminex® Performance Assay under supervision. I conducted the statistical analyses of the data.

5.2 Background

Cardiac sphingolipid accumulation occurs in all cardiac cell types resulting in LVH, myocardial inflammation, fibrosis and scar (26). These effects contribute to the high prevalence of arrhythmia in FD, and it is noteworthy that SCD is the most common form of FD mortality (217, 218). Studies indicate that the frequency of malignant ventricular arrhythmia may be as high as 30% (11). AF, brady-arrhythmia, ventricular tachyarrhythmia and SCD may indeed be the first manifestation of cardiomyopathy before clinical or imaging abnormalities (11).

Risk factors for tachyarrhythmia in FD include male gender, presence of LGE, advancing age, and elevated MSSI score. Risk factors for bradyarrhythmia and AF requiring intervention include age, LVH and LA dilatation (11, 23). Both ischaemia and inflammation have the potential to increase arrhythmic risk in FD, with myocardial Gb3 accumulation traditionally causing microvascular dysfunction, alteration of oxygen demand-supply mismatch due to LVH and reduced arterial compliance. Added to this, FD patients may have conventional risk factors for atherosclerotic coronary disease including hypertension, hypercholesterolaemia and co-existing renal disease (219-221).

LSDs, particularly FD, have a significant pro-inflammatory effect which is likely to be multi-organ (222). In the general population, various conditions of inflammation including inflammatory bowel disease and sepsis predispose to incident AF (223, 224), as do specific myocardial inflammatory disorders (225). In adults with FD undergoing endomyocardial biopsy, over half of the patients had evidence of myocarditis which

associated with a greater burden of arrhythmia on intermittent short term cardiac monitoring (110). However, neither the pro-arrhythmic potential of ischaemia nor inflammation have previously been studied in FD.

5.3 Hypotheses

Current risk factors, at present, do not adequately explain the increased risk of arrhythmia in FD. We hypothesised that adults with FD have an increased risk of atherosclerotic coronary disease with a high prevalence of cardiovascular risk factors, both of which contribute to the arrhythmia substrate and increase arrhythmic risk. With multiparametric CMR detecting myocardial inflammation at varying stages of FD cardiomyopathy, we also hypothesised that the arrhythmic substrate may reflect an inflammatory cardiomyopathy evidenced by released of pro-inflammatory cytokines at varying stages of disease.

5.4 Aims and Objectives

The aims of this chapter were to explore in detail the role of additional potential risk factors for arrhythmia. Particularly, the intention was to focus on the role of inflammation, ischaemia and atherosclerosis in arrhythmogenesis in FD. Specifically, the aim was to understand how each of these processes separately and in combination, affect FD patients risk of developing arrhythmia at varying degrees of cardiomyopathy stage.

5.5 Methods

5.5.1 Study population and design

5.5.1.1 Atherosclerotic risk in Fabry Disease

This was a single centre observational retrospective analysis of adults with genetic or enzymatic confirmation FD, currently on disease-modifying therapy including ERT or OCT at QEHB, UK. Baseline characteristics of cardiovascular risk factors were collected, including cardiac medication history, renal function, serum cholesterol and systolic blood pressure. In those who underwent formal testing due to symptoms potentially relating to ischaemia, data was collected from computed tomography coronary angiography (CTCA) invasive coronary angiography (ICA), or myocardial perfusion scanning (MPS).

5.5.1.2 Inflammation in Fabry Disease

This was a multicentre study of adults with genetic or enzymatic confirmation of FD enrolled to the RaILRoAD study (Chapter 6) who underwent serum and plasma collection at their baseline visit. Baseline characteristics were collected including demographics and comorbidities. Patients were categorised according to degree of FD cardiomyopathy. However, the classification was different to that of previous chapters in this thesis as the patients recruited to RaILRoAD were required to already have a degree of cardiomyopathy, as detailed in the inclusion criteria. Therefore patients were categorised into 2 groups: those with intermediate cardiomyopathy (ECG abnormalities associated with FD ± documented low T1 mapping on CMR), and those with advanced cardiomyopathy (elevated high-sensitivity troponin ± LGE on

CMR. Samples were also collected from a control cohort of non-FD patients, age and sex matched for comparison. The control cohort were recruited from the study “Effects of a Reduction in Renal Function on Cardiovascular Structure and Function: A 5-year Study of Kidney Donors”. The control cohort underwent detailed clinical assessment including biochemical testing (full blood count, renal and liver function tests), electrocardiography and CMR, all of which were normal.

5.5.2 Electrocardiography:

Standard 12 lead ECGs were acquired according to current standardised guidelines for acquisition and interpretation (226).

5.5.3 Transthoracic Echocardiography:

TTE (ie33 / EPIC, Phillips and Vivid, GE) was performed by an accredited sonographer according to the British Society of Echocardiography minimum dataset (140). Chamber size and function were measured according to current standard guidelines (227). Parameters for assessment of diastolic function were acquired according to the general principles for TTE assessment established by the American Society for Echocardiography in association with the European Association of Cardiovascular Imaging (164). Diastolic function was graded by an experienced Cardiologist specialising in TTE according to current guidelines (164).

5.5.4 Cardiac Magnetic Resonance Imaging.

Contrast-enhanced CMR (1.5T Avanto, Siemens Healthcare, Erlangen, Germany) was performed in line with standard protocols to obtain LV dimensions, volumes, and mass (197). A steady-state free precision single breath hold modified Looker Locker inversion recovery (MOLLI) sequence was used for T1 mapping in the basal and mid LV short axis levels and horizontal long-axis, before and 15-20 minutes after administration of gadolinium-based contrast agent (198). Imaging for assessment of LGE, calculation of regional and global T1 and myocardial extracellular volume were performed as previously described (199).

5.5.5 Bloods and urine

For both studies, routine biochemical and haematological tests were performed including cardiac biomarkers high-sensitivity troponin (I or T), NT-proBNP. For patients enrolled to the RaILRoAD study, additional serum and plasma samples were collected for future analysis and to run the Luminex® Performance Assay.

5.5.5.1 Luminex® Performance Assay

To explore the role of inflammation in FD cardiomyopathy, plasma samples from patients recruited to the RaILRoAD study were used to quantify the levels of multiple cytokines involved in angiogenesis, inflammation and leukocyte trafficking. This was conducted using a Luminex® Performance Assay (Human XL Cytokine Fixed Panel – Biotechne R&D Systems LKTM014B). The benefits of the Luminex® assays are that they allow for quantification of multiple analytes simultaneously in a single sample.

Plasma samples were also collected from healthy age and sex-matched non-FD controls for comparison.

5.5.5.1.1 *Preparation*

Plasma samples had been collected from patients consenting to the RaILRoAD study. Samples were taken at the time of consent and stored in a -80° C freezer. To minimise the effects of repeated freeze-thaw cycles, samples were thawed at the time of Luminex® preparation. The samples were run alongside 2 high and low controls and 7 standards in duplicates.

Analyte-specific antibodies were pre-coated onto magnetic microparticles, embedded with fluorophores at set ratios for each unique microparticle region. Samples were pipetted into wells along with microparticles and standards; the antibodies then bind to analytes of interest. Following a wash, cocktail specific antibodies to each of the analytes were added. Streptavidin-phycoerythrin conjugate was added to each well following another wash to bind to the biotinylated antibody. Multiple washes then removed unbound substances and microparticles were resuspended in buffer and read using the Luminex® machine. Detailed sample preparation was in accordance with the manufacturer's instructions.

5.5.5.1.2 *Procedure*

The Luminex® 100 machine (Biorad) was used which used 2 lasers for analysis. The first laser excited the dyes in each microparticle in order to identify the microparticle

region. The second laser was used to excite the phycoerythrin to measure and quantify the amount of analyte bound to the microparticle. Excitation emitted as each microparticle passed through the flow cell was analysed to differentiate excitation levels using a photomultiplier and an avalanche photodiode.

Values are expressed as observed concentrations. In some cases, values fell outside the standard curve (concentration too low for detection) but were within a pre-specified range. In these cases, concentrations were extrapolated and included in the analysis. If they were too low to fall within the pre-specified range, the lowest extrapolated reading was halved and included in the analysis.

5.6 Statistical analysis

The baseline demographics of the cohort were summarised, with continuous variables reported as means ± standard deviations (SDs). Where two continuous variables were being compared, normality was assessed using Shapiro-Wilks test. Where data was normally distributed, an unpaired t-test was performed. If the data was normally distributed but standard deviations were not equal, unpaired t-tests with Welch's correction were performed. Where data was not normally distributed, the Mann-Whitney test was used. Where more than two variables were being compared, an Ordinary one-way ANOVA was performed with Turkey's multiple comparisons test for normally distributed data. For non-normally distributed data where more than two variables were compared, the Kruskal-Wallis test was performed (with Dunn's test for multiple comparisons). A p-value <0.05 was deemed to be indicative of statistical significance throughout. All analyses were performed using GraphPad Prism version 9.3.1, GraphPad Software, San Diego, California, USA (www.graphpad.com).

5.7 Ethics

5.7.1 Atherosclerotic risk in Fabry Disease

Ethical approval was approved by West Midlands – South Birmingham Research Ethics Committee (23/WM/0180 IRAS 325613) for the use of retrospective clinical data for the secondary purpose of research. The study conducted in accordance with the local legislation and institutional requirements. The Ethics Committee / institutional review board waived the requirement of written informed consent for participation from the participants or participant's legal guardians / next of kin because data were acquired from a research database using routinely collected clinical data for the purpose of research

5.7.2 Inflammation in Fabry Disease

Ethical approval for the conduct of this study was approved by the NHS Health Research Authority and local NHS Research Ethics Committee (IRAS 224749 17/WM/0421). The study was also registered on ClinicalTrials.gov (NCT03305250). Informed consent was obtained from each study participant in accordance with Good Clinical Practice guidelines and patients were provided with a patient information leaflet to review prior to being consented. The use of plasma samples in non-FD healthy controls from the CRIB-DONOR study was approved by the West Midlands Solihull Research Ethics Committee (IRAS 214780 17/WM/0048) and approved by the Health Research Council. All healthy controls gave informed consent to take part in accordance with the principles set out in the Declaration of Helsinki.

5.8 Results

5.8.1 Atherosclerotic risk in Fabry Disease

5.8.1.1 Cohort characteristics

In this retrospective assessment of 47 adults with FD on disease-modifying therapy, mean age was 52.4 years and 47% were female. 32 (68%) were taking anti-hypertensive therapy, 18 (38%) were on a statin and 12 (26%) had a total cholesterol >5mmol/L. In total, 13 (28%) patients had stage 3-5 CKD and 14 (30%) stage 2. Moreover, 30 (63%) had proteinuria defined as an ACR >3mg/mmol. This represents a high frequency of conventional risk factors in adults with FD. Baseline characteristics are summarised in (**Table 5.1**).

Characteristic	N= 47 (%)
Gender	Male: 25 (53%) Female: 22 (47%)
Age (Years)	Male 51.4 Female 53.6 Overall 52.4
Enzyme replacement therapy / oral chaperone therapy	Fabrazyme: 10 (21%) Migalastat: 20 (43%) Replagal: 17 (36%)
Anti-hypertensive medication	0 anti-hypertensives – 15 (32%) 1 anti-hypertensive 20 (43%) 2 anti-hypertensives 7 (15%) 3 anti-hypertensives 5 (10%)
Angiotensin converting enzyme inhibitor / **angiotensin receptor blocker**	27 (57%)
Statin therapy	18 (38%)
T-Chol (mmol/L)	=< 5mmol/l: 35 (75%)

	> 5mmol/l: 12 (25%)
Systolic blood pressure (mmHg)	> 140: 16: (34) < 140 31: (66)
eGFR (ml/min)	>90: 11 (24%) 60-89: 23 (49%) 45-59: 10 (21%) 30-44: 1 (2%) 15-29: 1 (2%) <15: 1 (2%)
ACR (mg/mmol)	<3: 15 (32%) 3-30: 19 (41%) >30: 11 (23%) Not available: 2 (4%)

Table 5.1: Baseline characteristics of cardiovascular risk factors in a cohort of adults with FD on disease-modifying therapy

5.8.1.2 Ischaemia testing

Within the cohort of 47 patients, 25 (53%) had a formal assessment of their coronary arteries having experience ischaemic symptoms (**Table 5.2**). 12 (26%) underwent ICA and 13 (28%) underwent CTCA. Of those who underwent ICA, 7 (48%) had no evidence of flow-limiting coronary artery disease, and 5 (42%) had evidence of significant coronary disease necessitating revascularisation, 3 requiring coronary artery bypass grafting (CABG) and 2 percutaneous coronary intervention (PCI). In the CTCA group, no patients had flow-limiting coronary artery disease. However, 7 (54%) had mild-moderate coronary atheroma. Interestingly 9 (69%) had normal calcium scores with no evidence of coronary calcium. Most patients undergoing ischaemia testing were male (68%) and of advancing age (mean age 60 years).

5 patients underwent MPS to assess for perfusion defects in the context of experiencing chest pain. Of these, 3 were normal, 1 demonstrated ischaemic heart disease and the patient had undergone a previous CABG. Interestingly, this patient also had fixed perfusion defects in the basal inferolateral wall with associated LGE in the same region on CMR which suggests perfusion defects likely not related to ischaemic cardiomyopathy (**Figure 5.1**). The final MPS demonstrated reduced uptake in the anterior wall on stress with improvement at rest. Interestingly, this patient had also undergone ICA which demonstrated no flow-limiting disease, suggesting microvascular ischaemia and demand-supply oxygen mismatch.

Characteristic	ICA (N=12) (%)	CTCA (N=13) (%)	Total (N=25) (%)
Gender / Age	M: 9 (75%) F: 3 (25%) mean age 65	M: 8 (61%) F: 5 (39%) mean age 54	M: 17 (68%) F: 8 (32%) mean age 60
Angiography findings	Normal: 5 (41%) Mild Coronary Disease: 2 (17%) CABG with patent grafts: 3 (25%) PCI with patent stents: 2 (17%) Significant coronary disease (including occluded grafts/stents): 0 (0%)	No coronary stenosis: 6 (46%) Mild coronary stenosis: 6 (46%) Moderate coronary stenosis 1(8%) Significant coronary stenosis 0 (0%)	No coronary disease: 11 (44%) Mild/moderate coronary disease: 9 (36%) Coronary disease with patent grafts / stents: 5 (20%) Significant / Severe coronary disease: 0 (0%)
Hypertension	5 (41%)	3 (23%)	8 (32%)
Diabetes	0 (0%)	0 (0%)	0 (0%)
Cholesterol	<4mmol/L: 7 (58%) 4-5mmol/L: 3 (25%) > 5mmol/L: 2 (17%)	<4mmol/L: 3 (23%) 4-5mmol/L: 7 (54%) > 5mmol/L: 3 (23%)	<4mmol/L: 10 (40%) 4-5mmol/L: 10 (40%) > 5mmol/L: 5 (10%)
Family History	2 (17%)	2 (15%)	4 (16%)
Smoking History	1 (8%)	6 (46%)	7 (28%)

Table 5.2: ICA and CTCA findings in adults with FD on disease-modifying treatment including associated cardiovascular risk factors

.

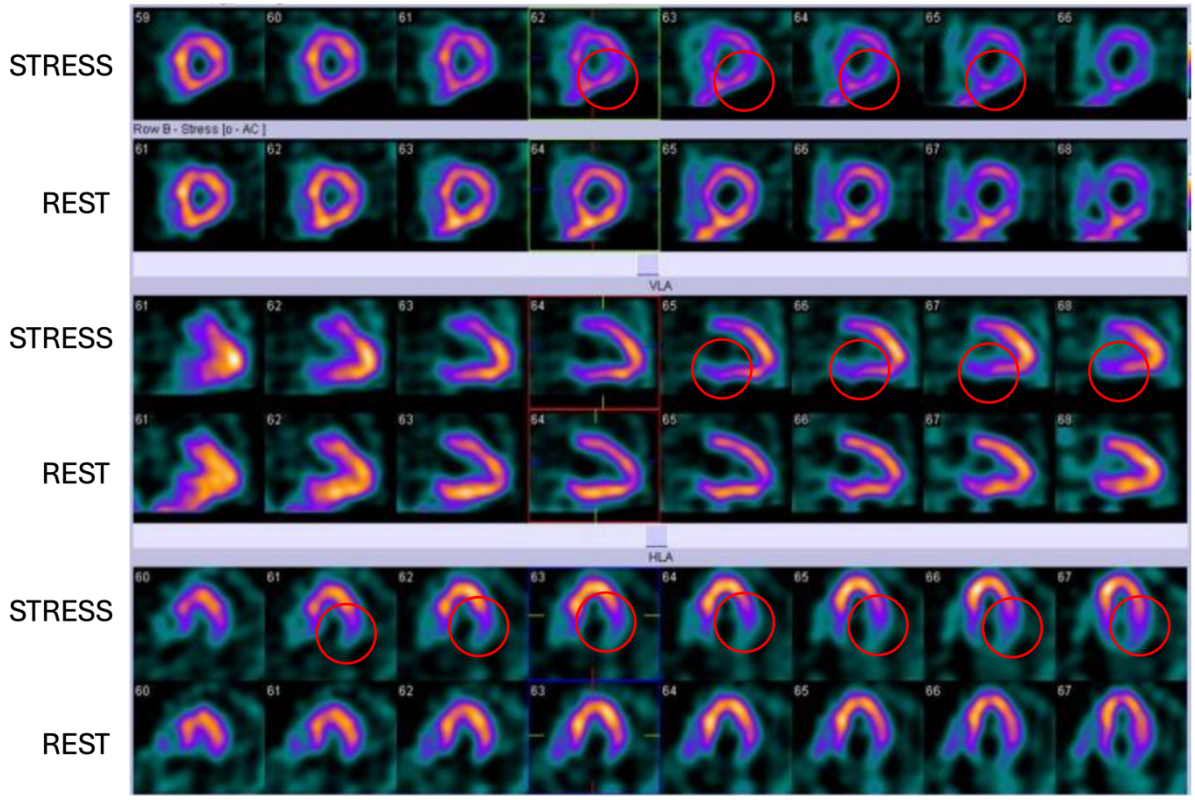

Figure 5.1: MPS of an adult with FD demonstrating with rest and stress imaging. Reversible perfusion defects in the basal inferolateral wall of the left ventricle under stress (defects circled in red) is typically seen in FD.

5.8.2 Inflammation in Fabry Disease

Cohort characteristics are summarised in **Table 5.3**. Patients were split into non-FD controls (N=38), FD with intermediate cardiomyopathy (N=14), and FD with advanced cardiomyopathy, (N=24). This allowed for sub-analysis of early-stage FD cardiomyopathy and advanced FD cardiomyopathy versus no FD. Mean age of the FD cohort was 41.2 ± 14.5 years in early-stage cardiomyopathy versus 55.4 ± 10.8 years in the advanced stage (mean age of the non-FD control group was 49.4 ± 12.3). In the early-stage cardiomyopathy group 9 (64%) were female compared with 12

(50%) in the advanced group versus 19 (50%) in the control group. The cohorts were appropriately age and sex matched on statistical assessment.

Findings from the Luminex® are summarised in **Table 5.4** and illustrated in **Figures 5.2-5.4** according to each patient group and individual analyte. In summary, numerous analytes were increased in FD patients compared to controls, with higher expression in more advanced disease. Highly significant ($p<0.0001$) changes were observed with Eotaxin, IL-6, MCP-1, VEGF and TNF-α (**Table 5.4**).

	Control (N=38)	Low T1/ECG (N=14)	High Trop / LGE (N=24)
Age (Years)	49.4 ± 12.3	41.2 ± 14.5	55.4 ± 10.8
Sex (% Female)	19 (50)	9 (64)	12 (50)
Systolic BP (mmHg)		132 ± 21	137 ± 16
Diastolic BP (mmHg)		75.7 ± 6	79.5 ± 8
Heart rate (bpm)		73 ± 11	70 ± 15
Weight (kg)		80.5 ± 17.6	87.4 ± 26.4
Height (cm)		170 ± 8.73	170 ± 10.6
Haemoglobin (g/l)		138 ± 12	140 ± 15
WCC (10*9/l)		6.8 ± 1.33	6.95 ± 1.62
Urea (mmol/l)		4.75 ± 1.00	6.70 ± 2.88
Creatinine (µmol/l)		70 ± 14	932± 40
Troponin-I (ng/l)		20 ± 12	144 ± 216
NT-proBNP (ng/l)		104 ± 96	2108 ± 4991
Total Cholesterol (mmol/l)		4.67 ± 0.770	4.80 ± 1.10
LDL-C (mmol/l)		2.71 ± 0.729	2.62 ± 0.962
HDL-C (mmol/l)		1.42 ± 0.441	1.58 ± 0.293

Table 5.3: Cohort characteristics for each Luminex® group

Analyte	Control (N=38)	Low T1/ECG (N=14)	High Trop / LGE (N=24)	P-Value
CD40 Ligand	5.05 (5.05-10.1)	68.2 (5.05-553)	316 (5.05-1016)	**0.001**
EDF	1.29 (0.110-12.5)	0.110 (0.110-8.06)	0.110 (0.110-0.110)	0.0617
Eotaxin	38.9 (22.5-57.0)	59.2 (35.6-108)	81.5 (56.1-129)	**<0.0001**
FGF-Basic	0.195 (0.195-0.195)	0.195 (0.195-0.195)	0.195 (0.195-0.195)	0.2236
Flt-3 Ligand	31.5 (24.6-42.3)	34.0 (26.9-36.3)	40.8 (34.7-51.7)	**0.0061**
G-CSF	0.320 (0.320-4.67)	6.86 (0.815-14.1)	4.02 (0.320-13.8)	**0.0052**
GM-CSF	0.820 (0.210-2.48)	0.620 (0.210-6.93)	3.02 (0.263-4.68)	0.2047
GRO-α	16.2 (9.16-32.5)	31.2 (19.0-48.8)	30.2 (20.5-44.5)	**0.0097**
Granzyme B	0.410 (0.410-0.410)	0.410 (0.410-2.10)	0.615 (0.410-5.29	**0.0002**
Gro-ß	109 (64.3-196)	154 (55.7-242)	115 (28.1-344)	0.878
IFN-α2	0.370 (0.100-0.700)	0.840 (0.230-1.18)	0.720 (0.115-1.27)	0.0997
IFN-ß	0.0600 (0.0600-0.0600)	0.0600 (0.0600-0.0600)	0.0600 (0.0600-0.0600)	0.9477
IFN-γ	0.490 (0.300-0.825)	0.690 (0.550-1.06)	0.745 (0.378-1.30)	0.066
IL-1α	0.0850 (0.0850-0.0850)	0.0850 (0.0850-3.66)	0.618 (0.0850-3.41)	**0.0025**

IL-1ß	0.760 (0.530-0.990)	1.29 (0.760-2.43)	1.22 (0.760-2.43)	**0.0035**
IL-1rα	138 (106-208)	219 (118-338)	236 (176-373)	**0.0015**
IL-2	0.0150 (0.0150-0.0150)	0.1 (0.0150-1.12)	0.0150 (0.0150-0.0450	**0.0104**
IL-4	0.570 (0.475-0.660)	0.550 (0.440-0.670)	0.540 (0.480-0.633)	0.8078
IL-6	3.15 (2.74-3.91)	4.41 (3.50-5.52)	5.05 (3.55-6.56)	**<0.0001**
IL-7	1.18 (0.660-1.35)	1.44 (0.898-3.89)	1.27 (0.830-3.12)	**0.0318**
IL-8	0.625 (0.385-1.37)	1.47 (0.525-3.04)	1.15 (0.810-2.82)	**0.0268**
IL-10	29.7 (23.0-63.4)	27.1 (18.9-37.4)	40.9 (26.3-53.4)	**0.0006**
IL-12 p70	4.57 (3.40-5.77)	8.90 (5.47-16.4)	6.70 (4.57-10.8)	**0.0023**
IL-13	6.38 (6.38-6.38)	6.38 (6.38-26.9)	12.8 (6.8-12.9)	**0.0023**
IL-15	0.500 (0.210-0.700)	0.965 (0.758-1.46)	0.910 (0.563-1.54)	**0.0005**
IL-17α	0.680 (0.390-0.858)	0.825 (0.680-1.37)	0.970 (0.680-1.78)	**0.0095**
IL-33	0.185 (0.185-0.185)	0.185 (0.185-3.62)	2.64 (0.185-10.0)	**0.0003**
IP10	29.9 (21.8-46.6)	29.3 (23.8-33.9)	33.7 (20.5-44.5)	0.9108
MCP-1	76.7 (67.1-109)	104 (85.1-149)	129 (98.0-167)	**<0.0001**

MIP-1ß	16.4 (16.4-16.4)	24.6 (16.4-60.8)	16.4 (16.4-62.1)	**0.0086**
MIP-3α	2.63 (1.31-5.10)	4.49 (2.82-8.16)	6.11 (3.42-8.30)	**0.004**
MIP-3ß	46.9 (368-54.1)	47.1 (39.7-56.5)	64.9 (45.1-97.6)	**0.0473**
PDGF-AA	431 (257-832)	1080 (592-3093)	1495 (644-4158)	**0.0008**
PDGF-AB BB	168 (90.2-308)	492 (213-1321)	373 (189-1262)	**0.0013**
PDL1- B17 H1	44.8 (36.6-57.8)	49.8 (34.1-66.8)	67.4 (49.8-91.7)	**0.0011**
RANTES	11457 (5929-16205)	13577 (7232-22327)	11131 (6180-32379)	0.7774
TGF-α	0.275 (0.275-0.275)	0.275 (0.275-0.344)	0.275 (0.275-0.275)	0.1357
TNF-α	2.06 (0.985-3.90)	2.42 (1.59-4.52)	4.92 (2.99-6.94)	**<0.0001**
TNF-ß	1.06 (0.780-1.48)	1.86 (0.548-2.27)	1.35 (0.690-2.04)	0.2331
TRAIL	10.0 (4.73-14.7)	12.6 (8.71-21.8)	16.5 (6.73-20.5)	0.2032
VEGF	22.0 (17.0-29.8)	33.9 (27.1-49.2)	47.7 (30.2-89.7)	**<0.0001**

Table 5.4: Mean observed concentrations of each analyte according to each cohort. Data expressed as median and interquartile ranges. P-values calculated from Kruskal-Wallis ANOVA test. Parameters with p<0.05 are highlighted in blue with bold p-values.

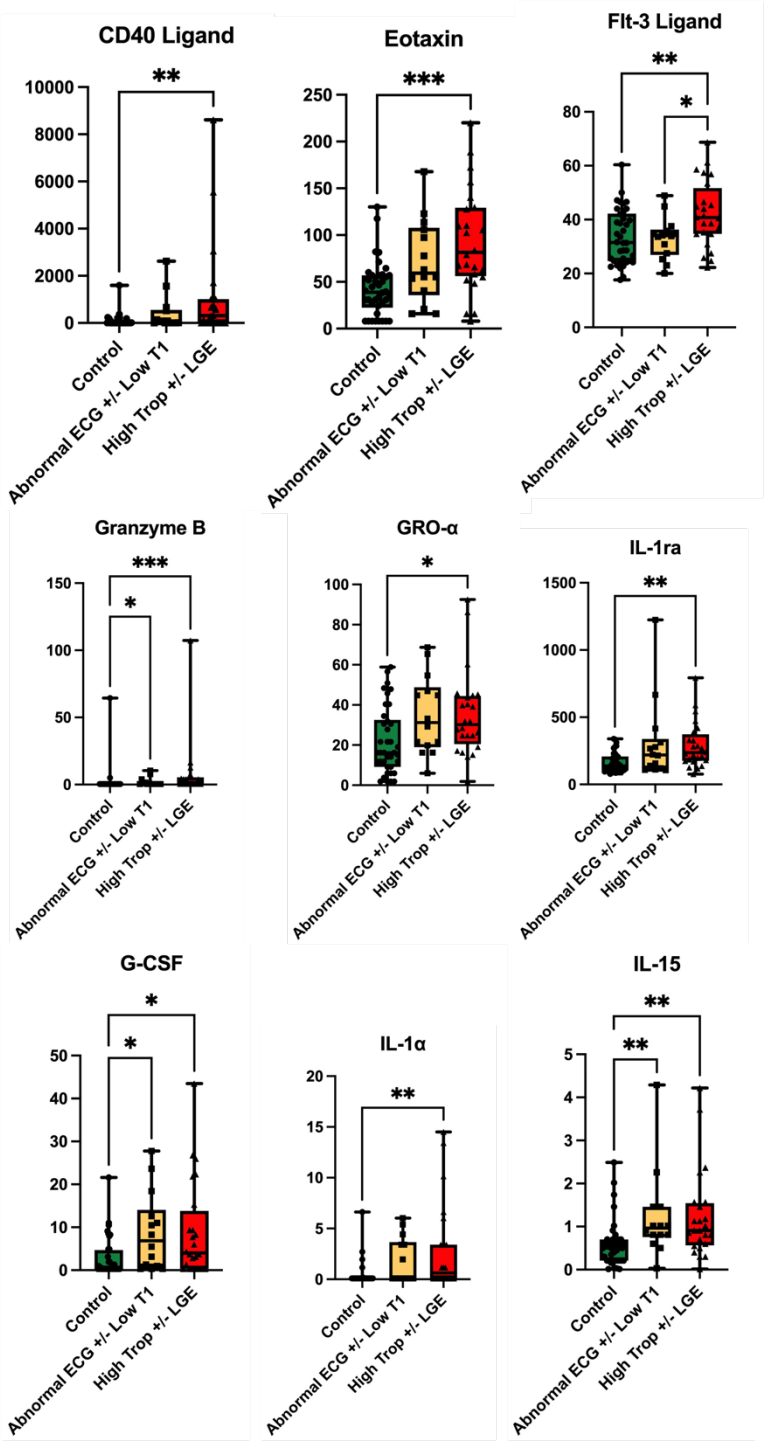

*Figure 5.2: Observed concentrations from the Luminex® assay. Analytes: CD40 Ligand, Eotaxin, Flt-3 Ligand, Granzyme B, Gro-α, IL-1rα, G-CSF, IL-1α, IL-15. Kruskal-Wallis ANOVA test was performed with Dunn's multiple comparison test between each group. *p<0.05, **p<0.01, ***p<0.001*

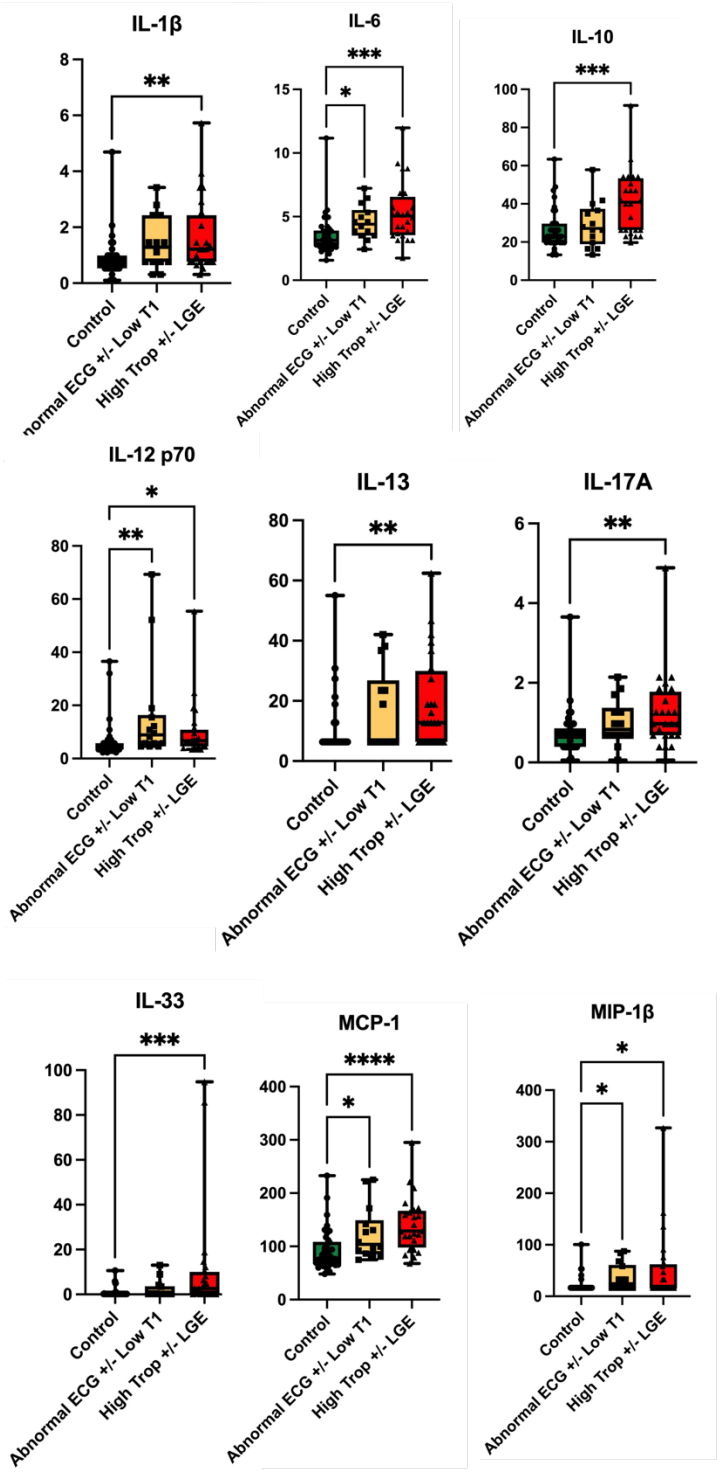

*Figure 5.3: Observed concentrations from the Luminex® assay. Analytes: IL-1ß, IL-6, IL-10, IL-12p70, IL-13, IL-17a, IL-33, MCP-1, MIP-1ß Kruskal-Wallis ANOVA test was performed with Dunn's multiple comparison test between each group. *p<0.05, **p<0.01, ***p<0.001, ****p<0.0001*

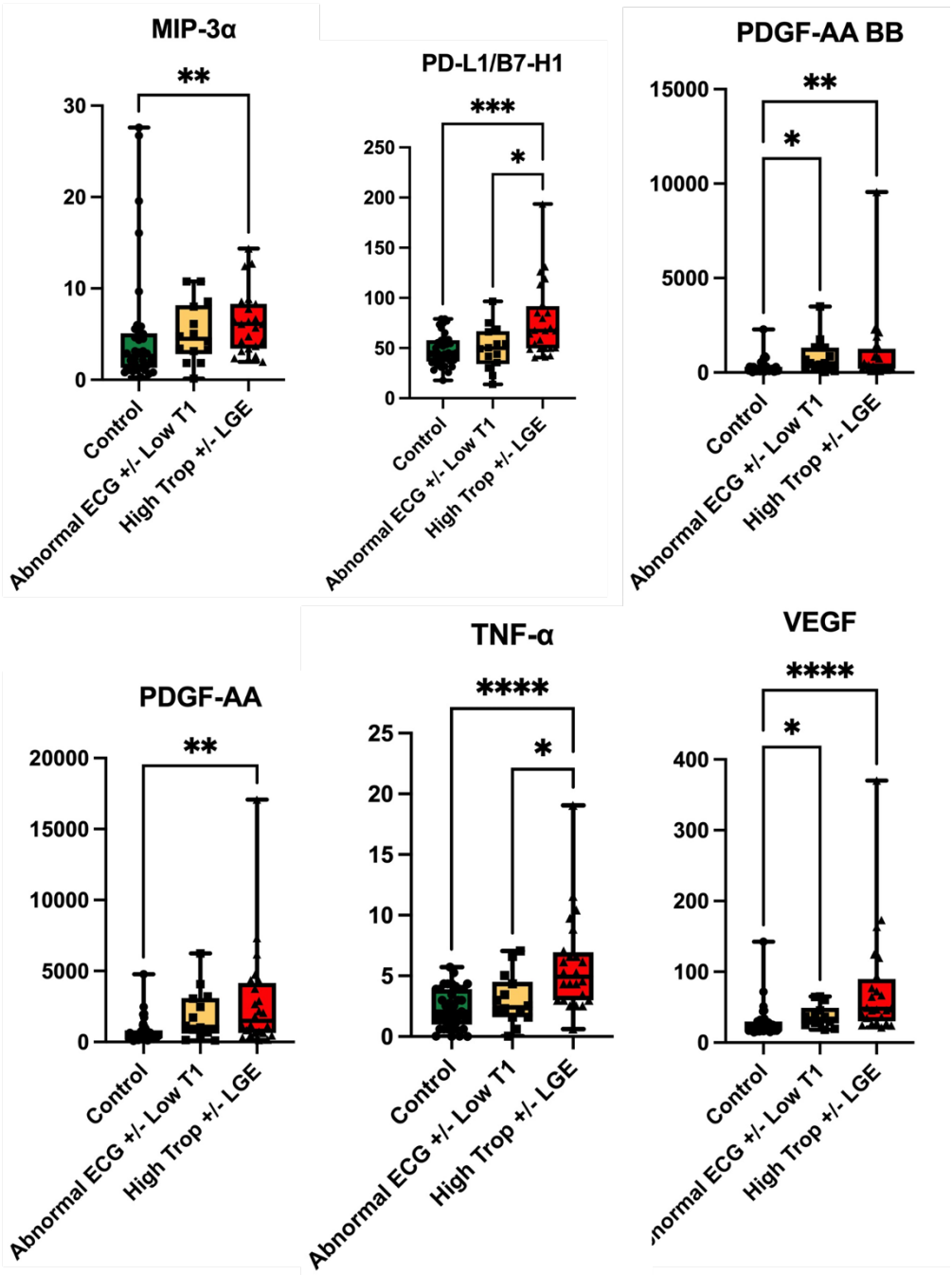

*Figure 5.4: Observed concentrations from the Luminex® assay. Analytes: MIP-3α, PD-L1/B7-H1, PDGF-AB-BB, PDGF-AA, TNF-α, VEGF. Kruskal-Wallis ANOVA test was performed with Dunn's multiple comparison test between each group. *p<0.05, **p<0.01, ***p<0.001, ****p<0.0001*

5.9 Discussion

5.9.1 Atherosclerotic risk in Fabry Disease

5.9.1.1 Conventional risk factors

The risk of atherosclerotic heart disease increases with age, particularly in males and a significant proportion of adverse cardiac events in the general population can be attributed to developing conventional risk factors for atherosclerosis (hypertension, hypercholesterolaemia, diabetes, renal impairment and obesity (228, 229). Registry data shows a high prevalence of hypertension, hypercholesterolaemia and CKD in the FD population and the data presented from our cohort reflects this (55, 182, 219, 220). Given the high frequency of these risk factors, atherosclerosis is likely to be accelerated via conventional pathophysiological processes in FD, thus increasing arrhythmic risk.

5.9.1.2 Fabry Disease-specific mechanisms of atherosclerosis

ICA and CTCA findings in this study support accelerated atherosclerosis in FD. Mechanisms specific to FD have also been postulated that accelerate atherosclerosis. Interestingly, autopsy studies of patients with FD identify atherosclerotic plaques that are concentric in pattern with a white discolouration (230). Gb3 infiltration may trigger the formation of reactive oxygen species (ROS) via microvascular dysfunction and increased arterial wall stress (231). This may further increase the risk of vascular dysfunction including superimposed atherosclerosis (232). Furthermore, elevated myeloperoxidase (MPO) levels have been observed in FD patients. MPO is a peroxidase enzyme secreted by neutrophils during cell degranulation and forms a key

component of atherosclerotic plaques, associated with lesion apoptosis, erosion and rupture (233, 234). In mouse models of α-Gal A deficiency, this associated with dysregulation of nitrous oxide. Excess nitrous oxide was found to accumulate in the atherosclerotic vessels of mice with α-Gal A deficiency, suggesting its role in enhancing atherogenesis (**Figure 5.5**) (235).

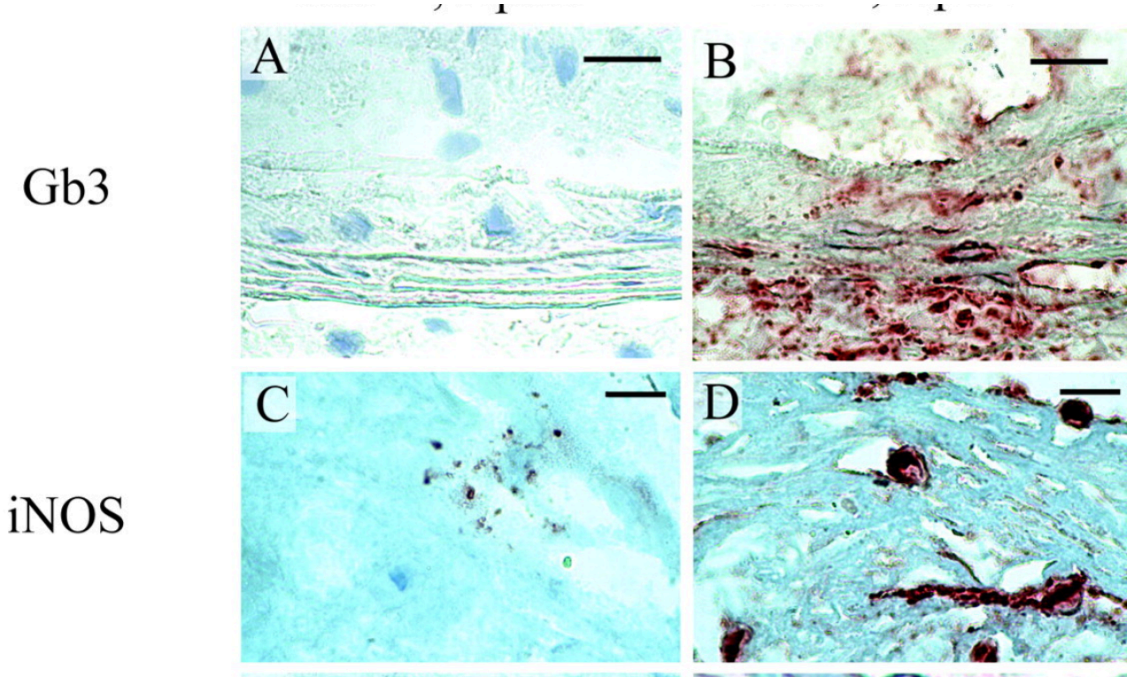

Figure 5.5: Immunostaining of Gb3 and NO in the atherosclerotic vessels of normal α-Gal A mice and α-Gal A deficient mice. A: GB3 stain in mice with normal α-Gal A levels. B: Gb3 stain in α-Gal A-deficient mice demonstrating significant over-accumulation compared to mice with normal α-Gal A. C: NO stain in mice with normal α-Gal A levels. D: NO stain in mice with α-Gal A-deficiency demonstrating significant accumulation of NO within the vasculature. Adapted from Bodary et al (235).

We demonstrate a high prevalence of hypercholesterolaemia in our cohort of FD patients undergoing ischaemia assessment, defined as an elevated serum total

cholesterol above the local reference range. Interestingly, elevated high-density lipoprotein cholesterol (HDL-C) has been observed in multiple FD studies (236, 237). Typically, a high HDL-C ratio compared with low-density lipoprotein cholesterol (LDL-C) has been associated with an improvement in cardiovascular risk profile (238). The reverse may be the case in FD due to its association with elevated levels of vascular endothelial growth factor (VEGF) and intracellular adhesion molecule-1 (ICAM-1) (239, 240). Both of these are early pro-atherosclerotic markers and have been associated with the development of microvascular ophthalmic lesions in FD, including compression of arteriovenous fundic vessels and increased arteriolar tortuosity and narrowing (241).

The high incidence of early onset vascular disease in FD (ischaemic heart disease, stroke and TIA) suggest a pro-thrombotic state (235). Thrombotic risk is heightened by the presence of CKD due to renal Gb3 accumulation and podocyte loss (242)..

5.9.1.3 Microvascular dysfunction

Non-invasive ischaemia assessment has allowed for the identification of small-vessel ischaemia in FD. ICA assessment in FD has demonstrated slow flow, slow run off and delayed distal vasculature opacification, not correlating with age, gender or extent of LVH, but correlating with degree of small vessel perfusion defects on PET CT. (243). The presence of slow-flow on ICA has been well documented in the context of microvascular disease in the general population and interestingly in the FD study, patients developed ischaemic signs on ECG during exercise and had stress-induced perfusion defects on non-invasive imaging (244).

Microvascular dysfunction has been confirmed on PET in FD patients with normal ICA studies (245). Coronary flow reserve and myocardial blood flow were significantly reduced compared to non-FD controls with no improvement when treated with ERT. Interestingly, the FD patients also had elevated serum total cholesterol levels with a higher HDL-C ratio, as has been documented in prior FD studies (236). The findings suggest that Gb3 deposition increases vascular resistance and myocardial oxygen demand due to LVH associated with FD cardiomyopathy.

Multiparametric CMR has been used to assess for microvascular dysfunction in FD. In a study of 44 adults with FD, impairments in myocardial blood flow were demonstrated in patients with LVH compared to those without. Interestingly, impairments were also demonstrated in the LVH-negative cohort when compared with non-FD controls, suggesting early microvascular dysfunction prior to the onset of LVH (79, 215). This has been supported on endomyocardial biopsies, where endothelial cell swelling and arteriolar luminal narrowing was demonstrated secondary to Gb3 storage (243). Mechanisms underpinning microvascular dysfunction in FD are summarised in **Figure 5.6**.

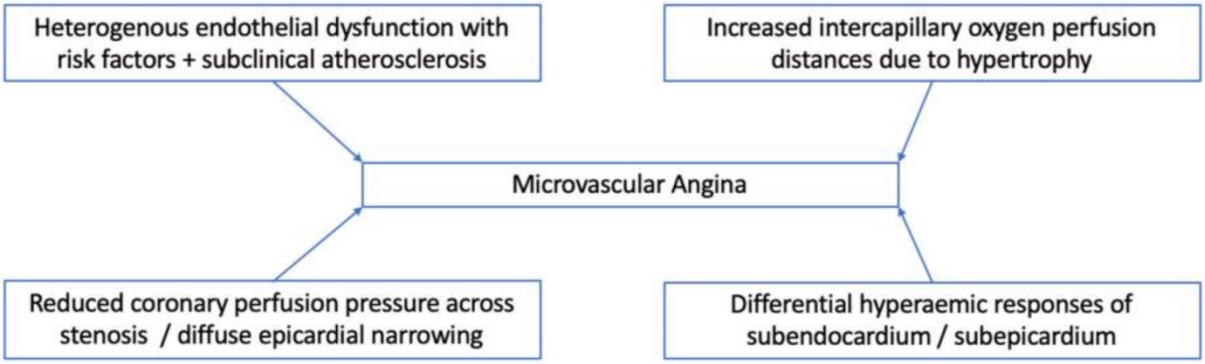

Figure 5.6: Mechanisms underpinning coronary flow in the absence of significant coronary artery disease in FD. Taken from Roy et al (63).

5.9.2 Inflammation in Fabry Disease

5.9.2.1 Luminex® Performance Assay

The results from the Luminex® Performance assay demonstrated signals from the majority of the analytes assessed with particularly significant signals in Eotaxin, Granzyme B, IL-6, 10, 15, 33, MCP-1, TNF-α, and VEGF in the FD cohort compared to non-FD controls with stepwise elevation from the intermediate cardiomyopathy stage (ECG abnormalities associated with FD +/- low T1 on CMR) to the advanced stage (elevated troponin +/- LGE on CMR).

5.9.2.1.1 *Myocardial inflammation in FD*

Lysosomal Gb3 accumulation disrupts physiological mechanisms of the innate immune system and triggers various pro-inflammatory pathways, release of inflammatory mediators, disruption of antigen presentation, all manifesting as systemic inflammation (104, 246). The role of myocardial inflammation and fibrosis related to

Gb3 accumulation are important when considering cardiac dysfunction particularly in the more advanced stages of the disease and in the context of arrhythmia. Gb3 and associated glycosphingolipids may act as antigens in activating toll-like-receptor signalling pathways, causing localised inflammation and pro-fibrotic signalling, leading to deposition of extracellular matrix with associated fibrosis (69, 247, 248). Interestingly, the role of inflammation in conduction disease has also been explored, with a study suggesting that oxidative damage to cardiomyocytes causes dysfunction and activation of apoptotic pathways, resulting in electrical instability and prolonged refractory times (29).

5.9.2.1.2 *Pro-inflammatory cytokines*

Increased levels of pro-inflammatory cytokines, specifically IL-6, TNF-α and matrix metalloprotease (MMP) have been observed with worsening FD cardiomyopathy severity (85, 249). In keeping with this published literature, our study confirms elevated plasma concentrations of IL-6 and TNF-α with a stepwise increase in both according to degree of FD cardiomyopathy when compared to non-FD age/sex matched controls. This highlights their potential role as biomarkers when used in conjunction with other relevant biochemical and imaging parameters to assess for cardiomyopathy progression or response to disease-modifying FD therapy. TNF-α is a pro-inflammatory cytokine primarily involved in triggering recruitment of inflammatory cytokines and chemokines (250). Activation of TNF-α receptors results in downstream signalling of complexes (II, IIa, IIb and IIc) each with specific pro-inflammatory responses (**Figure 5.7**) (251, 252).

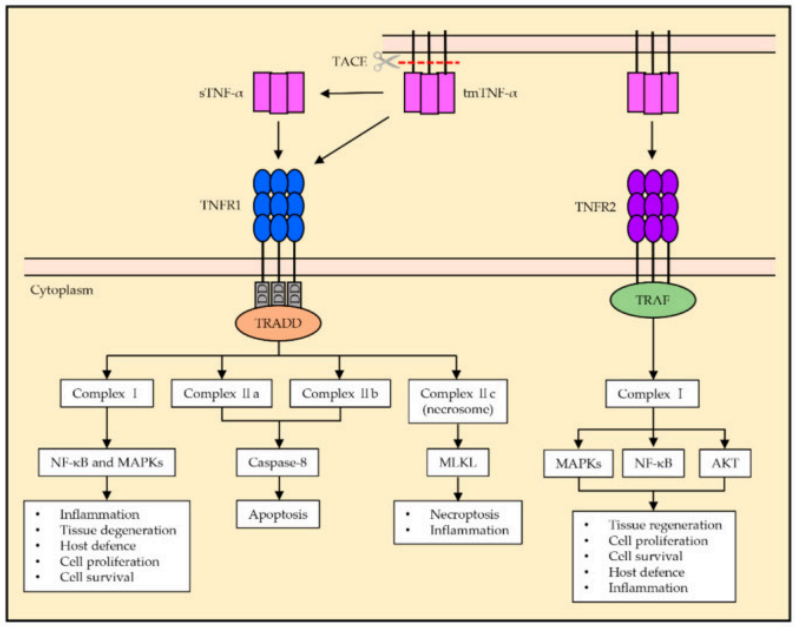

Figure 5.7: Various TNF-α signalling pathways including complexes I, IIa, IIb and IIc, activation, triggering the upregulation of various cytokines and chemokines, and the systemic effects of each. Taken from Jang et al (252).

IL-6 is involved in various acute and chronic inflammatory pathways, and likely has a key role in triggering inflammatory cascades in FD. High circulating levels of both IL-6 and the IL-6 receptor have been demonstrated in classical FD when compared to non-classical FD and non-FD controls (253). This implies IL-6 may have a role in the development of multisystemic damage associated with classical FD.

MCP-1 is a pro-inflammatory chemokine, functioning predominantly in leukocyte trafficking, to enhance expression, proliferation and migration of various immune cells including monocytes and macrophages (254). Studies have demonstrated elevated levels of MCP-1 in FD which reduce with ERT (249). Another study demonstrated significantly elevated levels in FD patients compared to non-FD controls, which also

reduced with 12 months ERT treatment (255). The results of our study document a similar trend of MCP-1 elevation, more pronounced in the advanced FD cardiomyopathy group.

Eotaxin is a potent chemokine, functioning to enhance expression and attract predominantly eosinophils (256, 257). It also acts as a chemotactic agent for T-cells and promotes T-cell adhesion to the endothelium (258). This study, for the first time, demonstrates elevated levels in the plasma of FD with a step-wise increase with FD cardiomyopathy severity, compared with non-FD controls. Eotaxin is most notably associated with asthma with accumulation in the lungs documented in patients with asthma, highlighting its inflammatory role in the pathophysiology of asthma (259). There is no previously documented association between Eotaxin and FD.

Granzyme B is a serin protease with pro-apoptotic functions, produced and secreted by various cells including T and B-cells, macrophages, monocytes, mast cells and basophils (260, 261). It enhances the function of cytotoxic T-lymphocytes and natural killer (NK) cells (262, 263). It also has various functions in extracellular matrix remodelling (264, 265). Granzyme B targets various components of the extracellular matrix, promoting degradation, activation of pro-inflammatory cytokines including IL-6 and GM-CSF, as well as perforin-dependent apoptosis (**Figure 5.8**) (266).

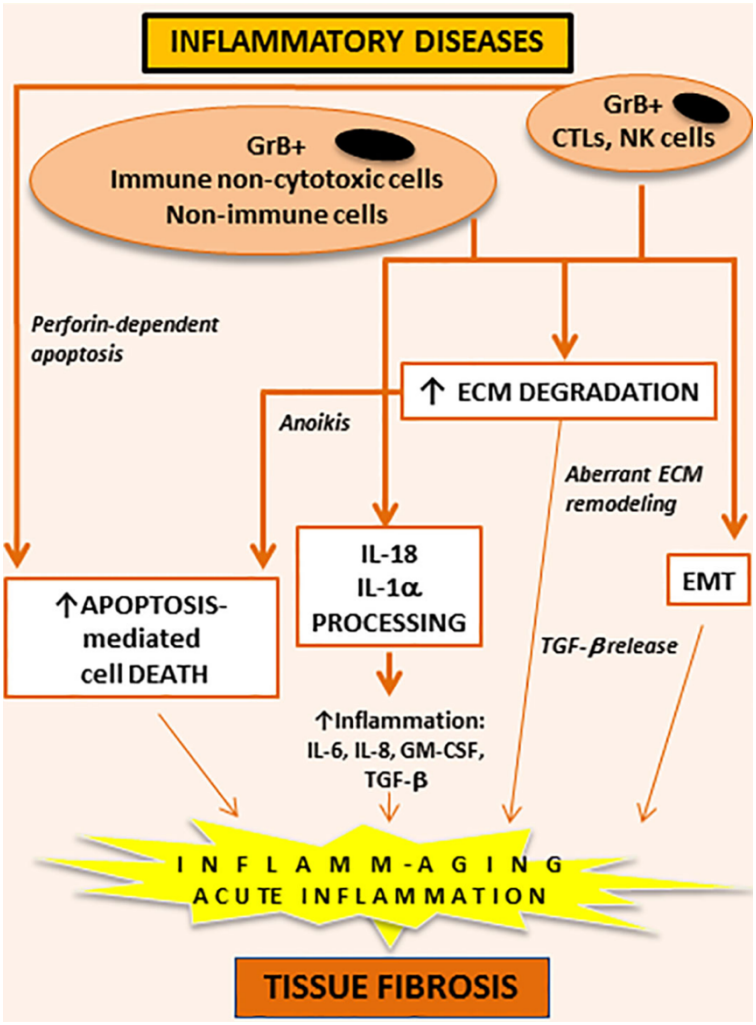

Figure 5.8: Contributions of Granzyme B to the development of systemic inflammation and fibrosis. Mechanisms include perforin-dependent apoptosis (activation of cytotoxic T-lymphocytes and NK cells), extracellular matrix degradation and subsequent anoikis, and activation of downstream pro-inflammatory cytokines. Abbreviations: GrB+: Granzyme B. Adapted from Velotti et al (266).

We demonstrate elevated plasma levels of Granzyme B in patients with FD cardiomyopathy with a stepwise increase according to degree of cardiac involvement when compared to non-FD controls. The higher concentration in patients with elevation of troponin +/- LGE on CMR fits with the extracellular role of Granzyme B as

a pro-fibrotic protease. Interestingly, we also demonstrate elevated plasma levels of pro-inflammatory cytokines IL-6 and IL-8, and IL-1α in patients with FD cardiomyopathy, compared to non-FD controls. IL-6 and IL-8 are both activated by granzyme B via IL-18 and IL-1α processing (**Figure 5.8**) (266).

IL-10 was also significantly upregulated in FD patients with stepwise increases in plasma levels from the intermediate to advanced cardiomyopathy groups, compared to non-FD controls. Traditionally, IL-10 has been considered a cytokine with predominantly anti-inflammatory properties, modulating the immune response and preventing host damage (267). However, it may also possess immunostimulatory properties, dependent on target cell, site and timing of secretion. The effects, both beneficial and deleterious, of IL-10 in the context of infection and inflammation are summarised in **Figure 5.9** (268). Interestingly, IL-10 may prevent B-cell apoptosis, enhance cell growth, and promote T-cell survival (269, 270). In keeping with our data on granzyme B, IL-10 also enhances production of granzyme (271). IL-10 also promotes proliferation, migration and increases activity of NK cells (272).

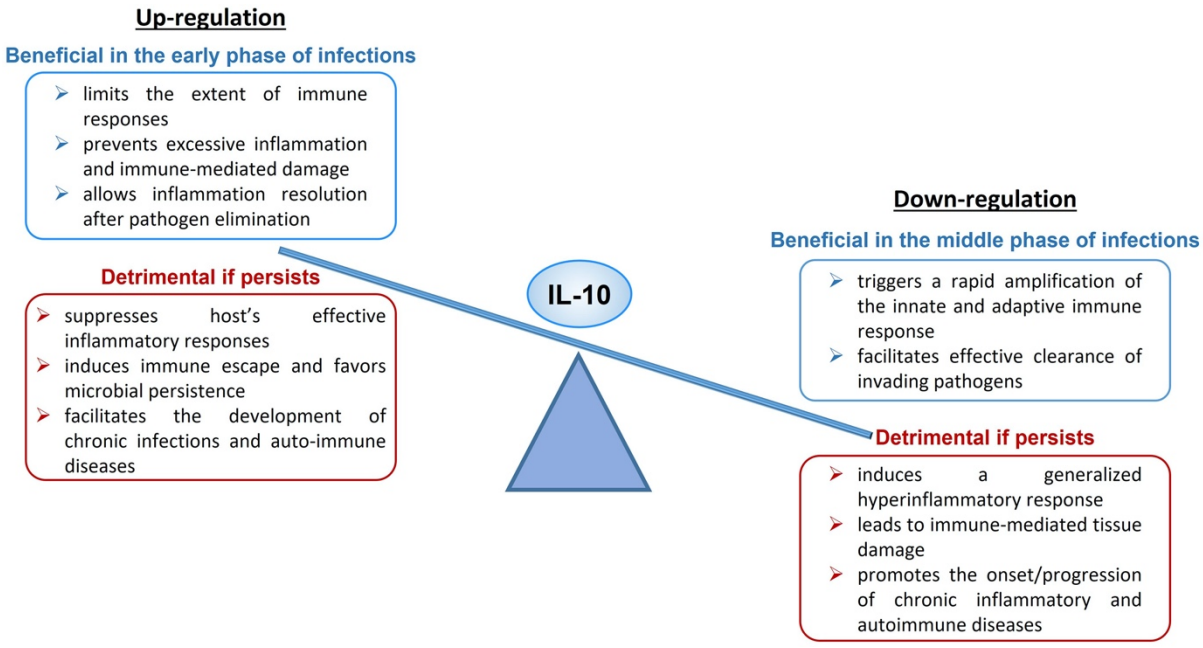

Figure 5.9: The effects of IL-10 upregulation and downregulation. Taken from Carlini et al (268).

In the context of FD, increased levels of IL-10 have been demonstrated in ERT-naïve patients which did not normalise with treatment (273). Interestingly a large proportion of these patients had early-stage renal impairment. In various renal diseases, elevated IL-10 has been documented and indeed podocytes may produce IL-10 as well as IL-6 (274, 275). The interplay of IL-10 with pro-fibrotic markers such as TGF-B1 and ILR suggests a potential pro-fibrotic role of IL-10 in FD (276, 277).

We also demonstrate a significant stepwise increase in plasma levels of IL-15 from non-FD controls to intermediate FD cardiomyopathy to the more advanced stage. IL-15 is a pro-inflammatory cytokine produced by a variety of immune cells including B-cells, T-cells, antigen presenting cells and mastocytes (278). IL-15 is involved in the

proliferation, and activation of NK cells, T-cells and pre-activated B-cells (279). Its overexpression has been documented in a variety of auto-immune conductions but not FD (280-283). Interestingly, IL-15 has also been shown to have a role in the expression of TNF-related apoptosis-inducing ligand (TRAIL) (284), though we did not demonstrate significant changes in plasma levels of TRAIL between the non-FD control and FD cohorts.

IL-33 is an alarmin cytokine with various roles in allergic and non-allergic inflammation, released on tissue injury, and activating various immune cells including T-helper cells, basophils, eosinophils, macrophages, NK cells and neutrophils (285, 286). High levels of IL-33 are present in vascular endothelial cells, epithelial cells from barrier tissue and fibroblastic cells (287, 288). It has been shown to play a role in asthma susceptibility and chronic obstructive pulmonary disease, but its role in FD has not been documented (289, 290). We demonstrate significantly elevated levels in the advanced FD cardiomyopathy group compared to non-FD controls with low levels expressed in the non-FD control group and intermediate FD-cardiomyopathy group. This highlights the potential role of IL-33 in the more advanced stages of FD cardiomyopathy where inflammation is likely to play a crucial role in the development of LGE on CMR with subsequent troponin elevation and T2 elevation on CMR.

5.9.2.1.3 *Markers of angiogenesis*

In the context of FD vasculopathy with microvascular dysfunction, as well as LVH, expansion of the coronary vasculature takes place to maintain oxygen perfusion. Angiogenesis proteins that trigger this cascade include that of VEGF and FGF-2, both

of which trigger proliferation of endothelial cells to promote angiogenesis (291). Studies in FD patients demonstrate greater circulating levels of VEGF-A and FGF-2 which correlated with levels of lyso-Gb3 (292). In keeping with the literature, we also demonstrate an increase in levels of VEGF in FD patients with a stepwise increase according to degree of FD cardiomyopathy, when compared to non-FD controls.

In a similar trend, PDGF-AA and BB (homodimers of PDGF) are expressed in higher concentrations in the FD cohorts compared to non-FD controls. Expression of PDGF has been shown in atherosclerotic arterial walls and infiltrating inflammatory cells (293). Indeed, in the context of the “response-to-injury” hypothesis in the pathogenesis of atherosclerosis, PDGF is released from aggregating platelets at sites of endothelial injury (294). PDGF is also shown to have a role in fibrosis, specifically in the deposition of extracellular matrix (295). Many pro-inflammatory cytokines promote upregulation of receptors of PDGF, triggering proliferation of mesenchymal cells (296). Mouse-models treated with PDGF receptor blockers demonstrated reduced myocardial collagen deposition, and PDGF-AA is a potent induced of cardiac fibroblast proliferation (297, 298). The role of PDGF in inflammation and fibrosis in the context of FD has not been explored but likely plays a key role given its involvement in inflammation and fibrosis pathogenesis in other cardiovascular diseases.

5.10 Limitations

5.10.1 Atherosclerotic risk in Fabry Disease

As with the utilisation of ILRs, the main limitation of this study is the small sample size, given this was a single centre study. Furthermore, patients were pre-selected on the ground of having symptoms to suggest myocardial ischaemia. The study was also limited to those on disease-modifying therapy in the form of ERT

5.10.2 Inflammation in Fabry Disease

As with the atherosclerosis study, the main limitation of the Luminex® study is the small sample size. Another unavoidable limitation is that to run such experiments from plasma samples which have been frozen and stored at -80C, the samples would undergo a freeze-thaw cycle prior to conducting the experiment. Repeated freeze-thaw cycling may cause denaturation, aggregation and subsequent functional loss of circulating proteins (299, 300). In order to minimise the number of freeze-thaw cycles, samples were thawed on the day of running the Luminex. Conducting the Luminex® assay from fresh samples would have been a logistical challenge as patients were recruited to the study at various timepoints and so will not have had samples collected at the same time.

5.11 Conclusions

These experiments clearly show an involvement of inflammation in FD, for the first time shown with a wide panel of inflammatory markers. Inflammation likely plays a key

role in the progression of cardiomyopathy in FD and arrhythmogenesis. Inflammation is likely to begin early in cardiomyopathy onset and not solely in the advanced stages as previously thought. Ischaemia and atherosclerosis in FD are common, and secondary to diverse mechanisms relating to microvascular disease, altered coronary vasoreactivity and perfusion mismatch all likely secondary to Gb3 deposition. Accelerated atherosclerosis is likely to take place through a variety of mechanisms in FD, leading to ischaemic cardiomyopathy which contributes to the arrhythmia substrate. This highlights the importance of investigating ischaemic symptoms in FD to exclude macrovascular or microvascular coronary artery disease.

6 Chapter 6 – Clinical ILR utilisation in Fabry Disease and their role in detecting arrhythmia compared to standard of care cardiac monitoring in a multicentre clinical trial

Data from this chapter is based on the first author published article where this data was first presented:

Roy A, Vijapurapu R, Kurdi H, Orsborne C, Woolfson P, Kalla M, et al. Clinical utilisation of implantable loop recorders in adults with Fabry disease-a multi-centre snapshot study. *Front Cardiovasc Med*. 2023;10:1323214.

6.1 Personal Contribution

I was responsible for screening the cohorts and collection of data across all sites. Following data collection, I conducted the statistical analysis, wrote the subsequent manuscript and subsequent revisions. For the RaILRoAD study I screened for eligibility and recruited patients from the 2 major recruiting centres in the UK.

6.2 Background

Cardiac monitoring is paramount in the documentation of cardiac arrhythmia requiring intervention. Whilst current FD guidelines recommend annual cardiac monitoring with 24-hour Holter in FD, this is not always carried out (53). Even if annual Holter monitoring does take place, these are often not diagnostic given that arrhythmia in FD may be sporadic and asymptomatic. Confirmation of arrhythmia, however, is essential before initiation of anti-arrhythmic therapy. Current evidence of the utility of 24-hour Holter is based on single centre studies with small patient cohorts. Short-term monitoring is generally used (<48 hours) with little evidence from large multi-centre collaborative studies.

Given the limitations of intermittent cardiac monitoring, continuous monitoring may be a more suitable method of detecting arrhythmia in FD. In the general population, ILR implantation is indicated in adults with recurrent unexplained symptoms with potential arrhythmic aetiology, following detailed initial assessment including clinical history, examination, ECG and TTE (301). There are no specific guidelines for ILR implantation in FD, but these offer the advantage of long term, continual rhythm monitoring (up to three years) at low risk. In FD, this may be particularly useful given that FD cardiomyopathy is insidious, progressive and often asymptomatic. The risks of ILR are minimal. Implantation of an ILR is a minimally invasive procedure conducted by clinicians or specialist physiologist. It involves a small incision on the chest wall with the ILR implanted subcutaneously. The risks associated include that of bleeding, infection and damage to local structures. In general, the procedure takes around 10 minutes with patients able to be discharged without restrictions on the same day. The

benefits of ILR monitoring over intermittent cardiac monitoring in documenting significant arrhythmia requiring intervention, however, has not been explored.

6.3 Hypotheses

We hypothesised that in adults with FD and ILRs implanted on clinical grounds, arrhythmia detection requiring clinical intervention will be high, and greater than that of the general population. FD patients undergoing ILR implantation are likely to be in the advanced stages of FD cardiomyopathy.

6.4 Aims and Objectives

The aims of this chapter were to explore arrhythmic risk in FD by providing a comprehensive evaluation of the clinical utilisation of ILR in FD and their impact on therapy. Further to this, understanding the cardiovascular phenotype of adults with FD undergoing clinically indicated ILR implantation was also explored. The findings from these data informed the set-up of a multi-centre clinical trial to highlight the potential beneficial role of early ILR implantation in FD, which is also described in this chapter. This study is titled, “A randomised controlled trial evaluating arrhythmia burden, risk of SCD and stroke in patients with Fabry Disease: the role of implantable loop recorders (RaILRoAD) compared with current standard practice. The study will quantify the true rate of arrhythmia in FD with cardiac involvement and provide information on specific risk factors predisposing to arrhythmia (on biomarkers, ECG and cardiovascular imaging) to provide clarity on SCD risk

6.5 Methods

6.5.1 Study population and design

This was an observational, retrospective, cross-sectional multicentre snapshot review of cardiovascular data collected from adults over 18 years with a genetic or enzymatic confirmation of FD. Patients were referred to three large centres in the United Kingdom managing adult patients with FD. These included Queen Elizabeth Hospital, Birmingham, Salford Royal Hospital, Salford and Royal Free Hospital, London. These centres provide a one-stop service for FD patients attending clinic. Patients undergo detailed clinical assessment including history/examination, 12-lead ECG, TTE, CMR and ambulatory cardiac monitoring according to current guidelines (71). All patients were screened and those with prior or current ILR were included in the analysis. Data was extracted from investigations performed within the preceding 12 months. The exclusion criteria for this study were having an existing therapeutic cardiac device or ILR implantation on research grounds. The inclusion criteria for this study are detailed below:

1. Adults over 18 years of age
2. Genetic or enzyme confirmation of FD
3. History of prior or current ILR implantation on clinical grounds

6.5.2 12-lead ECG

Standard 12 lead ECGs were acquired according to current standardised guidelines for acquisition and interpretation (226).

6.5.3 Transthoracic Echocardiography:

TTE (ie33 / EPIC, Phillips and Vivid, GE) was performed by an accredited sonographer according to the British Society of Echocardiography minimum dataset (140). Chamber size and function were measured according to current standard guidelines (227). Parameters for assessment of diastolic function were acquired according to the general principles for TTE assessment established by the American Society for Echocardiography in association with the European Association of Cardiovascular Imaging (164). Diastolic function was graded by an experienced Cardiologist specialising in TTE according to current guidelines (164).

6.5.4 Cardiac Magnetic Resonance Imaging.

Contrast-enhanced CMR (1.5T Avanto, Siemens Healthcare, Erlangen, Germany) was performed in line with standard protocols to obtain LV dimensions, volumes, function, and mass (197). A steady-state free precision single breath hold MOLLI sequence was used for T1 mapping in the basal and mid LV short axis levels and horizontal long-axis, before and 15-20 minutes after administration of gadolinium-based contrast agent (198). Imaging for assessment of LGE, calculation of regional and global T1 and myocardial extracellular volume were performed as previously described (199).

6.5.5 Bloods and urine

Routine biochemical and haematological tests were performed including cardiac biomarkers high-sensitivity troponin (I or T), NT-proBNP.

6.6 Statistical analysis

The baseline demographics of the cohort were summarised, with continuous variables reported as means ± SDs. Where two continuous variables were being compared, normality was assessed using Shapiro-Wilks test. Where data was normally distributed, an unpaired t-test was performed. When comparing the relationships between two quantitative and independent variables, simple linear regression was performed. A p-value <0.05 was deemed to be indicative of statistical significance throughout. All analyses were performed using GraphPad Prism version 9.3.1, GraphPad Software, San Diego, California, USA (www.graphpad.com).

6.7 Ethics

This study was approved by local clinical governance committees (CARMS-13350) and confirmed to the principles of Good Clinical Practice guidelines. Ethical approval was obtained for the conduct of this study by the NHS Health Research Authority and local NHS Research Ethics Committee (IRAS 325613 23/WM/0180). The data was collected on clinical grounds and used for the secondary purpose of research. Therefore, the requirement for written consent from patients was waived by the ethics committee.

6.8 Results

6.8.1 Cohort Characteristics

In this snapshot assessment, 915 patients with FD across three specialist treatment centres in England were identified between 1/1/2000 and 1/9/2022. Of these, 22 (2.4%) patients underwent clinically indicated ILR implantation. Mean age at time of implantation was 49.6 ± 9.9 years and thirteen (59%) were female. Mean systolic BP was 127mmHg ± 24 and diastolic BP 75mmHg ±13. Mean BMI was 27 ± 8. BMI and systolic BP significantly increased with age (p=0.0434 and p=0.0287 respectively) as illustrated in **Figure 6.1**. At time of implantation, six (27%) had hypertension, three (14%) had renal impairment defined as an eGFR< 90ml/min, six (27%) had a prior cerebrovascular accident (CVA) and eighteen (82%) were on enzyme replacement therapy (ERT). Cohort characteristics are described in **Table 6.1**

At the time of implantation, 21 (96%) were in sinus rhythm and one patient was in AF. Mean heart rate, PR interval, QRS duration and QTc were in the normal range. 21 (95%) patients had TTE imaging data available. Mean LVEF was in the upper/normal range (64% ± 6) and wall thickness was elevated (MWT16mm ± 8). Mean LA volume was normal (44ml ± 18). Of those where diastolic function could be assessed fourteen (67%) had evidence of diastolic dysfunction.

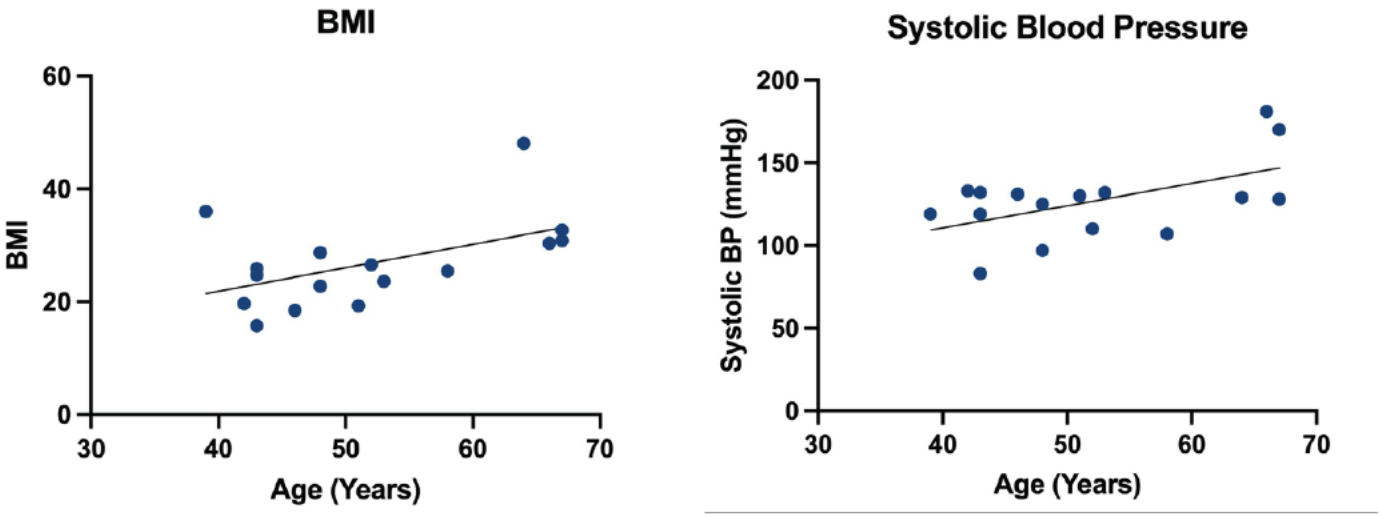

Figure 6.1: Simple linear regression of age versus BMI and systolic blood pressure

Eighteen (82%) patients had CMR imaging data available. Of these, sixteen (89%) had LVH. Mean LVMi was elevated (123g/m2 ± 54) and wall thickness was elevated (MWT 18mm ± 6). Mean LVEDVi was 68ml/m2 ± 16 and LVESVi 20ml/m2 ± 8. Mean LVEF was supranormal (70% ± 5). Nine (50%) had reduced septal T1 relaxation times indicative of sphingolipid accumulation (mean 898ms ± 99). Fourteen (78%) had evidence of LGE indicative of myocardial fibrosis.

Variable	Number	Mean	Std. Deviation
Demographics			
Age at implant	22	49.6	9.9
HR (bpm)	16	72	11
Systolic BP (mmHg)	16	127	24
Diastolic BP (mmHg)	16	75	13

Height (m)	21	1.68	0.09
Weight (kg)	21	76	19
BMI	16	26.8	7.9
Electrocardiogram			
PR interval (ms)	21	149	21.8
QRSd (ms)	22	105	20.3
Cardiac Magnetic Resonance Imaging			
LVMi (g/m2)	13	123	53.5
MWT (mm)	16	18.2	5.86
LVEDVi (ml/m2)	16	67.9	16.2
LVESVi (ml/m2)	16	20.2	8.02
LVSVi (ml/m2)	15	37.4	18.3
LVEF (%)	18	70.4	5.28
Septal T1 (ms)	13	898	98.8
Transthoracic Echocardiogram			
LVEF (%)	20	64.2	6.11
MWT (mm)	19	15.6	3.75
LA volume (ml)	17	44.1	17.8

Table 6.1: ILR utilisation cohort characteristics including demographic data, ECG, CMR and TTE, where available.

6.8.2 Indications for ILR implantation

Indications for ILR implantation varied. 12 (55%) underwent implantation for recurrent and persistent symptoms despite normal ECG and Holter monotiling. Of these, 8 patients had palpitations and 4 reported syncopal episodes. 5 (23%) were asymptomatic but underwent implantation to seek undiagnosed AF as an aetiology following cryptogenic CVA. 4 (18%) were asymptomatic but underwent implantation due to abnormal Holter monitoring (1 NSVT under five seconds, two sinus pauses

between one and two seconds, and one AF detection under 10 seconds). None of the arrhythmias detected on Holter mandated therapy. These patients were all deemed high risk for arrhythmia with evidence of LVH and LGE on CMR with a broad QRSd on ECG. 1 (4%) patient was asymptomatic with a normal Holter monitor but underwent ILR implantation as was deemed high risk for arrhythmia with LVH and LGE on CMR with a broad QRS duration on ECG.

6.8.3 Arrhythmia detection on ILR

Following ILR implantation, 9 (41%) patients had arrhythmia detected, requiring initiation or modification of therapy. Of these, 6 episodes of arrhythmia were detected on ILR and 3 were within 1 year following ILR battery depletion. Within these patients, 1 was in the group of four with documented arrhythmia on Holter monitoring; the remaining 3 did not develop arrhythmia on ILR or post- ILR. Of the 6 patients with arrhythmia on ILR, 3 had recurrent and prolonged AHREs over 6 hours. Given the duration and frequency of AHREs, they were commenced on anticoagulation. None of these patients had documented arrhythmia prior to ILR implantation. 1 had a high burden of symptomatic ventricular ectopy (11%) and was initiated on a beta blocker. This patient had NSVT on Holter prior to implantation. 2 had symptomatic NSVT and were also commenced on beta blockers. Of the 3 with arrhythmia 1-year post-ILR battery depletion, 1 was admitted acutely with syncope and found to have prolonged pauses and complete heart block requiring isoprenaline. They subsequently underwent dual chamber ICD implantation. 2 were admitted with syncope and found to have bursts of sustained VT on inpatient telemetry. Both patients underwent dual chamber ICD implantation. None of the three patients with documented arrhythmia post ILR had evidence of arrhythmia on prior Holter. Comparing characteristics in the

arrhythmia cohort versus those without, those in the arrhythmia group had a significantly shorter PR-interval (though still normal) on 12-lead ECG compared to those without (p=0.0402), illustrated in **Figure 6.2** with no other ECG changes. Otherwise, there were no significant differences observed between the 2 groups.

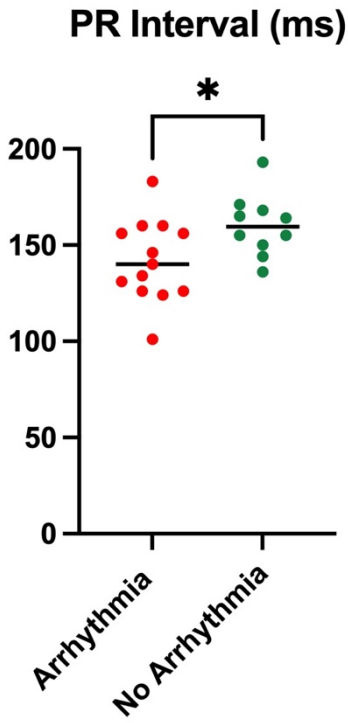

*Figure 6.2: Changes in PR interval in the arrhythmia versus no arrhythmia cohort. *p<0.05*

6.9 Discussion

6.9.1 High burden of arrhythmia detected on ILR

This multicentre snapshot assessment is the first to report the clinical utilisation of ILRs in FD. This demonstrated that the UK practice of ILR implantation rate in FD is low and uncovers a higher-than-expected burden of arrhythmia requiring initiation or

modification of therapy. The findings are in keeping with previously published single centre data in adults with FD and advanced cardiomyopathy, where a high burden of arrhythmia was detected on ILR but not Holter monitoring (31). It should be noted however, that the patients in the published study were included based on having advanced FD cardiomyopathy and did not undergo ILR implantation on clinical grounds. Interestingly, in our study, the burden of arrhythmia detected is higher than that of prior single and multi-centre studies. In a single centre study of non-FD patients, post-cryptogenic CVA with no prior history of arrhythmia, no patients who underwent ILR implantation developed arrhythmia (302). In a multicentre study of adults aged between 70 and 90 years with no prior CVA history but at least one documented risk factor for CVA, 31.8% had documented arrhythmia requiring modification of therapy following ILR implantation (303).

6.9.2 ILR implantation in patients with advanced cardiomyopathy

Another significant finding from this assessment is that those undergoing ILR implantation on clinical grounds in the UK have advanced FD cardiomyopathy. This is evidenced by advancing age, increased LVMi, MWT, supranormal LVEF and high burden of LGE on CMR. These factors in part explain the high detection of arrhythmia in this cohort as it is well established that such factors predispose to arrhythmogenesis in FD (11, 23). No significant differences were observed in LVMi, MWT, LVEF and burden of LGE on CMR in those with ILR and documented arrhythmia compared to those without arrhythmia. This largely reflects the heterogeneity within this cohort and that those undergoing ILR implantation have advanced disease already, at time of decision to implant.

6.9.3 Obesity cardiomyopathy

"Obesity cardiomyopathy" is a term describing metabolic, morphological and functional cardiac dysfunction due to the effects of obesity, including remodelling (LVH), fibrosis and diastolic dysfunction (**Figure 6.3**) (304). Morphological changes related to obesity has been shown to predispose to arrhythmia including AF (305). Alterations in myocardial haemodynamics secondary to obesity, including hypertension, increased cardiac output, increased blood volume, abnormal pulmonary haemodynamics and increased LV wall stress all predispose to ventricular remodelling and dysfunction (304, 306-309). The mechanisms relating to systemic inflammation described in obesity cardiomyopathy may share comparisons with FD where the prevalence of cardiovascular risk factors is increased. Similar mechanisms may be underpinning obesity cardiomyopathy in FD. Furthermore, we also demonstrate that the BMI of patients in this cohort increases with advancing age. The effects described, relating to BMI elevation are likely to be involved in this cohort and contribute, alongside Gb3 accumulation, to the development of LVH and increasing arrhythmic risk.

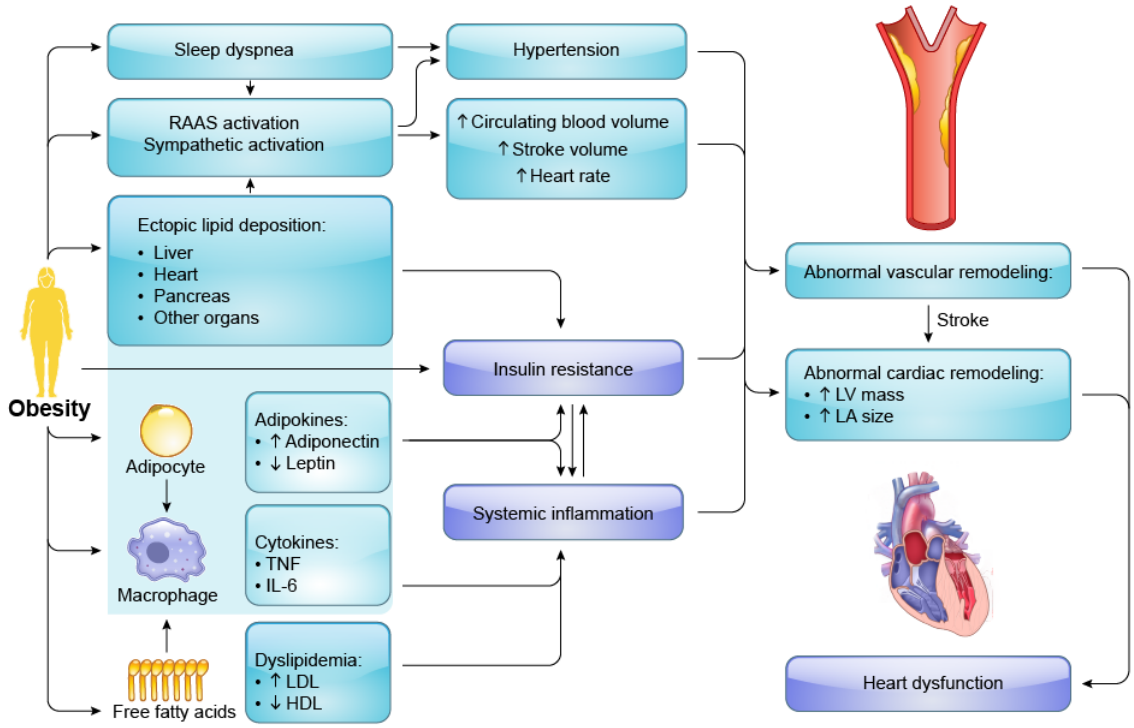

Figure 6.3: Mechanisms of obesity cardiomyopathy highlighting to role of lipid deposition, insulin resistance, inflammation and vascular remodelling. Taken from Ren et al (304).

6.9.4 Benefits of ILR monitoring in Fabry Disease

The main benefit of ILRs over short term cardiac monitoring is that they allow for continuous uninterrupted recording for a longer duration of time, accounting for sporadic arrhythmia. They can also record episodes of AHREs which have been demonstrated. AHREs may closely resemble AF, prompting clinicians to commence anticoagulation in patients for stroke prevention (310), especially given that in cohorts such as these, cardiovascular risk factors for stroke are prevalent (65, 219, 220), and stroke risk in FD is greater than the general population (50). A large multi-centre study

was conducted comparing initiation of anticoagulation for stroke prevention versus no anticoagulation in non-FD adults with AHREs detected on implantable devices including ILR and at least one risk factor for stroke (311). This was a large study of 2536 patients (1270 in anticoagulation group versus 1266 in placebo) with a mean age of 78 years and 37.4% female. The trial was terminated early due to safety concerns. Death or major bleeding was higher in the anticoagulation group (5.9% per patient-year) compared to placebo (4.5% per patient-year) with no significant reduction in the incidence of stroke or systemic embolism (stroke incidence roughly 1% per patient-year in both groups). These data suggest that even in the presence of additional risk factors for stroke, commencing formal anticoagulation for ILR-detected AHREs without 12-lead ECG conformation for AF is unlikely to reduce prevalence of stroke but may cause an additional risk of major bleeding. For patients in this cohort when anticoagulation was commenced due to the presence of AHREs, it was deemed that the risk of anticoagulation was outweighed by the potential benefit of stroke prevention given the frequency of AHREs. The large study of 2536 patients suggested this is not likely to be the case and it remains unclear whether these patients would benefit from anticoagulation.

6.9.5 Low rate of implantation in Fabry Disease

Outcome data for FD suggests that the prevalence of cardiac symptoms experienced by patients is high, reported to be over 60% in males and 45% females. Common symptoms include angina, palpitations, dyspnoea and syncope. Given this and the high prevalence of documented arrhythmia on short term cardiac monitoring in FD, the rate of ILR implantation in this cohort is disproportionately low. ILR implantation

appears to be largely restricted to those with the most advanced stages of FD cardiomyopathy which appears to be the case for patients in the UK with FD.

6.9.6 P-wave changes and arrhythmia

A notable finding on 12-lead ECGs of patients who had documented arrhythmia on ILR compared to those with no arrhythmia was alterations in the P-wave characteristics, namely a shortening of the PR-interval, though still within the normal range. PR-interval changes are frequently reported in FD and shortening of the PR-interval may be one of the earliest manifestations of FD cardiomyopathy. This has been demonstrated in a single centre study comparing 50 healthy non-FD controls with 30 FD patients with no evidence of LVH (24). The study demonstrated shortening of the PQ-interval in FD patients (131ms ± 18) compared with non-FD controls (155ms ± 20). Specifically, the change appeared to be within the P-wave itself with a shortening of P-wave duration in FD patients (74ms ±16) compared to non-FD controls (105ms ± 14). The major limitation of this study was that it was conducted 15 years ago, and the criteria used to define early disease was an absence of LVH. With the advancement of multimodality imaging in FD (159), it is now possible to detect early Gb3 accumulation (reduction in T1 mapping on CMR, impairment in GLS and diastolic dysfunction). Whilst the patients in the study may have not had LVH, they had not undergone the detailed multimodality, multiparametric assessment that they would likely have now to detect early FD cardiomyopathy. Nevertheless, the findings are significant and complement the P-wave changes observed in our study.

6.9.7 *Cardiac monitoring following battery depletion*

The major benefit of ILR over short term cardiac monitoring is the ability to continually document cardiac rhythm for a minimum of three years duration, until battery depletion. Interestingly, in this snapshot assessment, after three years ILR monitoring, a proportion of the cohort subsequently went on to suffer major adverse arrhythmic events. These patients all went on to require therapeutic cardiac device therapy for secondary prevention. Due a lack of documented arrhythmia on ILR for these patients, none underwent repeat ILR implantation following battery depletion. Added to this, of those within this group who subsequently underwent Holter assessment post ILR battery depletion, no arrhythmia was detected on these either. This highlights that despite the effectiveness of three years continual cardiac monitoring with ILRs, ongoing vigilance and surveillance is necessary in patients with FD, particularly in those with advancing FD cardiomyopathy, given the progressive nature of the disease. In line with national guidelines, FD patients are required to continually undergo frequent ambulatory cardiac monitoring, especially given the progressive and insidious nature of FD cardiomyopathy with arrhythmic risk increasing with age and cardiomyopathy progression.

6.10 Limitations

Within a large, pooled cohort of 915 patients, a small number of patients underwent clinically indicated ILR implantation. This is despite the pooling of data from three of the UKs largest centres for managing patients with FD. The small number of patients reflects low ILR utilisation as a total number of 915 patients represents one of the largest adult cohorts available in FD worldwide.

There were patients in this study who underwent ILR implantation with prior documentation of arrhythmia on short term cardiac monitoring. The rationale for implantation was for prolonged cardiac monitoring to facilitate decision-making regarding therapeutic device implantation or added cardioprotective pharmacological therapy. These patients specifically will be pre-selected for an arrhythmia substrate and are more likely to have arrhythmia documented on continuous cardiac monitoring compared to those without prior arrhythmia documented.

Finally, it should be noted that three patients developed arrythmia following ILR battery depletion, suggesting that whilst ILRs allow for prolonged screening, arrhythmia can be missed. There will therefore remain a select group of patients who are deemed high risk for arrhythmia whereby it may be considered for re-implantation of ILR following battery depletion.

6.11 RaILRoAD

The results from the clinical utilisation study informed the RaILRoAD study. This is a prospective multicentre, open label, randomised clinical trial in adults over 18 with genetic or enzymatic confirmation of FD and evidence of FD cardiomyopathy detectable on cardiovascular imaging (TTE or CMR) and/or ECG.

6.11.1 Study population and design

Patients were recruited from the following 7 centres:

1. QEHB, Birmingham, UK
2. Salford Royal Hospital, Salford, UK
3. Royal Free Hospital, London, UK
4. Addenbrookes Hospital, Cambridge, UK
5. Northen General Hospital, Sheffield, UK
6. University Hospital of Wales, Cardiff, UK
7. Westmead Hospital, Sydney, Australia

Inclusion criteria for the study was as follows:

1. Adults over 18 years with confirmed FD (genetic or enzymatic confirmation)
2. Evidence of cardiac involvement related to FD including:
    a. ECG abnormalities due to FD: short or prolonged PR-interval, QRS >120 ms, T-wave inversion in at least 2 contiguous leads, prolonged QTc interval.
    b. Low T1 relaxation times on CMR
    c. LVT on TTE or CMR (MWT >12mm)

The exclusion criteria included patients with an existing cardiac device or dual pathology (ischaemic heart disease requiring revascularisation or co-existing cardiomyopathy disease-causing mutation).

166 patients were recruited to the study and randomly assigned to either the intervention group with 3-years ILR monitoring or the control group with standard of care intermittent cardiac monitoring (Holter). Block randomisation was performed by a UHB statistician in accordance with number of “high risk features” for arrhythmia to ensure each arm was enriched with equal risk factors for arrhythmia (**Figure 6.4**). High risk features included:

1. Increased LVMi (2 SDs above age, sex and indexed BSA) or MWT > 12mm
2. LA dilatation on TTE or CMR (M-mode >40mm or biplane volume >34mL)
3. Elevation in high-sensitivity troponin above local reference range
4. QRS duration >120ms on ECG
5. Presence of LGE on CMR
6. MSSI score >20

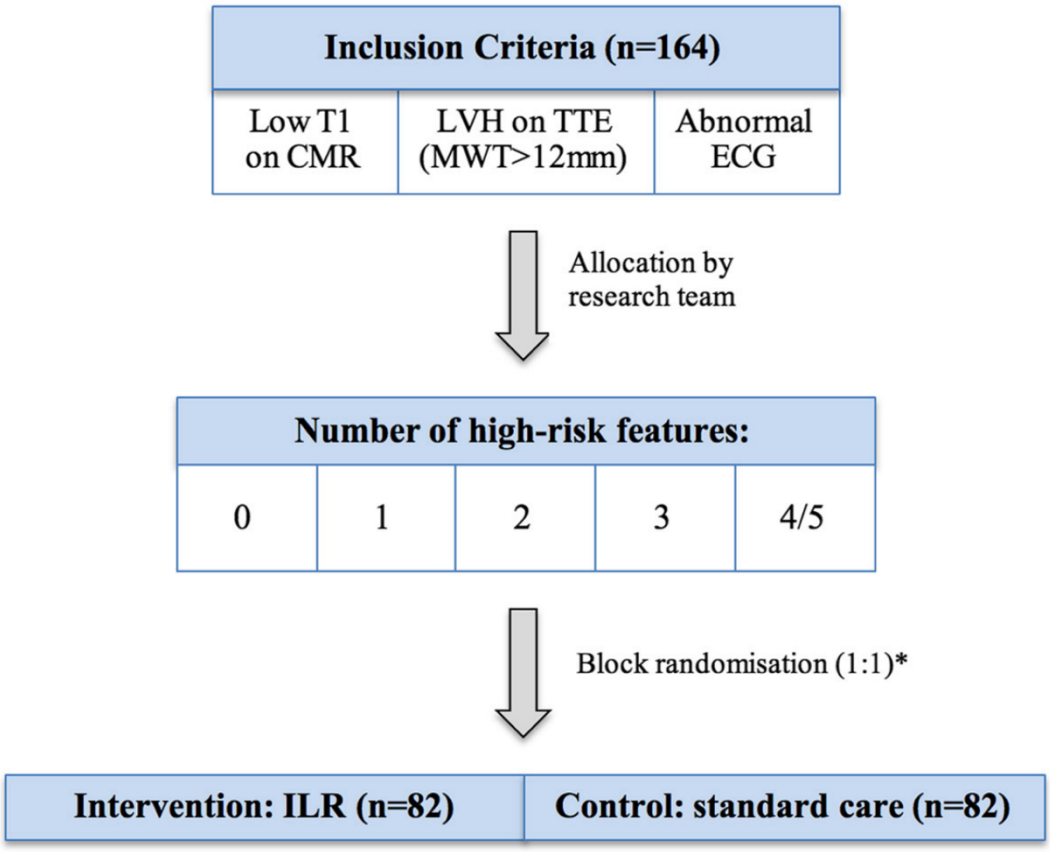

*Figure 6.4: Block randomisation process with inclusion criteria and high-risk features breakdown. * There will be a variable number of patients from each high-risk feature group to ensure variable risk profile within the study cohort. Taken from Vijapurapu et al (122).*

The study timeline for patients recruited to the RaILRoAD study is highlighted in (**Table 6.2**)

Visit	Screening	Baseline	Tests done according to national standard care for patients with FD during routine clinical review in line with each sites local policies and procedures (except QOL)		
	V1		V2	V3	End of study
Informed consent	X				
Clinical Hx and examination	X				X
QOL questionnaire		X			x
Drug Hx	X		X	X	x
CMR		X	X	X	X
Echocardiography		X	X	X	x
24hr/5-day ECG		X	X	X	x
12-lead ECG		X	X	X	x
Clinical blood tests		X	X	X	x
Stored blood/urine samples		X			
Advanced ECG		X			
ILR insertion		X			
ILR monitoring (FocusOn)			X	X	
ILR removal					X

Table 6.2: RaILRoAD study timeline

6.11.2 Outcome Measures

The primary endpoint was defined as a clinically significant arrhythmia requiring initiation or modification of therapy. This included:

- AHREs requiring anticoagulation
- Bradyarrhythmia requiring cardiac device implantation
- Tachyarrhythmia requiring cardiac device implantation, ablation or pharmacological therapy

Secondary outcome measures included:

- Assessment of arrhythmic burden in those with LGE, abnormalities in T1 or T2 mapping on CMR.
- Assessing the value of changes in ECG parameters (P-wave and QRS) in the prediction of arrhythmia.
- Evaluating the role of atrial size and burden of atrial high-rate episodes
- Evaluating the effect of changes in biochemical markers relevant to FD in the pathogenesis and burden of arrhythmia.

6.11.3 Ethics

Ethical approval for the conduct of the RaILRoAD study was approved by the NHS Health Research Authority and local NHS Research Ethics Committee (IRAS 224749 17/WM/0421) and the Human Research Ethics Committee of the Northern Sydney Local Health District (HREC/18/HAWKE/27). The study was also registered on ClinicalTrials.gov (NCT03305250). Informed consent was obtained from each study participant in accordance with Good Clinical Practice guidelines and patients were provided with a patient information leaflet to review prior to being consented. The use

of plasma samples in non-FD healthy controls was approved by the West Midlands Solihull Research Ethics Committee (17/WM/0048) and approved by the Health Research Council. All healthy controls gave informed consent to take part in accordance with the principles set out in the Declaration of Helsinki.

6.11.4 Recruitment

As of June 2023, 166 patients were recruited to the study, meeting the recruitment target of 164 across the 7 participating centres with all patients randomised (**Figure 6.5**). Those randomised to ILR have had these implanted. 5 patients met primary endpoints for cardiac device therapy based on arrhythmia detected on ILR. Arrhythmia data from ILR will not be presented in this thesis.

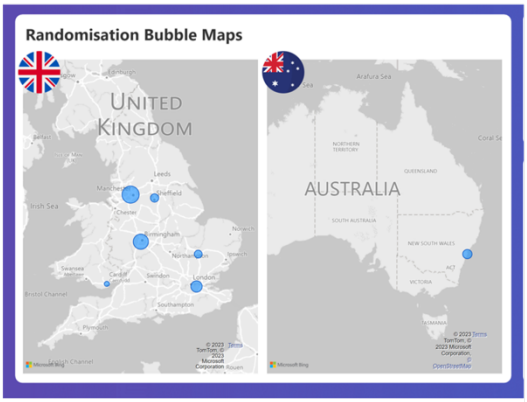

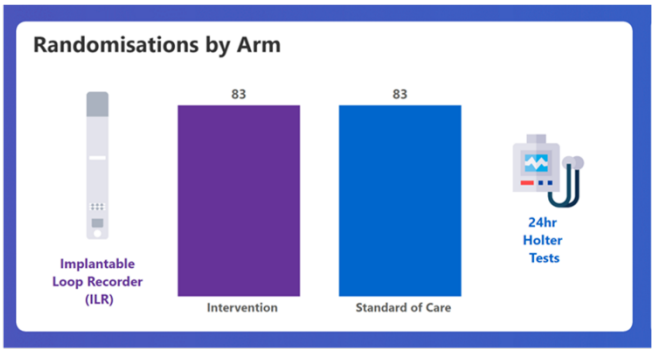

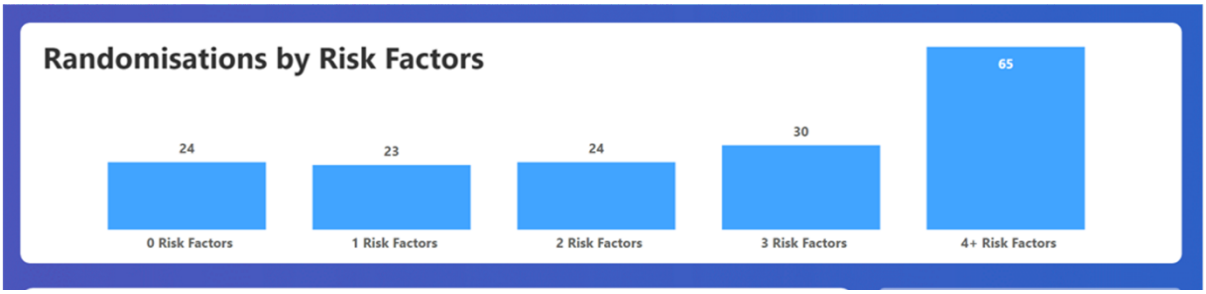

Figure 6.5: Top: Breakdown of randomisation by participating centre. Middle left: Participating centres accordingly to geographical area. Middle Right: Breakdown of randomisation according to study arm. Bottom: breakdown of randomisation according to number of high-risk features group.

The impact of the coronavirus 2019 pandemic (COVID-19) had been significant in that the study was required to pause for a long period of time due to various prolonged lockdowns, and re-deployment of research staff to clinical settings with only COVID-19 related research allowed to continue. This led to pauses in recruitment, study visits, and multiple extensions to the recruitment deadline. In August 2022, an audit was undertaken by the study sponsor (QEHB) and various recommendations were made to remain compliant with the study protocol. As such, a substantial amendment was made to the protocol and new standard operating procedures were put in place for the randomisation process. During the audit, the study was paused for 12 months for the amendments to be put in place. This further delayed recruitment.

The various extensions of the recruitment study did not impact the integrity of the study, or the patients already recruited. Data collected from recruited patients was entered onto a secure online database (REDCap) for electronic data capture. The data presented in this chapter are for the patients where baseline data has been entered and verified. As this is not complete for all the recruited patients, the data does not represent the complete patient cohort.

6.11.5 Baseline cohort characteristics

Baseline characteristics are summarised in **Table 6.3**. The mean age of the cohort was 52 ± 12 years (51 ± 12 years in the standard of care arm versus 52 ± 11 years in the ILR arm) and 56% were of female gender (49% in the standard of care arm versus 63% in the ILR arm). Interestingly 95% of patients were of white-Caucasian ethnicity which was equal across both study arms. In keeping with the atherosclerosis data, there was a high proportion of patients with conventional risk factors for atherosclerotic disease. 35 (25%) were treated for hypertension (17% in the standard of care arm versus 33% in the ILR arm), 11 (8%) patients had a diagnosis of CKD (7% in the standard of care arm versus 9% in the ILR arm) and 7 (5%) had a diagnosis of dyslipidaemia (3% in the standard of care arm versus 7% in the ILR arm). 119 (74%) reported FD-related symptoms (roughly equal split across both arms) and 122 (76%) were taking some form of cardiac medications (equal split across both arms).

	N	**Whole Cohort**	**Standard Care**	**ILR**
Baseline Demographics				
Recruiting Centre	161			
Salford		47 (29%)	22 (27%)	25 (32%)
UHB		45 (28%)	25 (30%)	20 (25%)
Royal Free		27 (17%)	13 (16%)	14 (18%)
Sheffield		16 (10%)	8 (10%)	8 (10%)
Cambridge		15 (9%)	9 (11%)	6 (8%)
Australia		9 (6%)	5 (6%)	4 (5%)

Cardiff		2 (1%)	0 (0%)	2 (3%)
Age (Years)	160	52 ± 12	51 ± 12	52 ± 11
Female Gender	161	90 (56%)	40 (49%)	50 (63%)
White Ethnicity	161	153 (95%)	78 (95%)	75 (95%)
Smoking Status	143			
Non- *Ex-* *Current*		100 (70%) 16 (11%) 27 (19%)	54 (76%) 8 (11%) 9 (13%)	46 (64%) 8 (11%) 18 (25%)
Weight (kg)	148	79 ± 19	81 ± 19	78 ± 19
Height (cm)	143	170 ± 10	171 ± 10	168 ± 10
BSA	143	1.93 ± 0.26	1.95 ± 0.25	1.90 ± 0.26
Heart Rate (bpm)	147	68 ± 13	69 ± 13	67 ± 12
Systolic Blood Pressure (mmHg)	147	131 ± 17	131 ± 18	130 ± 15
Diastolic Blood Pressure (mmHg)	147	77 ± 10	78 ± 10	77 ± 10
Other Comorbidities				
Any Other Comorbidities	139	52 (37%)	19 (27%)	33 (48%)
Hypertension	139	35 (25%)	12 (17%)	23 (33%)
Chronic Kidney Disease	139	11 (8%)	5 (7%)	6 (9%)
Dyslipidaemia	139	7 (5%)	2 (3%)	5 (7%)
Diabetes Mellitus	139	5 (4%)	1 (1%)	4 (6%)
Obesity	139	5 (4%)	1 (1%)	4 (6%)

Cerebrovascular Events	139	3 (2%)	2 (3%)	1 (1%)
Family History of CAD	139	0 (0%)	0 (0%)	0 (0%)
Peripheral Vascular Disease	139	0 (0%)	0 (0%)	0 (0%)
Others	139	6 (4%)	4 (6%)	2 (3%)

Table 6.3: Cohort characteristics, where data available, for the RaILRoAD cohort.

6.11.6 Risk factors for arrhythmia

The cohort was enriched with various high-risk features for arrhythmia with a relatively equal split between the ILR and standard of care arms (**Table 6.4**). 89 (55%) had LGE on CMR with 89 (55%) also having elevation of high-sensitivity troponin. 113 (70%) had low T1 mapping on CMR, 105 (65%) had LVH on TTE or CMR and 127 (79%) had ECG abnormalities associated with FD. There was also a roughly even split of patients with number of high-risk features: 18 (11%) with 0, 28 (17%) with 1, 23 (14%) with 2, 34 (21%) with 3, 37 (23%) with 4, 15 (9%) with 5 and 6 (4%) with 6, again with a roughly equal split across the ILR and standard of care arms.

	N	**Whole Cohort**	**Standard Care**	**ILR**
Features Included in Stratification for Randomisation				
LVH / Elevated LV Wall Thickness / Elevated LV Mass	161	109 (68%)	57 (70%)	52 (66%)
LA Dilatation / M-Mode >40mm / Biplane Volume >34ml	161	61 (38%)	30 (37%)	31 (39%)

Elevated Biomarkers	161	89 (55%)	47 (57%)	42 (53%)
QRS Duration >120ms	161	32 (20%)	19 (23%)	13 (16%)
Late Gadolinium Enhancement	161	89 (55%)	45 (55%)	44 (56%)
Mainz Severity Score				
Mean ± SD	145	18 ± 10	18 ± 10	18 ± 10
Score >20	161	55 (34%)	24 (29%)	31 (39%)
Total High-Risk Features	161			
0		18 (11%)	9 (11%)	9 (11%)
1		28 (17%)	14 (17%)	14 (18%)
2		23 (14%)	11 (13%)	12 (15%)
3		34 (21%)	18 (22%)	16 (20%)
4		37 (23%)	20 (24%)	17 (22%)
5		15 (9%)	8 (10%)	7 (9%)
6		6 (4%)	2 (2%)	4 (5%)
Other Features				
Low T1 on CMR	161	113 (70%)	63 (77%)	50 (63%)
LVH on Echo	161	105 (65%)	52 (63%)	53 (67%)
Fabry-Related Abnormality on ECG	161	127 (79%)	62 (76%)	65 (82%)

Table 6.4: Split of RaILRoAD cohort according to high-risk feature categories

6.11.7 Summary of baseline data

Existing literature suggests that the burden of arrythmia and SCD in FD cardiomyopathy is considerable. Yet the predictive factors for arrythmia requiring

initiation or modification of therapy are currently not defined. At present there is no FD-specific guideline for primary prevention cardiac device implantation as there is in the case of sarcomeric HCM, which uses the risk calculator, incorporating various aspects of the patient's clinical history and routine cardiac investigations.

The preliminary results from the baseline data collection in the RaILRoAD study confirm an equal distribution of patients across the 2 randomisation arms with a wide range of "high-risk" features for cardiomyopathy. This is important, as the majority of studies documenting risk of arrhythmia in FD refer to the more advanced markers of cardiomyopathy, with less of an emphasis on early markers which may be predictive (11, 23, 31).

6.11.8 Limitations

The limitations of the RaILRoAD study were the major delays to recruitment with the study paused due internal audit and the coronavirus 2019 pandemic. Also, given the multi-centre aspect of the study, study sites had varying levels of staffing which led to delays in data entry. Also, as the investigations in the protocol were in line with the patient standard of care, not all patients will have undergone the full list of cardiac investigations (e.g. not all patients will have undergone annual CMR or TTE). The coronavirus 19 pandemic means that many visits were switched to remote from face-to face which would have impacted the amount of data available for the baseline visit. Finally, not all participating centres will have as advanced multimodality imaging (e.g. not all centres will have T1 and T2 mapping on CMR), which limits the amount of

imaging data collected for analysis. The main limitation of RaILRoAD in the context of this thesis is that formal analysis of baseline data is not yet possible to undertake as the data collection and verification is not formally complete

6.12 Conclusions

A high burden of arrhythmia is detected in adults with FD compared to the general population on ILR, due to patients having advanced FD cardiomyopathy on implantation, at a stage where arrhythmic risk will be high due to the presence of LVH, LGE, advancing age and supranormal LVEF. This suggests that ILRs are being implanted late and highlights the need for these to be considered at an earlier stage in disease to detect both ventricular and atrial arrhythmia. Documentation of AHRE should be followed by AF confirmation on 12-lead ECG or Holter prior to anticoagulation to reduce the risk of major bleeding in the absence of stroke prevention benefit. Further large-scale multicentre data is required to understand which patients with FD are likely to benefit most from ILR implantation. This highlights the importance of multicentre studies such as RaILRoAD.

7 Chapter 7 – General Discussion

This body of work investigates the natural progression of cardiomyopathy in FD including mechanisms of arrhythmia, focusing on early cardiac changes detectable through ECG, imaging, biochemistry, and symptoms that may indicate an increased risk of arrhythmia. The research employs ECG analysis, multimodality cardiovascular imaging, symptom assessment through exercise testing and biochemical analysis to identify early markers of cardiomyopathy as well as the role of inflammation in arrhythmogenesis. A significant component of the study is the development of an atrial iPSC model with the GLA p. N215S variant demonstrating intrinsic intracellular changes contributing to an increased arrhythmic substrate. This complements the findings of early detectable changes in multimodality imaging and symptoms, as well the detection of early electrical abnormalities in the ECGs of patients without overt cardiac disease. Overall, this work provides new insights into FD cardiomyopathy, emphasising the importance of early detection and monitoring, paving the way for targeted early intervention strategies to mitigate arrhythmic risk, prevent long-term cardiovascular complications and improve long-term clinical outcomes in FD. Future research will focus on expanding the understanding of arrhythmogenesis in FD through various approaches. These would include the use of patient-derived iPSCs to validate identified cellular changes and collaborate on in-silico atrial modelling to simulate electrophysiological differences between FD and non-FD cardiomyocytes. Another key direction is testing the impact of disease-modifying therapies on reversing pro-arrhythmic changes. Additionally, a cardiac registry incorporating multimodal imaging and biochemical analysis will be developed to improve risk assessment and track disease progression. Future work will also investigate the relationship between

inflammation, atherosclerosis, and arrhythmic risk in FD by analysing cytokine profiles and conducting early-phase clinical trials. Moreover, longitudinal studies will assess how therapy affects imaging parameters, exercise capacity, and cardiac biomarkers to refine treatment timing and effectiveness.

The natural history of the cardiovascular phenotype in FD is well documented with typical manifestations including LVH and diastolic dysfunction in the early stages; myocardial fibrosis, inflammation, and arrhythmia in the advanced stages. Symptoms are common and frequent, affecting 60% of FD patients (70). Advances in multiparametric CMR, speckle tracking strain on TTE and automated ECG analysis have facilitated detection of cardiomyopathy at an earlier stage. This has significant implications as current guidelines recommend initiation of disease-modifying therapy when patients have developed LVH and LGE, although there is no clear evidence that these processes are reversible. It is feasible that this is a contributing reason why cardiovascular-related manifestations (predominantly arrhythmia) remain the most significant contributor to FD morbidity and mortality, despite initiation of ERT / OCT. Furthermore, there remains a lack of evidence relating to the underlying mechanisms involved in development of the cardiovascular phenotype, including damage to atrial structure and function, the role of inflammation at all stages of cardiomyopathy and the cause behind exercise limitation, a frequently experienced symptom at all stages of FD. Considering the high prevalence of ischaemic CVA in disproportionately young FD patients, it is important to explore the potential cardiac mechanisms that contribute to this burden. With studies reporting a high prevalence of AF in FD, and emerging imaging techniques available to detect atrial dysfunction, this allows for identification

of atrial involvement relating to Gb3 accumulation triggering arrhythmia and subsequent cardioembolic stroke.

This thesis provides insights into specific underlying mechanisms related to FD cardiomyopathy and their onset. Specifically, this thesis addresses topics relating to primary atrial myopathy, early markers of FD cardiomyopathy, predictors and associated mechanisms of arrhythmia relating to ischaemia, inflammation and Gb3 deposition, and how early imaging biochemical, and exercise markers change with cardiomyopathy progression. As such, the main findings of this thesis are as follows:

1. In patients previously thought to be "phenotype-negative" for FD cardiomyopathy, novel ECG changes were documented which may relate to early myocardial Gb3 accumulation. Specifically, we demonstrate P-wave duration and PQ shortening in early-stage FD cardiomyopathy. These findings are reflected in an *in-vitro* iPSC-CM model for FD with confirmed α-GAL A deficiency and Gb3 accumulation, where atrial iPSC-CMs demonstrated a quicker upstroke velocity. Novel contraction and calcium handling changes were also identified in this novel model for FD.

2. Traditionally, monitoring progression of cardiomyopathy has been limited to changes in LVMi over time. Longitudinal data in this thesis suggest that atrial dilatation and dysfunction, alongside impaired LV and RV longitudinal contraction and deformation, begin early and may be better markers of progression. These imaging changes coincide with a worsening of cardiac-biomarkers, specifically NT-proBNP and troponin. In combination, if confirmed

in larger populations, these could form the endpoints for future studies of disease-modifying therapy.

3. Regarding early markers of cardiomyopathy in FD, we confirm the onset of impaired aerobic capacity in gene-positive patients in the absence of overt cardiac phenotype, including T1 mapping, LV mass on cardiac MRI and deformation imaging on echocardiography. $\dot{V}O_{2peak}$ falls progressively with cardiac disease stage alongside increasing NT-proBNP and troponin without associated worsening of FEV_1. This provides novel insights into exercise intolerance experienced by FD patients.

4. In adults with FD and varying degrees of cardiac involvement, inflammation is likely to play a key role in cardiomyopathy onset and arrhythmogenesis. This may relate to endothelial cell activation, leukocyte trafficking, angiogenesis and thrombo-inflammation. Accelerated coronary atherosclerosis and subsequent myocardial ischaemia are likely to contribute this via conventional mechanisms and mechanisms specific to Gb3 deposition.

5. Continuous cardiac monitoring using devices such as ILRs are particularly useful in FD cardiomyopathy where arrhythmia may be sporadic in onset. However, utilisation in such devices is low and restricted to those with more advanced cardiomyopathy. In those with ILRs implanted, arrhythmia detection is much higher than that of the general population.

7.1 Molecular and electrophysiological changes in an atrial "disease in a dish" model of Fabry cardiomyopathy

As documented in this thesis, arrhythmia and stroke are responsible for the large burden of cardiovascular mortality in FD. Whilst predisposing factors and pathophysiological mechanisms for VA are established, there is less evidence for mechanisms of atrial myopathy and arrhythmia. AF prevalence is high and a likely contributor to stroke burden. The earliest detectable cardiac manifestations in FD are PQ changes on ECG; however, the mechanisms are not well understood.

This chapter has demonstrated that using signal-averaged P-wave analysis, P-wave duration and PQ interval shortens in adults with FD and no overt cardiovascular phenotype. This prolongs as cardiomyopathy progresses, most likely due to atrial structural remodelling including dilation and impairment in atrial strain. Data from the *in-vitro* component of this chapter identified several mechanisms for atrial arrhythmogenesis. We demonstrate alterations in contraction, calcium handling and excitability in gene-edited *GLA* p. *N215S* atrial IPSC-CMs which under-express α-GAL A and accumulate Gb3, compared to WT.

The atrial iPSC-CM data supports the early clinical ECG findings in FD, suggesting that electrical instability and remodelling in atrial cardiomyocytes begins early and progresses insidiously, forming a substrate for atrial arrhythmia. The combined use of *in-vivo* and *in-vitro* data may be applicable to other cardiomyopathies. These insights

into early alterations in atrial electrical conduction and contraction suggest there may be a need for more proactive, early monitoring of patients for AF. Further research into targeted therapy to reduce the atrial substrate for arrhythmia is required, thus reducing the prevalence of AF and stroke in FD. The work also supports the data generated from the other chapters documenting "early changes" in the cardiovascular phenotype of FD with insidious onset and progression.

7.1.1 Future work

The successful generation of gene-edited iPSC-CMs with model validation, evidenced by enzyme deficiency and Gb3 accumulation, opens up avenues for future work exploring arrhythmogenesis in FD. The cells used for gene-editing in this project were from healthy volunteers. Future projects include the use of patient-derived iPSCs to confirm the presence of identified changes in this cohort of patients. This will require ethical approval.

There are significant molecular implications when considering GLA p. *N215S* in the clinical manifestations of FD. The gene variant involves the substitution of a serine for an asparagine on α-GAL A at codon 215. The N-linked glycan attached to N215 is involved in the facilitation of trafficking α-GAL A to the lysosome, stabilising glycoproteins and folding of macromolecules (312). The GLA p. *N215S* variant lacks this glycan. When modelling out the structure of α-GAL, the N215 carbohydrate is located away from the surface of the protein (313). With the absence of the N-linked glycan in the GLA p. *N215S* variant, the serine incorporates into the structure of α-GAL A, however the subcellular distribution of α-GAL A is altered (39). This has consequences altering the folding of α-GAL and its trafficking to the lysosome. Future

work should therefore assess the implications of protein misfolding in the context of GLA p. *N215S.* Furthermore, future work could also utilise LysoTracker™ to stain the lysosomes in live cells. This may enable to identification of lysosomal Gb3 accumulation, which in turn, gives an indicator of the effects of alterations in α-GAL A ultrastructure (including loss of the N-linked glycan) and enzyme activity.

We are also in collaboration with an institution specialising in computer modelling and simulation work, with a plan to develop *in-silico* atrial cardiomyocyte models and provide a mechanistic explanation to the identified differences between *GLA* p. *N215S* and WT atrial iPSC-CMs, as well as FD patients and non-FD controls. The properties of the atrial IPSC-CM models, capturing any electrophysiological changes induced by *GLA* p. *N215S* would be used to describe the electrical activity of a human bi-atrial model. The characteristic structural, electrical and functional changes in the LA seen in our FD cohort will contribute to the development of the model. PACs will also be replicated *in-silico* by assessing changes in P-wave morphology after applying ectopic stimuli in different locations of the human atrial model. Comparing P-wave morphology between *in-silico* and clinical PACs may identify initiation sites of abnormal electrical impulses. This will characterise the electrophysiological substrate induced by FD.

The next step in the *in-vitro* aspect of this chapter would be to test the effects of disease modifying therapy (ERT / OCT) on the identified changes to ascertain if therapy exhibited any reversibility in the pro-arrhythmic changes. If positive, this would add to the rationale for early therapy-initiation at a stage where pathological changes could potentially be reversed. Ethical approval will be required and this could be

combined with multi-centre ethical approval in order to use ECGs from FD patients to test the effects of early-phase therapy initiation on alterations in P-wave morphology and duration.

Finally, next steps in the ECG work would be to create patient-specific models of cardiac excitation in the atria of FD patients, using these models to try and improve risk stratification for arrhythmia. Subsequently, pharmacological treatment could be tested in these models for arrhythmia termination and/or prevention. This goes in hand with the *in-silico* atrial models using the *in-vitro* data but also extends to use *in-vivo* data. The models would be created by defining atrial anatomy, structure and electrophysiology. This would be done using anatomical meshes, generated from patient-derived CMRs and/or TTE, to define atrial anatomy and function. Cardiac electrophysiology would be modelled by modifying established “healthy” models of atrial cardiomyocytes informed by P-wave changes on ECG. Arrhythmia inducibility would be assessed in these models using methods including S1 and S2 pacing. This would establish arrhythmia risk. The effects of disease-modifying therapy would then be assessed to test prevention or treatment. To test pharmacological modifications, this would be done by global modification of target proteins, for example specific ion channels / pumps in the case of common anti-arrhythmic drugs, e.g. Flecainide. This adds to the theme of delivering therapy which is personalised and individualised to specific disease mechanisms of the patient.

7.2 Longitudinal changes in transthoracic echocardiography and biochemical markers in Fabry Disease

This chapter identifies novel trends in conventional imaging markers on TTE and biochemical markers which, if used in conjunction with multiparametric CMR and ECG-monitoring, enables accurate assessment of stage and progression of cardiomyopathy, related to FD. Alongside the pro-inflammatory cytokines identified in the Luminex® assay from Chapter 2, there is a trend towards a worsening of conventional biochemical parameters (specifically NT-proBNP and troponin) over time. Troponin in the context of FD is likely to represent myocardial necrosis related to fibrosis (102) and chronic inflammation (82). This is further supported by the stepwise increase in concentration of pro-inflammatory cytokines from the Luminex® assay according to degree of FD cardiomyopathy.

The trends identified on TTE highlight the importance of documenting early changes in cardiac function. Timing of initiation of disease-modifying therapy is crucial to optimise outcomes in FD. By the time LVH and LGE develop, OCT / ERT appears to be of limited benefit in terms of reversibility or reduction in rate of progression (81). However, onset of LVH with or without LGE, is the main cardiac-specific indication for therapy initiation (53). Knowledge of the changes in LV TDI and LV GLS, longitudinal RV function or atrial deformation may prove more useful in deciding when to start therapy and how to monitor change over time. Indeed reversibility has been demonstrated on TDI in FD patients with diastolic dysfunction commenced on ERT, without LVH or advanced features of FD cardiomyopathy (73). This has also been

demonstrated more recently in pre-hypertrophic FD patients whereby Gb3 clearance was confirmed, evidenced by stable appearances on endomyocardial biopsy after ERT treatment (**Figure 7.1**).

Further findings in this chapter include increasing LA volume with progressive impairment of LA strain over time. This is consistent with the findings in Chapter 5, where intracellular abnormalities were identified, relating to atrial electrophysiology, contraction and calcium handling dynamics in gene-edited atrial iPSC-CMs, and Chapter 4 where impairment in atrial function likely contribute to aerobic capacity impairment in early-stage FD cardiomyopathy.

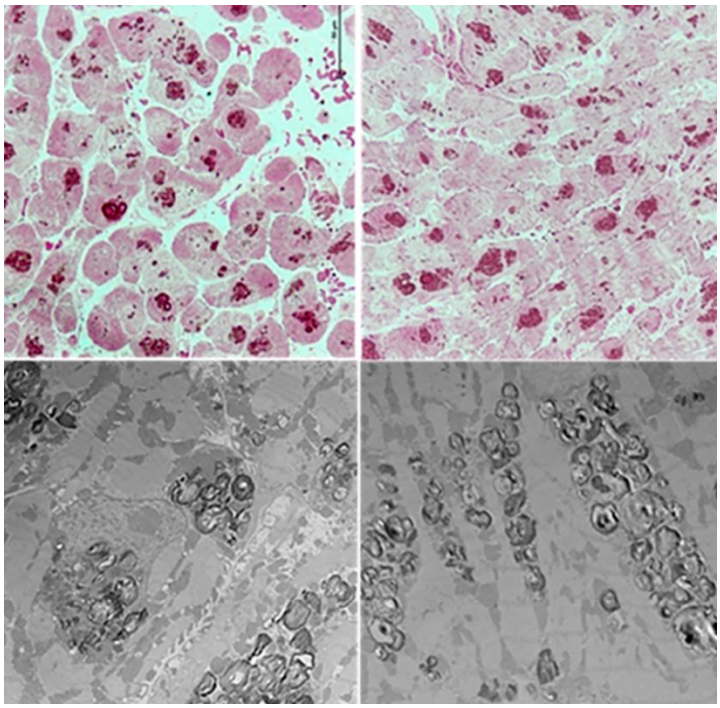

Figure 7.1: Endomyocardial biopsy of a 24-year-old male with FD at baseline and following 20 years ERT. Top left: Emethin section of Epon-embedded endomyocardial

biopsy samples demonstrating mildly hypertrophic cardiomyocytes with Gb3 storage material. Top right: Unchanged appearances of cardiomyocytes following 20 years ERT. Bottom left: Ultrastructural evidence of storage material with myelin bodies at baseline. Bottom right: Unchanged appearances of storage material following 20 years ERT. Adapted from Frustaci et al (171).

7.2.1 Future work

7.2.1.1 Effects of therapy on TTE parameters

One of the main limitations of this study was that the data was not able to provide information on how disease-modifying FD therapy may have impacted the TTE trends. In part, this was due to the small sample size. More importantly, since this was a longitudinal study of a single clinical cohort, disease severity was a major consideration when deciding about initiation of therapy. This meant that the phenotype of the treated and non-treated groups would likely be different. This issue raises the problem of reverse causality. As patients on therapy may have more severe disease, these patients would likely have faster disease progression as the progression itself would have resulted in consideration of treatment. Subsequently, the rate of disease progression would influence decisions for consideration of disease-modifying therapy, rather than therapy influencing the rate of disease progression. This could over-estimate the rate of disease progression in the treatment arm, underestimating the potential beneficial effect of treatment, and would produce misleading results. To assess the effects of disease-modifying therapy on TTE parameters, future work would need to involve a before-and-after intervention study. This would include

patients initially not on therapy, but who then commenced therapy during the study. This creates a “before” period where longitudinal trends in TTE could be assessed, and an “after” period where trends can be assessed on therapy.

7.2.1.2 Cardiac Registry

Given the ethical approval of multi-centre retrospective FD work, future work will be in the form of developing a cardiac registry. This will utilise multimodality imaging including TTE and multiparametric CMR, biochemical analysis, as well as CPEX to identify longitudinal trends relating to various stages of FD cardiomyopathy and if / how they may correlate with major adverse cardiac events (MACE). Data are currently lacking on the prognostic importance of changes in T1, LVMi and presence and quantity of LGE. With the identified TTE parameters in this study, these could be used in conjunction with CMR to improve risk stratification. Data from multimodality imaging, biochemistry and serial CPEX will be inputted into a multi-centre research database for adults with FD. By collecting and analysing these data in conjunction, this would identify the incremental value of various TTE, CMR, ECG, CPEX and biochemical parameters on MACE, specifically arrhythmia.

Pseudonymised data will be entered from participating centres onto a secure, online, web-based electronic data capture application. Using data from multiple centres will allow for a larger group of FD patients to be studied, where meaningful trends can be identified. The long-term aim is to build a collaborative project around the role of cardiovascular imaging and outcomes in FD. Retrospective work would build a database that incorporates image analysis of all clinically acquired CMR and TTE

scans for analysis with the prospective aim to offer images acquired for analysis by machine learning and to investigator-led research.

7.3 Changes in peak oxygen consumption on exercise and cardiomyopathy stage in Fabry Disease

This chapter highlighted the benefits of formal investigation of exercise intolerance in FD. Specifically, the work from this chapter identified $\dot{V}O_{2peak}$ as a potential biomarker for monitoring or assessing treatment response. $\dot{V}O_{2peak}$ was impaired in patients classified as "phenotype-negative" for FD cardiomyopathy. The fact that $\dot{V}O_{2peak}$ deteriorated with advancing stage of cardiac disease, and correlated with increasing cardiac biomarkers, suggests cardiac dysfunction as a likely cause for this impairment. This result is consistent with the gradual accumulation of Gb3 and lyso-Gb3, and the results of Chapter 3 that showed early changes in LV TDI and GLS, RV longitudinal contraction, and LA function on TTE that progressed over time.

The results of this chapter should give hope to the FD community by providing rationale for exercise intolerance, which can be attributed to reduced aerobic capacity, and quantified by a reduction in $\dot{V}O_{2peak}$. This is important because patients consider fatigue and effort intolerance to be a major issue for which there is no current effective therapy. Identifying a patient-specific factor that could be monitored opens possibilities for future research into pathogenesis and treatment. The assumption is that this likely reflects myocardial Gb3 deposition and raises the possibility of tracking response to

reduction in Gb3 and lyso-Gb3 with disease-modifying drugs before any other phenotypic change.

7.3.1 Future work

Many of the patients who have undergone CPEX in the study report symptoms relating to exercise intolerance. Also, the majority have only undergone a single test in order to ascertain the underlying aetiology. Future work will need to involve formal CPEX testing in a large FD cohort to confirm the findings, and then to perform serial testing to enhance our understanding of how $\dot{V}O_{2peak}$ changes with disease progression, measured using serial ECG and cardiac imaging. Determining reproducibility of CPEX by repeat-testing in a sub-group with FD would be an important part of this work. Discussions are taking place with pharmaceutical companies regarding early-phase study set up. This would incorporate not only exercise testing, but ECG and cardiovascular imaging, in light of the findings in Chapters 3 and 5. Given the lack of a healthy control group in our work and having to rely on normative values, any future study would benefit from a comparison with healthy controls matched for age and sex.

7.4 The role of atherosclerosis and inflammation on arrhythmia risk stratification in Fabry Disease

Inflammation is a key driver of FD, specifically in the development of cardiomyopathy. Activation and infiltration of immune cells triggered by Gb3 deposition, leads to local inflammation, pro-fibrotic signalling and deposition of the extracellular matrix (222). These are likely to be key underlying mechanisms in the development of LVH, fibrosis

and focal myocardial oedema as evidenced by elevated T2 mapping on multiparametric CMR. The findings from the Luminex® Performance Assay which demonstrate a stepwise increase in concentration of numerous pro-inflammatory cytokines from patients with FD and intermediate cardiomyopathy up to the more advanced stage, when compared to non-FD controls supports the key role of inflammation. The results of the assay reveal novel pro-inflammatory pathways related to angiogenesis, leukocyte trafficking, endothelial cell activation and thrombo-inflammation. Elevation in a subset of these cytokines (mainly related to angiogenesis) have been documented previously in FD but the majority have been shown for the first time.

This reveals the complex role of inflammation in the progression of organ dysfunction in FD, specifically cardiomyopathy. It suggests that inflammation, as with other relevant markers highlighted in this thesis, begins early in the disease, also progresses insidiously, and is not always detectable using current biochemical protocols. Elevated T2 on CMR with uptake of 18FDG PET in FD patients likely reflects inflammation that is detectable using advanced cardiovascular imaging. However, many of the earlier stages of inflammation may be undetected. The specific cytokines that demonstrated stepwise elevation according to cardiomyopathy stage show potential role as biomarkers in monitoring disease progression or response to therapy.

7.4.1 Future Work

Future work will involve running a second Luminex® assay. This assay will include the remaining patients of the RaILRoAD study who have had plasma samples taken. It will also include supernatant from the mature atrial iPSC-CMs (day 30), both from *GLA* p. *N215S* as well as WT iPSC-CMs. The intention of running this alongside human plasma samples is to identify if pro-inflammatory cytokines are expressed *in-vitro* in highly immature gene-edited cells. This will provide useful insights into understanding the precise onset of specific inflammatory cascades.

By understanding the potential role of identified cytokines as biomarkers, an early phase clinical trial would utilise such assays to assess response to therapy. An early phase clinical trial with disease-modifying therapy would utilise cardiovascular imaging, biochemistry, CPEX, automated ECG analysis and plasma analysis of pro-inflammatory cytokines, to understand not only the early detectable changes, but how these changes respond to therapy.

Future work to investigate atherosclerosis and ischaemia in FD will involve expanding the cohort to all patients and not exclusively those on disease-modifying FD therapy. Given the implementation of the RaILRoAD study and multi-centre ethical approval for the use of clinical data for the secondary purpose of research, this work will also expand to other FD centres in the UK, further increasing the cohort number. Many of those who are not established on ERT or OCT are likely to report cardiac symptoms, specifically those relating to myocardial ischaemia. It is likely that patients may have

also experienced ischaemic symptoms prior to a diagnosis of FD. Indeed, many patients ultimately are diagnosed with FD after repeated hospital admissions with troponin-positive chest pain with myocardial ischaemia and normal coronary arteries (MINOCA) diagnosed (314, 315). Subsequent CMR imaging then identifies patterns of fibrosis and hypertrophy consistent with FD (316).

7.5 Clinical ILR utilisation in Fabry Disease and their role in detecting arrhythmia compared to standard of care cardiac monitoring in a multicentre clinical trial

This chapter provides insights into the current practice in the UK for continuous cardiac monitoring using ILRs in FD. ILRs are particularly useful given the sporadic and unpredictable nature of arrhythmia in FD patients, who may or may not have cardiac-sounding symptoms (31, 317). ILR monitoring has proven sensitivity in various cardiovascular disorders for accurate detection of arrhythmia (318).

The role of ILR-detection of AF and need for subsequent treatment remains controversial. Atrial arrhythmias that have been detected on ILR which resembles AF are termed AHREs if not confirmed on 12-lead ECG monitoring. In large-scale non-FD studies of ILR and associated cardiac device-detected AHREs, in the absence of 12-lead ECG confirmation, formal commencement of anticoagulation did not reduce the burden of stroke but increased risk of major bleeding when compared to the non-anticoagulated group (311). This study was in a cohort of patients aged 65 years or

above with at least 1 risk factor for stroke. One of the secondary outcome measures of the RaILRoAD study was to assess the potential benefit of ILRs in detection of AHREs requiring anticoagulation (defined as AF over 30 seconds) (122). However, in light of the published data and the ASSERT trial which demonstrated a high risk of stroke in certain patients with AHREs detected on cardiac devices, the definition in the protocol was modified to reflect the fact that anticoagulation in the context of AHREs remains a somewhat evidence free area (319, 320). Accepting the higher stroke risk in FD compared to the normal population, anticoagulation was recommended only after discussing the risks and benefits with the patients and if detected continuously for over 24 hours on ILR.

Although ILR implantation appears to be useful in detecting arrhythmia in FD, the clinical ILR utilisation sub-chapter suggests under-utilisation. This supports the need for the RaILRoAD study, a multicentre study in FD patients with varying degrees of cardiomyopathy. RaILRoAD should clarify the clinical utility of ILRs in FD.

7.5.1 Future Work

The findings from the RaILRoAD study are likely to provide new insights into the sub-groups of FD patients most at risk of arrhythmia, as well as information on the ECG, biochemical and imaging markers that are most discriminatory. The next steps in this study are to verify the baseline data and complete follow-up. Specific analyses from the ILRs will include quantifying the burden of alerts, frequency of non-sustained supraventricular and ventricular arrhythmia that may not have resulted in modification

of therapy and beat-to-beat AI-based analysis of PDF records from the alerts. Data will also be analysed to identify longitudinal trends in multimodality imaging, biochemical and ECG parameters and how these may alter arrhythmic risk

7.6 Conclusions

The contents of this thesis have enhanced our knowledge on mechanisms of atrial cardiomyopathy in FD, including the identifying of intrinsic intracellular pro-arrhythmic changes in atrial iPSC-CMs with electrophysiological changes resembling that of P-wave changes in early FD-cardiomyopathy. Novel early changes have also been identified on TTE, CMR, oxygen uptake and pro-inflammatory cytokine expression, which in the future may serve as biomarkers for monitoring disease progression and response to therapy. These highlight how myocardial Gb3 accumulation triggers the early onset and insidious progression of FD cardiomyopathy. The findings also confirm the multitude of complex mechanisms involved, many of which hold promise for targeted therapy in the future.

8 Chapter 8 – Appendix

8.1 Published work related to thesis

8.1.1 Oral presentation

- A Disease in Dish model for Fabry disease using atrial iPSC-CMs. Institute of Cardiovascular Sciences Research Seminar Series, University of Birmingham (2022)

- Arrhythmia in Fabry Disease. Fabry International Network Meeting, Amsterdam (2023)

- Understanding atrial arrhythmia in Fabry Disease, the development of patient-specific *in-silico* atrial models. Fabry Matters Conference (2024)

- Mechanisms of arrhythmia in Fabry Disease: a mixed *in-vivo* and *in-vitro* model. British Cardiovascular Society Young Investigator Award. Manchester (2024)

8.1.2 Poster Presentation

- Atherosclerosis in Fabry Disease - British Cardiovascular Society, Manchester (2022)

- Family Screening in Fabry Disease - Fabry Update, Wurzburg, Germany (2022)

- Clinical utilisation of ILRs in adults with Fabry Disease – a snapshot multi-centre study. WORLD Symposium, Orlando, USA (2023)

- A systematic review on the incidence and clinical risk predictors of atrial fibrillation and permanent pacemaker implantation for bradycardia in Fabry Disease. British Cardiovascular Society, Manchester (2023)

- Generation of a Disease in Dish Model in Fabry Disease International Society for Heart Research meeting. Porto, Portugal (2023)

- Longitudinal Assessment of biochemical markers in Fabry Disease. WORLD Symposium, 2024, San Diego USA (2024)

- Early contractile changes in atrial cardiomyocytes – A Disease in dish model for Fabry disease. Fabry Update 2024. Hamburg, Germany (2024)

- Longitudinal changes on transthoracic echocardiography in Fabry disease. American Society of Echocardiography Meeting. Portland, USA (2024)

- Changes in peak oxygen consumption in Fabry Disease and associations with cardiomyopathy severity. European Society of Cardiology Congress, London (2024)

- Atrial remodelling drives arrhythmia in Fabry Disease. American Heart Association Scientific Sessions, Chicago, USA (2024)

8.1.3 Awards and Prizes

- British Heart Foundation Accelerator Award (2021)
- Metchley Park Fellowship Consumables Grant (2021)
- Society for Mucopolysaccharide Diseases Research Grant (2023)
- Fabry Matters Conference Research Grant (2024)
- British Cardiac Society Young Investigator Award Runner Up (2024)
- Basic Cardiovascular Sciences International Travel Grant (2024)

8.1.4 Publications

- **Roy A,** Umar H, Ochoa-Ferraro A, Warfield A, Lewis N, Geberhiwot T, Steeds R. Atherosclerosis in Fabry Disease – A Contemporary Review. *J. Clin. Med.* 2021: 10 (19) 4422

- **Roy A,** Mansour M, Oxborough D, Geberhiwot T, Steeds R. Multi-Modality Cardiovascular Imaging Assessment in Fabry Disease. *Appl Sci* 2022 12: 1605

- Vijapurapu R, **Roy A**, Demetriades P, Warfield, A, Hughes D, Moon J, Woolfson P, de Bono J, Geberhiwot T, Kotecha D, Steeds RP. Systematic review of the incidence and clinical risk predictors of atrial fibrillation and permanent pacemaker implantation for bradycardia in Fabry disease. *Open Heart* 2023 10: 2316

- **Roy A,** Vijapurapu R, Kurdi H, Orsborne C, Woolfson P, Kalla M, et al. Clinical utilisation of implantable loop recorders in adults with Fabry disease-a multi-centre snapshot study. *Front Cardiovasc Med*. 2023;10:1323214.

- **Roy A,** Cumberland MJ, O"Shea C, Holmes AP, Kalla M, Gehmlich K, Geberhiwot T, Steeds RP. Arrhythmogenesis in Fabry Disease. *Curr Cardiol Rep* 2024

- **Roy A**, Thompson S, Hodson J, van Vliet J, Condon N, Alvior A, O'Shea C et al. Changes in peak oxygen consumption in Fabry Disease and associations with cardiomyopathy severity. *Heart* 2024

- **Roy A**, Thompson S, Hodson J, Win K, Alvior A, Cumberland M, Ochoa-Ferraro A et al. Longitudinal changes on transthoracic echocardiogram and biochemical markers in Fabry Disease. *Canadian Journal of Cardiology Open* (in press)

- **Roy A**, O'Shea C, Dasi Martinez A, Patel L, Cumberland M, Nieves D, Canagarajah H, Thompson S et al. Early atrial remodelling drives arrhythmia in Fabry Disease. *Circulation: Arrhythmia and Electrophysiology* (undergoing revisions)

- Church Smith CL, **Roy A**, Steeds S, Tuzcuoglu N, Wingrove C, Aitchison K, et al. Underdiagnosis of Fabry disease in minority ethnic groups. *Mol Genet Metab Rep*. 2025;42:101194.

8.2 Published work not related to thesis

8.2.1 Oral Presentations

- Alström in the Adult Heart. Alström Society International Conference, Baltimore (2023)

8.2.2 Publications

- Cumberland MJ, Riebel LL, **Roy A**, O'Shea C, Holmes AP, Denning C, Kirchhof P, Rodriguez B, Gehmlich K Basic Research Approaches to Evaluate Cardiac Arrhythmia in Heart Failure and Beyond. *Front Physiol* 2022 13: 806366

- Patel L, **Roy A**, Alvior AM, Yuan M, Baig S, Bunting KV, Hodson J, Gehmlich K, Lord J, Geberhiwot T, Steeds RP. Phenoage and longitudinal changes on

transthoracic echocardiography in Alström syndrome: a disease of accelerated ageing. *Geroscience* 2023

- **Roy A**, Patel L, Yuan M, O'Shea C, Alvior AM, Charalambides M, Moxon D, Baig S, Bunting KV, Gehmlich K, Geberhiwot T, Steeds RP. Defining the cardiovascular phenotype of adults with Alström syndrome. *Int J Cardiol* 2024

- **Roy A**, Patel L, Yuan M, O'Shea C, Alvior AM, Charalambides M, Moxon D, Baig S, Bunting KV, Gehmlich K, Geberhiwot T, Steeds RP. Reply to Letter to the Editor: "Defining the cardiovascular phenotype of adults with Alström syndrome". *Int J Cardiol* 2024

- Patel L, **Roy A**, Barlow J, O'Shea C, Nieves D, Azad AJ, et al. Characterisation of infantile cardiomyopathy in Alström syndrome using ALMS1 knockout induced pluripotent stem cell derived cardiomyocyte model. *Mol Genet Metab*. 2024;143(1-2):108575.

9 Chapter 9 – References

1. Brady RO, Gal AE, Bradley RM, Martensson E, Warshaw AL, Laster L. Enzymatic defect in Fabry's disease. Ceramidetrihexosidase deficiency. N Engl J Med. 1967;276(21):1163-7.

2. Desnick RJ, Brady R, Barranger J, Collins AJ, Germain DP, Goldman M, et al. Fabry disease, an under-recognized multisystemic disorder: expert recommendations for diagnosis, management, and enzyme replacement therapy. Ann Intern Med. 2003;138(4):338-46.

3. Mehta A, Beck M, Eyskens F, Feliciani C, Kantola I, Ramaswami U, et al. Fabry disease: a review of current management strategies. QJM. 2010;103(9):641-59.

4. Desnick RJ, Blieden LC, Sharp HL, Hofschire PJ, Moller JH. Cardiac valvular anomalies in Fabry disease. Clinical, morphologic, and biochemical studies. Circulation. 1976;54(5):818-25.

5. Saito S, Ohno K, Sakuraba H. Fabry-database.org: database of the clinical phenotypes, genotypes and mutant α-galactosidase A structures in Fabry disease. J Hum Genet. 2011;56(6):467-8.

6. Saito S. Fabry Database

http://fabry-database.org/ [

7. Fabry J. Ein Beitrag zur Kenntniss der Purpura haemorrhagica nodularis (Purpura papulosa haemorrhagica Hebrae). Arch f Dermat. 1898;43:187-200.

8. Fabry H. Angiokeratoma corporis diffusum--Fabry disease: historical review from the original description to the introduction of enzyme replacement therapy. Acta Paediatr Suppl. 2002;91(439):3-5.

9. POMPEN AW, RUITER M, WYERS HJ. Angiokeratoma corporis diffusum (universale) Fabry, as a sign of an unknown internal disease; two autopsy reports. Acta Med Scand. 1947;128(3):234-55.

10. PC L, P B, M L. Dermatologic Aspects of Fabry Disease. Journal of Inborn Errors of Metabolism and Screening. 2016;4.

11. Baig S, Edward NC, Kotecha D, Liu B, Nordin S, Kozor R, et al. Ventricular arrhythmia and sudden cardiac death in Fabry disease: a systematic review of risk factors in clinical practice. Europace. 2018;20(FI2):f153-f61.

12. Nair V, Belanger EC, Veinot JP. Lysosomal storage disorders affecting the heart: a review. Cardiovasc Pathol. 2019;39:12-24.

13. Kampmann C, Wiethoff CM, Whybra C, Baehner FA, Mengel E, Beck M. Cardiac manifestations of Anderson-Fabry disease in children and adolescents. Acta Paediatr. 2008;97(4):463-9.

14. Güzel T, Çağlar FNT, Ekici B, Kış M, Öztaş S, Öz A, et al. Prevalence of Fabry Disease in patients with left ventricular hypertrophy in Turkey: Multicenter study (LVH-TR subgroup analysis). Int J Cardiovasc Imaging. 2023;39(6):1143-55.

15. Biegstraaten M, Arngrímsson R, Barbey F, Boks L, Cecchi F, Deegan PB, et al. Recommendations for initiation and cessation of enzyme replacement therapy in patients with Fabry disease: the European Fabry Working Group consensus document. Orphanet J Rare Dis. 2015;10:36.

16. Spada M, Pagliardini S, Yasuda M, Tukel T, Thiagarajan G, Sakuraba H, et al. High incidence of later-onset fabry disease revealed by newborn screening. Am J Hum Genet. 2006;79(1):31-40.

17. Laney DA, Fernhoff PM. Diagnosis of Fabry disease via analysis of family history. J Genet Couns. 2008;17(1):79-83.

18. Azevedo O, Marques N, Reis L, Cruz I, Craveiro N, Antunes H, et al. Predictors of Fabry disease in patients with hypertrophic cardiomyopathy: How to guide the diagnostic strategy? Am Heart J. 2020;226:114-26.

19. Niemann M, Herrmann S, Hu K, Breunig F, Strotmann J, Beer M, et al. Differences in Fabry cardiomyopathy between female and male patients: consequences for diagnostic assessment. JACC Cardiovasc Imaging. 2011;4(6):592-601.

20. Sun Z, Fan J, Wang Y. X-Chromosome Inactivation and Related Diseases. Genet Res (Camb). 2022;2022:1391807.

21. Belmont JW. Genetic control of X inactivation and processes leading to X-inactivation skewing. Am J Hum Genet. 1996;58(6):1101-8.

22. Echevarria L, Benistan K, Toussaint A, Dubourg O, Hagege AA, Eladari D, et al. X-chromosome inactivation in female patients with Fabry disease. Clin Genet. 2016;89(1):44-54.

23. R V, A R, P D. Systematic review of the incidence and clinical risk predictors of atrial fibrillation and permanent pacemaker implantation for bradycardia in Fabry disease. Open Heart. 2023;10:2316.

24. Namdar M, Steffel J, Vidovic M, Brunckhorst CB, Holzmeister J, Lüscher TF, et al. Electrocardiographic changes in early recognition of Fabry disease. Heart. 2011;97(6):485-90.

25. Namdar M. Electrocardiographic Changes and Arrhythmia in Fabry Disease. Front Cardiovasc Med. 2016;3:7.

26. Shah JS, Hughes DA, Sachdev B, Tome M, Ward D, Lee P, et al. Prevalence and clinical significance of cardiac arrhythmia in Anderson-Fabry disease. Am J Cardiol. 2005;96(6):842-6.

27. Krämer J, Niemann M, Störk S, Frantz S, Beer M, Ertl G, et al. Relation of burden of myocardial fibrosis to malignant ventricular arrhythmias and outcomes in Fabry disease. Am J Cardiol. 2014;114(6):895-900.

28. Acharya D, Robertson P, Kay GN, Jackson L, Warnock DG, Plumb VJ, et al. Arrhythmias in Fabry cardiomyopathy. Clin Cardiol. 2012;35(12):738-40.

29. Frustaci A, Morgante E, Russo MA, Scopelliti F, Grande C, Verardo R, et al. Pathology and function of conduction tissue in Fabry disease cardiomyopathy. Circ Arrhythm Electrophysiol. 2015;8(4):799-805.

30. Patel V, O'Mahony C, Hughes D, Rahman MS, Coats C, Murphy E, et al. Clinical and genetic predictors of major cardiac events in patients with Anderson-Fabry Disease. Heart. 2015;101(12):961-6.

31. Weidemann F, Maier SK, Störk S, Brunner T, Liu D, Hu K, et al. Usefulness of an Implantable Loop Recorder to Detect Clinically Relevant Arrhythmias in Patients With Advanced Fabry Cardiomyopathy. Am J Cardiol. 2016;118(2):264-74.

32. Orsborne C, Bradley J, Bonnett LJ, Pleva LA, Naish JH, Clark DG, et al. Validated Model for Prediction of Adverse Cardiac Outcome in Patients With Fabry Disease. J Am Coll Cardiol. 2022;80(10):982-94.

33. Meucci MC, Lillo R, Del Franco A, Monda E, Iannaccone G, Baldassarre R, et al. Prognostic Implications of the Extent of Cardiac Damage in Patients With Fabry Disease. J Am Coll Cardiol. 2023;82(15):1524-34.

34. Vijapurapu R, Geberhiwot T, Jovanovic A, Baig S, Nordin S, Kozor R, et al. Study of indications for cardiac device implantation and utilisation in Fabry cardiomyopathy. Heart. 2019;105(23):1825-31.

35. Pelliccia F, Pasceri V, Limongelli G, Autore C, Basso C, Corrado D, et al. Long-term outcome of nonobstructive versus obstructive hypertrophic cardiomyopathy: A systematic review and meta-analysis. Int J Cardiol. 2017;243:379-84.

36. Elliott PM, Gimeno JR, Thaman R, Shah J, Ward D, Dickie S, et al. Historical trends in reported survival rates in patients with hypertrophic cardiomyopathy. Heart. 2006;92(6):785-91.

37. Roy A, Cumberland MJ, O'Shea C, Holmes A, Kalla M, Gehmlich K, et al. Arrhythmogenesis in Fabry Disease. Curr Cardiol Rep. 2024.

38. Weidemann F, Niemann M, Störk S, Breunig F, Beer M, Sommer C, et al. Long-term outcome of enzyme-replacement therapy in advanced Fabry disease: evidence for disease progression towards serious complications. J Intern Med. 2013;274(4):331-41.

39. Germain DP, Brand E, Burlina A, Cecchi F, Garman SC, Kempf J, et al. Phenotypic characteristics of the p.Asn215Ser (p.N215S) GLA mutation in male and female patients with Fabry disease: A multicenter Fabry Registry study. Mol Genet Genomic Med. 2018.

40. Vijapurapu R, Roy A, Demetriades P, Warfield A, Hughes DA, Moon J, et al. Systematic review of the incidence and clinical risk predictors of atrial fibrillation and permanent pacemaker implantation for bradycardia in Fabry disease. Open Heart. 2023;10(2).

41. Hagège A, Réant P, Habib G, Damy T, Barone-Rochette G, Soulat G, et al. Fabry disease in cardiology practice: Literature review and expert point of view. Arch Cardiovasc Dis. 2019;112(4):278-87.

42. Lobo T, Morgan J, Bjorksten A, Nicholls K, Grigg L, Centra E, et al. Cardiovascular testing in Fabry disease: exercise capacity reduction, chronotropic

incompetence and improved anaerobic threshold after enzyme replacement. Intern Med J. 2008;38(6):407-14.

43. Wilson HC, Hopkin RJ, Madueme PC, Czosek RJ, Bailey LA, Taylor MD, et al. Arrhythmia and Clinical Cardiac Findings in Children With Anderson-Fabry Disease. Am J Cardiol. 2017;120(2):251-5.

44. Di LZ, Pichette M, Nadeau R, Bichet DG, Poulin F. Severe bradyarrhythmia linked to left atrial dysfunction in Fabry disease-A cross-sectional study. Clin Cardiol. 2018;41(9):1207-13.

45. O'Mahony C, Coats C, Cardona M, Garcia A, Calcagnino M, Murphy E, et al. Incidence and predictors of anti-bradycardia pacing in patients with Anderson-Fabry disease. Europace. 2011;13(12):1781-8.

46. Sené T, Lidove O, Sebbah J, Darondel JM, Picard H, Aaron L, et al. Cardiac device implantation in Fabry disease: A retrospective monocentric study. Medicine (Baltimore). 2016;95(40):e4996.

47. Pichette M, Serri K, Pagé M, Di LZ, Bichet DG, Poulin F. Impaired Left Atrial Function in Fabry Disease: A Longitudinal Speckle-Tracking Echocardiography Study. J Am Soc Echocardiogr. 2017;30(2):170-9.e2.

48. Talbot AS, Lewis NT, Nicholls KM. Cardiovascular outcomes in Fabry disease are linked to severity of chronic kidney disease. Heart. 2015;101(4):287-93.

49. Deva DP, Hanneman K, Li Q, Ng MY, Wasim S, Morel C, et al. Cardiovascular magnetic resonance demonstration of the spectrum of morphological phenotypes and patterns of myocardial scarring in Anderson-Fabry disease. J Cardiovasc Magn Reson. 2016;18:14.

50. Sims K, Politei J, Banikazemi M, Lee P. Stroke in Fabry disease frequently occurs before diagnosis and in the absence of other clinical events: natural history data from the Fabry Registry. Stroke. 2009;40(3):788-94.

51. Roy A, Mansour M, Oxborough D, Geberhiwot T, Steeds R. Multi-Modality Cardiovascular Imaging Assessment in Fabry Disease. *Appl Sci* 2022;12(3):1605.

52. Roy A, Vijapurapu R, Kurdi H, Orsborne C, Woolfson P, Kalla M, et al. Clinical utilisation of implantable loop recorders in adults with Fabry disease-a multi-centre snapshot study. Front Cardiovasc Med. 2023;10:1323214.

53. Hiwot T, Hughes D, Ramaswami U. Guidelines for the treatment of Fabry Disease. British Inherited Metabolic Diseases Group2020.

54. Vijapurapu R, Bradlow W, Leyva F, Moon JC, Zegard A, Lewis N, et al. Cardiac device implantation and device usage in Fabry and hypertrophic cardiomyopathy. Orphanet J Rare Dis. 2022;17(1):6.

55. Arends M, Wanner C, Hughes D, Mehta A, Oder D, Watkinson OT, et al. Characterization of Classical and Nonclassical Fabry Disease: A Multicenter Study. J Am Soc Nephrol. 2017;28(5):1631-41.

56. Politei JM, Bouhassira D, Germain DP, Goizet C, Guerrero-Sola A, Hilz MJ, et al. Pain in Fabry Disease: Practical Recommendations for Diagnosis and Treatment. CNS Neurosci Ther. 2016;22(7):568-76.

57. Lakomá J, Rimondini R, Donadio V, Liguori R, Caprini M. Pain related channels are differentially expressed in neuronal and non-neuronal cells of glabrous skin of fabry knockout male mice. PLoS One. 2014;9(10):e108641.

58. Hopkin RJ, Jefferies JL, Laney DA, Lawson VH, Mauer M, Taylor MR, et al. The management and treatment of children with Fabry disease: A United States-based perspective. Mol Genet Metab. 2016;117(2):104-13.

59. Fall B, Scott CR, Mauer M, Shankland S, Pippin J, Jefferson JA, et al. Urinary Podocyte Loss Is Increased in Patients with Fabry Disease and Correlates with Clinical Severity of Fabry Nephropathy. PLoS One. 2016;11(12):e0168346.

60. Najafian B, Svarstad E, Bostad L, Gubler MC, Tøndel C, Whitley C, et al. Progressive podocyte injury and globotriaosylceramide (GL-3) accumulation in young patients with Fabry disease. Kidney Int. 2011;79(6):663-70.

61. Ortiz A, Cianciaruso B, Cizmarik M, Germain DP, Mignani R, Oliveira JP, et al. End-stage renal disease in patients with Fabry disease: natural history data from the Fabry Registry. Nephrol Dial Transplant. 2010;25(3):769-75.

62. Ortiz A, Germain DP, Desnick RJ, Politei J, Mauer M, Burlina A, et al. Fabry disease revisited: Management and treatment recommendations for adult patients. Mol Genet Metab. 2018;123(4):416-27.

63. Idrus EA, Iskandar E. Cornea verticillata in Fabry disease. QJM. 2024;117(6):452-3.

64. Kolodny E, Fellgiebel A, Hilz MJ, Sims K, Caruso P, Phan TG, et al. Cerebrovascular involvement in Fabry disease: current status of knowledge. Stroke. 2015;46(1):302-13.

65. Roy A, Umar H, Ochoa-Ferraro A, Warfield A, Lewis N, Geberhiwot T, et al. Atherosclerosis in Fabry Disease-A Contemporary Review. J Clin Med. 2021;10(19).

66. Bolsover FE, Murphy E, Cipolotti L, Werring DJ, Lachmann RH. Cognitive dysfunction and depression in Fabry disease: a systematic review. J Inherit Metab Dis. 2014;37(2):177-87.

67. Esposito R, Russo C, Santoro C, Cocozza S, Riccio E, Sorrentino R, et al. Association between Left Atrial Deformation and Brain Involvement in Patients with Anderson-Fabry Disease at Diagnosis. J Clin Med. 2020;9(9).

68. Kampmann C, Linhart A, Baehner F, Palecek T, Wiethoff CM, Miebach E, et al. Onset and progression of the Anderson-Fabry disease related cardiomyopathy. Int J Cardiol. 2008;130(3):367-73.

69. Pieroni M, Moon JC, Arbustini E, Barriales-Villa R, Camporeale A, Vujkovac AC, et al. Cardiac Involvement in Fabry Disease: JACC Review Topic of the Week. J Am Coll Cardiol. 2021;77(7):922-36.

70. Ortiz A, Abiose A, Bichet DG, Cabrera G, Charrow J, Germain DP, et al. Time to treatment benefit for adult patients with Fabry disease receiving agalsidase β: data from the Fabry Registry. J Med Genet. 2016;53(7):495-502.

71. Linhart A, Germain DP, Olivotto I, Akhtar MM, Anastasakis A, Hughes D, et al. An expert consensus document on the management of cardiovascular manifestations of Fabry disease. Eur J Heart Fail. 2020;22(7):1076-96.

72. Yeung DF, Sirrs S, Tsang MYC, Gin K, Luong C, Jue J, et al. Echocardiographic Assessment of Patients with Fabry Disease. J Am Soc Echocardiogr. 2018;31(6):639-49.e2.

73. Pieroni M, Chimenti C, Ricci R, Sale P, Russo MA, Frustaci A. Early detection of Fabry cardiomyopathy by tissue Doppler imaging. Circulation. 2003;107(15):1978-84.

74. Spinelli L, Giugliano G, Pisani A, Imbriaco M, Riccio E, Russo C, et al. Does left ventricular function predict cardiac outcome in Anderson-Fabry disease? Int J Cardiovasc Imaging. 2021;37(4):1225-36.

75. O'Brien C, Britton I, Karur GR, Iwanochko RM, Morel CF, Nguyen ET, et al. Left Ventricular Mass and Wall Thickness Measurements Using Echocardiography and Cardiac MRI in Patients with Fabry Disease: Clinical Significance of Discrepant Findings. Radiol Cardiothorac Imaging. 2020;2(3):e190149.

76. Sado DM, White SK, Piechnik SK, Banypersad SM, Treibel T, Captur G, et al. Identification and assessment of Anderson-Fabry disease by cardiovascular magnetic resonance noncontrast myocardial T1 mapping. Circ Cardiovasc Imaging. 2013;6(3):392-8.

77. Nordin S, Kozor R, Baig S, Abdel-Gadir A, Medina-Menacho K, Rosmini S, et al. Cardiac Phenotype of Prehypertrophic Fabry Disease. Circ Cardiovasc Imaging. 2018;11(6):e007168.

78. Pica S, Sado DM, Maestrini V, Fontana M, White SK, Treibel T, et al. Reproducibility of native myocardial T1 mapping in the assessment of Fabry disease and its role in early detection of cardiac involvement by cardiovascular magnetic resonance. J Cardiovasc Magn Reson. 2014;16:99.

79. Knott KD, Augusto JB, Nordin S, Kozor R, Camaioni C, Xue H, et al. Quantitative Myocardial Perfusion in Fabry Disease. Circ Cardiovasc Imaging. 2019;12(7):e008872.

80. Dass S, Suttie JJ, Piechnik SK, Ferreira VM, Holloway CJ, Banerjee R, et al. Myocardial tissue characterization using magnetic resonance noncontrast t1 mapping in hypertrophic and dilated cardiomyopathy. Circ Cardiovasc Imaging. 2012;5(6):726-33.

81. Vijapurapu R, Baig S, Nordin S, Augusto JB, Price AM, Wheeldon N, et al. Longitudinal Assessment of Cardiac Involvement in Fabry Disease Using Cardiovascular Magnetic Resonance Imaging. JACC Cardiovasc Imaging. 2020;13(8):1850-2.

82. Augusto JB, Nordin S, Vijapurapu R, Baig S, Bulluck H, Castelletti S, et al. Myocardial Edema, Myocyte Injury, and Disease Severity in Fabry Disease. Circ Cardiovasc Imaging. 2020;13(3):e010171.

83. Imbriaco M, Nappi C, Ponsiglione A, Pisani A, Dell'Aversana S, Nicolai E, et al. Hybrid positron emission tomography-magnetic resonance imaging for assessing different stages of cardiac impairment in patients with Anderson-Fabry disease: AFFINITY study group. Eur Heart J Cardiovasc Imaging. 2019;20(9):1004-11.

84. Spinelli L, Imbriaco M, Nappi C, Nicolai E, Giugliano G, Ponsiglione A, et al. Early Cardiac Involvement Affects Left Ventricular Longitudinal Function in Females Carrying α-Galactosidase A Mutation: Role of Hybrid Positron Emission Tomography and Magnetic Resonance Imaging and Speckle-Tracking Echocardiography. Circ Cardiovasc Imaging. 2018;11(4):e007019.

85. Yogasundaram H, Nikhanj A, Putko BN, Boutin M, Jain-Ghai S, Khan A, et al. Elevated Inflammatory Plasma Biomarkers in Patients With Fabry Disease: A Critical Link to Heart Failure With Preserved Ejection Fraction. J Am Heart Assoc. 2018;7(21):e009098.

86. Straus SM, Kors JA, De Bruin ML, van der Hooft CS, Hofman A, Heeringa J, et al. Prolonged QTc interval and risk of sudden cardiac death in a population of older adults. J Am Coll Cardiol. 2006;47(2):362-7.

87. Jastrzebski M, Bacior B, Dimitrow PP, Kawecka-Jaszcz K. Electrophysiological study in a patient with Fabry disease and a short PQ interval. Europace. 2006;8(12):1045-7.

88. Aryana A, Fifer MA, Ruskin JN, Mela T. Short PR interval in the absence of preexcitation: a characteristic finding in a patient with Fabry disease. Pacing Clin Electrophysiol. 2008;31(6):782-3.

89. Vijapurapu R, Maanja M, Schlegel T, Augusto J, Kurdi H, Moon JC, et al. Advanced electrocardiography predicts early cardiac involvement and incident arrhythmias in Fabry disease. EP Europace. 2022;24(1):euac053.30.

90. Maruyama H, Taguchi A, Nishikawa Y, Guili C, Mikame M, Nameta M, et al. Medullary thick ascending limb impairment in the Gla. FASEB J. 2018;32(8):4544-59.

91. Ballabio A, Bonifacino JS. Lysosomes as dynamic regulators of cell and organismal homeostasis. Nat Rev Mol Cell Biol. 2020;21(2):101-18.

92. Waldek S, Feriozzi S. Fabry nephropathy: a review - how can we optimize the management of Fabry nephropathy? BMC Nephrol. 2014;15:72.

93. Puertollano R, Ferguson SM, Brugarolas J, Ballabio A. The complex relationship between TFEB transcription factor phosphorylation and subcellular localization. EMBO J. 2018;37(11).

94. Ivanova M. Altered Sphingolipids Metabolism Damaged Mitochondrial Functions: Lessons Learned From Gaucher and Fabry Diseases. J Clin Med. 2020;9(4).

95. Chimenti C, Hamdani N, Boontje NM, DeCobelli F, Esposito A, Bronzwaer JG, et al. Myofilament degradation and dysfunction of human cardiomyocytes in Fabry disease. Am J Pathol. 2008;172(6):1482-90.

96. Barbey F, Brakch N, Linhart A, Rosenblatt-Velin N, Jeanrenaud X, Qanadli S, et al. Cardiac and vascular hypertrophy in Fabry disease: evidence for a new mechanism independent of blood pressure and glycosphingolipid deposition. Arterioscler Thromb Vasc Biol. 2006;26(4):839-44.

97. Birket MJ, Raibaud S, Lettieri M, Adamson AD, Letang V, Cervello P, et al. A Human Stem Cell Model of Fabry Disease Implicates LIMP-2 Accumulation in Cardiomyocyte Pathology. Stem Cell Reports. 2019;13(2):380-93.

98. Choi L, Vernon J, Kopach O, Minett MS, Mills K, Clayton PT, et al. The Fabry disease-associated lipid Lyso-Gb3 enhances voltage-gated calcium currents in sensory neurons and causes pain. Neurosci Lett. 2015;594:163-8.

99. Choi S, Kim JA, Na HY, Cho SE, Park S, Jung SC, et al. Globotriaosylceramide induces lysosomal degradation of endothelial KCa3.1 in fabry disease. Arterioscler Thromb Vasc Biol. 2014;34(1):81-9.

100. Cumberland MJ, Riebel LL, Roy A, O'Shea C, Holmes AP, Denning C, et al. Basic Research Approaches to Evaluate Cardiac Arrhythmia in Heart Failure and Beyond. Front Physiol. 2022;13:806366.

101. Moon JC, Sachdev B, Elkington AG, McKenna WJ, Mehta A, Pennell DJ, et al. Gadolinium enhanced cardiovascular magnetic resonance in Anderson-Fabry disease. Evidence for a disease specific abnormality of the myocardial interstitium. Eur Heart J. 2003;24(23):2151-5.

102. Seydelmann N, Liu D, Krämer J, Drechsler C, Hu K, Nordbeck P, et al. High-Sensitivity Troponin: A Clinical Blood Biomarker for Staging Cardiomyopathy in Fabry Disease. J Am Heart Assoc. 2016;5(6).

103. Zarate YA, Hopkin RJ. Fabry's disease. Lancet. 2008;372(9647):1427-35.

104. Vitner EB, Platt FM, Futerman AH. Common and uncommon pathogenic cascades in lysosomal storage diseases. J Biol Chem. 2010;285(27):20423-7.

105. Rigante D, Cipolla C, Basile U, Gulli F, Savastano MC. Overview of immune abnormalities in lysosomal storage disorders. Immunol Lett. 2017;188:79-85.

106. Schmid D, Dengjel J, Schoor O, Stevanovic S, Münz C. Autophagy in innate and adaptive immunity against intracellular pathogens. J Mol Med (Berl). 2006;84(3):194-202.

107. Hsing LC, Rudensky AY. The lysosomal cysteine proteases in MHC class II antigen presentation. Immunol Rev. 2005;207:229-41.

108. De Francesco PN, Mucci JM, Ceci R, Fossati CA, Rozenfeld PA. Fabry disease peripheral blood immune cells release inflammatory cytokines: role of globotriaosylceramide. Mol Genet Metab. 2013;109(1):93-9.

109. Rigoldi M, Concolino D, Morrone A, Pieruzzi F, Ravaglia R, Furlan F, et al. Intrafamilial phenotypic variability in four families with Anderson-Fabry disease. Clin Genet. 2014;86(3):258-63.

110. Frustaci A, Verardo R, Grande C, Galea N, Piselli P, Carbone I, et al. Immune-Mediated Myocarditis in Fabry Disease Cardiomyopathy. J Am Heart Assoc. 2018;7(17):e009052.

111. Nordin S, Kozor R, Bulluck H, Castelletti S, Rosmini S, Abdel-Gadir A, et al. Cardiac Fabry Disease With Late Gadolinium Enhancement Is a Chronic Inflammatory Cardiomyopathy. J Am Coll Cardiol. 2016;68(15):1707-8.

112. Nappi C, Altiero M, Imbriaco M, Nicolai E, Giudice CA, Aiello M, et al. First experience of simultaneous PET/MRI for the early detection of cardiac involvement in patients with Anderson-Fabry disease. Eur J Nucl Med Mol Imaging. 2015;42(7):1025-31.

113. Germain DP, Charrow J, Desnick RJ, Guffon N, Kempf J, Lachmann RH, et al. Ten-year outcome of enzyme replacement therapy with agalsidase beta in patients with Fabry disease. J Med Genet. 2015;52(5):353-8.

114. Silva CAB, Moura-Neto JA, Dos Reis MA, Vieira Neto OM, Barreto FC. Renal Manifestations of Fabry Disease: A Narrative Review. Can J Kidney Health Dis. 2021;8:2054358120985627.

115. Mc Causland FR, Tumlin JA, Roy-Chaudhury P, Koplan BA, Costea AI, Kher V, et al. Intradialytic Hypotension and Cardiac Arrhythmias in Patients Undergoing

Maintenance Hemodialysis: Results from the Monitoring in Dialysis Study. Clin J Am Soc Nephrol. 2020;15(6):805-12.

116. O'Mahony C, Jichi F, Pavlou M, Monserrat L, Anastasakis A, Rapezzi C, et al. A novel clinical risk prediction model for sudden cardiac death in hypertrophic cardiomyopathy (HCM risk-SCD). Eur Heart J. 2014;35(30):2010-20.

117. Boyd AC, Lo Q, Devine K, Tchan MC, Sillence DO, Sadick N, et al. Left atrial enlargement and reduced atrial compliance occurs early in Fabry cardiomyopathy. J Am Soc Echocardiogr. 2013;26(12):1415-23.

118. Hasselberg NE, Edvardsen T, Petri H, Berge KE, Leren TP, Bundgaard H, et al. Risk prediction of ventricular arrhythmias and myocardial function in Lamin A/C mutation positive subjects. Europace. 2014;16(4):563-71.

119. Okada DR, Smith J, Derakhshan A, Gowani Z, Misra S, Berger RD, et al. Ventricular Arrhythmias in Cardiac Sarcoidosis. Circulation. 2018;138(12):1253-64.

120. Laptseva N, Rossi VA, Sudano I, Schwotzer R, Ruschitzka F, Flammer AJ, et al. Arrhythmic Manifestations of Cardiac Amyloidosis: Challenges in Risk Stratification and Clinical Management. J Clin Med. 2023;12(7).

121. Sammani A, Kayvanpour E, Bosman LP, Sedaghat-Hamedani F, Proctor T, Gi WT, et al. Predicting sustained ventricular arrhythmias in dilated cardiomyopathy: a meta-analysis and systematic review. ESC Heart Fail. 2020;7(4):1430-41.

122. Vijapurapu R, Kozor R, Hughes DA, Woolfson P, Jovanovic A, Deegan P, et al. A randomised controlled trial evaluating arrhythmia burden, risk of sudden cardiac death and stroke in patients with Fabry disease: the role of implantable loop recorders (RaILRoAD) compared with current standard practice. Trials. 2019;20(1):314.

123. Baig S, Vijapurapu R, Alharbi F, Nordin S, Kozor R, Moon J, et al. Diagnosis and treatment of the cardiovascular consequences of Fabry disease. QJM. 2019;112(1):3-9.

124. Krämer J, Bijnens B, Störk S, Ritter CO, Liu D, Ertl G, et al. Left Ventricular Geometry and Blood Pressure as Predictors of Adverse Progression of Fabry Cardiomyopathy. PLoS One. 2015;10(11):e0140627.

125. Ammirati E, Contri R, Coppini R, Cecchi F, Frigerio M, Olivotto I. Pharmacological treatment of hypertrophic cardiomyopathy: current practice and novel perspectives. Eur J Heart Fail. 2016;18(9):1106-18.

126. Kirchhof P, Camm AJ, Goette A, Brandes A, Eckardt L, Elvan A, et al. Early Rhythm-Control Therapy in Patients with Atrial Fibrillation. N Engl J Med. 2020;383(14):1305-16.

127. Reasor MJ, Kacew S. Drug-induced phospholipidosis: are there functional consequences? Exp Biol Med (Maywood). 2001;226(9):825-30.

128. Fine NM, Wang Y, Khan A. Acute Decompensated Heart Failure After Initiation of Amiodarone in a Patient With Anderson-Fabry Disease. Can J Cardiol. 2019;35(1):104.e5-.e7.

129. Lip GY, Nieuwlaat R, Pisters R, Lane DA, Crijns HJ. Refining clinical risk stratification for predicting stroke and thromboembolism in atrial fibrillation using a novel risk factor-based approach: the euro heart survey on atrial fibrillation. Chest. 2010;137(2):263-72.

130. Reisin RC, Romero C, Marchesoni C, Nápoli G, Kisinovsky I, Cáceres G, et al. Brain MRI findings in patients with Fabry disease. J Neurol Sci. 2011;305(1-2):41-4.

131. Weidemann F, Niemann M, Breunig F, Herrmann S, Beer M, Störk S, et al. Long-term effects of enzyme replacement therapy on fabry cardiomyopathy: evidence for a better outcome with early treatment. Circulation. 2009;119(4):524-9.

132. Benjamin ER, Della Valle MC, Wu X, Katz E, Pruthi F, Bond S, et al. The validation of pharmacogenetics for the identification of Fabry patients to be treated with migalastat. Genet Med. 2017;19(4):430-8.

133. Hughes DA, Nicholls K, Shankar SP, Sunder-Plassmann G, Koeller D, Nedd K, et al. Oral pharmacological chaperone migalastat compared with enzyme replacement therapy in Fabry disease: 18-month results from the randomised phase III ATTRACT study. J Med Genet. 2017;54(4):288-96.

134. Lenders M, Nordbeck P, Kurschat C, Karabul N, Kaufeld J, Hennermann JB, et al. Treatment of Fabry's Disease With Migalastat: Outcome From a Prospective Observational Multicenter Study (FAMOUS). Clin Pharmacol Ther. 2020;108(2):326-37.

135. Gatterer C, Beitzke D, Graf S, Lenz M, Sunder-Plassmann G, Mann C, et al. Long-Term Monitoring of Cardiac Involvement under Migalastat Treatment Using Magnetic Resonance Tomography in Fabry Disease. Life (Basel). 2023;13(5).

136. Kyem G, Okorozo A, Hamdan H, Tuffaha AM. A Case Report of Kidney After Heart Transplant in Patient With Fabry Disease. Transplant Proc. 2023;55(8):1975-7.

137. Kotecha D, Piccini JP. Atrial fibrillation in heart failure: what should we do? Eur Heart J. 2015;36(46):3250-7.

138. Namdar M, Kampmann C, Steffel J, Walder D, Holzmeister J, Lüscher TF, et al. PQ interval in patients with Fabry disease. Am J Cardiol. 2010;105(5):753-6.

139. Sommerfeld LC, Holmes AP, Yu TY, O'Shea C, Kavanagh DM, Pike JM, et al. Reduced plakoglobin increases the risk of sodium current defects and atrial

conduction abnormalities in response to androgenic anabolic steroid abuse. J Physiol. 2024.

140. Robinson S, Rana B, Oxborough D, Steeds R, Monaghan M, Stout M, et al. A practical guideline for performing a comprehensive transthoracic echocardiogram in adults: the British Society of Echocardiography minimum dataset. Echo Res Pract. 2020;7(4):G59-G93.

141. Gilchrist M, Casanova F, Tyrrell JS, Cannon S, Wood AR, Fife N, et al. Prevalence of Fabry disease-causing variants in the UK Biobank. J Med Genet. 2023;60(4):391-6.

142. Cumberland MJ, Euchner J, Azad AJ, T N Vo N, Kirchhof P, Holmes AP, et al. Generation of a human iPSC-derived cardiomyocyte/fibroblast engineered heart tissue model. F1000Res. 2023;12:1224.

143. Gehmlich K, Dodd MS, Allwood JW, Kelly M, Bellahcene M, Lad HV, et al. Changes in the cardiac metabolome caused by perhexiline treatment in a mouse model of hypertrophic cardiomyopathy. Mol Biosyst. 2015;11(2):564-73.

144. Workman AJ, Kane KA, Rankin AC. The contribution of ionic currents to changes in refractoriness of human atrial myocytes associated with chronic atrial fibrillation. Cardiovasc Res. 2001;52(2):226-35.

145. Holmes AP, Saxena P, Kabir SN, O'Shea C, Kuhlmann SM, Gupta S, et al. Atrial resting membrane potential confers sodium current sensitivity to propafenone, flecainide and dronedarone. Heart Rhythm. 2021;18(7):1212-20.

146. Sala L, van Meer BJ, Tertoolen LGJ, Bakkers J, Bellin M, Davis RP, et al. MUSCLEMOTION: A Versatile Open Software Tool to Quantify Cardiomyocyte and Cardiac Muscle Contraction In Vitro and In Vivo. Circ Res. 2018;122(3):e5-e16.

147. O'Shea C, Holmes AP, Yu TY, Winter J, Wells SP, Correia J, et al. ElectroMap: High-throughput open-source software for analysis and mapping of cardiac electrophysiology. Sci Rep. 2019;9(1):1389.

148. Ali ZS, Bhuiyan A, Vyas P, Miranda-Arboleda AF, Tse G, Bazoukis G, et al. PR prolongation as a predictor of atrial fibrillation onset: A state-of-the-art review. Curr Probl Cardiol. 2024;49(4):102469.

149. Parham WA, Mehdirad AA, Biermann KM, Fredman CS. Hyperkalemia revisited. Tex Heart Inst J. 2006;33(1):40-7.

150. Berecki G, Wilders R, de Jonge B, van Ginneken AC, Verkerk AO. Re-evaluation of the action potential upstroke velocity as a measure of the Na+ current in cardiac myocytes at physiological conditions. PLoS One. 2010;5(12):e15772.

151. Fan JL, Su B, Zhao X, Zhou BY, Ma CS, Wang HP, et al. Correlation of left atrial strain with left ventricular end-diastolic pressure in patients with normal left ventricular ejection fraction. Int J Cardiovasc Imaging. 2020;36(9):1659-66.

152. Biegstraaten M, van Schaik IN, Wieling W, Wijburg FA, Hollak CE. Autonomic neuropathy in Fabry disease: a prospective study using the Autonomic Symptom Profile and cardiovascular autonomic function tests. BMC Neurol. 2010;10:38.

153. Landstrom AP, Dobrev D, Wehrens XHT. Calcium Signaling and Cardiac Arrhythmias. Circ Res. 2017;120(12):1969-93.

154. Baines O, Sha R, Kalla M, Holmes AP, Efimov IR, Pavlovic D, et al. Optical mapping and optogenetics in cardiac electrophysiology research and therapy: a state-of-the-art review. Europace. 2024;26(2).

155. Mechmann S, Pott L. Identification of Na-Ca exchange current in single cardiac myocytes. Nature. 1986;319(6054):597-9.

156. Asakura K, Cha CY, Yamaoka H, Horikawa Y, Memida H, Powell T, et al. EAD and DAD mechanisms analyzed by developing a new human ventricular cell model. Prog Biophys Mol Biol. 2014;116(1):11-24.

157. Kistamás K, Veress R, Horváth B, Bányász T, Nánási PP, Eisner DA. Calcium Handling Defects and Cardiac Arrhythmia Syndromes. Front Pharmacol. 2020;11:72.

158. Krämer J, Niemann M, Liu D, Hu K, Machann W, Beer M, et al. Two-dimensional speckle tracking as a non-invasive tool for identification of myocardial fibrosis in Fabry disease. Eur Heart J. 2013;34(21):1587-96.

159. Roy A, Mansour M, Oxborough D, Geberhiwot T, Steeds R. Multi-Modality Cardiovascular Imaging Assessment in Fabry Disease. *Appl Sci* 2022;12(3):1605.

160. Morris DA, Blaschke D, Canaan-Kühl S, Krebs A, Knobloch G, Walter TC, et al. Global cardiac alterations detected by speckle-tracking echocardiography in Fabry disease: left ventricular, right ventricular, and left atrial dysfunction are common and linked to worse symptomatic status. Int J Cardiovasc Imaging. 2015;31(2):301-13.

161. Feustel A, Hahn A, Schneider C, Sieweke N, Franzen W, Gündüz D, et al. Continuous cardiac troponin I release in Fabry disease. PLoS One. 2014;9(3):e91757.

162. Torralba-Cabeza M, Olivera S, Hughes DA, Pastores GM, Mateo RN, Pérez-Calvo JI. Cystatin C and NT-proBNP as prognostic biomarkers in Fabry disease. Mol Genet Metab. 2011;104(3):301-7.

163. Wharton G, Steeds R, Allen J, Phillips H, Jones R, Kanagala P, et al. A minimum dataset for a standard adult transthoracic echocardiogram: a guideline protocol from the British Society of Echocardiography. Echo Res Pract. 2015;2(1):G9-G24.

164. Nagueh SF, Smiseth OA, Appleton CP, Byrd BF, Dokainish H, Edvardsen T, et al. Recommendations for the Evaluation of Left Ventricular Diastolic Function by

Echocardiography: An Update from the American Society of Echocardiography and the European Association of Cardiovascular Imaging. Eur Heart J Cardiovasc Imaging. 2016;17(12):1321-60.

165. Devereux RB, Reichek N. Echocardiographic determination of left ventricular mass in man. Anatomic validation of the method. Circulation. 1977;55(4):613-8.

166. Levin A, Stevens PE, Bilous RW, Coresh J, De Francisco ALM, De Jong PE. Kidney disease: Improving global outcomes (KDIGO) CKD work group. KDIGO 2012 clinical practice guideline for the evaluation and management of chronic kidney disease . Kidney Int Suppl. 2013;3(1):1-150.

167. Koo TK, Li MY. A Guideline of Selecting and Reporting Intraclass Correlation Coefficients for Reliability Research. J Chiropr Med. 2016;15(2):155-63.

168. Germain DP, Elliott PM, Falissard B, Fomin VV, Hilz MJ, Jovanovic A, et al. The effect of enzyme replacement therapy on clinical outcomes in male patients with Fabry disease: A systematic literature review by a European panel of experts. Mol Genet Metab Rep. 2019;19:100454.

169. Frustaci A, Verardo R, Scialla R, Bagnato G, Verardo M, Alfarano M, et al. Downregulation of Mannose-6-Phosphate Receptors in Fabry Disease Cardiomyopathy: A Potential Target for Enzyme Therapy Enhancement. J Clin Med. 2022;11(18).

170. Bergmann O, Bhardwaj RD, Bernard S, Zdunek S, Barnabé-Heider F, Walsh S, et al. Evidence for cardiomyocyte renewal in humans. Science. 2009;324(5923):98-102.

171. Frustaci A, Verardo R, Galea N, Alfarano M, Magnocavallo M, Marchitelli L, et al. Long-Term Clinical-Pathologic Results of Enzyme Replacement Therapy in

Prehypertrophic Fabry Disease Cardiomyopathy. J Am Heart Assoc. 2024;13(8):e032734.

172. El Dib R, Gomaa H, Carvalho RP, Camargo SE, Bazan R, Barretti P, et al. Enzyme replacement therapy for Anderson-Fabry disease. Cochrane Database Syst Rev. 2016;7(7):CD006663.

173. Orsborne C, Black N, Naish JH, Woolfson P, Reid AB, Schmitt M, et al. Disease-specific therapy for the treatment of the cardiovascular manifestations of Fabry disease: a systematic review. Heart. 2023;110(1):19-26.

174. Umer M, Kalra DK. Treatment of Fabry Disease: Established and Emerging Therapies. Pharmaceuticals (Basel). 2023;16(2).

175. Nordin S, Kozor R, Medina-Menacho K, Abdel-Gadir A, Baig S, Sado DM, et al. Proposed Stages of Myocardial Phenotype Development in Fabry Disease. JACC Cardiovasc Imaging. 2019;12(8 Pt 2):1673-83.

176. Graziani F, Laurito M, Pieroni M, Pennestrì F, Lanza GA, Coluccia V, et al. Right Ventricular Hypertrophy, Systolic Function, and Disease Severity in Anderson-Fabry Disease: An Echocardiographic Study. J Am Soc Echocardiogr. 2017;30(3):282-91.

177. Niemann M, Breunig F, Beer M, Herrmann S, Strotmann J, Hu K, et al. The right ventricle in Fabry disease: natural history and impact of enzyme replacement therapy. Heart. 2010;96(23):1915-9.

178. Huntjens PR, Zhang KW, Soyama Y, Karmpalioti M, Lenihan DJ, Gorcsan J. Prognostic Utility of Echocardiographic Atrial and Ventricular Strain Imaging in Patients With Cardiac Amyloidosis. JACC Cardiovasc Imaging. 2021;14(8):1508-19.

179. Hiemstra YL, Debonnaire P, Bootsma M, Schalij MJ, Bax JJ, Delgado V, et al. Prevalence and Prognostic Implications of Right Ventricular Dysfunction in Patients With Hypertrophic Cardiomyopathy. Am J Cardiol. 2019;124(4):604-12.

180. Meucci MC, Lillo R, Mango F, Lombardo A, Lanza GA, Parisi V, et al. Right ventricular strain in Fabry disease: Prognostic implications. Int J Cardiol. 2023;374:79-82.

181. Shi Q, Chen J, Pongmoragot J, Lanthier S, Saposnik G. Prevalence of Fabry disease in stroke patients--a systematic review and meta-analysis. J Stroke Cerebrovasc Dis. 2014;23(5):985-92.

182. Mehta A, Ricci R, Widmer U, Dehout F, Garcia de Lorenzo A, Kampmann C, et al. Fabry disease defined: baseline clinical manifestations of 366 patients in the Fabry Outcome Survey. Eur J Clin Invest. 2004;34(3):236-42.

183. Politei J, Schenone B, Andrea, Burlino A, Blanco M, Lescano S, Szlago M, et al. Vertebrobasilar Dolichoectasia in Fabry Disease: The Earliest Marker of Neurological Involvement? 2014.

184. Hauser R, Nielsen AB, Skaarup KG, Lassen MCH, Duus LS, Johansen ND, et al. Left atrial strain predicts incident atrial fibrillation in the general population: the Copenhagen City Heart Study. Eur Heart J Cardiovasc Imaging. 2021;23(1):52-60.

185. Halfmann MC, Altmann S, Schoepf UJ, Reichardt C, Hennermann JB, Kreitner KF, et al. Left atrial strain correlates with severity of cardiac involvement in Anderson-Fabry disease. Eur Radiol. 2023;33(3):2039-51.

186. Sheppard MN, Cane P, Florio R, Kavantzas N, Close L, Shah J, et al. A detailed pathologic examination of heart tissue from three older patients with Anderson-Fabry disease on enzyme replacement therapy. Cardiovasc Pathol. 2010;19(5):293-301.

187. Mueller C, McDonald K, de Boer RA, Maisel A, Cleland JGF, Kozhuharov N, et al. Heart Failure Association of the European Society of Cardiology practical guidance on the use of natriuretic peptide concentrations. Eur J Heart Fail. 2019;21(6):715-31.

188. Kawasaki T, Sakai C, Harimoto K, Yamano M, Miki S, Kamitani T. Usefulness of high-sensitivity cardiac troponin T and brain natriuretic peptide as biomarkers of myocardial fibrosis in patients with hypertrophic cardiomyopathy. Am J Cardiol. 2013;112(6):867-72.

189. Coats CJ, Parisi V, Ramos M, Janagarajan K, O'Mahony C, Dawnay A, et al. Role of serum N-terminal pro-brain natriuretic peptide measurement in diagnosis of cardiac involvement in patients with anderson-fabry disease. Am J Cardiol. 2013;111(1):111-7.

190. Heeg JE, de Jong PE, van der Hem GK, de Zeeuw D. Reduction of proteinuria by angiotensin converting enzyme inhibition. Kidney Int. 1987;32(1):78-83.

191. Faro DC, Losi V, Rodolico MS, Torrisi EM, Colomba P, Duro G, et al. Sex Differences in Anderson-Fabry Cardiomyopathy: Clinical, Genetic, and Imaging Analysis in Women. Genes (Basel). 2023;14(9).

192. Spinelli L, Nicolai E, Acampa W, Imbriaco M, Pisani A, Rao MA, et al. Cardiac performance during exercise in patients with Fabry's disease. Eur J Clin Invest. 2008;38(12):910-7.

193. Pietilä-Effati P, Söderström J, Saarinen JT, Löyttyniemi E, Kantola I. Pulmonary manifestations and the effectiveness of enzyme replacement therapy in Fabry Disease with the p. Arg227Ter (p.R227*) mutation. Mol Genet Genomic Med. 2022;10(5):e1915.

194. Gambardella J, Fiordelisi A, Cerasuolo FA, Buonaiuto A, Avvisato R, Viti A, et al. Experimental evidence and clinical implications of Warburg effect in the skeletal muscle of Fabry disease. iScience. 2023;26(3):106074.

195. Bayonas-Ruiz A, Muñoz-Franco FM, Ferrer V, Pérez-Caballero C, Sabater-Molina M, Tomé-Esteban MT, et al. Cardiopulmonary Exercise Test in Patients with Hypertrophic Cardiomyopathy: A Systematic Review and Meta-Analysis. J Clin Med. 2021;10(11).

196. Olivotto I, Oreziak A, Barriales-Villa R, Abraham TP, Masri A, Garcia-Pavia P, et al. Mavacamten for treatment of symptomatic obstructive hypertrophic cardiomyopathy (EXPLORER-HCM): a randomised, double-blind, placebo-controlled, phase 3 trial. Lancet. 2020;396(10253):759-69.

197. Luu JM, Gebhard C, Ramasundarahettige C, Desai D, Schulze K, Marcotte F, et al. Normal sex and age-specific parameters in a multi-ethnic population: a cardiovascular magnetic resonance study of the Canadian Alliance for Healthy Hearts and Minds cohort. J Cardiovasc Magn Reson. 2022;24(1):2.

198. Maceira AM, Prasad SK, Khan M, Pennell DJ. Normalized left ventricular systolic and diastolic function by steady state free precession cardiovascular magnetic resonance. J Cardiovasc Magn Reson. 2006;8(3):417-26.

199. Vijapurapu R, Hawkinds F, Liu B, Edwards N, Steeds R. A study of the different methodologies used in calculation of extra-cellular volume by CMR imaging. Heart. 2018;104:A14-A5.

200. Magrì D, Limongelli G, Re F, Agostoni P, Zachara E, Correale M, et al. Cardiopulmonary exercise test and sudden cardiac death risk in hypertrophic cardiomyopathy. Heart. 2016;102(8):602-9.

201. Coats CJ, Rantell K, Bartnik A, Patel A, Mist B, McKenna WJ, et al. Cardiopulmonary Exercise Testing and Prognosis in Hypertrophic Cardiomyopathy. Circ Heart Fail. 2015;8(6):1022-31.

202. Powell AW, Jefferies JL, Hopkin RJ, Mays WA, Goa Z, Chin C. Cardiopulmonary fitness assessment on maximal and submaximal exercise testing in patients with Fabry disease. Am J Med Genet A. 2018;176(9):1852-7.

203. Graves RS, Mahnken JD, Perea RD, Billinger SA, Vidoni ED. Modeling Percentile Rank of Cardiorespiratory Fitness Across the Lifespan. Cardiopulm Phys Ther J. 2015;26(4):108-13.

204. American college of Sports Medicine. ACSM's Guidelines for Excercise Testing and Prescription. 9th ed. Baltimore, Maryland, USA: Lippincott Williams & Wilkins; 2014.

205. Bowerman C, Bhakta NR, Brazzale D, Cooper BR, Cooper J, Gochicoa-Rangel L, et al. A Race-neutral Approach to the Interpretation of Lung Function Measurements. Am J Respir Crit Care Med. 2023;207(6):768-74.

206. Laboratories ACoPSfCPF. ATS statement: guidelines for the six-minute walk test. Am J Respir Crit Care Med. 2002;166(1):111-7.

207. Bierer G, Balfe D, Wilcox WR, Mosenifar Z. Improvement in serial cardiopulmonary exercise testing following enzyme replacement therapy in Fabry disease. J Inherit Metab Dis. 2006;29(4):572-9.

208. Tuan SH, Chiu PC, Liou IH, Lu WH, Huang HY, Wu SY, et al. Serial Analysis of Cardiopulmonary Fitness and Echocardiography in Patients with Fabry Disease Undergoing Enzyme Replacement Therapy. J Rehabil Med Clin Commun. 2020;3:1000028.

209. Svensson CK, Feldt-Rasmussen U, Backer V. Fabry disease, respiratory symptoms, and airway limitation - a systematic review. Eur Clin Respir J. 2015;2.

210. Morrissey RP, Philip KJ, Schwarz ER. Cardiac abnormalities in Anderson-Fabry disease and Fabry's cardiomyopathy. Cardiovasc J Afr. 2011;22(1):38-44.

211. Vijapurapu R, Nordin S, Baig S, Liu B, Rosmini S, Augusto J, et al. Global longitudinal strain, myocardial storage and hypertrophy in Fabry disease. Heart. 2019;105(6):470-6.

212. Schiffmann R, Warnock DG, Banikazemi M, Bultas J, Linthorst GE, Packman S, et al. Fabry disease: progression of nephropathy, and prevalence of cardiac and cerebrovascular events before enzyme replacement therapy. Nephrol Dial Transplant. 2009;24(7):2102-11.

213. Webb KL, Gorman EK, Morkeberg OH, Klassen SA, Regimbal RJ, Wiggins CC, et al. The relationship between hemoglobin and [Formula: see text]: A systematic review and meta-analysis. PLoS One. 2023;18(10):e0292835.

214. Viggiano E, Politano L. X Chromosome Inactivation in Carriers of Fabry Disease: Review and Meta-Analysis. Int J Mol Sci. 2021;22(14).

215. Knott KD, Seraphim A, Augusto JB, Xue H, Chacko L, Aung N, et al. The Prognostic Significance of Quantitative Myocardial Perfusion: An Artificial Intelligence-Based Approach Using Perfusion Mapping. Circulation. 2020;141(16):1282-91.

216. Sayegh ALC, Dos Santos MR, Sarmento AO, de Souza FR, Salemi VMC, Hotta VT, et al. Cardiac and peripheral autonomic control in restrictive cardiomyopathy. ESC Heart Fail. 2017;4(3):341-50.

217. Frustaci A, Chimenti C. Images in cardiovascular medicine. Cryptogenic ventricular arrhythmias and sudden death by Fabry disease: prominent infiltration of cardiac conduction tissue. Circulation. 2007;116(12):e350-1.

218. Igawa O, Miake J, Hisatome I. Ventricular tachycardias and dilated cardiomyopathy caused by Fabry disease. Pacing Clin Electrophysiol. 2005;28(10):1142-3.

219. Kleinert J, Dehout F, Schwarting A, de Lorenzo AG, Ricci R, Kampmann C, et al. Prevalence of uncontrolled hypertension in patients with Fabry disease. Am J Hypertens. 2006;19(8):782-7.

220. Patel MR, Cecchi F, Cizmarik M, Kantola I, Linhart A, Nicholls K, et al. Cardiovascular events in patients with fabry disease natural history data from the fabry registry. J Am Coll Cardiol. 2011;57(9):1093-9.

221. Jaurretche S, Antogiovanni N, Perretta F. Prevalence of chronic kidney disease in fabry disease patients: Multicenter cross sectional study in Argentina. Mol Genet Metab Rep. 2017;12:41-3.

222. Kurdi H, Lavalle L, Moon JCC, Hughes D. Inflammation in Fabry disease: stages, molecular pathways, and therapeutic implications. Front Cardiovasc Med. 2024;11:1420067.

223. Kristensen SL, Lindhardsen J, Ahlehoff O, Erichsen R, Lamberts M, Khalid U, et al. Increased risk of atrial fibrillation and stroke during active stages of inflammatory bowel disease: a nationwide study. Europace. 2014;16(4):477-84.

224. Walkey AJ, Greiner MA, Heckbert SR, Jensen PN, Piccini JP, Sinner MF, et al. Atrial fibrillation among Medicare beneficiaries hospitalized with sepsis: incidence and risk factors. Am Heart J. 2013;165(6):949-55.e3.

225. Adegbala O, Olagoke O, Akintoye E, Adejumo AC, Oluwole A, Jara C, et al. Predictors, Burden, and the Impact of Arrhythmia on Patients Admitted for Acute Myocarditis. Am J Cardiol. 2019;123(1):139-44.

226. Hancock EW, Deal BJ, Mirvis DM, Okin P, Kligfield P, Gettes LS, et al. AHA/ACCF/HRS recommendations for the standardization and interpretation of the electrocardiogram: part V: electrocardiogram changes associated with cardiac chamber hypertrophy: a scientific statement from the American Heart Association Electrocardiography and Arrhythmias Committee, Council on Clinical Cardiology; the American College of Cardiology Foundation; and the Heart Rhythm Society. Endorsed by the International Society for Computerized Electrocardiology. J Am Coll Cardiol. 2009;53(11):992-1002.

227. Harkness A, Ring L, Augustine DX, Oxborough D, Robinson S, Sharma V. Normal reference intervals for cardiac dimensions and function for use in echocardiographic practice: a guideline from the British Society of Echocardiography. Echo Res Pract. 2020;7(1):X1.

228. Herrington W, Lacey B, Sherliker P, Armitage J, Lewington S. Epidemiology of Atherosclerosis and the Potential to Reduce the Global Burden of Atherothrombotic Disease. Circ Res. 2016;118(4):535-46.

229. Head T, Daunert S, Goldschmidt-Clermont PJ. The Aging Risk and Atherosclerosis: A Fresh Look at Arterial Homeostasis. Front Genet. 2017;8:216.

230. Case records of the Massachusetts General Hospital. Weekly clinicopathological exercises. Case 2-1984. A 47-year-old man with coronary-artery disease and variable neurologic abnormalities. N Engl J Med. 1984;310(2):106-14.

231. Simoncini C, Torri S, Montano V, Chico L, Gruosso F, Tuttolomondo A, et al. Oxidative stress biomarkers in Fabry disease: is there a room for them? J Neurol. 2020;267(12):3741-52.

232. Laurindo FR, Pedro MeA, Barbeiro HV, Pileggi F, Carvalho MH, Augusto O, et al. Vascular free radical release. Ex vivo and in vivo evidence for a flow-dependent endothelial mechanism. Circ Res. 1994;74(4):700-9.

233. Kaneski CR, Moore DF, Ries M, Zirzow GC, Schiffmann R. Myeloperoxidase predicts risk of vasculopathic events in hemizgygous males with Fabry disease. Neurology. 2006;67(11):2045-7.

234. Senders ML, Mulder WJM. Targeting myeloperoxidase in inflammatory atherosclerosis. Eur Heart J. 2018;39(35):3311-3.

235. Bodary PF, Shen Y, Vargas FB, Bi X, Ostenso KA, Gu S, et al. Alpha-galactosidase A deficiency accelerates atherosclerosis in mice with apolipoprotein E deficiency. Circulation. 2005;111(5):629-32.

236. Cartwright DJ, Cole AL, Cousins AJ, Lee PJ. Raised HDL cholesterol in Fabry disease: response to enzyme replacement therapy. J Inherit Metab Dis. 2004;27(6):791-3.

237. Stepien KM, Hendriksz CJ. Lipid profile in adult patients with Fabry disease - Ten-year follow up. Mol Genet Metab Rep. 2017;13:3-6.

238. Sacks FM, Cholesterol EGoH. The role of high-density lipoprotein (HDL) cholesterol in the prevention and treatment of coronary heart disease: expert group recommendations. Am J Cardiol. 2002;90(2):139-43.

239. Tsai WC, Li YH, Huang YY, Lin CC, Chao TH, Chen JH. Plasma vascular endothelial growth factor as a marker for early vascular damage in hypertension. Clin Sci (Lond). 2005;109(1):39-43.

240. Kitagawa K, Matsumoto M, Sasaki T, Hashimoto H, Kuwabara K, Ohtsuki T, et al. Involvement of ICAM-1 in the progression of atherosclerosis in APOE-knockout mice. Atherosclerosis. 2002;160(2):305-10.

241. Katsuta H, Tsuboi K, Yamamoto H, Goto H. Correlations Between Serum Cholesterol and Vascular Lesions in Fabry Disease Patients. Circ J. 2018;82(12):3058-63.

242. Wattanakit K, Cushman M, Stehman-Breen C, Heckbert SR, Folsom AR. Chronic kidney disease increases risk for venous thromboembolism. J Am Soc Nephrol. 2008;19(1):135-40.

243. Chimenti C, Morgante E, Tanzilli G, Mangieri E, Critelli G, Gaudio C, et al. Angina in fabry disease reflects coronary small vessel disease. Circ Heart Fail. 2008;1(3):161-9.

244. Beltrame JF, Limaye SB, Horowitz JD. The coronary slow flow phenomenon--a new coronary microvascular disorder. Cardiology. 2002;97(4):197-202.

245. Elliott PM, Kindler H, Shah JS, Sachdev B, Rimoldi OE, Thaman R, et al. Coronary microvascular dysfunction in male patients with Anderson-Fabry disease and the effect of treatment with alpha galactosidase A. Heart. 2006;92(3):357-60.

246. Castaneda JA, Lim MJ, Cooper JD, Pearce DA. Immune system irregularities in lysosomal storage disorders. Acta Neuropathol. 2008;115(2):159-74.

247. Rozenfeld P, Feriozzi S. Contribution of inflammatory pathways to Fabry disease pathogenesis. Mol Genet Metab. 2017;122(3):19-27.

248. Mauhin W, Lidove O, Masat E, Mingozzi F, Mariampillai K, Ziza JM, et al. Innate and Adaptive Immune Response in Fabry Disease. JIMD Rep. 2015;22:1-10.

249. Chen KH, Chien Y, Wang KL, Leu HB, Hsiao CY, Lai YH, et al. Evaluation of Proinflammatory Prognostic Biomarkers for Fabry Cardiomyopathy With Enzyme Replacement Therapy. Can J Cardiol. 2016;32(10):1221.e1-.e9.

250. Horiuchi T, Mitoma H, Harashima S, Tsukamoto H, Shimoda T. Transmembrane TNF-alpha: structure, function and interaction with anti-TNF agents. Rheumatology (Oxford). 2010;49(7):1215-28.

251. Brenner D, Blaser H, Mak TW. Regulation of tumour necrosis factor signalling: live or let die. Nat Rev Immunol. 2015;15(6):362-74.

252. Jang DI, Lee AH, Shin HY, Song HR, Park JH, Kang TB, et al. The Role of Tumor Necrosis Factor Alpha (TNF-α) in Autoimmune Disease and Current TNF-α Inhibitors in Therapeutics. Int J Mol Sci. 2021;22(5).

253. Lenzini L, Iori E, Vettore M, Gugelmo G, Radu C, Padoan A, et al. Increased Soluble Interleukin 6 Receptors in Fabry Disease. J Clin Med. 2023;13(1).

254. Singh S, Anshita D, Ravichandiran V. MCP-1: Function, regulation, and involvement in disease. Int Immunopharmacol. 2021;101(Pt B):107598.

255. Alonso-Núñez A, Pérez-Márquez T, Alves-Villar M, Fernández-Pereira C, Fernández-Martín J, Rivera-Gallego A, et al. Inflammatory and Cardiovascular Biomarkers to Monitor Fabry Disease Progression. Int J Mol Sci. 2024;25(11).

256. Quackenbush EJ, Aguirre V, Wershil BK, Gutierrez-Ramos JC. Eotaxin influences the development of embryonic hematopoietic progenitors in the mouse. J Leukoc Biol. 1997;62(5):661-6.

257. Quackenbush EJ, Wershil BK, Aguirre V, Gutierrez-Ramos JC. Eotaxin modulates myelopoiesis and mast cell development from embryonic hematopoietic progenitors. Blood. 1998;92(6):1887-97.

258. Quackenbush EJ, Gutierrez-Ramos J-C. Mast Cells and Basophils - Modulation of Mast Cell Development from Embroyonic Haemapoetic Progenitors by Eotaxin: Elsevier Ltd.; 2000.

259. Conroy DM, Williams TJ. Eotaxin and the attraction of eosinophils to the asthmatic lung. Respir Res. 2001;2(3):150-6.

260. Bulati M, Buffa S, Martorana A, Candore G, Lio D, Caruso C, et al. Trafficking phenotype and production of granzyme B by double negative B cells (IgG(+)IgD(-)CD27(-)) in the elderly. Exp Gerontol. 2014;54:123-9.

261. Kim WJ, Kim H, Suk K, Lee WH. Macrophages express granzyme B in the lesion areas of atherosclerosis and rheumatoid arthritis. Immunol Lett. 2007;111(1):57-65.

262. Velotti F, Palmieri G, D'Ambrosio D, Piccoli M, Frati L, Santoni A. Differential expression of granzyme A and granzyme B proteases and their secretion by fresh rat natural killer cells (NK) and lymphokine-activated killer cells with NK phenotype (LAK-NK). Eur J Immunol. 1992;22(4):1049-53.

263. Chowdhury D, Lieberman J. Death by a thousand cuts: granzyme pathways of programmed cell death. Annu Rev Immunol. 2008;26:389-420.

264. Boivin WA, Cooper DM, Hiebert PR, Granville DJ. Intracellular versus extracellular granzyme B in immunity and disease: challenging the dogma. Lab Invest. 2009;89(11):1195-220.

265. Buzza MS, Zamurs L, Sun J, Bird CH, Smith AI, Trapani JA, et al. Extracellular matrix remodeling by human granzyme B via cleavage of vitronectin, fibronectin, and laminin. J Biol Chem. 2005;280(25):23549-58.

266. Velotti F, Barchetta I, Cimini FA, Cavallo MG. Granzyme B in Inflammatory Diseases: Apoptosis, Inflammation, Extracellular Matrix Remodeling, Epithelial-to-Mesenchymal Transition and Fibrosis. Front Immunol. 2020;11:587581.

267. Saraiva M, O'Garra A. The regulation of IL-10 production by immune cells. Nat Rev Immunol. 2010;10(3):170-81.

268. Carlini V, Noonan DM, Abdalalem E, Goletti D, Sansone C, Calabrone L, et al. The multifaceted nature of IL-10: regulation, role in immunological homeostasis and its relevance to cancer, COVID-19 and post-COVID conditions. Front Immunol. 2023;14:1161067.

269. Wilke CM, Wei S, Wang L, Kryczek I, Kao J, Zou W. Dual biological effects of the cytokines interleukin-10 and interferon-γ. Cancer Immunol Immunother. 2011;60(11):1529-41.

270. Wang S, Wang J, Ma R, Yang S, Fan T, Cao J, et al. IL-10 enhances T cell survival and is associated with faster relapse in patients with inactive ulcerative colitis. Mol Immunol. 2020;121:92-8.

271. Oft M. Immune regulation and cytotoxic T cell activation of IL-10 agonists - Preclinical and clinical experience. Semin Immunol. 2019;44:101325.

272. Wang Z, Guan D, Huo J, Biswas SK, Huang Y, Yang Y, et al. IL-10 Enhances Human Natural Killer Cell Effector Functions via Metabolic Reprogramming Regulated by mTORC1 Signaling. Front Immunol. 2021;12:619195.

273. Laffer B, Lenders M, Ehlers-Jeske E, Heidenreich K, Brand E, Köhl J. Complement activation and cellular inflammation in Fabry disease patients despite enzyme replacement therapy. Front Immunol. 2024;15:1307558.

274. Sinuani I, Beberashvili I, Averbukh Z, Sandbank J. Role of IL-10 in the progression of kidney disease. World J Transplant. 2013;3(4):91-8.

275. Su H, Lei CT, Zhang C. Interleukin-6 Signaling Pathway and Its Role in Kidney Disease: An Update. Front Immunol. 2017;8:405.

276. Zhang J, Li Y, Shan K, Wang L, Qiu W, Lu Y, et al. Sublytic C5b-9 induces IL-6 and TGF-β1 production by glomerular mesangial cells in rat Thy-1 nephritis through p300-mediated C/EBPβ acetylation. FASEB J. 2014;28(3):1511-25.

277. Rozenfeld PA, de Los Angeles Bolla M, Quieto P, Pisani A, Feriozzi S, Neuman P, et al. Pathogenesis of Fabry nephropathy: The pathways leading to fibrosis. Mol Genet Metab. 2020;129(2):132-41.

278. Jabri B, Abadie V. IL-15 functions as a danger signal to regulate tissue-resident T cells and tissue destruction. Nat Rev Immunol. 2015;15(12):771-83.

279. Waldmann TA. The biology of interleukin-2 and interleukin-15: implications for cancer therapy and vaccine design. Nat Rev Immunol. 2006;6(8):595-601.

280. McInnes IB, al-Mughales J, Field M, Leung BP, Huang FP, Dixon R, et al. The role of interleukin-15 in T-cell migration and activation in rheumatoid arthritis. Nat Med. 1996;2(2):175-82.

281. Vaknin-Dembinsky A, Brass SD, Gandhi R, Weiner HL. Membrane bound IL-15 is increased on CD14 monocytes in early stages of MS. J Neuroimmunol. 2008;195(1-2):135-9.

282. Villadsen LS, Schuurman J, Beurskens F, Dam TN, Dagnaes-Hansen F, Skov L, et al. Resolution of psoriasis upon blockade of IL-15 biological activity in a xenograft mouse model. J Clin Invest. 2003;112(10):1571-80.

283. Aringer M, Stummvoll GH, Steiner G, Köller M, Steiner CW, Höfler E, et al. Serum interleukin-15 is elevated in systemic lupus erythematosus. Rheumatology (Oxford). 2001;40(8):876-81.

284. Zhang C, Zhang J, Niu J, Tian Z. Interleukin-15 improves cytotoxicity of natural killer cells via up-regulating NKG2D and cytotoxic effector molecule expression as well as STAT1 and ERK1/2 phosphorylation. Cytokine. 2008;42(1):128-36.

285. Liew FY, Girard JP, Turnquist HR. Interleukin-33 in health and disease. Nat Rev Immunol. 2016;16(11):676-89.

286. Cayrol C, Girard JP. Interleukin-33 (IL-33): A nuclear cytokine from the IL-1 family. Immunol Rev. 2018;281(1):154-68.

287. Smithgall MD, Comeau MR, Yoon BR, Kaufman D, Armitage R, Smith DE. IL-33 amplifies both Th1- and Th2-type responses through its activity on human basophils, allergen-reactive Th2 cells, iNKT and NK cells. Int Immunol. 2008;20(8):1019-30.

288. Alves-Filho JC, Sônego F, Souto FO, Freitas A, Verri WA, Auxiliadora-Martins M, et al. Interleukin-33 attenuates sepsis by enhancing neutrophil influx to the site of infection. Nat Med. 2010;16(6):708-12.

289. Grotenboer NS, Ketelaar ME, Koppelman GH, Nawijn MC. Decoding asthma: translating genetic variation in IL33 and IL1RL1 into disease pathophysiology. J Allergy Clin Immunol. 2013;131(3):856-65.

290. Byers DE, Alexander-Brett J, Patel AC, Agapov E, Dang-Vu G, Jin X, et al. Long-term IL-33-producing epithelial progenitor cells in chronic obstructive lung disease. J Clin Invest. 2013;123(9):3967-82.

291. Khurana R, Simons M, Martin JF, Zachary IC. Role of angiogenesis in cardiovascular disease: a critical appraisal. Circulation. 2005;112(12):1813-24.

292. Ivanova MM, Dao J, Slayeh OA, Friedman A, Goker-Alpan O. Circulated TGF-β1 and VEGF-A as Biomarkers for Fabry Disease-Associated Cardiomyopathy. Cells. 2023;12(16).

293. Raines EW. PDGF and cardiovascular disease. Cytokine Growth Factor Rev. 2004;15(4):237-54.

294. Ross R. The pathogenesis of atherosclerosis: a perspective for the 1990s. Nature. 1993;362(6423):801-9.

295. Andrae J, Gallini R, Betsholtz C. Role of platelet-derived growth factors in physiology and medicine. Genes Dev. 2008;22(10):1276-312.

296. Bonner JC. Regulation of PDGF and its receptors in fibrotic diseases. Cytokine Growth Factor Rev. 2004;15(4):255-73.

297. Zymek P, Bujak M, Chatila K, Cieslak A, Thakker G, Entman ML, et al. The role of platelet-derived growth factor signaling in healing myocardial infarcts. J Am Coll Cardiol. 2006;48(11):2315-23.

298. Simm A, Nestler M, Hoppe V. Mitogenic effect of PDGF-AA on cardiac fibroblasts. Basic Res Cardiol. 1998;93 Suppl 3:40-3.

299. Chaigneau C, Cabioch T, Beaumont K, Betsou F. Serum biobank certification and the establishment of quality controls for biological fluids: examples of serum biomarker stability after temperature variation. Clin Chem Lab Med. 2007;45(10):1390-5.

300. Kisand K, Kerna I, Kumm J, Jonsson H, Tamm A. Impact of cryopreservation on serum concentration of matrix metalloproteinases (MMP)-7, TIMP-1, vascular growth factors (VEGF) and VEGF-R2 in Biobank samples. Clin Chem Lab Med. 2011;49(2):229-35.

301. Brignole M, Moya A, de Lange FJ, Deharo JC, Elliott PM, Fanciulli A, et al. 2018 ESC Guidelines for the diagnosis and management of syncope. Eur Heart J. 2018;39(21):1883-948.

302. Dion F, Saudeau D, Bonnaud I, Friocourt P, Bonneau A, Poret P, et al. Unexpected low prevalence of atrial fibrillation in cryptogenic ischemic stroke: a prospective study. J Interv Card Electrophysiol. 2010;28(2):101-7.

303. Svendsen JH, Diederichsen SZ, Højberg S, Krieger DW, Graff C, Kronborg C, et al. Implantable loop recorder detection of atrial fibrillation to prevent stroke (The LOOP Study): a randomised controlled trial. Lancet. 2021;398(10310):1507-16.

304. Ren J, Wu NN, Wang S, Sowers JR, Zhang Y. Obesity cardiomyopathy: evidence, mechanisms, and therapeutic implications. Physiol Rev. 2021;101(4):1745-807.

305. Lavie CJ, Pandey A, Lau DH, Alpert MA, Sanders P. Obesity and Atrial Fibrillation Prevalence, Pathogenesis, and Prognosis: Effects of Weight Loss and Exercise. J Am Coll Cardiol. 2017;70(16):2022-35.

306. Alpert MA, Lavie CJ, Agrawal H, Kumar A, Kumar SA. Cardiac Effects of Obesity: PATHOPHYSIOLOGIC, CLINICAL, AND PROGNOSTIC CONSEQUENCES-A REVIEW. J Cardiopulm Rehabil Prev. 2016;36(1):1-11.

307. Obokata M, Reddy YNV, Pislaru SV, Melenovsky V, Borlaug BA. Evidence Supporting the Existence of a Distinct Obese Phenotype of Heart Failure With Preserved Ejection Fraction. Circulation. 2017;136(1):6-19.

308. Syme C, Shin J, Richer L, Gaudet D, Paus T, Pausova Z. Sex Differences in Blood Pressure Hemodynamics in Middle-Aged Adults With Overweight and Obesity. Hypertension. 2019;74(2):407-12.

309. Frank RC, Min J, Abdelghany M, Paniagua S, Bhattacharya R, Bhambhani V, et al. Obesity Is Associated With Pulmonary Hypertension and Modifies Outcomes. J Am Heart Assoc. 2020;9(5):e014195.

310. Toennis T, Bertaglia E, Brandes A, Dichtl W, Fluschnik N, de Groot JR, et al. The influence of atrial high-rate episodes on stroke and cardiovascular death: an update. Europace. 2023;25(7).

311. Kirchhof P, Toennis T, Goette A, Camm AJ, Diener HC, Becher N, et al. Anticoagulation with Edoxaban in Patients with Atrial High-Rate Episodes. N Engl J Med. 2023;389(13):1167-79.

312. Hebert DN, Lamriben L, Powers ET, Kelly JW. The intrinsic and extrinsic effects of N-linked glycans on glycoproteostasis. Nat Chem Biol. 2014;10(11):902-10.

313. Lee K, Jin X, Zhang K, Copertino L, Andrews L, Baker-Malcolm J, et al. A biochemical and pharmacological comparison of enzyme replacement therapies for the glycolipid storage disorder Fabry disease. Glycobiology. 2003;13(4):305-13.

314. Graziani F, Leccisotti L, Lillo R, Bruno I, Ingrasciotta G, Leone AM, et al. Coronary Microvascular Dysfunction Is Associated With a Worse Cardiac Phenotype in Patients With Fabry Disease. JACC Cardiovasc Imaging. 2022;15(8):1518-20.

315. Graziani F, Lillo R, Biagini E, Limongelli G, Autore C, Pieroni M, et al. Myocardial infarction with non-obstructive coronary arteries in hypertrophic cardiomyopathy vs Fabry disease. Int J Cardiol. 2022;369:29-32.

316. Camporeale A, Diano A, Tondi L, Pica S, Pasqualin G, Ciabatti M, et al. Cardiac Magnetic Resonance Features of Fabry Disease: From Early Diagnosis to Prognostic Stratification. Rev Cardiovasc Med. 2022;23(5):177.

317. Bisignani A, De Bonis S, Mancuso L, Ceravolo G, Bisignani G. Implantable loop recorder in clinical practice. J Arrhythm. 2019;35(1):25-32.

318. van Veldhuisen DJ, van Woerden G, Gorter TM, van Empel VPM, Manintveld OC, Tieleman RG, et al. Ventricular tachyarrhythmia detection by implantable loop recording in patients with heart failure and preserved ejection fraction: the VIP-HF study. Eur J Heart Fail. 2020;22(10):1923-9.

319. Healey JS, Connolly SJ, Gold MR, Israel CW, Van Gelder IC, Capucci A, et al. Subclinical atrial fibrillation and the risk of stroke. N Engl J Med. 2012;366(2):120-9.

320. Van Gelder IC, Healey JS, Crijns HJGM, Wang J, Hohnloser SH, Gold MR, et al. Duration of device-detected subclinical atrial fibrillation and occurrence of stroke in ASSERT. Eur Heart J. 2017;38(17):1339-44.